LBL-37532
UC-413

Lawrence Berkeley Laboratory
UNIVERSITY OF CALIFORNIA

Presented at the Workshop on Tibet Cosmic Ray Experiment and Related Physics Topics, Beijing, China, April 4–13, 1995, and to be published in the Proceedings

Current Trends in Non-Accelerator Particle Physics

Y. He

July 1995

iNPA

Institute for Nuclear and Particle Astrophysics

Nuclear Science and Physics Divisions

REFERENCE COPY
Does Not
Circulate
Bldg. 50 Library.
LBL-37532
Copy 1

Prepared for the U.S. Department of Energy under Contract Number DE-AC03-76SF00098

DISCLAIMER

This document was prepared as an account of work sponsored by the United States Government. While this document is believed to contain correct information, neither the United States Government nor any agency thereof, nor The Regents of the University of California, nor any of their employees, makes any warranty, express or implied, or assumes any legal responsibility for the accuracy, completeness, or usefulness of any information, apparatus, product, or process disclosed, or represents that its use would not infringe privately owned rights. Reference herein to any specific commercial product, process, or service by its trade name, trademark, manufacturer, or otherwise, does not necessarily constitute or imply its endorsement, recommendation, or favoring by the United States Government or any agency thereof, or The Regents of the University of California. The views and opinions of authors expressed herein do not necessarily state or reflect those of the United States Government or any agency thereof, or The Regents of the University of California.

Lawrence Berkeley National Laboratory
is an equal opportunity employer.

DISCLAIMER

This document was prepared as an account of work sponsored by the United States Government. While this document is believed to contain correct information, neither the United States Government nor any agency thereof, nor the Regents of the University of California, nor any of their employees, makes any warranty, express or implied, or assumes any legal responsibility for the accuracy, completeness, or usefulness of any information, apparatus, product, or process disclosed, or represents that its use would not infringe privately owned rights. Reference herein to any specific commercial product, process, or service by its trade name, trademark, manufacturer, or otherwise, does not necessarily constitute or imply its endorsement, recommendation, or favoring by the United States Government or any agency thereof, or the Regents of the University of California. The views and opinions of authors expressed herein do not necessarily state or reflect those of the United States Government or any agency thereof or the Regents of the University of California.

LBL-37532
UC-413
Preprint

CURRENT TRENDS IN NON-ACCELERATOR PARTICLE PHYSICS[1]

I. Neutrino Mass and Oscillation

II. High Energy Neutrino Astrophysics

III. Detection of Dark Matter

IV. Search for Strange Quark Matter

V. Magnetic Monopole Searches

Yudong He

Department of Physics, Space Science Laboratory
and Center for Particle Astrophysics
University of California at Berkeley, Berkeley, CA 94720, USA

and

Institute for Nuclear and Particle Astrophysics
and Nuclear Science Division
Lawrence Berkeley National Laboratory, Berkeley, CA 94720, USA

July 1995

[1]This work was supported by the Director, Office of Energy Research, Office of High Energy and Nuclear Physics, Division of High Energy Physics of the U. S. Department of Energy under Contract No. DE-AC03-76SF00098.

CURRENT TRENDS IN NON-ACCELERATOR PARTICLE PHYSICS[1]

Yudong He[2]
Department of Physics, Space Science Laboratory
and Center for Particle Astrophysics
University of California at Berkeley, Berkeley, CA 94720, USA
and
Institute for Nuclear and Particle Astrophysics
and Nuclear Science Division
Lawrence Berkeley National Laboratory, Berkeley, CA 94720, USA

The emphasis in particle physics is changing today, as the growing symbiosis with astrophysics and cosmology becomes more widely appreciated than ever. Various astrophysical sites and, in a more general sense, the Universe itself have become a laboratory for the study of particle physics – a laboratory in which a unique experiment is still continuing. Non-accelerator particle physics has, in fact, been pushing forward the frontiers of our understanding the fundamentals in nature. It represents alternative opportunities to explore novel physics beyond the standard model of particle physics at energy scales inaccessible to man-made accelerators. On a practical ground, accelerator physics is experiencing a challenge, and what has been called "big science" in a narrow sense may have to await its next machine for at least 10 years. In this situation, the value of emphasizing different approaches dramatically increases. With the aim of extending our knowledge far beyond its present limits, theorists have been plunging into regions beyond the standard model. It is indeed the time for experimentalists to continue their efforts and move ahead to exploit new opportunities.

The purpose of the CCAST Workshop on Tibet Cosmic Ray Experiments and Related Physics Topics was to review the field of ultrahigh energy γ-ray astronomy, in particular the exciting results that have been flowing from the Tibet Air Shower Array, and in a more general view, to take a critical look at the various possibilities for future opportunities and directions in non-accelerator particle physics. This last point was conceivable when I was asked by the organizers to give a series of talks on current trends in non-accelerator particle physics in the workshop. To overview this merging field, I covered the following five topics. The selection of these topics reflects more or less my personal taste rather than established overview, as some of them may even not belong to the well-defined mainstream. Nevertheless, I believe such a choice illustrates the current trends in the field and especially the increasingly appreciated interplay between particle physics and astrophysics and cosmology. My topics are as follows:

[1]Invited lectures presented at the Workshop on Tibet Cosmic Ray Experiment and Related Physics Topics, CCAST (China Center for Advanced Science and Technology), Beijing, April 4-13, 1995.

[2]Mailing address: Department of Physics, University of California, Berkeley, CA 94720, USA. Email address: yudong@physics.berkeley.edu.

I. **Neutrino mass and oscillation** are to me fascinating topics. This amusing but elusive particle postulated as a way of explaining an otherwise intractable problem appears to play a crucial role in the collapse processes of astrophysical objects and the evolution and structure of the Universe. New results from the solar and atmospheric neutrino experiments seem to show a consistent picture that neutrinos may have *non-zero* masses, pointing toward new physics beyond the standard model. It appears to be a possibility that the study of physics at a low energy scale ($m_\nu \sim 10^{-3}$ eV) may provide information about energy regime on the scale of the grand unification mass ($M_{\rm GUT} \sim 10^{15}$ GeV).

II. **High energy neutrino astrophysics** with its known and encouraging prospects appears to be on the dramatic rise in recent years. High energy astrophysical neutrinos would provide information otherwise unattainable for the understanding of hadronic processes on various cosmic sites. The scientific promise of the subject apparently attracts the interest of an increasing number of researchers. With prototype experiments now underway, the field is at the turning point from a dream of theorists to an experimental reality. The endeavor is expected to have a great reward.

III. **Detection of dark matter** represents a great quest of science, as the dark matter problem remains as one of the most puzzling aspects in cosmology. In theory, the understanding of its nature involves new physics such as supersymmetry that is uniquely amenable to its detection. In experiment, the detection employs knowledge of nuclear physics and advanced applied technologies. Searches for various candidates that make up more than 90% of the Universe are exciting but are an experimental challenge.

IV. **Search for strange quark matter** may help us to identify the true ground state of the strongly interacting system. Moreover, the existence of strange quark matter may lead to a number of interesting consequences in cosmology and astrophysics and may fill the void of 55 orders of magnitude between known nuclides and the ultradense neutron stars. While present theories are incapable of deciding if strange matter is stable or not, the answer needs to be found experimentally with searches for relics in terrestrial materials and in galactic cosmic rays, and in "the Little Bang" simulated by ultrarelativistic heavy ion collisions.

V. **Magnetic monopole searches**, either the point-like ones of Dirac or the structured ones of 't Hooft-Polyakov, have great impact on physical theories. Monopole searches have never stopped either in high energy interactions or in galactic cosmic rays. As a topological defect, monopoles may have played a very crucial role in the very early Universe. Along with neutrino mass and proton decay, monopoles are one of the few predictions of grand unification theories that can be studied in our present "low energy" environment.

These topics contain many fundamental problems that are interconnected in our current exploration. For example, the mass of neutrinos seems to hold the secret to some of the most pivotal questions in nuclear physics (e.g., weak interaction in β decay and double β decay), particle physics (e.g., lepton number conservation, mass generation mechanism), astrophysics (e.g., stellar evolution, especially stellar collapse and explosion process), and cosmology (e.g, dark matter problem). The study of astrophysical neutrinos is an example of attacking fundamental physics at microscopic scale ("point-like" ν) by studying stellar phenomena at cosmic scale! As one of the dark matter candidates, strange quark matter might have been created in quark-hadron phase transition after the Big Bang. The study of monopoles, whose relic may constitute part of dark matter, may shed the light on the earlest moment ($t \sim 10^{-34}$ sec after the Big Bang) of the Universe governed by the grand unification theories at energies $\sim 10^{15}$ GeV. Preparing these talks and writing up these papers have given me a fantastic excursion through the world that is characterized by the explosive progress vs severe limits, and a number of intriguing ideas vs an enormous number of unknowns in our understanding of nature. As we know from history, it is these unknowns that will drive us into a new era.

It should be noted that I did not intend to give complete reviews on the field of non-accelerator particle physics. Instead, I discussed some general trends in the field by examining some important discoveries in the history and by highlighting the most recent developments which I think are important. The references cited in each paper may be far from complete and I apologize in advance for any omission of important work. As the camera-ready manuscripts go to press, I am responsible for all the errors contained in these papers – errors of typography and errors of physics.

It was my great pleasure to be selected as a member of the CCAST Young Returning Scientists Program. I wish to record my indebtedness to Professor T. D. Lee for his invitation. I thank Professor Minghan Ye and all the CCAST staff for their hospitality during my stay at CCAST and Professor Yang Pang for coordinating the program. I thank Professor Linkai Ding and Anxiang Huo for putting together such a wonderful workshop. The workshop was, all around, a productive and enjoyable experience. It has provided me a chance to learn more recent developments, to meet colleagues and friends, and to interact with young researchers.

I acknowledge the support from my home institutions, University of California at Berkeley and Lawrence Berkeley National Laboratory. I thank my colleagues with whom I have had enjoyable discussions. In particular, I thank Professor Buford Price who has read all the manuscripts and made helpful comments. I also thank Dr. Bob Stokstad of INPA for his useful suggestions. This work was supported in part by the Director, Office of Energy Research, Office of High Energy and Nuclear Physics, Division of High Energy Physics of the U. S. Department of Energy under Contract No. DE-AC03-76SF00098.

I would like to dedicate this series of papers to all the teachers of mine who have given me guidance, advice, and friendship at various stages of my academic career.

July 1995
Berkeley, California

NEUTRINO MASS AND OSCILLATION[1]

Yudong He[2]
Department of Physics, Space Science Laboratory
and Center for Particle Astrophysics
University of California at Berkeley, Berkeley, CA 94720, USA
and
Institute for Nuclear and Particle Astrophysics
and Nuclear Science Division
Lawrence Berkeley National Laboratory, Berkeley, CA 94720, USA

Abstract

I review the recent development of neutrino studies, focusing primarily on the neutrino mass, flavor transition, and related interesting topics. The Kamiokande scattering experiment and two recent Ga experiments which are sensitive to pp neutrinos from the Sun have supported the solar neutrino deficit discovered by the Cl experiment over the last two decades. Among various explanations, the MSW effect is favored. The possible anomaly found in atmospheric neutrinos by the Kamiokande and IMB Collaborations has shown some hints for neutrino oscillation. The new result of accelerator oscillation experiment from LSND, if confirmed, will be a direct evidence for neutrino oscillation. All these seem to show a consistent picture that neutrinos may have non-zero masses, pointing toward new physics beyond the standard model of particle physics.

Neutrino physics is largely an art of learning a great deal by observing nothing. – Haim Harari (1988)[3]

1 The Elusive Neutrino: An Introduction

The most elusive particle discovered so far in nature may be the neutrino. Facts about neutrinos that we know today are: they are stable, neutral, spin 1/2 fermions, they may have a tiny mass if not zero, they may have a small magnetic moment if not zero, and there are three generations (or flavors): electron neutrino, muon neutrino, and tau neutrino. We know little about their fundamental properties. For example, do they have a *non-zero* mass? Can a neutrino of one flavor transform into a different flavor intrinsically? These

[1]This topic is one of a series of lectures on "Current Trends in Non-Accelerator Particle Physics" given at CCAST Workshop on Tibet Cosmic Ray Experiment and Related Physics Topics, Beijing, April 4-13, 1995. This work was supported in part by the U. S. Department of Energy under Contract No. DE-AC03-76SF00098.

[2]Mailing address: Department of Physics, University of California, Berkeley, CA 94720, USA. Email address: yudong@physics.berkeley.edu.

[3]H. Harari, in *Proc. 13th Intern. Conf. on Neutrino Physics and Astrophysics*, Boston (Medford), 1988, p. 574.

questions seem to hold the key to some of the most important unanswered questions in nuclear physics (e.g., weak interaction in β decay and double β decay), particle physics (e.g., lepton number conservation, mass generation mechanism), astrophysics (e.g., stellar evolution, especially stellar collapse and explosion process), and cosmology (e.g, dark matter problem). The study of neutrino physics has a long history and there are many excellent books available [1, 2, 3]. In my talk, I focus only on recent studies on the neutrino mass and flavor oscillation.

The idea of neutrino was introduced *apologetically* by Pauli[4] [4] in 1930 in order to resolve the puzzling continuous electron spectrum in nuclear β decay. The β decay spectrum was so mysterious that it seemed to challenge other fundamental laws such as energy conservation[5]. Since Pauli's proposal, various aspects of neutrinos have occupied the thoughts of many brilliant physicists of this century. The exploration of neutrinos has, in fact, played a crucial role in the advancement of our understanding of fundamental physics.

Shortly after Pauli's suggestion, a theory regarding the interaction of a massless neutrino with matter was formulated by Fermi[6]. Much of the work since then, for over a quarter of a century, was aimed at determining the nature of the weak interactions. It was finally settled that it takes the following form:

$$\frac{1}{\sqrt{2}} G_{\mathrm{F}} \overline{p} \gamma_\mu (1 - \lambda \gamma_5) n \overline{e} \gamma^\mu (1 - \gamma_5) \nu \tag{1}$$

after the discovery of parity violation by Lee and Yang [7] and the experimental confirmation by Wu *et al.* [8]. In the modern view, the $(1-\gamma_5)$ structure is taken as being the first evidence which indicates that massless particles play a basic role in the weak interaction, and the constant $\lambda \neq 1$ indicates that nucleons have structures which renormalize the strength of the axial coupling.

On the experimental side, it took a long period of time to find ways to detect neutrinos. The early "indirect" way of establishing the existence of neutrinos besides nuclear β decay was suggested by Wang in a short note[7] published in 1942. He proposed to use K electron capture reaction of β^+-radioactive atoms to detect neutrinos by measuring the recoil energy and momentum of the resulting atom alone. A specific example he proposed is Be^7 which decays in ~ 43 days with K capture in two different processes:

$$\begin{aligned} \mathrm{Be}^7 + e_{\mathrm{K}} \rightarrow \quad & \mathrm{Li}^7 + \nu + (1\,\mathrm{MeV}) \\ \mathrm{Be}^7 + e_{\mathrm{K}} \rightarrow \quad & (\mathrm{Li}^7)^* + \nu + (0.55\,\mathrm{MeV}) \\ & \hookrightarrow \mathrm{Li}^7 + (h\nu) + (0.45\,\mathrm{MeV}). \end{aligned}$$

[4]Wolfgang Pauli once said: "I have done a terrible thing, I have postulated a particle that cannot be detected." (1948). He dared not publish anything about the idea, and other than archival conference proceedings he never did write a paper proposing the existence of the new particle.

[5]For example, Neils Bohr was willing to entertain the possibility that the energy conservation must be abandoned in the nuclear realm and is only statistically valid [5].

[6]This brilliant work of Fermi was unfortunately rejected by *Nature* and was eventually published in *Z. Phys.* [6].

[7]This important paper was submitted from Guizhou, China during World War II and published in *Phys. Rev.* [9]. But unfortunately it did not receive timely adequate attention.

The actual experiment along this line followed the suggestion of Crane in 1948 [10]. In the K-capture reaction in ^{37}Ar:

$$^{37}\mathrm{Ar} + e^- \rightarrow {}^{37}\mathrm{Cl} + \nu + Q, \tag{2}$$

the recoil of the Auger electrons can be neglected, so that the momentum of the neutrinos manifests itself only in the recoil of the Cl atoms. Rodeback and Allen [11] used this reaction to detect neutrinos indirectly.

In 1946, Pontecorvo [12] proposed an idea of establishing the existence of neutrinos directly by using inverse β-decay:

$$\nu + {}^{37}\mathrm{Cl} \rightarrow \beta^- + {}^{37}\mathrm{Ar}. \tag{3}$$

Bethe [13] calculated that the cross section for the absorption of a neutrino by a nucleus, in inverse β decay, was so small that the neutrino was very likely undetectable. Some time later, eqn. (3) became the tool used by Davis to begin the first solar neutrino experiment.

The first direct detection of free neutrinos (in fact anti-neutrinos!) was carried out by Reines and Cowan[8] [15]. Using anti-neutrinos created in a reactor, they studied the process:

$$\overline{\nu}_e + p \rightarrow n + e^+. \tag{4}$$

Almost immediately following this process, the positron would annihilate with an electron into a pair of back-to-back γ-rays. The neutron would be captured by a cadmium nucleus some 5 ms after the annihilation γ-rays had emerged, which would then emit some more γ-rays.

In 1959, Schwartz [16], inspired by Lee's concern with the unitarity crisis in the weak interactions, proposed to study the neutrino interactions using a beam of neutrinos from the decay of high energy pions. A similar idea was also proposed independently by Pontecorvo [17]. Later, it was demonstrated that $\nu_\mu \neq \overline{\nu}_e$ and the concept of flavor was established [18]. At CERN, neutrinos were eventually used to help unify two of the fundamental forces (electromagnetic and weak) and explore the deep structure of nucleons [19].

The experimental effort carried out over the last two decades has established that the interaction of the neutrino with matter is just as described by the standard electroweak theory. Current interest is focused on the mass of the neutrino and its related phenomena beyond the standard model.

Neutrino physics involves many seemingly independent disciplines, both theoretical (involving nuclear, atomic, particle physics, and astrophysics) and experimental (involving nuclear chemistry, nuclear physics, geochemistry, high energy physics, and astronomy). In section 2, I will first give a brief introduction to the neutrino mass and oscillation formulation which are necessary to understand the subject. In section 3, I will present two examples of laboratory searches for the neutrino mass. In section 4, I will discuss

[8]Pauli wrote a note to Reines and Cowan in 1956 (but never received until 1986): "Everything comes to him who knows how to wait" [14].

non-accelerator neutrino experiments including the solar, supernova, and atmospheric neutrinos. Finally in section 5, I will comment on the present status and discuss future directions.

2 Neutrino Mass and Oscillation

2.1 Dirac Neutrino and Majorana Neutrino

If a neutrino indeed has a finite mass, many questions would arise concerning its properties. The first question is perhaps whether the neutrino is of the Dirac type or the Majorana type. Generation mixing would also be a very important issue, which would provide a hint to our understanding of the mass problem in particle physics. If the neutrino does not have a finite mass, the distinction between the Dirac type and the Majorana type becomes meaningless.

In the context of the Dirac Lagrangian for spin 1/2 particles, the mass term serves to change helicity from left-handed to right-handed partner or vice versa. There are two possible mass terms – the Dirac mass term $m(\overline{\psi}_{\rm R}\psi_{\rm L} + h.c.)$ and the Majorana mass term $M(\overline{\psi}^{\rm c}_{\rm L}\psi_{\rm L} + h.c.)$, where $\psi^{\rm c} = C\gamma^{\rm o}\psi^*$ is the charge conjugated field of ψ and $\psi^{\rm c}_{\rm L} \equiv (\psi_{\rm L})^{\rm c} = (1+\gamma_5)\psi^{\rm c}/2$ has a right-handed chirality. The first mass term gives a mass to quarks and charged leptons. The existence of the second term violates lepton-number conservation by two units, and makes a particle and its antiparticle indistinguishable. When neutrinos have a Majorana mass component, they are usually called the "Majorana neutrino". If there exists a right-handed neutrino $\nu_{\rm R}$ in addition to a left-handed neutrino $\nu_{\rm L}$ one can construct a Dirac mass term and treat the neutrino mass in parallel to the mass term for other charged particles. If only the $\nu_{\rm L}$ exists, the Majorana mass is the only possible form to give the neutrino a finite mass. Within the standard Weinberg-Salam theory, however, the Majorana mass term is necessarily non-renormalizable, and is taken as an effective interaction that arises from more fundamental interactions at a higher energy scale. In turn, this would provide an explanation as to why the mass of the neutrino (if any) is so small compared with the mass of other charged particles. The simplest example is the so-called see-saw mechanism [20], in which the right-handed neutrino $\nu_{\rm R}$ has a large Majorana mass M and the left-handed neutrino $\nu_{\rm L}$ is given a mass through leakage of the order of $\sim m/M$. The Dirac mass m causes mixing between $\nu_{\rm L}$ and $\nu_{\rm R}$ and is taken to be of the order of the other charged particle mass. Such a mechanism, indeed, plays a crucial role in grand unification theory, which usually requires that the neutrino Dirac mass and the charge $-2/3$ quark mass be related.

If the neutrino is of the Majorana type, the neutrinoless double β decay may take place, as pointed out by Furry [21]. The study of neutrinoless double β decay, which is important to test the lepton number violation and mass scale at higher energies, is in itself an active research field [22]. Pontecorvo [23] suggested that a neutrino may oscillate into its antipartner in the vacuum if the lepton number is not conserved, just like $K^{\rm o} - \overline{K}^{\rm o}$ oscillation in the case of CP violation. Oscillation among the different kinds of neutrinos was then proposed by Maki *et al.* [24]. Such a phenomenon may occur if some of the

neutrinos are massive and if there is a mixing between neutrinos.

2.2 Vacuum Oscillation

If flavor (or, current, or weak) eigenstates are not identical to mass eigenstates, intrinsic transitions between different flavors are indispensable. This is usually called flavor (or generation) oscillation.

Suppose neutrinos have 3 flavor eigenstates $|\nu_e>$, $|\nu_\mu>$, and $|\nu_\tau>$. The mass eigenstates are $|\nu_1>$, $|\nu_2>$, and $|\nu_3>$. The flavor eigenstates can be represented as linear combinations of the mass eigenstates:

$$|\nu_\alpha>=\sum_j U_{\alpha j}e^{-iE_jt}|\nu_j>, \tag{5}$$

in which U is a unitary matrix that can be chosen to be real if CP is conserved. For simplicity, let us consider a two flavor system. The mass matrix in this case is:

$$U=\begin{pmatrix} \cos\theta_v & \sin\theta_v \\ -\sin\theta_v & \cos\theta_v \end{pmatrix}, \tag{6}$$

where θ_v is the vacuum mixing angle. The probability of remaining in flavor α is:

$$|<\nu_\alpha|\nu_\alpha>|^2=1-\sin^2(2\theta_v)\sin^2\left[\frac{1}{2}(E_2-E_1)t\right], \tag{7}$$

in which we assume that the two mass eigenstates have the same momentum, which implies that they have slightly different energies if they have finite masses. The energy difference for relativistic neutrinos is:

$$E_2-E_1=\frac{m_2^2-m_1^2}{2E}\equiv\pm\frac{\Delta m^2}{2E}, \tag{8}$$

where $\Delta m^2\equiv|m_2^2-m_1^2|$, it takes $+$ when $m_2>m_1$ and $-$ when $m_2<m_1$. With the definition:

$$\frac{1}{2}(E_2-E_1)t\equiv\frac{\pi d}{L_v}, \tag{9}$$

$$L_v\equiv\frac{4\pi E}{\Delta m^2}, \tag{10}$$

the remaining probability in flavor α after traveling distance d is:

$$P_{\alpha\to\alpha}=1-\sin^2(2\theta_v)\sin^2\left(\frac{\pi d}{L_v}\right), \tag{11}$$

and the probability of transforming from flavor α into β is:

$$P_{\alpha\to\beta}=1-P_{\alpha\to\alpha}=\sin^2(2\theta_v)\sin^2\left(\frac{\pi d}{L_v}\right). \tag{12}$$

Table 1: The sensitive mass difference squared for different types of experiments.

Experiment	d/E (m/MeV)	$\sqrt{\Delta m^2}$ (eV)
Accelerator	$10^{-2} - 10^{1}$	$0.5 - 10$
Reactor	$10^{0} - 10^{2}$	$0.1 - 1$
Atmospheric	$10^{2} - 10^{4}$	$10^{-2} - 10^{-1}$
Solar	$10^{10} - 10^{11}$	$5 \times 10^{-6} - 10^{-5}$
Supernova	$10^{19} - 10^{20}$	$10^{-10} - 10^{-9}$

The vacuum oscillation length is given as:

$$L_\nu = \frac{4\pi E\hbar}{\Delta m^2 c^3} = 2.48 \text{ meter} \left(\frac{E}{1 \text{ MeV}}\right)\left(\frac{1 \text{ eV}^2}{\Delta \text{m}^2}\right). \tag{13}$$

This formula is often used to discuss terrestrial oscillation experiments that employ beams from reactor or accelerator. For discussions of astrophysical neutrino experiments, it is convenient to use:

$$\frac{\pi d}{L_\nu} = 1.9 \times 10^{11} \left(\frac{1 \text{ MeV}}{E}\right)\left(\frac{\Delta m^2}{1 \text{ eV}^2}\right)\left(\frac{d}{1 \text{ AU}}\right), \tag{14}$$

where 1 AU is the average distance between the Earth and the Sun. It is readily seen that the minimum mass difference squared Δm^2 that can be studied with an experiment is determined by $(\pi d/L_\nu) = 0.3$:

$$(\Delta m^2)_{\min} = 1.6 \times 10^{-12} \text{ eV}^2 \left(\frac{E}{1 \text{ MeV}}\right)\left(\frac{1 \text{ AU}}{\text{d}}\right). \tag{15}$$

For solar neutrinos, the minimum mass difference squared is on the order of $\sim 10^{-9}$ eV^2. It is worth noting that this minimum mass is many orders of magnitude smaller than can be achieved in terrestrial experiments. In Table 1, I list (d/E) and $\sqrt{\Delta m^2}$ for various types of neutrino experiments.

In the Hamiltonian formulation, an arbitrary neutrino state can be written in the flavor basis as:

$$|\nu >_t = C_\alpha(t)|\nu_\alpha > + C_\beta(t)|\nu_\beta > . \tag{16}$$

The time evolution of the coefficients is controlled by:

$$i\frac{d}{dt}\begin{pmatrix} C_\alpha(t) \\ C_\beta(t) \end{pmatrix} = M_\nu \begin{pmatrix} C_\alpha(t) \\ C_\beta(t) \end{pmatrix}, \tag{17}$$

in which the mass matrix is given as:

$$M_\nu = \pm\frac{\Delta_\nu}{2}\begin{pmatrix} -\cos(2\theta_\nu) & \sin(2\theta_\nu) \\ \sin(2\theta_\nu) & \cos(2\theta_\nu) \end{pmatrix}, \tag{18}$$

with

$$\Delta_{\rm v} = \frac{|\Delta m^2|}{2E}. \tag{19}$$

The mass eigenvalues obtained by diagonalizing the mass matrix are:

$$E_{1,2} = \text{const.} \pm \frac{1}{2}\Delta_{\rm v}. \tag{20}$$

The vacuum oscillation length is:

$$L_{\rm v} = \frac{2\pi}{|E_1 - E_2|} = \frac{2\pi}{\Delta_{\rm v}}, \tag{21}$$

which is equivalent to eqn. (13).

2.3 Matter Oscillation (The MSW Effect)

When neutrinos propagate through matter $\nu_{\rm e}$ and ν_μ (or ν_τ) feel different potential because $\nu_{\rm e}$ scatters off electrons via both neutral and charged currents, whereas ν_μ (or ν_τ) scatters only via the neutral current. This induces a *coherent* effect in which maximal conversion of $\nu_{\rm e}$ into ν_μ takes place even for a rather small intrinsic mixing angle in the vacuum, when the phase arising from the potential difference between the two neutrinos cancels the phase caused by the mass difference in the vacuum. This mechanism was pointed out by Mikheyev and Smirnov, and Wolfenstein (the MSW effect) [25, 26].

The enhancement of oscillation in matter can be formally represented as:

$$M \longrightarrow M_{\rm v} + M_{\rm matter}, \tag{22}$$

The new matrix:

$$M_{\rm matter} = \sqrt{2}G_{\rm F}n_{\rm e}P_{\rm e} = \sqrt{2}G_{\rm F}n_{\rm e}|\nu_{\rm e}><\nu_{\rm e}| \tag{23}$$

is due to the contribution of $\nu_{\rm e} - e$ scattering to the index of refraction of $\nu_{\rm e}$ in matter. The total mass matrix, for a two flavor system, becomes:

$$M = \pm\frac{\Delta_{\rm m}}{2}\begin{pmatrix} -\cos(2\theta_{\rm m}) & \sin(2\theta_{\rm m}) \\ \sin(2\theta_{\rm m}) & \cos(2\theta_{\rm m}) \end{pmatrix}, \tag{24}$$

where

$$\Delta_{\rm m} = \left\{[\pm\Delta_{\rm v}\cos(2\theta_{\rm v}) - \sqrt{2}G_{\rm F}n_{\rm e}]^2 + [\Delta_{\rm v}\sin(2\theta_{\rm v})]^2\right\}^{\frac{1}{2}}. \tag{25}$$

The eigenvalues of E are:

$$E_{1,2} = \text{const.} \pm \frac{1}{2}\Delta_{\rm m}. \tag{26}$$

The mixing angle in matter $\theta_{\rm m}$ is:

$$\tan(2\theta_{\rm m}) = \frac{\tan(2\theta_{\rm v})}{1 \pm \frac{L_{\rm v}}{L_{\rm e}} \frac{1}{\cos(2\theta_{\rm v})}}, \tag{27}$$

in which the $\nu_{\rm e} - e$ interaction length $L_{\rm e}$ is:

$$L_{\rm e} = \frac{\sqrt{2}\pi\hbar c}{G_{\rm F} n_{\rm e}} = 1.64 \times 10^5 \text{ m} \left(\frac{100 \text{ g cm}^{-3}}{\mu_{\rm e}\rho}\right) \tag{28}$$

where $\mu_{\rm e} = (1+X)/2$ and X is the mass fraction of H.

Eqn. (27) has resonant feature when $L_{\rm v}/L_{\rm e} \sim \cos(2\theta_{\rm v})$. The MSW resonant density is:

$$n_{\rm e}\Big|_{\rm resonance} = \frac{|\Delta m^2|}{2\sqrt{2}G_{\rm F}E}\cos(2\theta_{\rm v}), \tag{29}$$

or numerically:

$$n_{\rm e}\Big|_{\rm resonance} = 66 N_{\rm A}\cos(2\theta_{\rm v})\left(\frac{|\Delta m^2|}{10^{-4}\text{ eV}^2}\right)\left(\frac{10\text{ MeV}}{E}\right). \tag{30}$$

We note that for a very small $\theta_{\rm v}$, $\theta_{\rm m}$ can be large. Hence this is called matter enhancement of oscillation. The fact that $\theta_{\rm m}$ depends on E would change the energy spectrum of neutrinos. The MSW effect is rich and beautiful. For detailed discussions, see Ref. [3].

3 Search for Neutrino Mass in Laboratory

Neutrinos are produced on the Earth by natural radioactivity, by nuclear reactors, and by high energy accelerators. The dominant part of the current experimental effort with laboratory neutrinos is concerned with the search for a finite mass. The most straightforward is the search for the electron neutrino mass with nuclear β decay. The most sensitive method is to look for oscillations between flavors. In this section, I will discuss two examples. One is the classic nuclear β decay (with the 17 keV neutrino story) and the other is the LSND experiment (with its surprising new results).

3.1 Nuclear β Decay: The 17 keV Neutrino Story

Nuclear β decay:

$$^{\rm Z}{\rm A} \rightarrow {}^{\rm Z}({\rm A}-1) + {\rm e}^- + \overline{\nu}_{\rm e} \tag{31}$$

is a colorful example in modern physics. It was the origin of neutrino idea and its inverse process was used in its detection. Moreover, weak theory and symmetry test have been based on β decay. Additionally, one can search for non-zero mass neutrinos in β decay by looking for a distortion of the spectrum. Limits obtained from this method so far have been summarized by Particle Data Group [27] and discussed in some details by Robertson [28] and Kündig *et al.* [29]. I will only discuss the 17 keV story here.

Suppose that a component (fraction λ) of non-zero mass neutrino is produced in addition to the normal massless neutrino in β decay:

$$|\nu_e >= (1-\lambda)|\nu_1 > +\lambda|\nu_2 >, \tag{32}$$

the kinematic and phase space consideration leads to the following energy spectrum in the *incoherent* case here:

$$\frac{dN}{dp} = CSFp^2(1-\lambda^2)(E_{\rm end}-E)^2 + \lambda^2(E_{\rm end}-E)[(E_{\rm end}-E)^2 - m_2^2]^{1/2}, \tag{33}$$

where C, S, and F are constants that depend on nuclear physics. For a detector system with known response function $\mathcal{R}(p,p')$ and residual background $B_{\rm rsd}$, the observed spectrum will be:

$$\frac{\Delta N}{\Delta p} = \int_p^{p+\Delta p} dp' \Big\{ \Big[\Big(\frac{dN}{dp}\Big) + B_{\rm rsd} \Big] \mathcal{R}(p,p') \Big\}. \tag{34}$$

By minimizing the χ^2 fit of eqn. (33) to the observed spectrum, one obtains values of λ and m_2.

The first evidence for a 17 keV neutrino was found by Simpson [30] in ^{3}H decay using a Si detector. The result caused a certain amount of upheaval, as theorists tried to find out if their theories could accommodate a 17 keV neutrino, and experimental groups tried to find further evidence. Afterwards, several groups, using solid state detectors, reported new evidence in decay systems of ^{3}H, ^{35}S, ^{14}C, ^{71}Ge, ^{55}Fe, and ^{63}Ni. What is more interesting is that all the results seemed to converge to a notion that the neutrinos produced in β decay may contain a component of heavy neutrinos with mass $\sim$ 17 keV at a few percent level [31].

Recently, negative results have been continuously reported for the same isotopes from experiments using mainly magnet spectrometers. The case became controversial in the beginning of 90's[9]. Are there solid state effects that could mimic a neutrino like "kinks" in β spectrum? Or is the magnet spectrometer experiment indeed incapable of detecting the kind of spectral distortions sought?

Eventually, the case has been clarified by several conclusive experiments. In particular, it was demonstrated that the effect vanishes in spectrometers based on solid state detectors, when baffle scattering is eliminated by a solenoidal magnetic guiding field [32, 33]. All recent control experiments exclude a component of a 17 keV neutrino on the level of about 10^{-3} or somewhat better. Moreover, β-spectra were scanned carefully for heavy neutrino components at other energies. In the range of 10.5 eV $\leq m_\nu \leq$ 25.0 keV a null result was obtained excluding any component larger than 0.15% [34]. For an extended version of the story about the 17 keV neutrino and lessons learned from the story, see detailed discussions by Franklin [35] and by Wietfeldt and Norman [36].

[9]In defending his experiments, J. J. Simpson once said: "Contrary to one's intuition, a null result is not more reliable than a positive result."

3.2 LSND New Results: Oscillation Observed?

In the end of January this year, email messages circulating around the world seemed to indicate a possible discovery of neutrino oscillation at Los Alamos. The news apparently shocked the whole physics community, while no scientific document was available[10]. Here I briefly mention their results[11].

Using a proton beam at $\sim$ 800 MeV, LSND (Liquid Scintillation Neutrino Detector) studies:

$$\begin{aligned} \mathrm{p} + \text{target}\,(\mathrm{H_2O}) \rightarrow \quad & \pi^+ + \mathrm{X} \\ & \hookrightarrow \nu_\mu + \mu^+ \\ & \qquad\qquad \hookrightarrow \quad e^+(\mathrm{E} > 36\mathrm{MeV}) + \nu_\mathrm{e} + \overline{\nu}_\mu. \end{aligned}$$

Of course, π^-'s are also produced by protons, but they are absorbed. In this chain of the neutrino production, no $\overline{\nu}_\mathrm{e}$ is expected to be present if there is no oscillation either between flavor states ($\overline{\nu}_\mu \leftrightarrow \overline{\nu}_\mathrm{e}$) or between charge-conjugated states ($\nu_\mathrm{e} \leftrightarrow \overline{\nu}_\mathrm{e}$). The collaboration has searched for $\overline{\nu}_\mathrm{e}$ as a signal of oscillation via $\overline{\nu}_\mathrm{e} + p \rightarrow e^+ + n$ where the neutron will be captured by a proton, forming a deuteron and emitting a 2.2 MeV characteristic γ. Therefore, the signature in the detector is the coincident detection of a positron with energy larger than 36 MeV and an associated γ with energy $\sim$ 2.2 MeV. There are several potential sources of background that may contribute to the events including cosmic ray neutrinos. Usually, rejecting background at a level as small as 10^{-4} is extremely difficult in this type of experiment. The detailed procedures are unknown at this time. Nevertheless, it is claimed that after subtraction of possible background, events of $\overline{\nu}_\mathrm{e}$ were detected. Furthermore, the signal stays at $\sim$ 0.7% level of oscillation probability, roughly independent of the cuts applied (R parameter).

Given the importance of their results, more careful analysis is absolutely necessary before a discovery can be claimed. If they are unable to find a reasonable background to account for the detected events, their observation would imply a neutrino with mass of few to 10 eV, given the experiment configuration. Needless to say, this discovery, if confirmed, would be of great significance.

4 Astrophysical Neutrino Study

Neutrinos from space include solar, supernova, cosmic, and cosmological. As things stand no practical way to detect the relic cosmological neutrinos has yet been found. In this section, I will discuss solar, supernova, and atmospheric neutrinos.

[10]It has become a fashion to publicize a scientific discovery in newspaper first rather than publish a specialized paper in a refereed scientific journal these days [37].

[11]The new result has not been published and no preprints can be found at this time. If errors are contained in this presentation of their results, they are due to my own misunderstanding.

4.1 Solar Neutrinos: Deficit!

The Sun is an astronomical laboratory. Because of its proximity to the Earth, we are able to obtain information about the Sun that is not accessible for other stars. The Sun has the fundamental attraction of being the dynamo that drives life on the Earth. The nuclear fusion chains occurring in the solar core at high temperature are responsible for the energy generation in the Sun. Vast quantities of neutrinos are produced in these thermonuclear reactions involving weak interactions. These solar neutrinos can escape almost freely from the solar interior. Consequently, their detection can probe the physical state of the solar core very directly. By comparing measured neutrino fluxes and spectra with theoretical predictions, stellar structure models, in particular the standard solar model, can be experimentally tested. More importantly, solar neutrino measurements have the potential to unravel a nonvanishing neutrino mass by virtue of neutrino oscillation as I discussed in a previous section.

Even though solar neutrino flux is quite large (at the Earth $\sim 6 \times 10^{10}$ cm^{-2} s^{-1}), the detection is very difficult because of the extremely low interaction cross section (at sub-MeV, $10^{-46} - 10^{-42}$ cm^2). Typical event rates are indicated by the magnitude of the appropriately defined solar neutrino unit:

$$1 \text{ SNU} \equiv 1 \text{ event per } 10^{36} \text{ target atoms per second.} \tag{35}$$

So far some 10^3 neutrinos have been detected from the Sun over the past quarter of century. The history of solar neutrino problem, either theoretical or experimental, is quite interesting. Interested readers may find a historical account of the development and comprehensive review on the subject by one of the key players in Ref. [3].

In theory, given its mass and chemical composition, the structure and evolution of a star is uniquely defined. The standard ingredients of stellar models include hydrostatic equilibrium, the ideal gas equation of state, thermal equilibrium (energy production equals luminosity), radiation dominated energy transport in the dense interior, and secular energy production by nuclear reactions.

Parameters about the Sun are known best among all astrophysical objects. Knowledge of the nuclear cross sections for the relevant fusion reactions has come from laboratory measurements. The most explicit solar model calculations focusing on neutrino productions have been carried out and continuously updated by Bahcall during the past quarter century. In the diagram below, I list the pp chain and CNO cycle that are mainly responsible for solar neutrino production. For a central temperature of 15.6×10^6 K for the Sun, the dominant cycle is the pp chain, whereas the CNO cycle contributes only marginally to the energy production. Fig. 1 shows calculated solar neutrino spectra from different reactions [38]. As we see from this figure, the most abundant solar neutrinos are those produced in the initial pp reaction (6×10^{10} cm^{-2} s^{-1} at the Earth). After deuterium is burnt into ^{3}H, neutrinos are produced either in the ppII branch from electron capture of the intermittently produced ^{7}Be nuclei (^{7}Be neutrinos have a line spectrum) or, in the very rare ppIII branch from the e$^+$ decay of ^{8}B. Under each neutrino production process, I also list the neutrino energy.

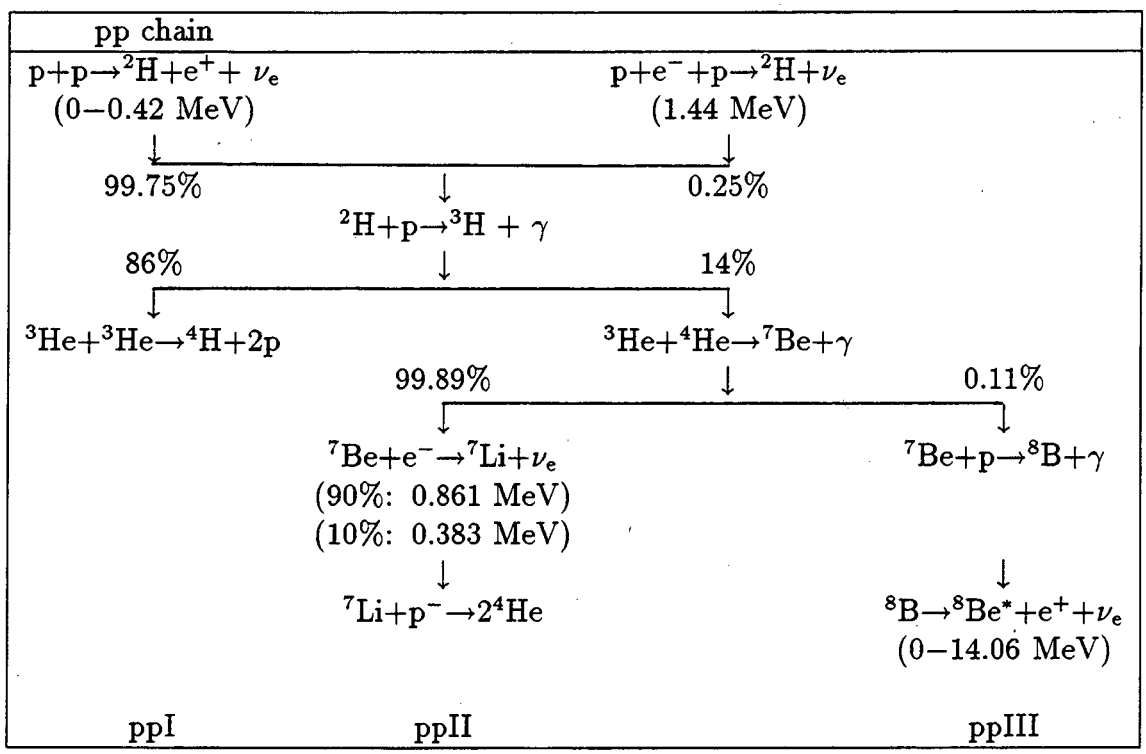

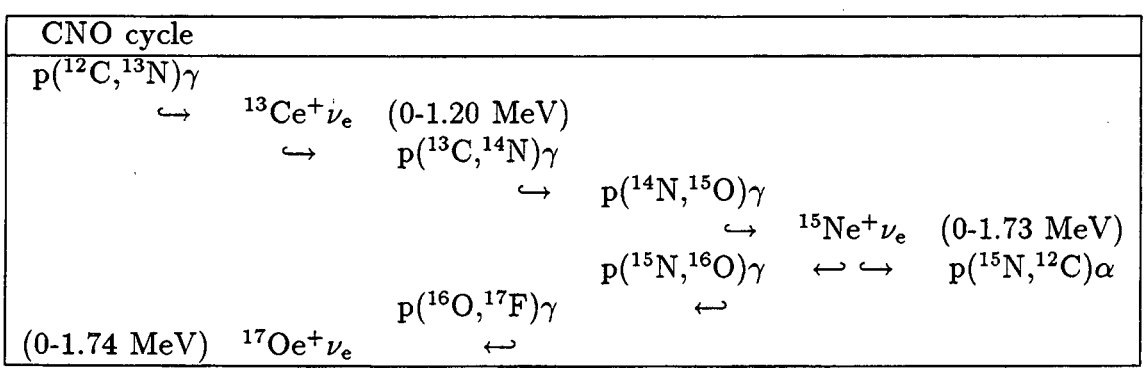

The detection of solar neutrinos was made possible for the first time by Davis [39]. In this remarkable experiment, neutrinos are detected at the bottom of a deep mine using a large tank containing 615 tons of C_2Cl_4. The target isotope ^{37}Cl can capture a neutrino, producing a radioactive isotope ^{37}Ar. The Cl experiment was the only solar neutrino experiment for about two decades until other solar neutrino detectors recently came on-line. In Table 2, I summarize most of reactions used in experimental detection including radiochemical technique, geochemical method, and real-time scattering experiment. Note the thresholds for each reaction are different from one experiment to another (also shown in Fig. 1).

For the Cl experiment, the predicted capture rate of solar neutrinos is shown in Fig. 2 as a function of time of publication [12]. The ^8B (+ ^7Be) neutrino flux observed by Davis

[12]Before one starts fitting the time variation of the predicted capture rate, one should read Bahcall's explanation in Ref. [3] first.

Table 2: Summary of some reactions used or to be used in the detection of neutrinos.

Detection Technique	Reaction	Threshold (MeV)	Sensitive Neutrinos	Group
Radiochemical	$^{37}Cl+\nu_e \rightarrow ^{37}Ar+e^-$	0.814	^8B (^7Be)	Homestake
	$^{71}Ga+\nu_e \rightarrow ^{71}Ge+e^-$	0.233	pp (^7Be)	GALLEX/SAGE
	$^7Li+\nu_e \rightarrow ^7Be+e^-$	0.862	pep	
	$^{81}Br+\nu_e \rightarrow ^{81}Kr+e^-$	0.470	all except pp	U Penn
	$^{127}I+\nu_e \rightarrow ^{127}Xe+e^-$	0.789	^7Be + ^8B	
Geochemical	$^{98}Mo+\nu_e \rightarrow ^{98}Tc^*+e^-$	1.68	^8B	Los Alamos
	$^{205}Tl+\nu_e \rightarrow ^{205}Pb+e^-$	0.054	pp	Alchar mine
Scattering	$\nu_e+e \rightarrow \nu_e'+e'$	~ 5	^8B (hep)	Kamiokande
				LVD
				ICARUS
				SUNLAB
		0.25	^7Be	BOREXINO
	$\nu_e + ^2H \rightarrow p + p + e^-$	~ 5	^8B (hep)	SNO
	$\nu_x + ^2H \rightarrow p + n + \nu_x$	~ 5	^8B (hep)	SNO
	$\nu_x + ^{40}Ar \rightarrow e^- + ^{40}K^*$	~ 5.885	^8B (hep)	ICARUS
	$^{115}In+\nu_e \rightarrow ^{115}Sn^*+e^-$	0.119	pp (^7Be)	European
	$^{11}B+\nu_e \rightarrow ^{11}B+\nu_e$	$4-5$	^8B	BOREX
	$^{11}B+\nu_e \rightarrow ^{12}C+e^-$	$4.5-5$	^8B	BOREX
	$^{19}F+\nu_e \rightarrow ^{12}Ne+e^-$	3.238	^8B	

is shown in Fig. 3 as a function of time[13]. We find that the observed neutrino flux is only $1/3 - 1/2$ of that expected. This is the long standing solar neutrino deficit problem.

This deficit is confirmed by the observation of solar ^8B neutrinos by Kamiokande. This scattering experiment is crucial to establish the case unambiguously with additional information such as timing, directionality (via the directionality of recoil electrons), and spectral sensitivity.

Two experiments using ^{71}Ga (GALLEX and SAGE), with its low threshold (0.233 MeV), are able to provide the first observational information about the dominated pp neutrinos ($E_{pp} < 0.42$ MeV). The pp neutrinos are believed to provide a critical test of explanations of the solar neutrino problem because the prediction of Ga has the highest reliability and the smallest error among all neutrino detection schemes. The reported results from both GALLEX and SAGE are summarized in Fig. 4. In Table 3, I collect all the published solar neutrino results.

[13]Is there any time variation or is there any anti-correlation between the neutrino flux and solar activity? The statistics are not enough to draw a convincing conclusion at present.

Table 3: The solar neutrino flux observations from four experiments now running.

Experiment	Principal Source	I_{exp}/I_{cal}	Ref.
Homestake	$^7B + ^8Be$	0.32 ± 0.03	[40]
Kamiokande	$^7B + ^8Be$	0.51 ± 0.07	[41]
GALLEX	pp	0.60 ± 0.09	[42]
SAGE	pp	0.54 ± 0.09	[43]

The deficit established by these four experiments implies two possibilities. One would be that the solar model is in question. Bahcall has examined a long list of possibilities and found each of these possibilities has its own problem and is constrained by other observations[14]. The other possibility would be that something is new in the physics of neutrinos. Again, one can have a long list of possibilities, but the most promising one is the neutrino oscillation in matter (the MSW effect). In fact, the results of all the experiments can be explained if either ν_ν or ν_τ has a mass of about 3×10^{-3} eV and has a small amount of mixing with a lighter ν_e. In this case, the ν_e produced at the center of the Sun are transformed (with a transformation probability that depends on the energy of ν_e) into ν_μ or ν_τ as they pass through the material medium of the Sun. Fig. 5 shows the allowed region in parameter space of Δm^2 vs $\sin^2(2\theta)$.

To summarize, four separate experiments to detect neutrinos from the Sun have now established a deficit in the flux relative to the prediction of the combination of standard theories of nuclear physics and the knowledge of the Sun. Among various explanations, the MSW effect is favored. Only future experiments can determine if this is indeed the correct explanation. A network of neutrino detectors around the world as shown in Fig. 6 is being established. New techniques for the next generation neutrino detectors are being developed. The Sudbury Neutrino Observatory (SNO), now under construction, will measure neutrino interactions via both $\nu_e + {}^2H \rightarrow p + p + e^-$ and $\nu_x + {}^2H \rightarrow p + n + \nu_x$. Note that the first reaction is sensitive to both the neutral current and the charged current, whereas the second one is sensitive only to the neutral current. This experiment will be able to identify signatures of new physics, independent of solar models and solar physics. Superkamiokande will, beginning in 1996, provide new data with an increase in neutrino-electron scattering event rate of a factor of 30. The change in the shape of the neutrino energy spectrum predicted by the MSW effect may be observable in this experiment via the spectrum of recoil energies of the scattered electrons. Both SNO and Superkamiokande detect only those neutrinos with energies above 5 MeV. Borex will observe intense flux of low-energy neutrinos via capture on ^{11}B.

[14]See Bahcall [3] for his definition of 3σ in the standard solar model prediction and his 1000 Monte-Carlo solar models.

Table 4: Some of physics constraints on neutrino properties obtained from SN1987A.

Physics	Limit	Comment
ν_e mass	$m_{\nu_e} \leq 25$ eV	Impressive limit
ν charge	$Q_\nu \leq 10^{-17}\|e\|$	Best limit
ν_e lifetime	$\gamma\tau \geq 1.6 \times 10^5$ yr	Rules out ν_e decay as solar ν solution
ν magnetic moment	$\mu_\nu \leq 10^{-12}\mu_B$	Best limit
Number of flavors	$N_\nu \leq 7$	Independent of nucleosynthesis argument

4.2 Supernova Neutrinos: What We Have Learned?

The Sun is not special in the sense that it is just one of the main sequence stars at its middle age. Other astrophysical sources of neutrinos are also accessible to us. However, the flux at the Earth is proportional to d^{-2}, where d is the distance between the source and the Earth. To detect neutrinos from a distant source, its luminosity needs to be high enough, which may momentarily be true in the case of a supernova in our own Galaxy.

Supernova neutrinos provide information not only on the physical processes in stellar collapse but also on the fundamental properties of neutrinos. SN1987A, the optically bright supernova, $d \sim 50$ kpc away from us in the Large Magellanic Cloud, is the only supernova from which neutrinos have been detected so far.

It is really amusing that 20 or so flashes of Čerenkov light in two arrays of photomultipliers (IMB and Kamiokande)[15] which lasted 10 seconds or so provided us a great deal of information. For this reason, I want to review the subject briefly.

A large number of papers [44] have appeared analyzing the observed events from SN1987A after the reports from Kamiokande [45] and IMB [46]. It was the first time that we were be able to check basic theories connecting stellar evolution, core collapse, and explosion process. The results are in satisfactory agreement with the conventional notions of a standard stellar collapse. We also learned about neutrino properties that would otherwise have been impossible. For example, based on the Kamiokande and IMB data, we obtained upper limit on the neutrino mass, charge, lifetime, magnetic moment, and the number of flavors. I collect these constraints and comment on each in Table 4.

We note some of the constraints are the best to date and otherwise unaccessible. Some of the constraints are no better than those obtained from current terrestrial experiments. However, the detection of a future collapse in our Galaxy might enable us to make significant improvements in limits such as neutrino mass of cosmological significance.

Supernova rate in our Galaxy is estimated to be $1 - 2$ per century, a too low rate to

[15]The Mt. Blanc UNO scintillation experiment [47] observed a cluster of five events in 7 second, but strangely enough the time of occurrence was about 5 hours earlier than that observed by Kamiokande and IMB. This anomaly still remains a mystery. The Baksan liquid scintillation telescope [49] also observed 5 events. But the initially reported time of the burst disagreed with the times observed in Kamiokande and IMB [48].

guarantee detection in our lifetime[16]. The extra-galactic supernova rate is estimated to be ~ 1 per year at 1-2 Mpc. This is a lot. But the flux we can detect at the Earth is proportional to d^{-2}. The neutrino events detectable are few for distant supernovae. Detection of neutrinos from either galactic or extra-galactic supernovae seems to be difficult.

4.3 Atmospheric Neutrinos: Anomaly?

Extensive air showers of particle production have been studied for a long time. The hadronic cascade production of neutrinos by cosmic ray protons or nuclei in the atmosphere is expected dominantly via:

$$\begin{aligned} p/A + \text{Air} \rightarrow X + \pi^{\pm} & \\ \hookrightarrow \quad \nu_\mu(\overline{\nu}_\mu) + \mu^{\pm} & \\ \hookrightarrow \quad e^{\pm} + \nu_e(\overline{\nu}_e) + \overline{\nu}_\mu(\nu_\mu) & \end{aligned}$$

At ground level, a shower contains various types of particles. Deep underground, however, nothing remains but the most penetrating component – energetic muons and almost all of the neutrinos. Underground detectors such as Kamiokande and IMB are capable of detecting neutrinos through the Čerenkov light generated by muons and electrons produced in interactions of neutrinos.

Irrespective of the complicated details, unimpeachable particle theory dictates that these hadronic showers produce, on average, twice as many $\nu_\mu' s$ as $\nu_e' s$. This can be seen from the above reactions in the zero-*th* order of approximation. The detailed calculation is very complicated and leaves wiggle room for a few percent departure from: $N_{\nu_e} \sim N_{\overline{\nu}_e} \sim N_{\nu_\mu}/2 \sim N_{\overline{\nu}_\mu}/2$. Monte-Carlo simulation is indispensably used, as the cascade is so complicated that analytic approach does not seem to apply. Even with a Monte-Carlo, the absolute flux of neutrinos cannot be correctly predicted. It is so because Monte-Carlo calculation involves uncertainties associated with the knowledge of low energy nuclear interactions, geomagnetic field cutoff, etc. Since the experimental detection makes a distinction between flavor states ($\nu_e/\overline{\nu}_e$ and $\nu_\mu/\overline{\nu}_\mu$) rather than between charge conjugate states (ν_e and $\overline{\nu}_e$, or ν_μ and $\overline{\nu}_\mu$), one calculates $R_{\rm MC} = (N_{\nu_\mu} + N_{\overline{\nu}_\mu})/(N_{\nu_e} + N_{\overline{\nu}_e})$ and compares with experimental data $R_{\rm exp}$. It has became a common practice that one examines the ratio of ratios: $\mathcal{R} \equiv R_{\rm exp}/R_{\rm MC}$[17]. I list $\mathcal{R}$ reported by several groups in Table 5.

The IMB collaboration [51] reported $\mathcal{R} = 0.54 \pm 0.05 \pm 0.07$ for its low-energy data. The Kamiokande collaboration [50] found the ratio $\mathcal{R} = 0.60 \pm 0.07$ for the sub-GeV data and $\mathcal{R} = 0.57 \pm 0.10$ for the higher-energy data. Data from Fréjus and Nusex seem to be consistent with the conventional theory. Recent data from the Soudan [54] and MACRO collaborations [55] support such an atmospheric neutrino anomaly.

[16]The detection of neutrinos from SN1987A by Kamiokande and IBM was an unexpected reward to these two groups with the original goal of looking for proton decay.

[17]This ratio of ratios is introduced to take account of detector idiosyncrasies as well as cancelling out much of the uncertainty due to flux normalization and shower phenomenology. This, in my opinion, is not a valid argument.

Table 5: Summary of $\mathcal{R}$ measured for contained neutrino events in various detectors.

Experiment	Scale (kton yr)	$\mathcal{R}$	Ref.
Kamiokande	6.10	$0.69 \pm 0.07 \pm 0.05$	[50]
IMB-3	7.70	$0.54 \pm 0.05 \pm 0.07$	[51]
Frejus	1.56	$0.87 \pm 0.16 \pm --$	[52]
Nusex	0.40	$0.99 \pm 0.29 \pm --$	[53]
Soudan 2	1.01	$0.64 \pm 0.17 \pm 0.09$	[54]

In the absence of neutrino oscillations or other new physics, $\mathcal{R}$ should be close to unity. This anomaly might be an indication of neutrino oscillations. However, I would like to point out that such low values of $\mathcal{R}$ by themselves do not necessarily imply a disappearance of ν_μ's. They might alternatively be pointing to an excess of electron or positron tracks in the detector.

The angular dependence of the high energy data from Kamiokande seems to add intriguing evidence in favor of neutrino oscillation [50]. In Fig. 7, I reproduce the zenith angle dependence of $\mathcal{R}$ for sub-GeV events. Note the apparent departure from isotropy at higher energies. The data can be fitted by a calculation assuming neutrino oscillation as shown in Fig. 8. For oscillations between ν_e and ν_μ, the fit yields $\Delta m^2 = 0.01$ eV^2 and a mixing $\sin\theta \sim 1$. For oscillations between ν_μ and ν_τ, an equally good fit is also obtained.

In conclusion, the atmospheric neutrino data seem to exhibit an anomaly. However, the case is still far from overwhelming. Moreover, the results depend primarily on the technique. Furthermore, phenomenological predictions of the fluxes are not in agreement as to whether the reported effect represents an excess of electrons or a deficit of muons. If the anomaly is indeed real and it is due to deficit in the number of observed muon neutrinos, as indicated by the angular dependence data, then the most likely explanation would be neutrino oscillations.

5 Discussions and Conclusions

5.1 A Consistent Picture?

In conclusion, there are "significant"[18] hints for a non-zero neutrino mass from the solar neutrino, atmospheric neutrino, and LSND experiment.

Do we have a consistent overall picture about neutrino mass and oscillation that fits all observations from solar and atmospheric neutrino studies? This is the goal of a dozen recent papers [56]. The basic argument is the following.

The solar neutrino suggests $\Delta m^2_{\nu_e\nu_x} \simeq 7 \times 10^{-6}$ eV^2 and $\sin^2(2\theta_{\nu_e\nu_x}) \simeq 5 \times 10^{-3}$. The atmospheric neutrino suggests $\Delta m^2_{\nu_\mu\nu_y} \simeq 2 \times 10^{-2}$ eV^2 and $\sin^2(2\theta_{\nu_\mu\nu_y}) \simeq 1$. The simplest

[18]How significant is the signal? It is extremely difficult to estimate the σ level based on present data.

scenario, which is in agreement with the finding that there are only three generations of neutrinos, would be $m_{\nu_e} \neq m_{\nu_\mu} \neq m_{\nu_\tau} \neq 0$. In particular, a configuration like $m_{\nu_e} \leq 10^{-6\sim-8}$ eV, $m_{\nu_\mu} \simeq 10^{-3}$ eV, and $m_{\nu_\tau} \simeq 10^{-1}$ eV, with small mixing between ν_e and ν_μ and large mixing between ν_μ and ν_τ, would be acceptable. Shown in Fig. 9 is the oscillation probability as a function of L/E for all the available experimental data. More sophisticated scenarios may involve a sterile neutrino[19].

Do we still have a consistent picture when we take the new LSND results into account? In this case, we have to consider one sterile neutrino in order to get a consistent pattern. Again, the solar neutrino result gives $\Delta m^2_{\nu_e\nu_x} \sim 10^{-5}$ eV^2 with a small mixing. The atmospheric neutrino result gives $\Delta m^2_{\nu_\mu\nu_y} \sim 10^{-2}$ eV^2 with a large mixing. A reactor experiment probably excludes $y = \nu_e$ with a large mixing, so atmospheric neutrino result indicates $\nu_\mu \leftrightarrow \nu_\tau$. The LSND claim suggests $\Delta m^2_{\nu_\mu\nu_e} \sim 10$ eV^2 with a small mixing and excludes $x = \nu_\mu$ in solar neutrino. So solar neutrino result gives $\nu_e \leftrightarrow \nu_s$.

Therefore, the simplest (but not beautiful in my opinion) pattern that is consistent with all the above is: $m_{\nu_\mu} \sim m_{\nu_\tau} \sim 2.4$ eV with a splitting of 10^{-2} eV, and $m_{\nu_e} \sim m_{\nu_s} \sim 3 \times 10^{-3}$ eV with a splitting of 10^{-6} eV. The mixing between ν_μ and ν_τ is large ($\sim 10^{-2}$) and the mixing between ν_e and ν_s is small (~ 1).

This scenario is particularly favored in a mixed cold + hot dark matter in terms of large scale structure formation, see Primack *et al.* for details [57].

5.2 New Physics Beyond Standard Model?

If we indeed find $m_\nu \neq 0$, so what? A non-zero neutrino mass would be of great significance in astrophysics, cosmology, and particle theory. In astrophysics, a neutrino mass as small as $\sim 10^{-2}$ eV would be sufficient to solve the solar neutrino problem if the MSW mechanism works. In cosmology, neutrinos with $\sum m_{\nu_i} \sim 25$ eV would be enough to constitute dark matter and to close the Universe. In the standard model of particle theory we have today, we know how to treat neutrino interactions if neutrino mass is zero. But questions such as why a neutrino has a vanishing mass cannot be answered within the framework of standard model. If neutrinos do have a non-vanishing small mass, however, we have at least one attractive explanation, going beyond the standard model. The explanation involves the grand unification mass scale. A typical value for the mass at which the strong and electromagnetic interactions are united is estimated to be $M_{\rm GUT} \sim 10^{15}$ GeV. The mass scale at which the weak and electromagnetic interactions are united is $M_{\rm EW} \sim 10^2$ GeV, which is much smaller than $M_{\rm GUT}$. Thus one can form dimensionally a small mass by considering $M^2_{\rm EW}/M_{\rm GUT} \sim 10^{-2}$ eV. An expression of exactly this form is embodied in the see-saw mechanism. The mass of a neutrino is related to the square of the mass of its associated quark or lepton:

$$m_{\nu_i} \cong \frac{m^2_{q_i}}{M_{\rm GUT}} \sim \frac{m_{l_i}}{M_{\rm GUT}}. \tag{36}$$

[19]A sterile neutrino does not contribute to the Z^o width, so it has not been ruled out yet.

Inserting $m_{q_i} \sim 100$ GeV for the heavest quark, one gets $m_{\nu_i} \sim 10^{-2}$ eV, about what is needed for the MSW effect to work effectively in the Sun.

The study of astrophysical neutrinos has been an example of attacking fundamental physics at microscopic scale ("point-like" ν) by studying stellar phenomena at cosmic scale! One would also be amused by the possibility that by studying physics at such a low energy scale would provide information about energies on the scale of the grand unification mass, 10^{15} GeV.

5.3 Future Perspectives

We definitely need more data for which there is no substitute. Uncertainties and unambiguities are key issues in neutrino experiments. It is essential not to rely upon just a few data points from one single experiment, because the history of science has shown that systematic uncertainties can sometimes lead to mistaken conclusions. This is particularly important when the measurements are as intrinsically difficult as they appear to be for neutrino experiments. Therefore, to establish a new physics and eventually understand the fundamentals involving in neutrino physics, it is indispensable to have several independent experiments using different techniques. There is much to be done to comfortably establish the MSW effect and to discover new physics beyond the standard model.

There are a dozen solar neutrino experiments in various stages of planning and operation around the world now, aiming primarily at resolving solar neutrino puzzle. Some experiments have the promise to provide information on the spectral shape which is especially crucial to establish the MSW effect (and to discriminate between alternative classes of explanation). Moreover, with data from detectors of different thresholds, one will be able to map out neutrino fluxes from various production reactions.

As to the atmospheric neutrino case, we certainly need improved data (and improved Monte-Carlo too!) in order to establish whether there is really an anomaly. Planned experiments such as Superkamiokande will provide more data with much higher statistics. However, I want to point out that cosmic ray cascade is not a very suitable neutrino source for oscillation testing. Ideally, one wants to start with an intense, well-characterized neutrino beam of known initial flavor, let it travel a specified distance and then look for any flavor change by directing the beam through a detector designed for the purpose.

Such experiments are planned. Using a 25 GeV ν_μ beam from the Super Proton Synchrotron, CHORUS will search for decay products of the heavy, short-lived τ leptons from ν_τ interactions 600 meters downstream. Almost a ton of photographic emulsion will be used to look for telltale track kinks a few hundred microns from neutrino collision vertices. Another interesting approach is to direct neutrino beams from accelerator facilities to large scale neutrino detectors through a long distance travel across the Earth. The beam energy and the distance between neutrino source and detectors determine what regions of the oscillation parameter space an experiment can probe.

Finally, let me point out that neutrino astronomy can provide a unique window by means of which one can see into the deepest interiors of stars and galaxies otherwise unaccessible. So far the only astrophysical neutrinos we have detected are from the Sun

and SN1987A. Much more is definitely expected at even higher energies as I will cover in my next lecture.

Acknowledgements

I am grateful to Prof. Stuart Freedman, Prof. Buford Price, and Guangjun Wang for reading the manuscript and making useful comments.

References

[1] K. Winter, *Neutrino Physics*, (Cambridge University Press, 1991).

[2] C. Sutton, *Spaceship Neutrino* (Cambridge University Press, 1992).

[3] J. N. Bahcall, *Neutrino Astrophysics*, (Cambridge University Press, 1989)

[4] W. Pauli, in a letter to L. Meitner *et al.*, in *Collected Scientific Papers by Wolfgang Pauli* (Wiley Interscience, New York, 1964), Vol. 2, ed. R. Kronig and V. F. Weisskopf, p. 1316.

[5] N. Bohr, in a letter to R. H. Fowler, in *Neils Bohr - Collected Works* (North-Holland, Amsterdam, 1986), Vol. 9, ed. R. Peirels, p. 555 and J. Chem. Soc. 349 (1932).

[6] E. Fermi, La Ricerca Scientifica 2 No 12 (1933); Z. Phys. **88**, 161 (1934).

[7] T. D. Lee and C. N. Yang, Phys. Rev. **104**, 254 (1956).

[8] C. S. Wu *et al.*, Phys. Rev. **105**, 1413 (1957).

[9] K. C. Wang, Phys. Rev. **62**, 92 (1942).

[10] H. R. Crane, Rev. Mod. Phys. **20**, 195 (1948).

[11] G. W. Rodeback and J. S. Allen, Phys. Rev. **86**, 446 (1952).

[12] B. Pontecorvo, Report PP-205 of the National Research Council of Canada, Division of Atomic Energy (1946).

[13] H. A. Bethe, Phys. Rev. **55**, 434 (1939).

[14] F. Reines, in *Discovery of the Neutrino*, (World Scientific, Singapore, 1993), ed. C. E. Lane and R. I. Steinberg, p. 166.

[15] F. Reines and C. L. Cowan Jr., Nature **178**, 446 (1956); C. L. Cowan *et al.*, Science **124**, 103 (1956); F. Reines and C. L. Cowan Jr., Phys. Rev. **113**, 273 (1959).

[16] M. Schwartz, Phys. Rev. Lett. **4**, 306 (1960).

[17] B. Pontecorvo, JETP **37**, 1236 (1960).

[18] G. Danby *et al.*, Phys. Rev. Lett. **9**, 36 (1962).

[19] M. M. Block *et al.*, Phys. Lett. **12**, 281 (1964); J. K. Bienlein *et al.*, Phys. Lett. **13**, 80 (1964); C. Bernardini *et al.*, Phys. Lett. **13**, 86 (1964); F. J. Hasert *et al.*, Phys. Lett. B **46**, 121 (1973).

[20] M. Gell-Mann, P. Ramond, and R. Slansky, in *Supergravity: Proc. Supergravity Workshop*, Stony Brook, ed. P. Van Nieuwenhuizen and D. Z. Freedman (Amsterdam: North-Holland), p. 315.

[21] W. H. Furry, Phys. Rev. **56**, 1184 (1939).

[22] For a review on double β decay, see M. K. Moe, Nucl. Phys. B (Proc. Suppl.) **19**, 158 (1991); and D. O. Caldwell, in *Neutrino Physics*, (Cambridge University, 1991), ed. K. Winter, p. 125.

[23] B. Pontecorvo, JETP **6**, 429 (1958).

[24] Z. Maki, M. Nakagawa, and S. Sakata, Prog. Theor. Phys. **28**, 870 (1962).

[25] S. P. Mikheyev and A. Yu. Smirnov, Sov. J. Nucl. Phys. **42**, 913 (1985).

[26] L. Wolfenstein, Phys. Rev. D **17**, 2369 (1978); and **20**, 2634 (1979).

[27] Particle Data Group, Phys. Rev. **50**, 1173 (1994).

[28] R. G. H. Robertson and D. A. Knapp, Ann. Rev. Nucl. Part. Sci. **38**, 185 (1988); and R. G. H. Robertson, in *Discovery of the Neutrino*, (World Scientific, Singapore, 1993), ed. C. E. Lane and R. I. Steinberg, p. 69.

[29] W. Kündig, E. Holzschuh, M. Frutschi, and H. Stüssi, in *Neutrino Physics*, (Cambridge University, 1991), ed. K. Winter, p. 144.

[30] J. J. Simpson, Phys. Rev. Lett. **54**, 1891 (1985).

[31] See, for example, A. Hime, Mod. Phys. Lett. A **7**, 1301 (1992) and references therein.

[32] J. L. Mortara *et al.*, Phys. Rev. Lett. **70**, 394 (1993).

[33] H. Abele *et al.*, Phys. Lett. B **316**, 26 (1993).

[34] T. Oshima, Phys. Rev. D **47**, 4840 (1993).

[35] A. Franklin, Rev. Mod. Phys. **67**, 457 (1995).

[36] F. E. Wietfeldt and E. B. Norman, Preprint LBL-37044 (1995) (submitted to Phys. Rep.).

[37] The New York Times, January 31, 1995.

[38] J. N. Bahcall and R. K. Ulrich, Rev. Mod. Phys. **60**, 297 (1988).

[39] R. Davis Jr., Phys. Rev. Lett. **12**, 303 (1964).

[40] R. Davis Jr., in *Frontiers of Neutrino Astrophysics*, ed. Y. Suzuki and K. Nakamura, (University Academy Press, Tokyo, 1993), p. 47; and B. T. Cleveland *et al.*, Nucl. Phys. B (Proc. Suppl.) **38**, 47 (1995).

[41] K. S. Hirata *et al.* Phys. Rev. Lett. **63**, 16 (1989); Y. Suzuki, Nucl. Phys. B (Proc. Suppl.) **38**, 54 (1995).

[42] P. Anselmann *et al.* Phys. Lett. B **285**, 376 (1992); *ibid*, **314**, 445 (1993); P. Anselmann *et al.*, Nucl. Phys. B (Proc. Suppl.) **38**, 68 (1995).

[43] A. I. Abazov *et al.* Phys. Rev. Lett. **67**, 3332 (1991); J. N. Abdurashitov *et al.*, Phys. Lett. B **328**, 234 (1994); J. N. Abdurashitov *et al.*, Nucl. Phys. B (Proc. Suppl.) **38**, 60 (1995).

[44] For a review, see Ref. [3] and references therein.

[45] K. S. Hirata *et al.*, Phys. Rev. Lett. **58**, 1490 (1987).

[46] R. M. Bionta *et al.*, Phys. Rev. Lett. **58**, 1494 (1987).

[47] M. Aglietta *et al.*, Europhys. Lett. **3**, 1315 (1987).

[48] E. N. Alekseev *et al.*, JETP Lett. **45**, 589 (1987).

[49] E. N. Alekseev *et al.*, Phys. Lett. B **205**, 209 (1988).

[50] Y. Fukuda *et al.* (Kamiokande Coll.), Phys. Lett. B **335**, 237 (1994).

[51] R. Becker-Szendy *et al.* (IMB Coll.), Phys. Rev. Lett. **69**, 1010 (1992).

[52] Ch. Berger *et al.* (Frejus Coll.), Phys. Lett. B **227**, 489 (1989).

[53] M. Aglietta *et al.* (NUSEX Coll.), Europhys. Lett. **8**, 611 (1989).

[54] M. C. Goodman *et al.* (Soudan 2 Coll.), Nucl. Phys. B **38**, 337 (1995).

[55] S. Ahlen *et al.* (MACRO Coll.), Phys. Rev. Lett. **72**, 608 (1994).

[56] See, for example, G. L. Fogli, E. Lisi, and D. Montanino, Phys. Rev. D **49**, 3626 (1994) and references therein; P. F. Harrison, D. H. Perkins, and W. G. Scott, Phys. Lett. B **349**, 137 (1995).

[57] J. R. Primack, J. Holtzman, A. Klypin, and D. O. Caldwell, Phys. Rev. Lett. **74**, 2160 (1995).

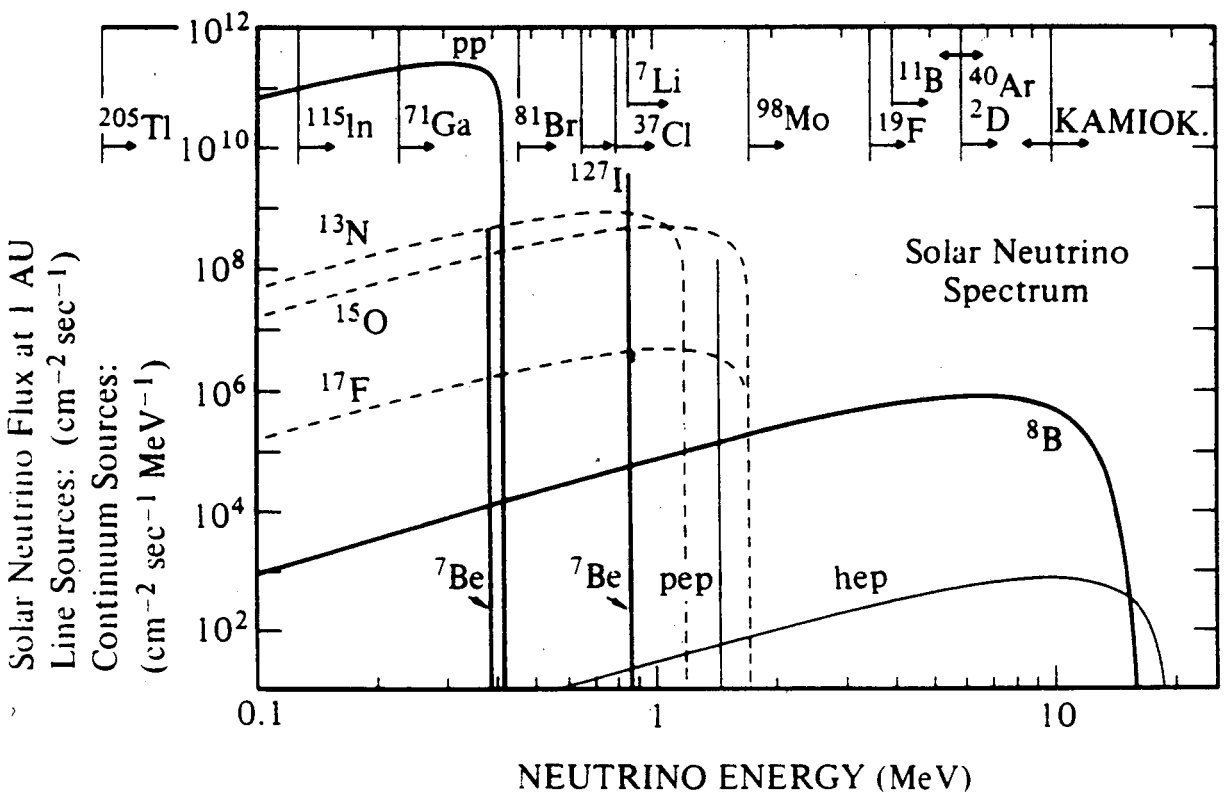

Fig. 1 Energy spectrum of solar neutrinos as calculated from the standard solar model [38]. Energy thresholds for various neutrino detection schemes also shown on the top portion.

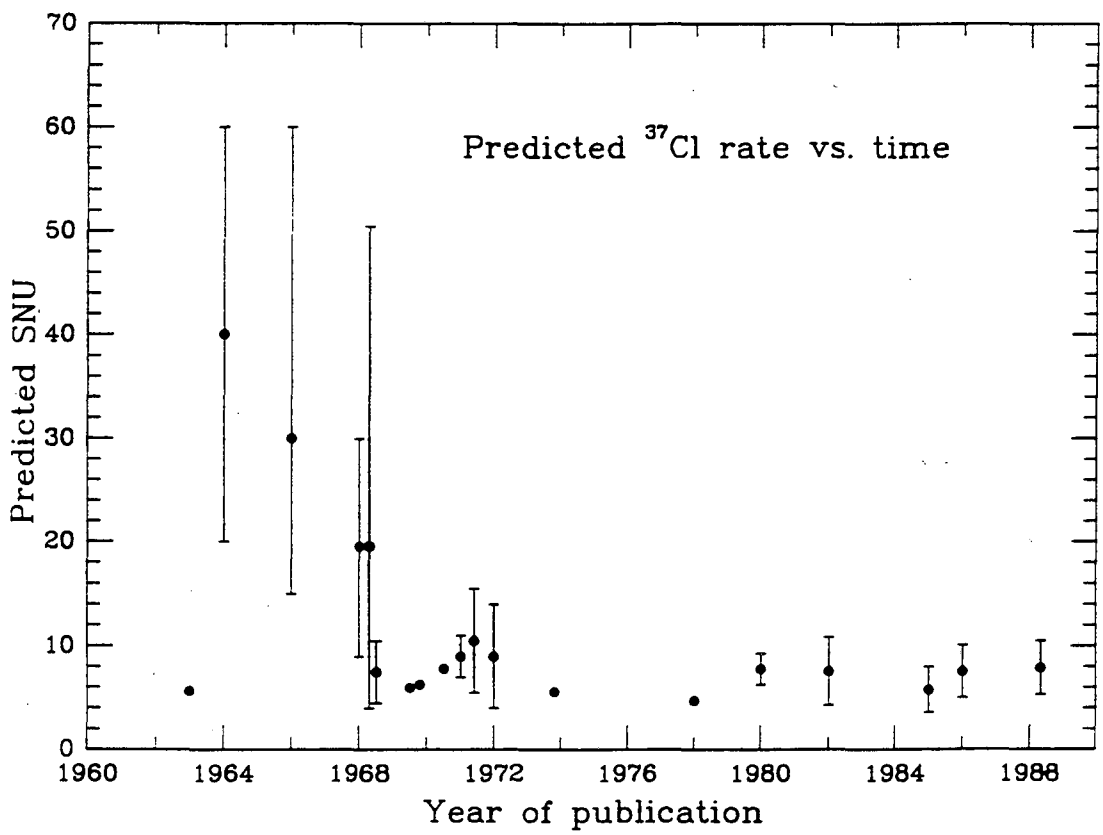

Fig. 2 Predicted capture rates of solar neutrinos in the ^{37}Cl experiment as a function of time of publication. See Ref. [3] for details.

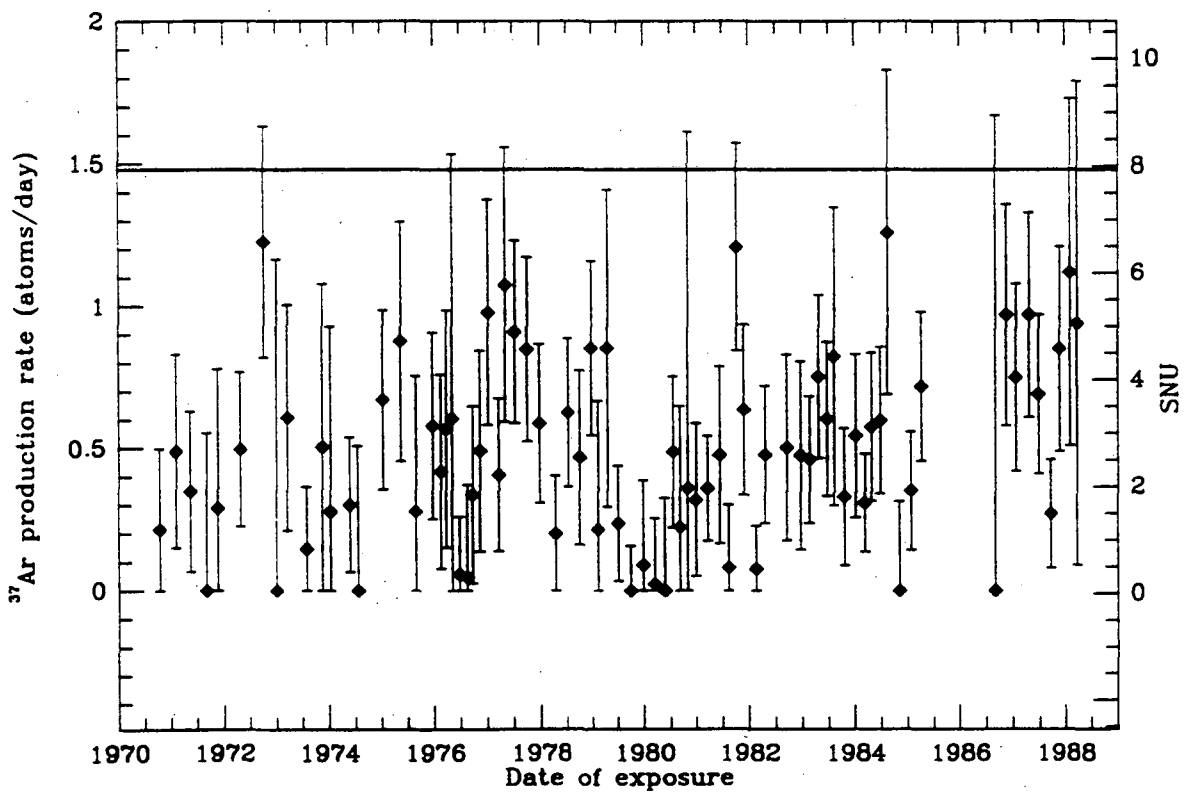

Fig. 3 Observed Ar production rates in the Cl solar neutrino experiment as a function of time. The line at 7.8 SNU represents the prediction of the standard model.

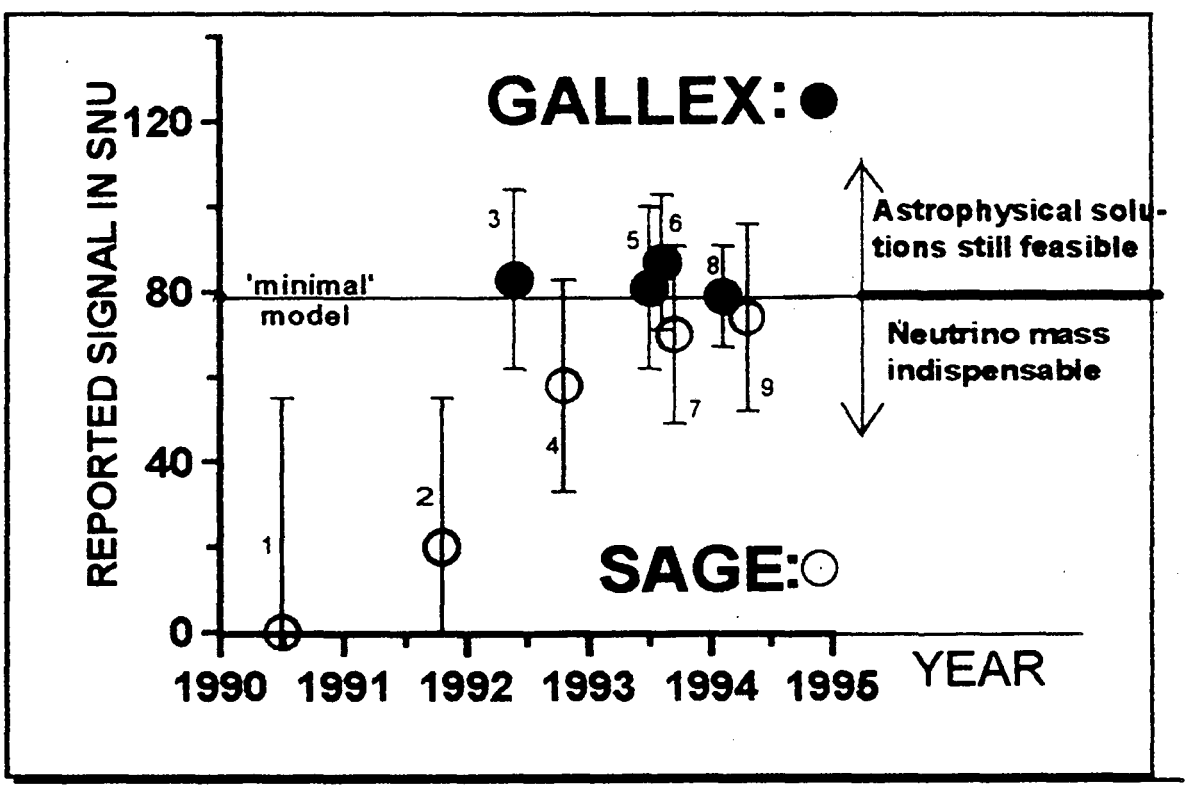

Fig. 4 The neutrino flux from the pp reaction in the Sun measured in the recent two Ga experiments GALLEX and SAGE. See text for details.

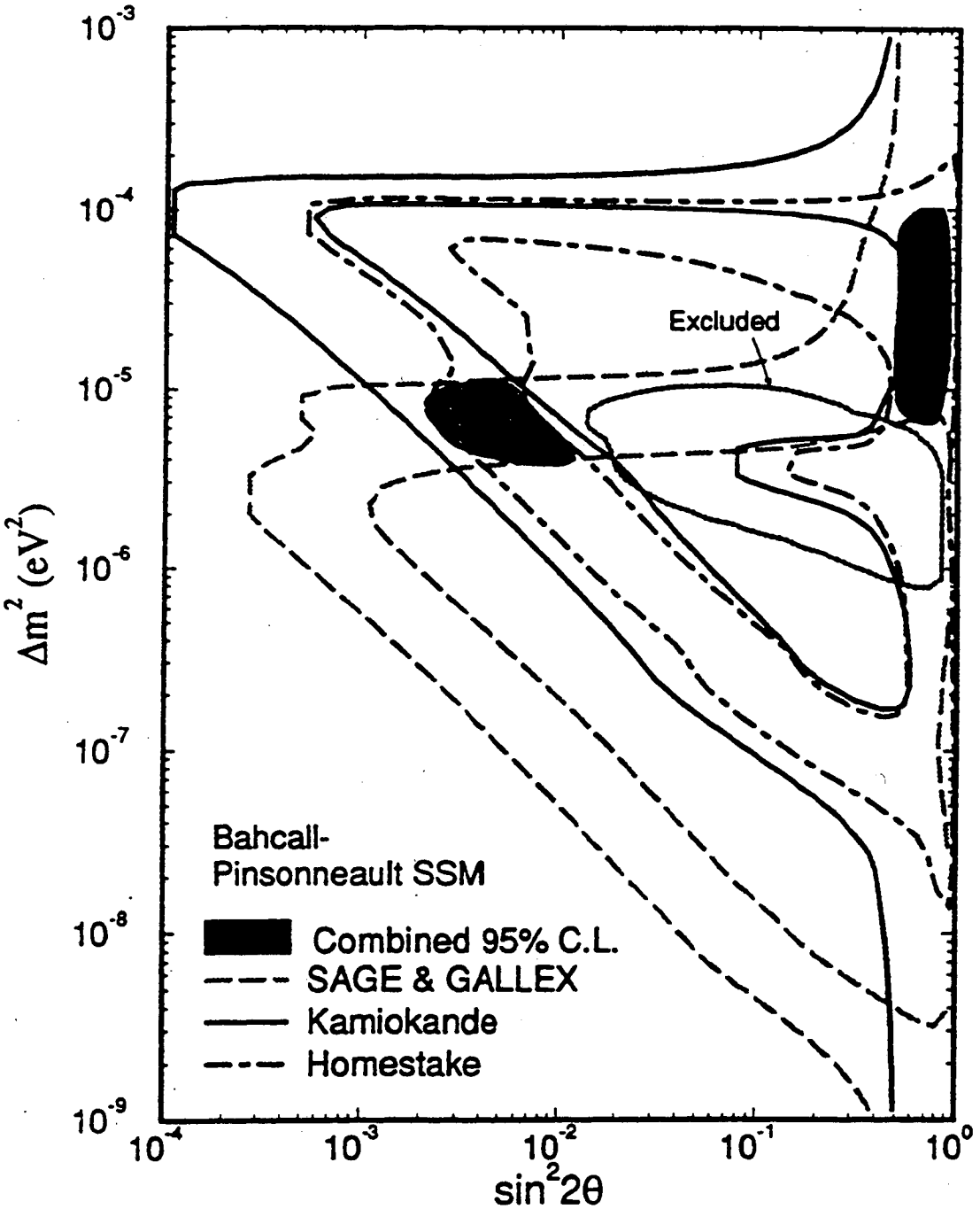

Fig. 5 The allowed regions in the parameter space Δm^2 vs $\sin^2(2\theta)$ derived from four solar neutrino experiments. The overlapped regions allowed by all the data are two black islands.

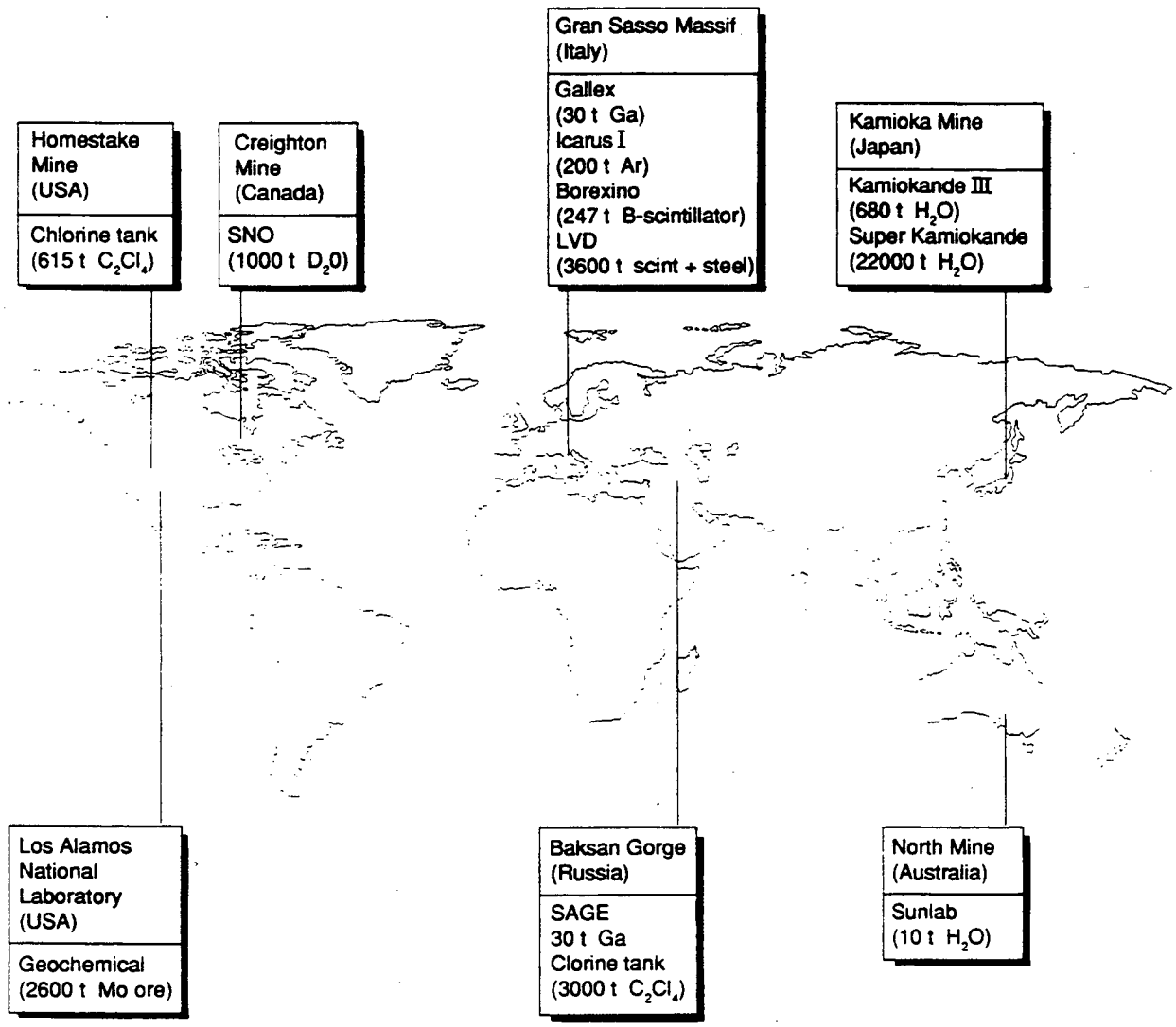

There are now a number of solar neutrino detectors around the world, in various stages from proposals to those that are up and running. This map shows the major detectors that are already built, or being built, at least in prototype form. It indicates the approximate size of the detector in tonnes (t) and the material used to capture the neutrinos. (Ga = gallium; C_2Cl_4 = perchloroethylene; H_2O = water; Ar = argon, B = boron; scint = scintillator; Mo = molybdenum; D_2O = heavy water.)

Fig. 6 A map of major solar neutrino detectors around the world either in the stage of operating or the stage of being built.

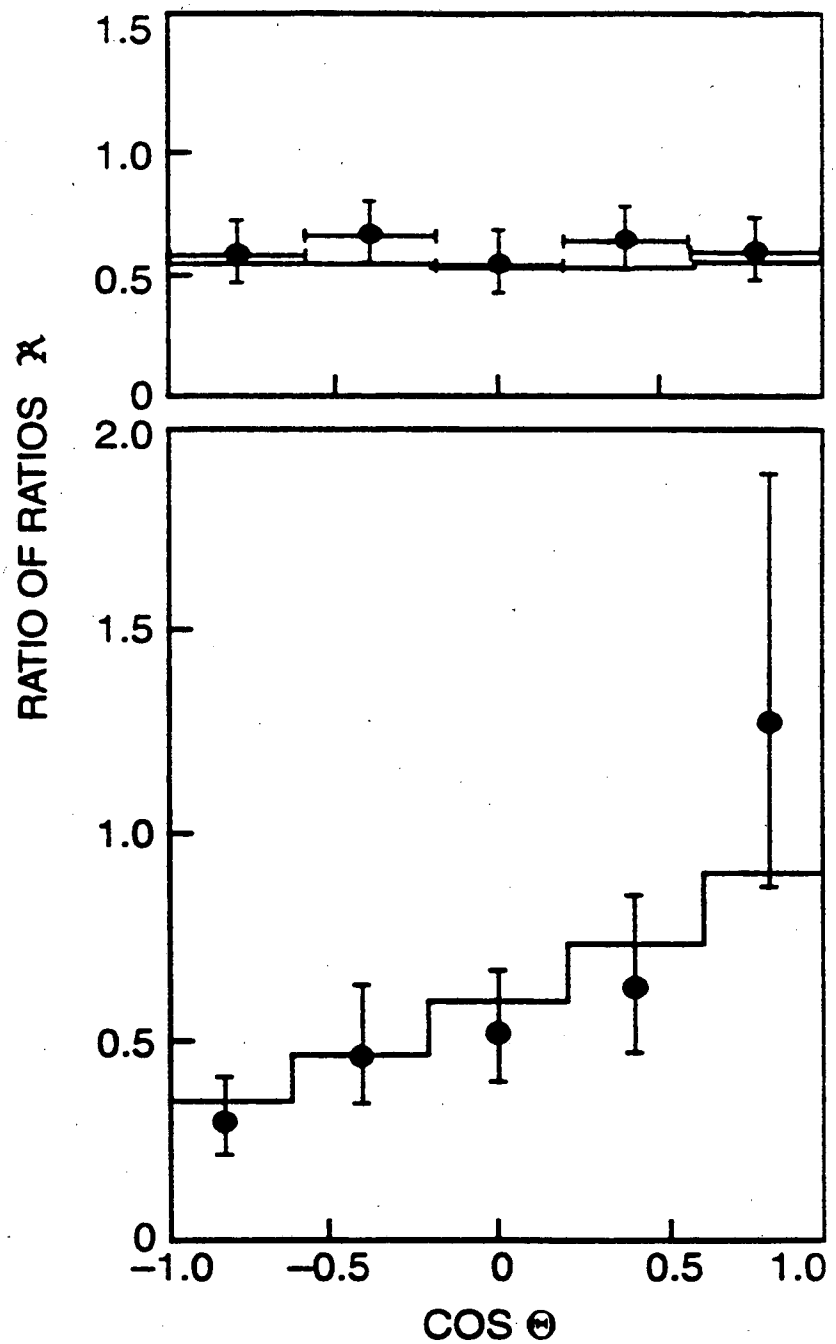

Fig. 7 The ratio of ratios $\mathcal{R}$ as a function of zenith angle for Kamiokande cosmic ray neutrino events with energies less than 1 GeV (top panel) and greater than 1 GeV (bottom panel). Data from Ref. [50].

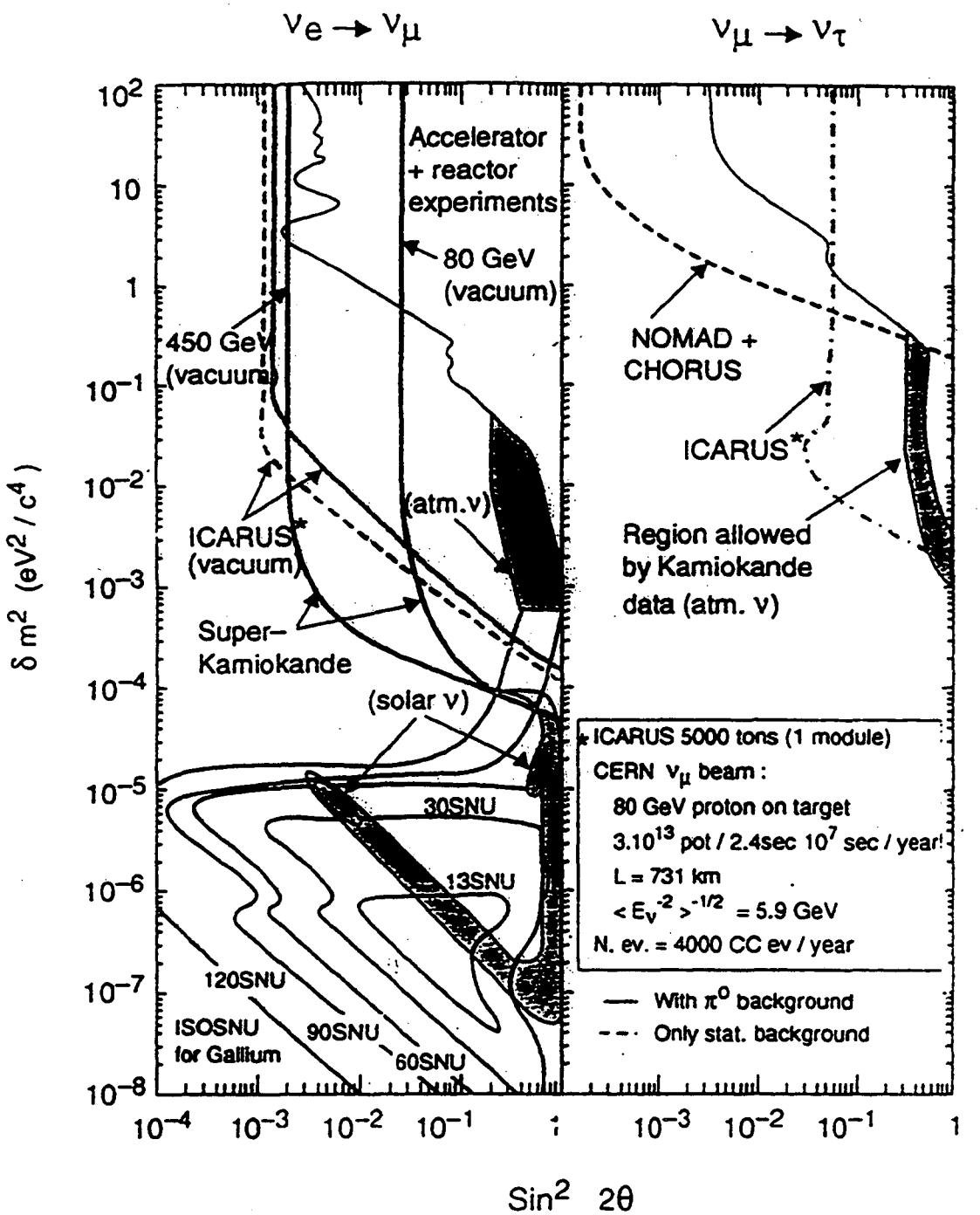

Fig. 8 The exclusive plots of neutrino mixing Δm^2 vs $\sin^2(2\theta)$ obtained from atmospheric neutrino data.

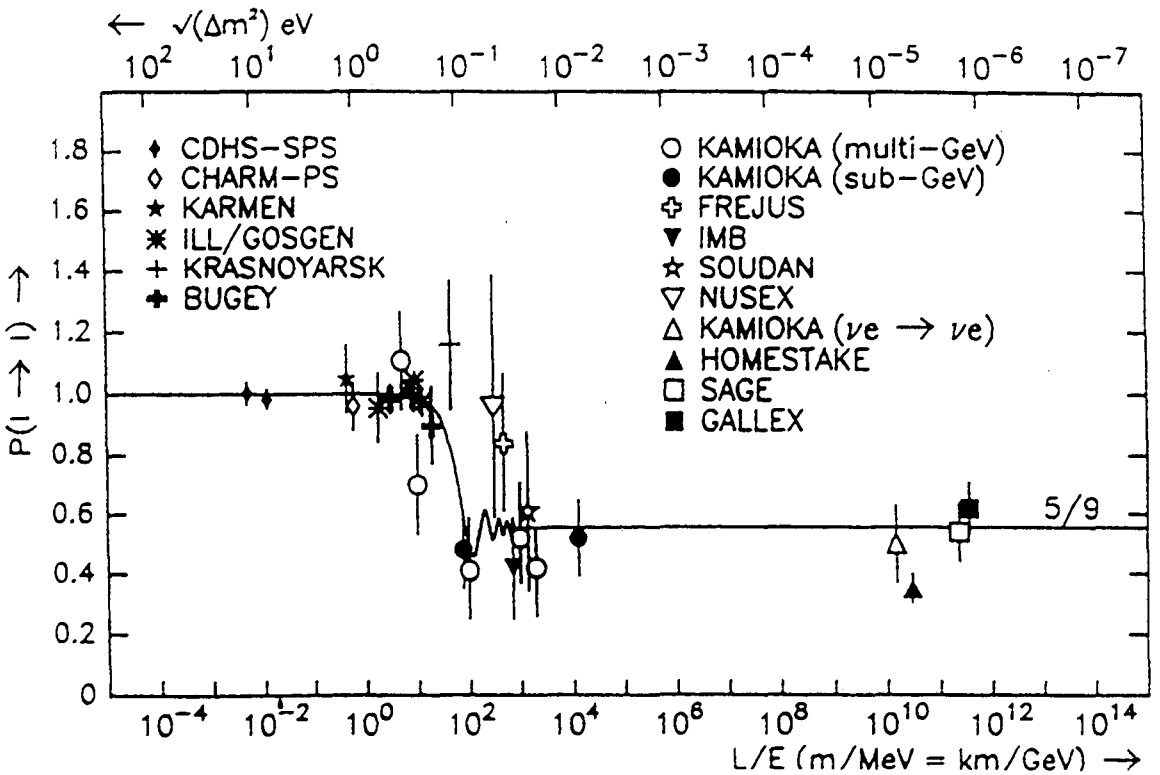

Fig. 9 An overall picture that summarizes most of the neutrino oscillation experiments.

HIGH ENERGY NEUTRINO ASTROPHYSICS[1]

Yudong He[2]
Department of Physics, Space Science Laboratory
and Center for Particle Astrophysics
University of California at Berkeley, Berkeley, CA 94720, USA
and
Institute for Nuclear and Particle Astrophysics
and Nuclear Science Division
Lawrence Berkeley National Laboratory, Berkeley, CA 94720, USA

Abstract

High energy astrophysical neutrinos would provide us with important, otherwise inaccessible information to understand physical processes in various cosmic sites. Detecting high energy neutrinos and mapping the sky in high energy neutrinos require a large scale array of detectors on the order of ~ 1 km^3. With several prototype experiments now underway and future efforts toward a 1 km^3 telescope, the goal is to open this unique window to the Universe. Other interesting investigations that could be carried out with such a telescope include indirect detection of galactic dark matter, study of neutrino oscillation, search for GUT monopoles that catalyze nucleon decay, and earth tomography.

1 Introduction: Neutrino Astrophysics

Doing astronomy by means of neutrinos was realized as early as the time when physicists found that nuclear reactions are responsible for energy generation in stars[3]. Neutrinos from astrophysical sites carry important information otherwise impossible to acquire on the hadronic processes at the source because they can penetrate matter either surrounding the source or on their way to the Earth due to their extremely small interaction cross section. For that very reason, detecting astronomical neutrinos has been found to be an extremely difficult enterprise. For instance, it has taken more than a quarter of century of experimental efforts to catch ~ 1000 solar neutrinos in a detector containing 615 tons of C_2Cl_4 in Homestake mine. The two heroic detectors, KAMIOKANDE and IMB, which contain a fiducial mass of 2140 and 6800 tons water respectively, detected only ~ 20

[1]This topic is one of a series of lectures on "Current Trends in Non-Accelerator Particle Physics" given at CCAST Workshop on Tibet Cosmic Ray Experiment and Related Physics Topics, Beijing, April 4-13, 1995. This work was supported in part by the U. S. Department of Energy under Contract No. DE-AC03-76SF00098.

[2]Mailing address: Department of Physics, University of California, Berkeley, CA 94720, USA. Email address: yudong@physics.berkeley.edu.

[3]Philip Morrison (1962) pointed out in Ref. [1]: "The neutrinos provide ... the only way to penetrate the massive shield of a star's body and see what the center is like ... this message comes constantly to us riding a beam as bright ... as sunlight itself, and yet we cannot detect it at all!"

neutrinos in total from Supernova 1987A. It is important to point out that it is this successful detection of neutrinos from the Sun and from Supernova 1987A that has driven the dream of neutrino astronomy to a reality though it is at its infancy.

It is believed that neutrino astronomy, conceived with the identification of thermonuclear fusion in the Sun and the particle processes controlling the fate of a nearby supernova, will reach outside the galaxy and make measurements relevant to cosmology. Inspired by a somewhat different dream, physicists have been trying to study high energy neutrinos from space. It should be noted that throughout this paper I use *high energy* to refer to an energy range above TeV-PeV which is most accessible experimentally as I will demonstrate later [in cosmic ray physics energy scales at GeV ($\equiv 10^9$ eV), TeV ($\equiv 10^{12}$ eV), PeV ($\equiv 10^{15}$ eV), and EeV ($\equiv 10^{18}$ eV) are traditionally called high energy (HE), very high energy (VHE), ultra high energy (UHE), and extremely high energy (EHE), respectively]. The neutrino, a weakly interacting neutral particle, will allow us to probe cosmic sites shielded from our view of photons of any energy by more than a few hundred grams of intervening matter. Hence, high energy neutrinos could reveal objects with no counterpart in any wavelength of radiation. Fig. 1 shows schematically the concept. Even though photons and protons are produced together with neutrinos at the astrophysical site, only neutrinos can penetrate the intervening matter and be unaffected by interstellar magnetic fields. Through this new and unique window to the Universe, we would hope to be able to discover and study various cosmic sources, to study and solve the long-standing problem of cosmic ray origin and acceleration, and more importantly, to discover and explore new phenomena unanticipated. Therefore, the endeavor is expected to have a great reward.

High energy neutrino astrophysics is now, in my opinion, at the turning point from a field of only theoretical calculations to a branch of experimental science. This will result from the pioneering experimental work of several groups now underway on detector arrays with an effective area of $\sim 10^4$ m^2. Optimistically, there might be some chance to detect a few high energy astrophysical neutrinos per year with these detectors. In some sense, the present generation of detectors will serve as prototype detectors for a future ~ 1 km^3 scale detector array that is required to do real high energy neutrino astronomy. Plans are advancing for an international consortium to propose a ~ 1 km^3 scale detector array. Local working groups have been formed at JPL and LBNL to carry out the effort toward a proposal.

It is not the intention of this paper to give a detailed review on the field of high energy neutrino astrophysics. The references cited in the paper may be far from complete and I apologize in advance for any omission of important work. In this paper, I discuss some general trends in the field by highlighting the most recent development which I think is important. In Section 2, I will briefly review various neutrino sources expected from theory and by doing so provide a solid motivation for high energy neutrino observation. In Section 3, I will discuss experimental techniques to detect high energy astrophysical neutrinos, pointing out a need of ~ 1 km^3 scale detector array based on event rate calculations. In Section 4, I will introduce the current experiments pioneering in the development of prototype detectors at four sites. In Section 5, I will illustrate examples of applications of a large scale detector array to interesting subjects other than astronomy. Finally in

Section 6, I will discuss my personal opinion on future directions.

2 High Energy Neutrino Sources Expected

In this section, I shall review possible high energy neutrino sources expected from theory. Since this subject has been a focus of a dozen recent papers [2] and has been reviewed by others in some detail [3, 4], I will only give a brief introduction, focusing mainly on the luminosity and spectral features of these expected sources. More relevant issues to an experimentalist such as the signal and detectability of these neutrinos in terms of upward going muons will be discussed in some detail in the next section.

2.1 Neutrino Production Mechanism

Let me start with a brief description of the generic production mechanism of high energy neutrinos. In space, as on the Earth (e.g., in the atmosphere), high energy neutrinos are produced in beam dumps consisting of a high energy proton (or nucleus) accelerator and a target (proton or photon) via dominantly:

$$\begin{array}{ccccccccccc} p/A & + & p/\gamma & \longrightarrow & \pi^\circ & + & \pi^+ & + & \pi^- & + & \cdots . \\ & & & & \downarrow & & \downarrow & & \downarrow & & \\ & & & & \gamma+\gamma & & \mu^+ + \nu_\mu & & \mu^- + \overline{\nu}_\mu & & \\ & & & & & & \downarrow & & \downarrow & & \\ & & & & & & e^+ + \nu_e + \overline{\nu}_\mu & & e^- + \overline{\nu}_e + \nu_\mu & & \end{array}$$

To the zero-*th* order of approximation, as many neutrinos of all flavors are produced as photons or three times as many as photons depending on kinematics and target density which determine whether muons decay or not. The production of neutrinos in $p\gamma$ interactions has a threshold requirement that a proton must have energy greater than $E_p \sim 100$ TeV $(E_\gamma/3\,\text{keV})$.

The sites of the cosmic accelerators can be pulsars, black holes, cosmic strings, and other unknown sites, while the target materials can be companion stars, accretion disc, radio cocoon, 3K cosmic photon field and others. I want to emphasize that in efficient cosmic beam dumps with an abundant amount of target material, high energy photons may be absorbed before escaping the source. Therefore, the most spectacular neutrino source may have no counterpart in high energy γ rays.

The cosmic beam dump for binary X-ray sources has been studied in which a collapsed object accelerates beams of particles, perhaps in the high fields of a pulsar or through conversion to the gravitational energy from accretion of matter from the companion star, into a target provided by the accreting matter. The pulsar in a young supernova can accelerate particles into the surrounding shell. A massive black hole can power beams into the dense photon cocoon in a radio galaxy. In all such systems neutral particles, i.e. photons, neutrinos, and neutrons, are emitted in directional beams, while stable charged particles such as protons and electrons leaving the source spiral in galactic or

extra-galactic magnetic fields. Unlike the neutrino flux, the γ-ray is only observed if it has not been attenuated by intervening matter in the source or by the cosmic photon background on its way to the Earth.

How certain is the existence of neutrinos in cosmic ray sources? The argument used frequently is as follows. The cosmic ray spectra we know today extends to $\sim 10^{20}$ eV. Photons and neutrinos are produced by cosmic ray particles interacting with (1) the interstellar medium, (2) the cosmic microwave background, (2) the Sun, and (4) the Earth's atmosphere. It is not difficult to estimate diffuse fluxes of neutrinos as well as γ rays from these beam dumps to within order of magnitude. In Fig. 2, energy spectra of these diffuse neutrinos are summarized in comparison with that of atmospheric neutrinos.

The neutrino energy spectrum dN_ν/dE_ν at the Earth is related to the source luminosity $\mathcal{L}_{\rm p}$ distance d away from us as:

$$\int dE_\nu \left[E_\nu \frac{dN_\nu}{dE_\nu}(E_\nu) \right] = \frac{1}{4\pi d^2} \epsilon_\nu \mathcal{L}_{\rm p}, \tag{1}$$

where ϵ_ν accounts for the fact that only a finite fraction of the proton energy goes into neutrino production. When we take the source proton spectrum as $dN_{\rm p}/dE_{\rm p} \propto E_{\rm p}^{-2}$, the neutrino production spectrum becomes:

$$\frac{dN_\nu}{dE_\nu} = \frac{1}{4\pi d^2} \frac{\epsilon_\nu \mathcal{L}_{\rm p}}{\ln \gamma_{\rm max}} E_\nu^{-2}, \tag{2}$$

where $\gamma_{\rm max} = E_{\rm p}^{\rm max}/E_{\rm p}^{\rm min}$ is the maximum Lorentz factor attained in the accelerator and, under optimal conditions, $\epsilon_\nu = 0.11$, 0.094, 0.042, and 0.029 for ν_μ, $\overline{\nu}_\mu$, $\nu_{\rm e}$, and $\overline{\nu}_{\rm e}$ respectively. Numerically, we have:

$$\frac{dN_\nu}{dE_\nu} \simeq 10^{-10}\ {\rm cm}^{-2}\ {\rm s}^{-1}\ {\rm TeV}^{-1} \left(\frac{d}{10\ {\rm kpc}} \right)^2 \left(\frac{\mathcal{L}_{\rm p}}{10^{38}\ {\rm erg\ s}^{-1}} \right) \left(\frac{E_\nu}{1\ {\rm TeV}} \right)^{-2}. \tag{3}$$

2.2 Neutrinos from Point Sources

Galactic sources are likely emitters of high energy neutrinos. Of particular interest are X-ray binary systems and young supernova remnants. Currently no air shower array has detected steady fluxes from any of the previously reported UHE γ-ray emitters, but X-ray binaries are still primary candidates for cosmic ray acceleration sites up to 10^{18} eV and possible neutrino production sites. X-ray binaries consist of a compact object (neutron star or black hole) and a more ordinary companion star. The dynamics of the system is complicated and involves mass transfer from the companion onto the compact object. Neutron stars are known to have a surface magnetic field as strong as 10^{12} G and millisecond periods. Both the accretion and the magnetic dipole radiation can be the energy source. The existence of high magnetic fields and plasma flows creates the environment necessary for the formation of strong shocks, and corresponding particle acceleration. The companion star itself, the accretion flow, or the heavy stellar winds might be targets for inelastic nucleon interactions and neutrino production. In the presence of UHE γ−ray

fluxes one can relate the γ-ray flux to the neutrino flux. For a γ-ray source spectrum $\frac{dN}{dE_\gamma} = IE_\gamma^{-\alpha}$, the neutrino spectrum can be derived from the kinematics of pion decay as:

$$\frac{dN}{dE_\nu} = I\left[1 - \left(\frac{m_\mu}{m_\pi}\right)^2\right]^{\alpha-1} E_\nu^{-\alpha}. \tag{4}$$

The actual neutrino flux depends strongly on the geometry of the source because of the possible absorption of γ-rays in the target. Detailed calculations of the neutrino flux expected from Cygnus X-3 have been done by different authors [5].

Young supernova remnants are another candidate for production of observable neutrino fluxes. As suggested by Berezinsky and Prilutsky [6], if protons are accelerated in a young supernova remnant, they will interact with material of the expanding shell and produce γ-rays and neutrinos until the adiabatic loss of the particle exceeds the collisions loss. Two modifications of the idea became necessary after the explosion of SN1987A and the proliferation of detailed supernova models [7].

The neutrino fluxes from several point sources are shown in Fig. 3. For comparison, the atmospheric neutrino flux scaled to 1° bin is also plotted.

2.3 Diffuse Neutrino Flux from AGN

The possibility that high energy neutrinos are produced in AGN has been suggested long ago [8]. Recently, this promising source of ultrahigh energy neutrinos has been discussed extensively in the literature [9]. In particular, the detections of GeV γ's from distant active galaxies like Mrk 421 by the EGRET instrument on the Compton GRO and TeV γ's by Whipple Čerenkov Observatory are intriguing. This has fueled considerable calculational effort to predict neutrino fluxes from AGN. These objects, the most luminous in the Universe, may well be emitting a significant fraction ($\sim 1/2$) of their gravitationally powered radiation in ultrahigh energy neutrinos [10, 11]. In fact the spectral signature is sufficiently shallow that the summed flux from all sources would be discernible over the atmospheric background.

In one scenario, it is assumed that a massive black hole as an accelerator at the center of the AGN is the source of jets [12]. These jets terminate in "hot spots" in the radio lobes which are dense clouds of photons. The termination shocks of the jet are supposed to accelerate protons and they bombard the photon cloud; thus neutrinos are produced through $p\gamma$ interaction. But the cloud is optically thick and γ-rays are unlikely to escape the source. Stecker *et al.* [10] pointed out that the radio-quiet AGN could also be a powerful emitter of neutrinos. Consider a massive black hole surrounded by an accretion disk in a very dense cloud of photons. High energy protons accelerated in the shocks in the accretion disk produce pions from collisions with photons in ultraviolet photons. All of the high energy photons generated in the beam dump cascade down to X-ray energy and should account for the observed X-ray spectrum. Even if the neutrino fluxes from individual AGN are small, the combined flux from hundreds of radio-quite sources can be larger than the atmospheric neutrino background at energies greater than ~ 100 TeV.

Fig. 4 summarizes the diffuse flux of AGN neutrinos calculated by various authors.

3 Detectability and Experimental Techniques

Let us agree that high energy neutrinos from space permit us to do interesting physics, astrophysics, cosmology, and even geophysics studies. The questions then are: How do we detect them? Are the expected fluxes accessible experimentally? What is the energy threshold? How large a detector is required? What are difficulties in experiments? I shall try to answer these questions in this section.

3.1 Energy Threshold and Detector Scale

It is illustrative to compare three classes of neutrino spectra. The first one is the atmospheric neutrino spectrum which forms the background for any experiment carried out on the Earth. The spectrum follows the primary cosmic ray spectrum with spectral index $\alpha \sim 2.7$ up to ~ 100 GeV and turns over to $\alpha \sim 3.7$ due to the competition between the decay and interaction of pions in the atmosphere. Other complications due to contributions of other channels and muon decays make $\alpha \sim 4.7$ in high energy end. The second is the neutrino spectrum produced by galactic cosmic rays in interactions with interstellar matter. This spectrum should follow the cosmic ray spectrum up to the highest energies since all interaction products decay. The last spectrum is the neutrino spectrum produced by cosmic rays at their acceleration sites. This spectrum should have a hard ($\alpha \sim 2.0 - 2.2$) cosmic ray source spectrum, which is not yet affected by the cosmic ray leakage from the Galaxy. At energies below 1 TeV, the atmospheric neutrinos dominate the total neutrino flux, and thus it is unlikely to be able to extract the signal from such a strong background. However, the steepening of atmospheric neutrino spectrum above 1 TeV allows for achieving a reasonable signal/noise ratio at such energies. Therefore, this crossing energy roughly defines the threshold of a detector for high energy neutrino astrophysics. The exact number depends on the luminosity of the source to be studied and is estimated to be around 1 TeV optimistically or around 1 PeV conservatively.

At $E_{\rm th} \sim 1$ TeV, the neutrino flux is estimated to be on the order of $\mathcal{F}_\nu \sim 10^{-10}$ cm^{-2} s^{-1} TeV^{-1}. The event rate in a detector with effective area $\mathcal{A}$ is roughly estimated to be $\mathcal{R}_\nu = \mathcal{F}_\nu \epsilon \mathcal{A}$. The overall detection efficiency of neutrinos is $\epsilon \sim 10^{-6}$ (I will discuss this factor below). Therefore, in a detector with $\mathcal{A} \sim 10^4$ m^2, less than 1 event per year is expected. To get good statistics for neutrino astrophysical study (say, ~ 100 yr^{-1}), the detector scale needs to be at least $\mathcal{A} \sim 10^6$ m^2.

The current operating detectors with high energy neutrino detection capability include NUSEX, KGF, SOUDAN, KAMIOKANDE, BAKSAN, IMB, LVD, and MACRO. But the effective area of these detectors ranges from 10 m^2 to few$\times$100 cm^2, which is too small to detect high energy neutrinos. A required detector of the order 1 km^3 is a factor of 25000 larger than IMB, or 1000 larger than MACRO or LVD.

3.2 Experimental Techniques

To achieve the large scale needed for high energy neutrino detection it appears to be impractical to adopt either the schemes used in traditional accelerator experiment (to use active detector to cover a given area)[4] or the method used in current generation detectors like IMB and KAMIOKANDE (to use a contained volume of detector medium). The most efficient way to detect high energy neutrinos seems to use the Earth as a target for neutrino interaction and to use naturally existing material as transparent detection medium such as ocean water or Antarctic ice.

The neutrino is a neutral particle with extremely great penetrating power. The detection of a neutrino is realized by observing its secondary charged products when it interacts in the detection medium. A well established technique is to identify neutrinos by detecting the Čerenkov light from charged muons produced in the neutrino-nucleon interaction. Based on the arrival times and amplitudes of the Čerenkov light recorded by phototubes positioned at a grid of a volume, the trajectory of muons can be reconstructed. The direction of the neutrino is then inferred from the muon trajectory. The accuracy is determined intrinsically by the angle between muon track and neutrino direction: $< \theta_{\nu-\mu} > \sim 1^\circ \sqrt{1\ \mathrm{TeV}/E_\nu}$.

The Čerenkov radiation is generated when a charged particle moves in a medium with a velocity $\beta > 1/n$ where n is the index of refraction. The number of photons emitted per unit length along the path of the muon is given by:

$$\frac{dN}{dl} = 2\pi\alpha \int_{\lambda_{\min}}^{\lambda_{\max}} d\lambda \left\{ \left[1 - \frac{1}{\beta^2 n(\lambda)^2} \right] \left(\frac{1}{\lambda^2} \right) \right\}. \tag{5}$$

For visible light, $\frac{dN}{dl} \sim 500 \sin^2\theta_c \mathrm{cm}^{-1}$ where the Čerenkov emission angle $\theta_c = \cos^{-1}(1/\beta n)$. The Čerenkov radiation is peaked towards the blue, generally being cut off in the ultraviolet by Rayleigh scattering. As the light propagates in the medium, its intensity would be attenuated and its direction would be changed or randomized by a number of scattering mechanisms. Therefore, both the attenuation length and scattering length of visible light are critical parameters for a detector medium. The former determines how far apart optical modules could be placed. The latter limits the capability of reconstructing the trajectory of muons.

The experimental challenge is to determine the muon direction with sufficient accuracy by sampling Čerenkov wavefront with a minimum number of optical modules. In order to extract the upward going muons due to neutrinos, one has to reject the much more numerous downward going cosmic ray muons. The up/down discrimination power must be better than 10^{-5} or 10^{-6}, depending on the depth of the detector array.

I emphasize that the Čerenkov technique has been well established for neutrino detection in current generation detectors such as IMB and KAMIOKANDE. Other approaches such as the acoustic detection [17] and radio detection [18] of particle cascades induced by neutrino interactions have been proposed long ago. However, they have not been used in

[4]John Learned figured out that to achieve 10^5 m^2 area of detector this way, one would need a total cost of order 10^9 dollars!

in-situ tests and more R & D needs to be done. In the following I will discuss experiments based on the Čerenkov technique.

3.3 Expected Event Rate: Accessible?

For a given differential flux of astrophysical neutrinos, the observed spectrum of muons in a detector array of effective area $\mathcal{A}$ and angular acceptance of $\Delta\Omega$ in unit time is estimated to be:

$$\frac{\Delta N_{\rm obs}}{\Delta E_\mu} = \mathcal{A}\Delta\Omega \int_{E_\mu}^{E_\mu+\Delta E_\mu} dE_\nu \left[\frac{dN_\nu}{dE_\nu}(E_\nu)\, P_{\nu\to\mu}(E_\nu, E_\mu)\, \eta(E_\mu)\right], \tag{6}$$

where $\eta(E_\mu)$ is the efficiency of detecting μ's as a function of E_μ. The ν to μ conversion probability $P_{\nu\to\mu}(E_\nu, E_\mu)$ is given as:

$$P_{\nu\to\mu}(E_\nu, E_\mu) = \left(\frac{\rho N_{\rm A}}{<A>}\right) \int_{E_\mu}^{E_\nu} dE'_\mu \left\{\left[\frac{d\sigma_\nu^{\rm cc}}{dE'_\mu}(E'_\mu, E_\nu)\right] R_\mu(E'_\mu, E_\mu)\right\}, \tag{7}$$

in which $\frac{\rho N_{\rm A}}{<A>}$ is the nucleon number density in the medium, $\frac{d\sigma_\nu^{\rm cc}}{dE_\mu}$ is the charged-current cross section of a neutrino producing the muon with energy E_μ, and $R_\mu(E'_\mu, E_\mu)$ is the effective range of μ generated with energy E'_μ to retain energy E_μ in the medium.

The calculated $P_{\nu\to\mu}(E_\nu, E_\mu)$ using different quark structure functions (especially at small x) is found to be a roughly linear function of E_ν. In the relevant range of $E_\nu = 1$ TeV to 1 PeV, the conversion efficiency for $E_{\rm th} = 100$ GeV is $P_{\nu\to\mu}(E_\nu, E_\mu = 100\,{\rm GeV}) = (0.3 - 1.2) \times 10^{-6}(E_\nu/1\,{\rm TeV})^\delta$ with $\delta \sim 0.8 - 1.2$. Using the Čerenkov techniques, the detection efficiency $\eta(E_\mu)$ for muons with $E_\mu > 0.2$ TeV resulting from neutrino interactions is almost 100%. If we define the overall detection efficiency of neutrinos as $\epsilon(E_\nu) = P_{\nu\to\mu}(E_\nu, E_\mu) \times \eta(E_\mu)$, we find $\epsilon(E_\nu) \sim 10^{-6}$ at $E_\nu \sim 1$ TeV. One needs to keep this number in mind as it serves roughly as a conversion factor from flux to event rate in a back-of-the-envelope estimate (I have used it in section 3.1).

The observed event rate above threshold $E_{\rm th}$ becomes:

$$N_{\rm obs}(E_\mu > E_{\rm th}) = \int_{E_{\rm th}}^{\infty} dE_\mu \left[\frac{\Delta N_{\rm obs}}{\Delta E_\mu}(E_\mu)\right]. \tag{8}$$

Another important fact is that at very high energies the neutrino flux from astrophysical sources will be attenuated by interactions inside the Earth before reaching the detector [19]. This effect reduces the event rate in eqn. (6) by rescaling the neutrino flux $\frac{dN_\nu}{dE_\nu}(E_\nu)$ by a shadowing factor:

$$\frac{dS}{d\Omega}(E_\nu) = \exp\left\{-\left(\frac{\rho N_{\rm A}}{<A>}\right)\sigma_{\nu N}(E_\nu) L(\theta)\right\}, \tag{9}$$

in which $L(\theta)$ is the distance traveled through the Earth for a source at zenith angle θ. This attenuation is roughly 0.1 for neutrinos at TeV-PeV from $\theta = 180°$. But for neutrinos at higher energies it becomes a serious problem. For example, at 10 PeV, the attenuation by the full length of the Earth can be as large as 10^{-4}.

Table 1: Examples of calculated neutrino flux for various sources.

Source	Energy Threshold	Flux (yr^{-1} $0.1km^{-2}$)	Atmospheric ν flux (yr^{-1} $0.1km^{-2}$)
Diffuse AGN	> 10 GeV	~ 3000	5000 (in 1°)
Diffuse AGN	> 1 TeV	~ 2000	200 (in 1°)
Diffuse AGN	> 1 PeV	~ 100	few (in 1°)
Point AGN	> 1 TeV	~ 10	2 (in 1°)
500 GeV WIMP	> 10 GeV	~ 100	10 (in 1°)

It should be noted that the uncertainties in the particle physics involved in the above neutrino detection scheme are small since $\frac{d\sigma_\nu^{cc}}{dE_\mu}$, R_μ, and thus $P_{\nu\to\mu}$ can be calculated to a good accuracy. It is worthwhile to note that the event rate given in eqn. (6) is proportional not only to the effective area, but also to the third dimension through the effective range of muons. For this reason, I use the effective area or the effective volume interchangeably, implying roughly a cubic detector array.

In Table 1, I list expected event rate for a few examples of neutrino sources estimated using the above equations. The event rates are for an array with effective area of 0.1 km^2.

3.4 Discussion on Detector Parameters

What is the best configuration of a detector array that optimizes the sensitivity, signal/noise ratio, and angular resolution? I think no one is ready to answer this question at present. First, there are a number of uncertainties involved in detector performance as well as in the expectation of neutrino sources. Second, answering such a question requires a tremendous amount of Monte-Carlo work which has not been done so far. Nevertheless, I think that it may be helpful for me to point out the following.

(1) The **sensitivity** to neutrino fluxes is proportional to the effective volume of a detector array. Since both the neutrino cross section and the range of muons increase with energy, the conversion probability $P_{\nu\to\mu}$ goes up nearly linearly with energy. However, the neutrino flux to be observed decreases with energy. For a spectrum of $\frac{dN}{dE_\nu} \propto E_\nu^{-1}$, $P_{\nu\to\mu}\frac{dN}{dE_\nu}$ to which the event rate is proportional is almost a constant. The actual source neutrino spectrum may be steeper than E_ν^{-1}. Therefore, for a given detector array, the sensitivity decreases with energy slightly (probably E_ν^{-1}) rather than strongly.

(2) The **signal/background ratio** improves with energy as $S/B \propto E_\nu^\alpha$ where $\alpha \sim 1.5$ because the source spectrum is harder than the atmospheric spectrum. At $\sim$ 1 TeV, $S/N \sim 0.1$. An additional background to be rejected is the downward going muons in residual cosmic rays at a detector site. The flux of cosmic ray muons decreases with increasing depth. Thus, for a detector at a shallow depth, more downward going muons needs to be rejected against the signal of upward going neutrino-induced muons. For

example, at $\sim$ 1 km depth, the up/down ratio is roughly estimated to be $\sim 10^{-6}$. At a fixed depth, the up/down discrimination power depends critically on the reconstruction capability and accuracy of muon tracks.

(3) The **angular resolution** is an issue in searching for point sources. The intrinsic angular resolution, which is determined by the angle between the incoming neutrino and the muon trajectory, improves with energy. The accuracy of muon trajectory reconstruction is determined by the noise level of phototubes, timing resolution at each phototubes, light scattering in the medium, and the number of phototubes used in a given volume, and the array geometry. In practice, the accuracy of muon trajectory reconstruction is worse than the intrinsic angular resolution.

The determination of the energy and direction of muons relies upon the properties of individual phototube and the array configuration. A large photon collecting power is desired. The noise in the optical modules will sprinkle a muon trigger with false signals. The geometry of an array, and in particular the spacing among optical modules are determined by the absorption and scattering length of visible light in the medium, and by the desired energy threshold.

4 Current Prototype Detectors

The current prototype detectors on the scale of $\sim 10^4$ m^2 include BAIKAL, AMANDA, NESTOR, and DUMAND (BAND, for short). I shall introduce the present status of each telescope and comment on its major characteristics below. Other on-going experiments with scales on the order of $\sim 10^2$ m^2 (e.g., IMB and KAMIOKANDE) or other proposed detectors near surface lakes or ponds (e.g., GRANDE, LENA, NET, and PAN) which require up/down rejection of $10^{-10} - 10^{-11}$ will not be discussed.

4.1 Antarctic Muon And Neutrino Detector Array (AMANDA)

AMANDA [3] uses clear ice at the South Pole as detector medium as shown in Fig. 5. The most important advantage for AMANDA is the substantially low noise level of photomultipliers (a factor of $\sim$ 40 lower than that in ocean water or lake Baikal) in the polar environment. However, its relatively shallow depth requires a better rejection power of up/down going muons than other deep ocean detectors (10^{-6} vs 10^{-4}). The most critical issue for AMANDA has been the transparency of ice for visible light[5]. In 1990, the group initiated a test in Arctic ice in Greenland with a short string of 3 phototubes suspended in a bore hole extending 100 m below the packed snow layer, and about 200 m below the surface. This short string detected downward going cosmic ray muons [20]. Four AMANDA strings of twenty phototubes 8 inch in diameter have been placed down at 800-1000 m depth in Antarctic ice in 1994 season. The hot water drilling technique

[5]Just as John Learned was once worried about giant monsters on large scales in the deep ocean, Buford Price is now worried about something different – ice physics on microscopic scale at extremely low temperature and high pressure.

and the deployment scheme have been demonstrated to be successful. The phototubes survived the freezing process of the holes. The group also has laser sources deployed for calibration purpose. Optical properties of the polar ice at the these depths have been derived from delayed timing distributions received by phototubes at various distances and depths (800-1000 m). In particular, fitting of the laser pulses diffusing between strings separated horizontally by 20-30 m permits deduction of both scattering and absorption lengths (as functions of wavelength) [21]. It has been shown [21] that the absorption length is much longer than had been inferred from laboratory measurements and than any other natural medium like the clearest ocean waters, in the range of $\sim$ 300 m. The scattering length, however, is quite small (10-20 cm scattering length) due presumably to the existence of bubbles. This is a challenge as such frequently occurring scattering makes the array incapable of any significant determination of muon direction based on the measurement of the arrival times of the Čerenkov wavefront at each of the phototubes. An even greater challenge is the up/down discrimination power required at such a depth is as low as $\sim 10^{-6}$. It points to a need to develop ways other than directionality to extract signal of muons induced by neutrino interactions, if an array at such a depth is to be used to detect astrophysical neutrinos. Price [22] has recently developed a model in which the depth dependence of air bubble concentration at South Pole is derived. This model predicts the dependence of the bubble-to-bubble scattering length on depth for ice at South Pole in Fig. 6. The bubble-to-bubble scattering length is $\sim$ 6 m at a depth of 1.3 km, 20 m at 1.4 km, and 130 m at 1.5 km. He also showed [23] that at depths greater than 1.4 km the scattering is governed by dust, soluble impurities, crystal boundaries in ice, and air hydrate crystals. The collaboration intends to place 6 strings at a depth of $1.5 - 1.9$ km in the next deployment scheduled for 1995-1996. The results obtained then would be crucial to determine the feasibility of detecting neutrinos in polar ice.

4.2 The BAIKAL Neutrino Telescope (NT-200)

The BAIKAL Neutrino Telescope [24] has 36 large photomultipliers installed and operating since 1993 at 1.1 km depth in Lake Baikal (the deepest freshwater lake on the Earth) in Eastern Siberia. In March 1995, 36 more photomultipliers were deployed [25]. The goal is to extend the current version to a full 200 module array NT-200 (Neutrino Telescope with 200 photomultipliers) as shown in Fig. 7, in the next few years. Its relatively shallow depth like AMANDA exposes it to a much higher downward going cosmic ray muon background than deep ocean detectors. At such a depth, the absorption length of light is $\sim$ 20 m at $\lambda = 480 - 500$ nm. The background counting rate in-situ is found to be as high as tens of Hz mainly from bioluminescence and radioactive decays. The group suppresses its background by pairing optical modules in the trigger and by clustering optical modules closely. Half of optical modules are pointing upwards in order to achieve a uniform acceptance over upper and lower hemispheres. Since the installation in 1992, the group has recorded a vast number of down-going muons, with a trigger rate of $\sim$ 20 Hz. Angular distributions have been obtained. The group has reached an up/down rejection ratio of 10^{-4}. According to their Monte-Carlo, the group might be able to reach the 10^{-6} goal of

detecting neutrinos when the full complement of 200 optical modules is deployed. This collaboration expects to deploy more optical modules in 1995. The depth of the lake is 1.4 km, so the experiment cannot expand downwards and will have to grow horizontally. It will be of particular interest to know whether the expected up/down rejection power is achievable at such a depth.

4.3 Deep Underwater Muon And Neutrino Detector (DUMAND)

DUMAND [26] has been proposed for a long time as the result of the continuous effort of cosmic ray community[6]. The project uses water in the ocean off Hawaii at a depth as deep as 4.7 km. In such deep water, the cosmic ray muon background is roughly 1000 times less at DUMAND than AMANDA and BAIKAL. However, background light is much greater in the deep ocean, due to the presence of radioactive decays from ^{40}K and emission from bioluminescent organisms. It has required years to develop the necessary technology and learn to work in the ocean environment[7]. The test short string with seven optical modules deployed in 1987 at the depth of 3.5 km demonstrated the feasibility of the technique. Data obtained not only revealed downward-going muons but even one upward-going muon, possibly due to a neutrino. The results also indicated that the single string of seven optical modules detected muons over $\sim$ 400 m^2, an area that is comparable to that of the whole IMB detector. DUMAND-II will consist of 9 strings of optical modules, eight arranged to form an octagon with sides 40 meters long, the ninth string being at the center of the octagon, as shown in Fig. 8. Each string will contain 24 downward looking 40 cm diameter hemispherical phototubes, placed on every 10 meters. The collaboration has already installed the 25 km long power and signal cables from detector site to shore as well as the junction box for deploying the strings in 1992. The first DUMAND-II string with 24 optical detectors was also installed in 1992, but failed due to a leak in the main electronics housing after 10 hours of operation [27]. During the operating period some data were collected. The string was recalled, brought back to the laboratory and repaired.

4.4 NEutrinos from Supernovae & TeV Sources, Ocean Range (NESTOR)

NESTOR [28] uses water as detector medium in the Mediterranean sea off the southwest coast of Greece. The group has carried out a test experiment in 4 km deep water, counting muons and verifying the adequacy of the deep sea site. The first "tower" now under construction will have a 12-story hexagonal floor of 7 omni-directional optical modules as shown in Fig. 9. Each floor is deployed as an umbrella-like Titanium structure which

[6]The project has its roots in discussions at the 13rd International Cosmic Ray Conference at Denver in 1973. Since then, there have been a series of DUMAND workshops.

[7]John Learned once recounts: "There were formidable potential problems that people had foreseen, such as monsters of the deep (not many below 2 km), brightly glowing fishes and bacteria (rare, and not much action as long as one does not jostle the instruments about) ... It had been a long struggle, but not at all without much fun."

Table 2: Compilation of features of high energy neutrino telescopes under construction.

Experiment	BAIKAL	AMANDA	NESTOR	DUMAND
Experimental Site	Siberia	South Pole	Greece	Hawaii
Depth (km)	1.0	> 1.5	3.7	4.7
PMT diameter (inch)	15	8	15	15
Number of PMTs	192	193	168	216
PMT noise rate (kHz)	50-100	1.3	60	50
Effective Area (m^2)	5,000	10,000	10,000	20,000
Solid Angle	0.8	0.9	1.0	1.2

opens in the water, with six spines. Each module has two photomultipliers in up/down pairs like BAIKAL. The angular response of the detector is being tuned to be much more isotropic than either AMANDA or DUMAND, which may give it advantages in the study of neutrino oscillations. NESTOR may have the potential to use neutrino beams from CERN to perform long baseline oscillation experiments, perhaps in conjunction with another detector in Grand Sasso. Using a higher density of photocathodes than the other detectors, NESTOR may be able to make local coincidences on lower energy events, even perhaps down to tens of MeV. If this is realized, the detector array will be sensitive to the supernova neutrinos at tens of MeV. As the name indicates, the detector array will engage in the detection of both low energy and high energy neutrinos. The full size NESTOR will have seven such towers and the effective area will be on the order of 10^5 m^2 in the next few years. Since it will be deployed in the deep water in ocean, the group will face the same problems as DUMAND.

4.5 Discussions on BAND

In Table 2, I compile the main features of these four experiments, BAND. Comparisons of these four experiments often lead to discussions of the advantages of one particular experiment over others in terms of the workability of different environments (ocean, lake, or south pole), the choice of two detector mediums for Čerenkov light (water vs ice), the level of noise background (bioluminescence and radioactive decays or no), the optimization of array configuration (e.g., optical module pair or not), the suitability of various trigger schemes, and of course the effectiveness of costs. Even though some of advantages for a particular experiment are easily foreseen, it is in fact difficult, at this stage, to assess and evaluate each advantage or disadvantage, and it is premature to predict which experiment is the best or which one is superior to others. I personally regard all these experiments as complementary to each other. In my opinion, they represent a variety of engineering tests (in different environment and medium, with different array configurations, with different trigger schemes) which are necessary to establish the feasibility of the technique for neutrino detection and to obtain an optimal detector array. The experience in hardware

construction and array deployment being gained or to be gained from BAND and data being collected or to be collected from BAND will definitely clarify the above issues and will be of critical values for the design of future 1 km^3 scale detector array.

5 Other Applications of Neutrino Detector Arrays

Such detector arrays designed for the observation of high energy neutrinos would be multi-purpose instruments. In fact, a number of interesting studies could be carried out ranging from astrophysics to particle physics and from cosmology to geophysics. Examples are search for neutrinos from the annihilation of dark matter particles in our galaxy, study of intrinsic properties of neutrinos such as flavor oscillation, observation of neutrinos from supernovae, search for magnetic monopoles predicted in grand unification theories, and neutrino tomography of the earth core. To illustrate the diversity, I shall cover three topics below: indirect detection of cold dark matter particles (in cosmology), study of neutrino oscillation (in particle physics), and neutrino tomography of the Earth (in geophysics).

5.1 Indirect Detection of Cold Dark Matter Particles

As an indirect approach, a high energy neutrino telescope can be used to detect weakly interacting massive particles (WIMPs) that may make up the cold dark matter in the Universe [29]. Among various candidates for WIMPs, the neutralino is a favored one predicted in the minimal supersymmetry model. If such WIMPs exist in our galactic halo, they would annihilate into neutrinos in the Sun or other stars. Consequently, the observation of neutrinos from WIMP annihilation in the Sun would provide indirect evidence for the existence of galactic WIMPs.

A WIMP (say, neutralino χ) falling on the Sun will loss its energy by scattering off nucleons in the Sun. The WIMP will be gravitationally trapped in the Sun as soon as its velocity falls below the escape velocity due to this continuous energy loss. These trapped WIMPs eventually reach equilibrium temperature, and therefore come to rest at the center of the Sun, building up WIMP density in the Sun. The energy density (ρ_χ) and velocity (v_χ) distributions of WIMPs in our galaxy are well defined if such WIMPs constitute the dark matter in our galactic halo. The capture rate of WIMPs in the Sun is related to the WIMP flux $\mathcal{F}_\chi = v_\chi \rho_\chi / m_\chi$ and interaction cross section with nucleons $\sigma_{\chi N}$ as: $\mathcal{R}_{\rm cap} = \mathcal{F}_\chi \mathcal{N}_\odot \sigma_{\chi N}$ where $\mathcal{N}_\odot$ is the total number of nucleons in the Sun $\mathcal{N}_\odot = m_\odot / m_{\rm N}$.

On the other hand, WIMP may annihilate into any open fermion, gauge boson, or Higgs channels. As the result of the competition between the capture and annihilation, an equilibrium will be inevitably reached: $\mathcal{R}_{\rm ann} = \mathcal{R}_{\rm cap}$. The leptonic decays from annihilation channels such as $b\bar{b}$ heavy quarks and W^+W^- pairs turn the Sun into a source of high energy neutrinos. I point out that such neutrinos from WIMP annihilation have energies in the range of GeV-TeV depending on the WIMP mass. As comparison, neutrinos from thermonuclear burning in the Sun are characterized by keV to MeV range. At the steady state in which the capture rate and annihilation rate of WIMPs are in equilibrium, the generation rate of neutrinos in the Sun is given as: $\mathcal{R}_\nu = f_{\chi\bar{\chi}\to\nu_\mu} \mathcal{R}_{\rm ann}$. The factor

$f_{\chi\bar{\chi}\to\nu_\mu}$ represents that only a fraction of WIMP annihilation results in a neutrino as final decay product. This branching ratio ranges from 1% to 10% depending on particle physics and the mass of WIMPs. The corresponding neutrino flux at the Earth is estimated to be $\mathcal{F}_\nu = \mathcal{R}_\nu/(4\pi D_\odot^2)$ where $D_\odot$ is the distance between the Sun and the Earth, i.e., 1 A.U. Numerically, the neutrino flux for a WIMP with energy density ρ_χ, mean velocity v_χ, and mass m_χ is:

$$\mathcal{F}_\nu \simeq 3.6 \times 10^{-8}\mathrm{cm}^{-2}\,\mathrm{s}^{-1}\left(\frac{f_{\chi\bar{\chi}\to\nu_\mu}}{10\%}\right)\left(\frac{\rho_\chi}{0.4\,\mathrm{GeV\,cm}^{-3}}\right)\left(\frac{v_\chi}{300\,\mathrm{km\,s}^{-1}}\right)\left(\frac{500\,\mathrm{GeV}}{m_\chi}\right), \quad (10)$$

in which I keep all the dependences on WIMP parameters. Of interest to experimentalists is the comparison of the neutrino flux due to WIMP annihilation in the Sun with the cosmic ray neutrino flux from the Sun and the atmospheric neutrino flux in 1 degree bin. These fluxes can be translated to event rates in a detector array with area 1 km^2 using the formulation given in section 3.3. The result is shown in Fig. 10. In a simple calculation I performed, I find that it is possible to observe the signal for a WIMP mass of several hundred GeV. The event rate for WIMPs with $m_\chi \sim 200$ GeV is estimated to be 3000 yr^{-1}. If WIMP mass exceeds ~ 1 TeV, the chance of distinguishing the signal from background becomes unlikely.

5.2 Study of Neutrino Oscillations

Study of neutrino mass and oscillation is of great significance in particle physics, astrophysics, and cosmology as I discussed in another paper [30]. It has been proposed to study the neutrino oscillation using a large scale neutrino detector array. Recently, Learned and Pakvasa [31] have suggested an interesting detection scheme to study ν_τ oscillation which I will discuss briefly below.

A large neutrino detector array, given the presence of significant numbers of neutrinos in the PeV energy range as predicted by various models of AGN, can make unique measurements of the properties of neutrinos. In particular, the interaction of high energy ν_τ's in such detectors will present a spectacular "double bang" signature. Let us consider a process shown in Fig. 11. A ν_τ interaction produces a big hadronic shower (first bang). A τ produced in the interaction would fly ~ 100 m before it decays. The τ decay then produces an even larger particle cascade (second bang). The numbers of detectable photons from these three segments scale roughly as $10^{11} : 2 \times 10^6 : 2 \times 10^{11}$. Such large bursts of light would be visible at photomultipliers positioned at distances of hundreds of meters away. The charged τ will be difficult to resolve from bright Čerenkov light of the cascades, and the photons arrival times will not be very different. However, simply connecting the two cascades by the speed of light will suffice to make an unambiguous association of the two bursts. Learned and Pakvasa found such double bang signal is nearly background free. Following their argument, I am convinced that the double bang event topology appears to be a unique signal for real τ production by ν_τ's, thus permitting the "discovery" of the ν_τ, and inferring mixing of neutrino flavors.

The problem is that the existence of such events depends on the presence of PeV neutrinos in adequate numbers. Optimistically we estimate the event rate of the double bang type to be $\sim$ 1000 per year in a $\sim$ 1 km^3 array or $\sim$ 1 event per year in the BAND detectors under construction now using the neutrino fluxes from all AGN by Szabo and Protheroe [11]. As shown by Learned and Pakvasa [31] ν_τ's are unlikely to have originated in commonly considered astrophysical sources, but are likely to appear due to neutrino mass and mixing, over a large range of allowable (and even favored, if the solar neutrino puzzle and the atmospheric neutrino anomaly have anything to do with oscillation) neutrino mixing parameter space. The point is that in the general energy range of a few PeV there exists a powerful tool for searching for τ mixing, over an unequaled parameter space, with unambiguous identification of the τ. We know of no other way to make a ν_τ appearance experiment with cosmic rays, no way has been proposed for an accelerator experiment except for the use of emulsions making observations of relatively large $\Delta m^2 > 1$ eV^2, and no way of detecting ν_τ's except statistically at proposed long baseline accelerator experiments.

In conclusion, it will be possible to observe the existence of the ν_τ, measure its mixing with other flavors, and measure the ν_τ interaction cross section. Of particular interest is to test the mixing pattern for all three flavors based upon the mixing parameters suggested by the solar and atmospheric neutrino data. This depends on correctness of assumption that very few ν_τ's are produced at sources.

5.3 Earth Tomography Using Astrophysical Neutrinos

The role of high energy neutrinos has been considered not only in physics and cosmology as discussed above, but also in geophysics. An interesting possibility, considered first in 1974 by Volkova and Zatsepin [32], would be to use high energy beams of neutrinos from accelerators to probe the varying density of the Earth, rather as X-rays reveal the varying density within a human body. The basic idea would be to direct neutrino beam across a whole range of angles through the Earth, and to detect the neutrinos as they emerge on the opposite side. However, it has been argued [33] that to work properly for this inverse problem, as in a whole body X-ray scanner, such a scheme requires that both the source of particles and the detector can be moved around the object to be scanned. This is hardly practical with a large particle accelerator on the Earth as a source and a detector like one of the BAND. An alternative would be to have a network of detectors (BAND) observing neutrinos from an astrophysical source. The Earth's rotation would ensure that the source moved around the object. While it is apparently unrealistic at present using the artificial accelerator neutrino beams, it would be possible to fulfill the same task using simply the natural neutrino beams from heaven, if a strong high energy neutrino source is ever found. This possibility of earth tomography using astrophysical neutrinos from either point source or diffuse background has been recently considered in some detail [34, 35]. The burning question is: Can we get enough neutrinos?

6 Concluding Remarks

Neutrino astrophysics offers the potential to peer deeper into astronomical bodies than is possible with any electromagnetic radiation. The recent calculations of neutrino fluxes from AGN provide a promising case for high energy neutrino astrophysics. The uncertainties in particle physics processes involved in the neutrino production calculations are minimal. Although the neutrino cross sections have not been experimentally measured in the laboratory at the energies of interest, our understanding is good enough for reasonable extrapolations. The big uncertainties come from a variety of astrophysics assumptions, that are essential for the evaluation of neutrino signal. Simply because of these uncertainties, the neutrino fluxes could not be calculated within an order of magnitude. The predicted fluxes would serve as only a reference point for the experimental design and indicate roughly how far experimental efforts need to go.

The energy regime of interest extends from a few tens of GeV, which may characterize neutrinos coming from the annihilation of WIMPs in the Sun, into the TeV and PeV regime, which may characterize neutrinos from sources like AGN. The performance of detectors is expected to be improved with increasing energy, despite the fact that the neutrino fluxes decrease with energy. For instance, the overall detection efficiency, signal/background ratio, and angular resolution all improve with energy. At 6.3 PeV, the signal would be enhanced by orders of magnitude due to the Glashow resonant peak in the electron antineutrino cross section [36]. This may serve as a benchmark of energy calibration for a detector array.

Given the expected neutrino fluxes, the question is whether we are within striking distance of being able to detect them. Present estimates suggest that detectors with a scale on the order of 1 km^3 are required. The current experiments, BAND, are only on the order of 10^4 m^2. Even though these arrays are designed to be easily expandable to a required scale, the limited production rate of Čerenkov photons (200 cm^{-1}), their limited absorption length ($\sim$ 50 m), and the high cost of equipment may make it impractical to scale up to 1 km^3. In this connection new detection techniques to cover a larger sensitive volume with a reasonable cost are highly desired.

Acoustic detection of particle cascades is of great interest because of the possibility that a very large detector volume might be built economically. If the energy threshold of acoustic signal generation due to the energy deposition by an electromagnetic cascade is really around few PeV, the technique might be very useful. The great attraction is that the attenuation length for sound in water or ice is in the range of km for frequencies of interest (10-30 kHz). An important advantage of acoustic detectors may be the larger scattering length at ice boundaries and air hydrate boundaries and dust than for light. This approach appears to be a natural and economical choice for km^3 scale effective volume aiming at PeV AGN neutrinos. Therefore, it is worthwhile to undertake further investigations and in particular in-situ testing of this detection scheme. Radio detection of particle cascades is another possibility of high threshold.

If PeV neutrinos from astrophysical sources were detected in adequate rates, there would open up chances to study interesting problems other than astronomy. Of particular

interests are to search for dark matter in our galaxy via annihilation in the Sun, to study ν_τ oscillation using double bang signature, and to probe the density profile of the earth core.

In conclusion, high energy neutrino astrophysics is now being transformed from a dream of theorists to an experimental reality. The future of the field will be largely determined by preliminary results to be obtained by the experimental groups of BAND in the next few years. With the BAND, we are marching into a new era of high energy neutrino astrophysics, and the goal seems to be within the horizon.

Acknowledgements

I thank Prof. Buford Price, Dr. Douglas Lowder, and other AMANDAers for useful discussions.

References

[1] P. Morrison, Scientific American, August 1962, p.91.

[2] See for example, F. Halzen, Nucl. Phys. B (Proc. Suppl.) **38**, 472 (1995) and references therein.

[3] S. W. Barwick *et al.* (AMANDA Coll.), J. Phys. G **18**, 225 (1992).

[4] T. K. Gaisser, F. Halzen, T. Stanev, Preprint MAD/PH/847, to be published in Phys. Rep. (1995).

[5] T. K. Gaisser and T. Stanev, Phys. Rev. Lett. **54**, 2265 (1985); E. W. Kolb, M. S. Turner, and T. P. Walker, Phys. Rev. D **32**, 1145 (1985); V. S. Berezinsky, C. Castagnoli, and P. Galeotti, IL Nuovo Cim. C **8**, 185 (1985).

[6] V. S. Berezinsky and O. F. Prilutsky, Astron. Astrophys. **66**, 325 (1978).

[7] T. K. Gaisser, A. K. Harding, and T. Stanev, Astrophys. J. **345**, 423 (1989).

[8] V. S. Berezinsky, in *Proc. Neutrinos 77* (Nauka, Moscow, 1977) **1**, p.177; R. Silberberg and M. M. Shapiro, in *Proc. 16th Intern. Cosmic Ray. Conf.* v.10, p. 357 (1979); V. S. Berezinsky and V. L. Ginzburg, Mon. Not. Royal Astr. Soc. **194**, 3 (1981).

[9] M. Sikora *et al.*, Astrophys. J. Lett. **320**, L81 (1987); P. L. Biermann and P. A. Strittmatter, Astrophys. J. **322**, 643 (1987); K. Mannheim and P. L. Biermann, Astron. Astrophys. **23**, 211 (1989); M. C. Begelman, B. Rudak and M. Sikora, Astrophys. J. **362**, 38 (1990).

[10] F. W. Stecker, C. Done, M. H. Salamon, and P. Sommers, Phys. Rev. Lett. **66**, 2697 (1991) and **69**, 2738(E) (1992).

[11] A. Szabo and R. J. Protheroe, in *Proc. Workshop on High Energy Neutrino Astrophysics*, ed V. J. Stenger, J. G. Learned, S. Pakvasa, and X. Tata, (World Scientific, Singapore, 1992), p.24.

[12] K. Mannheim, T. Stanev, and P. L. Biermann, Astron. Astrophys. **260**, L1 (1992).

[13] V. Berezinsky, in *Proc. Neutrinos 77* (Nauka, Moscow, 1977), p.177.

[14] M. Sikora and M. C. Begelman, in *Proc. Workshop on High Energy Neutrino Astrophysics*, ed V. J. Stenger, J. G. Learned, S. Pakvasa, and X. Tata, (World Scientific, Singapore, 1992), p.114.

[15] P. L. Biermann, in *Proc. Workshop on High Energy Neutrino Astrophysics*, ed V. J. Stenger, J. G. Learned, S. Pakvasa, and X. Tata, (World Scientific, Singapore, 1992), p.86.

[16] V. S. Berezinsky and L. Ozernoy, Astron. Astrophys. **98**, 50 (1981).

[17] P. B. Price, Nucl. Instr. Meth. B **325**, 346 (1993) and references therein.

[18] F. Halzen, E. Zas, and T. Stanev, Phys. Lett. B **257**, 432 (1991) and references therein.

[19] M. Honda and M. Mori, Prog. Theor. Phys. **78**, 963 (1987); R. H. Reno and C. Quigg, Phys. Rev. D **37**, 657 (1988).

[20] D. M. Lowder *et al.* (AMANDA Coll.), Nature **353**, 331 (1991).

[21] P. Askebjer *et al.* (AMANDA Coll.), Science **267**, 1147 (1995).

[22] P. B. Price, Science **267**, 1802 (1995).

[23] P. B. Price *et al.* (AMANDA Coll.), paper submitted to 24th Intern. Cosmic Ray Conf., Rome (1995).

[24] G. Domogatsky *et al.* (BAIKAL Coll.), in *Proc. 3rd NESTOR Intern. Workshop*, ed. L. K. Resvanis, U. Athens (1994).

[25] I. A. Belolaptikov *et al.* (BAIKAL Coll.), paper submitted to 24th Intern. Cosmic Ray Conf., Rome (1995).

[26] A. Roberts, Rev. Mod. Phys. **64**, 259 (1992).

[27] J. Learned *et al.* (DUMAND Coll.), Nucl. Phys. B (Proc. Suppl.) **38**, 484 (1995).

[28] L. K. Resvanis *et al.* (NESTOR Coll.), in *Proc. Workshop on High Energy Neutrino Astrophysics*, ed V. J. Stenger, J. G. Learned, S. Pakvasa, and X. Tata, (World Scientific, Singapore, 1992), p.325.

[29] F. Halzen, T. Stelzer, and M. Kamionkowski, Phys. Rev. D **45**, 4439 (1992).

[30] Y. D. He, this proceedings.

[31] J. G. Learned and S. Pakvasa, Astropart. Phys. **3**, 267 (1995).

[32] L. V. Volkova and G. Zatsepin, Acad. Sci. U. S. S. R., Bull. Phys. Ser. **38**, 151 (1974).

[33] T. Wilson, Nature **309**, 38 (1984).

[34] A. Nicolaidis, M. Jannane, and A. Tarantola, J. Geophys. Res. **96**, 21881 (1991).

[35] C. Kuo *et al.*, Earth and Planetary Sciences Letters (1995) in press.

[36] S. L. Glashow, Phys. Rev. **118**, 316 (1960); F. Wilczek, Phys. Rev. Lett. **55**, 1252 (1985).

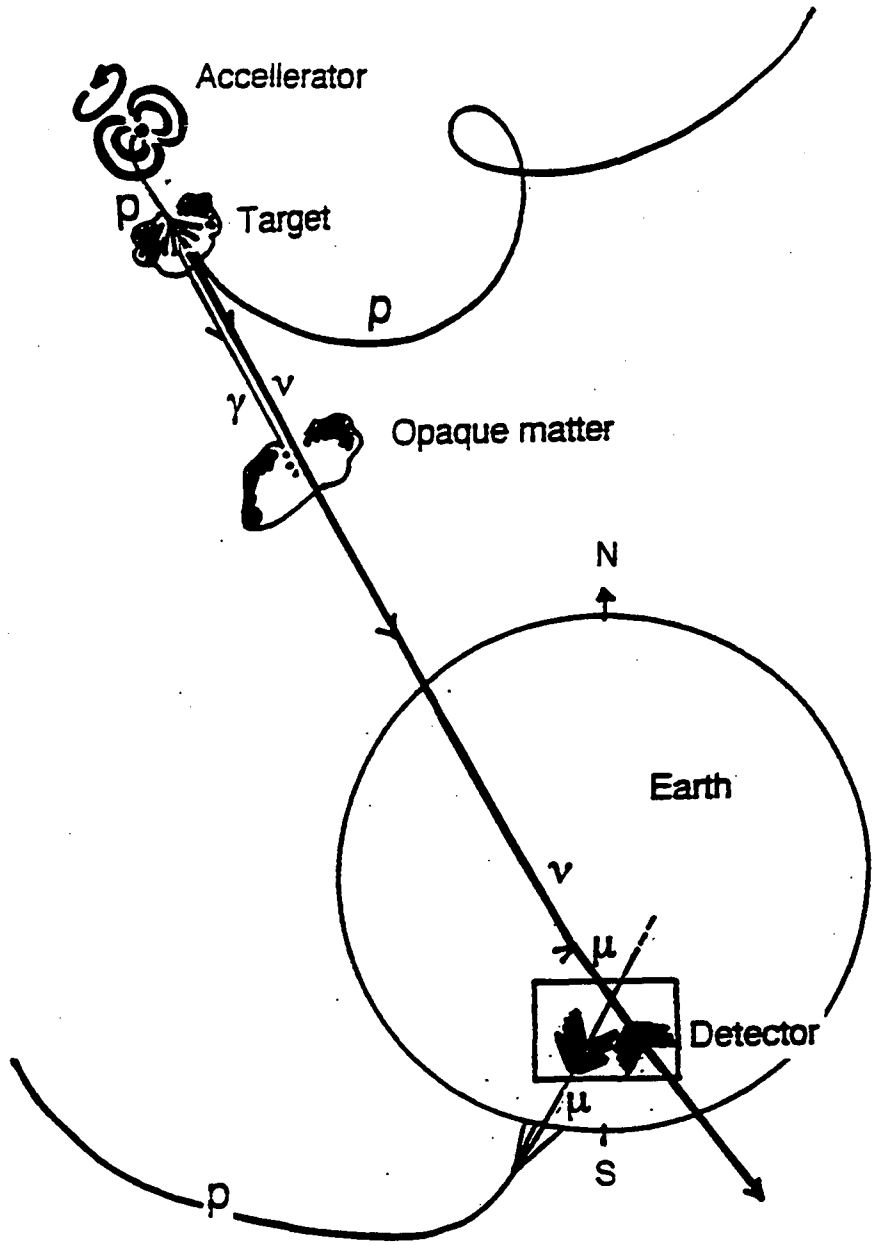

Fig. 1 Unlike either photons which may be absorbed before escaping the source or on the way to the Earth or protons which may be affected by interstellar magnetic fields and lose their directionality, neutrinos can penetrate all the way to the Earth and hence carry the source information.

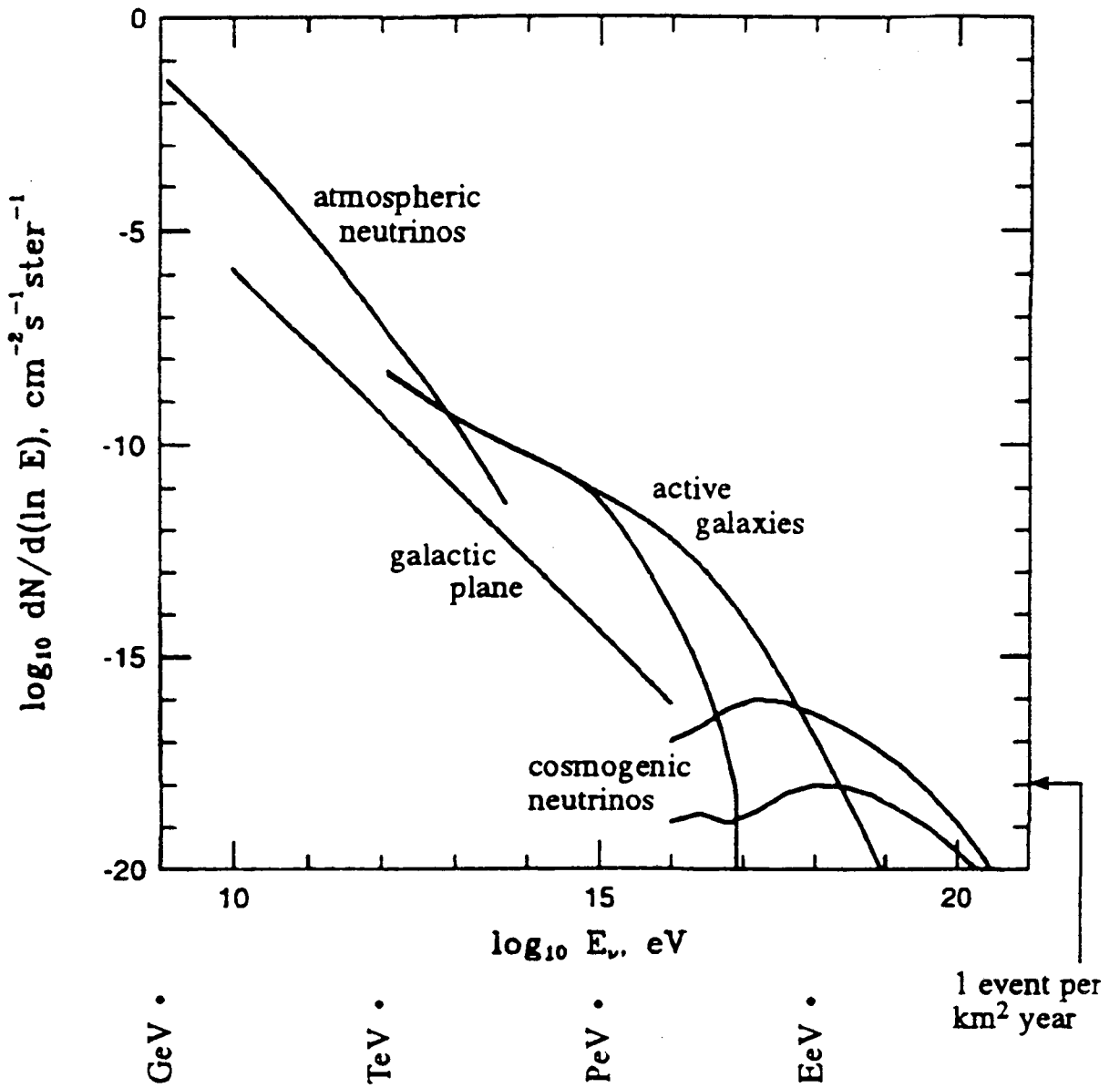

Fig. 2 Estimated neutrino fluxes from the galactic plane and diffuse fluxes of neutrinos from active galaxies and from the interaction of extra-galactic cosmic rays with cosmic photons. Also shown is the atmospheric neutrino flux.

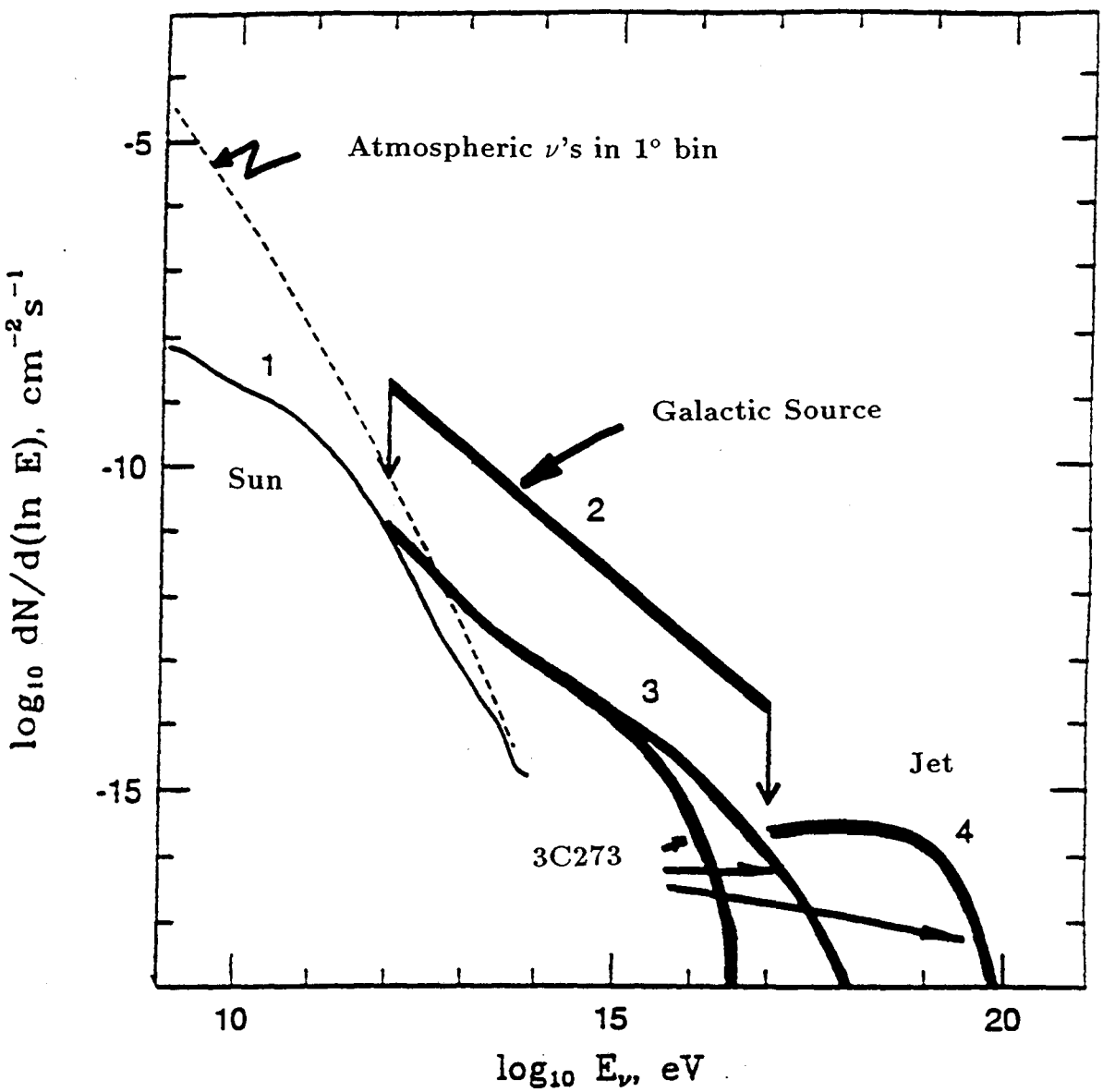

Fig. 3 Estimated neutrino fluxes from galactic source and other point sources. For comparison, the atmospheric neutrino flux in 1° bin and the neutrino flux from cosmic ray interactions in the Sun are also shown.

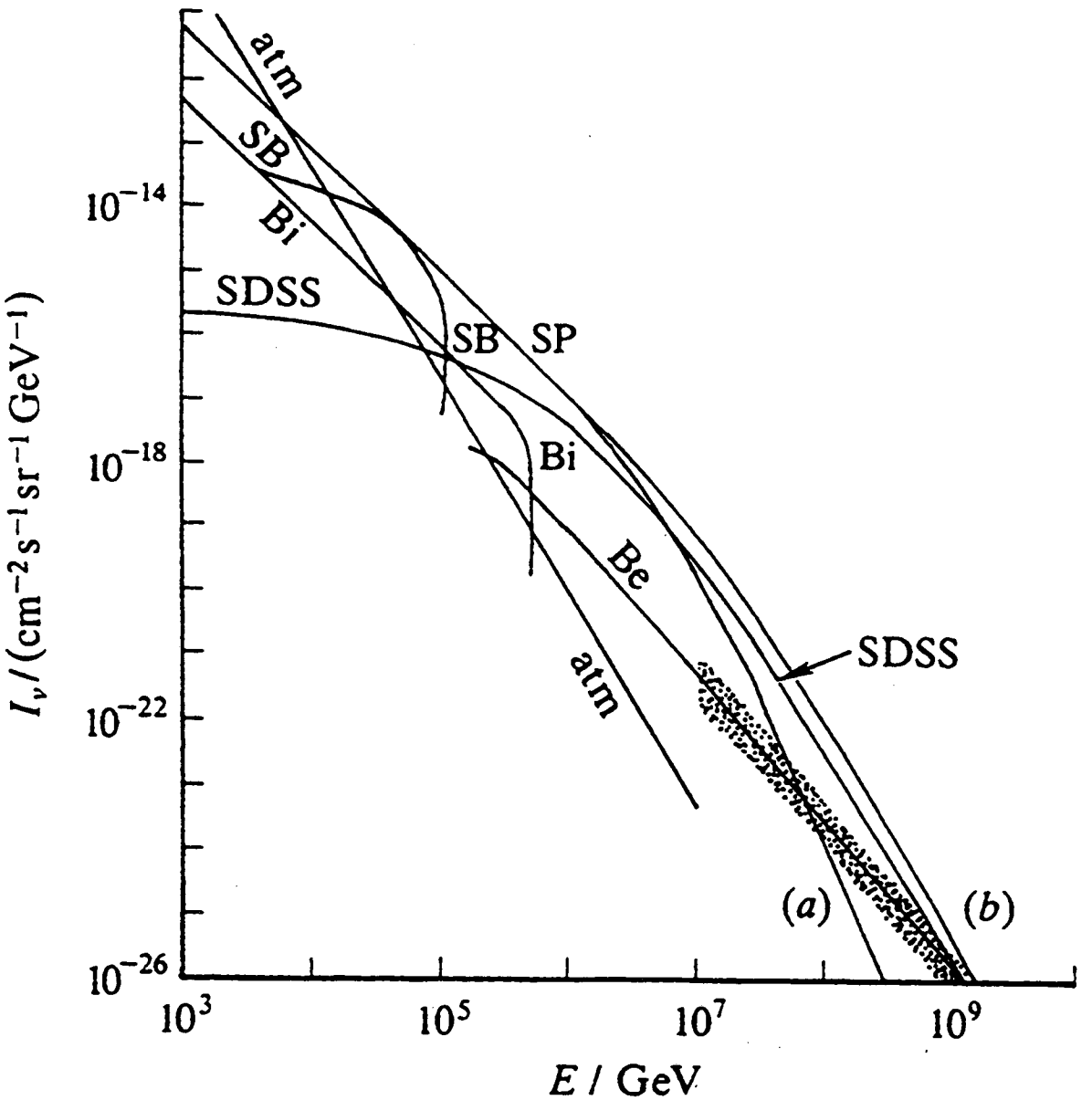

Fig. 4 Calculated spectrum of diffuse neutrinos from active galactic nuclei in comparison with the atmospheric spectrum. The spectra are taken from Be [13], SDSS [10], SP [11], SB [14], and Bi [15]. The shaded region refers to the flux from bright phase in galaxy evolution [16].

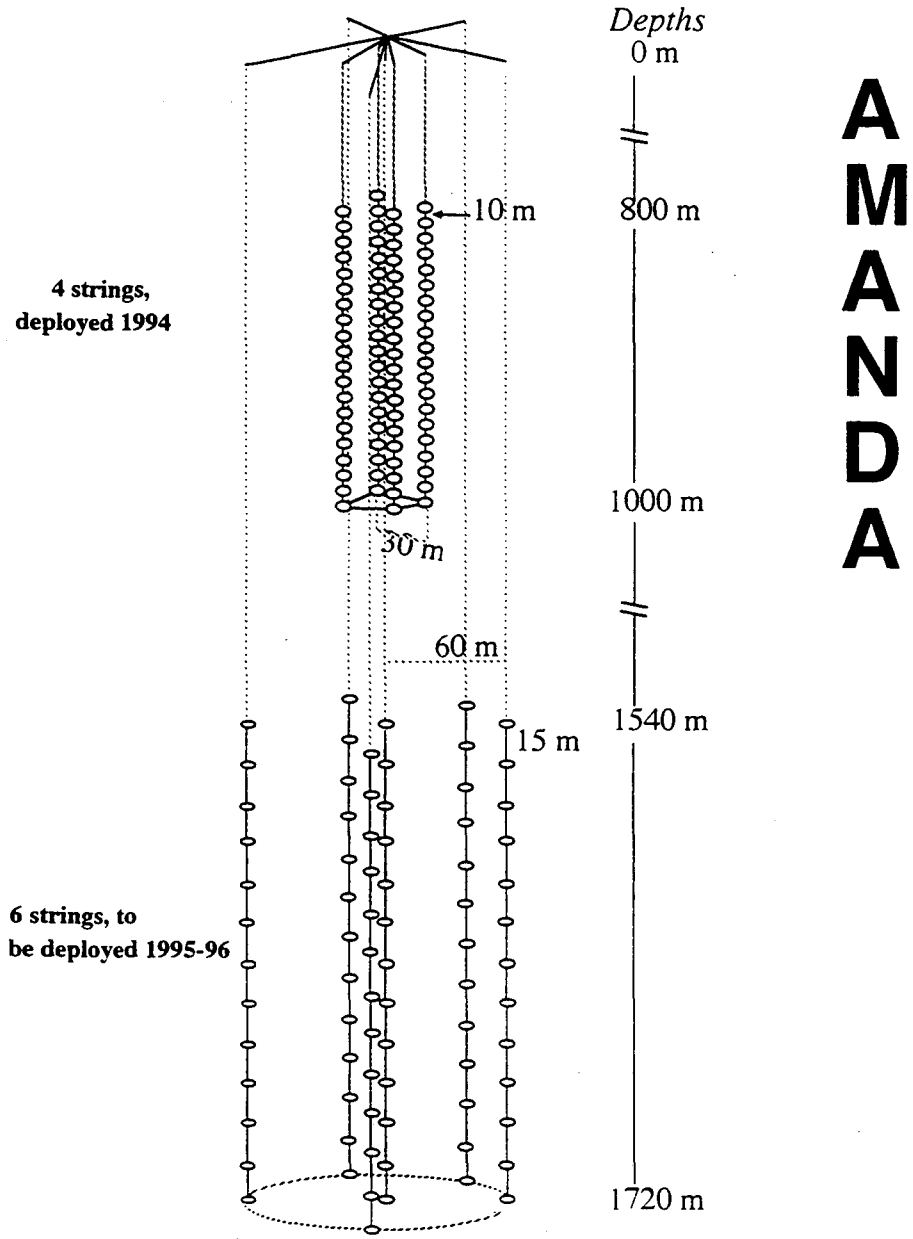

Fig. 5 The sketch of AMANDA. Four strings at 0.8 – 1 km are operating and six more strings have been scheduled to be deployed at 15. – 1.9 km this year.

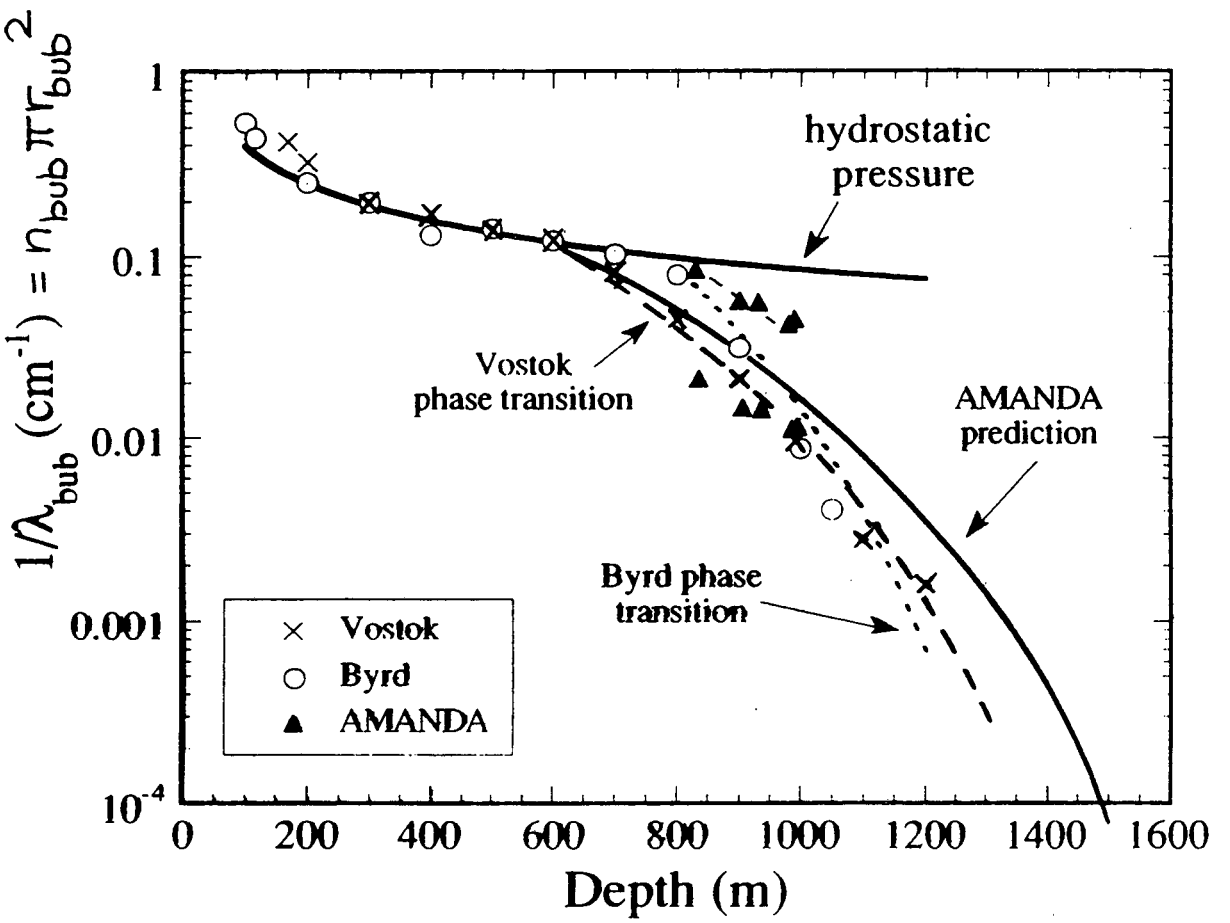

Fig. 6 Reciprocal of bubble-to-bubble scattering length as a function of depth predicted by Price [22]. At depth of 1.4 km, the scattering length is estimated to be $\sim$ 20 m.

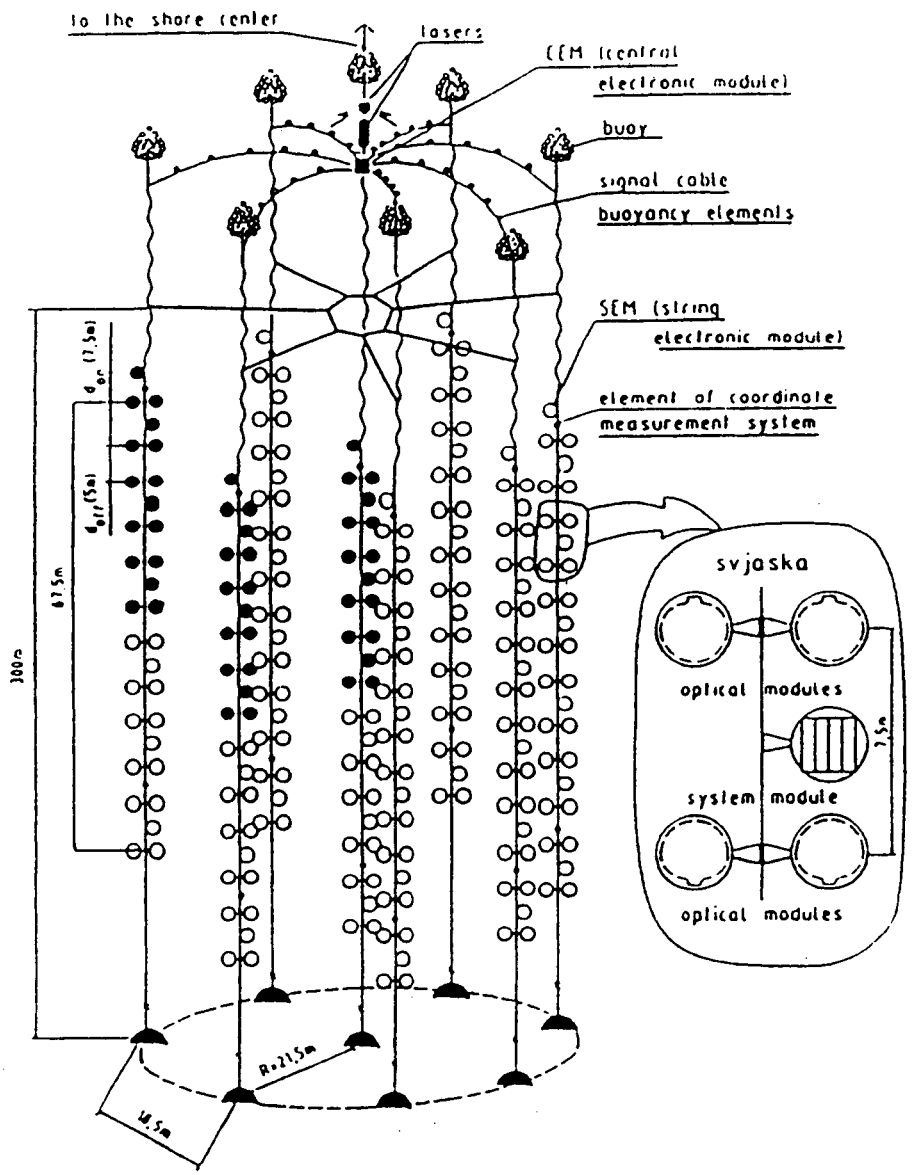

Fig. 7 The schematical layout of the BAIKAL NT-200 detector. The black modules are NT-36 that has been operating since 1993.

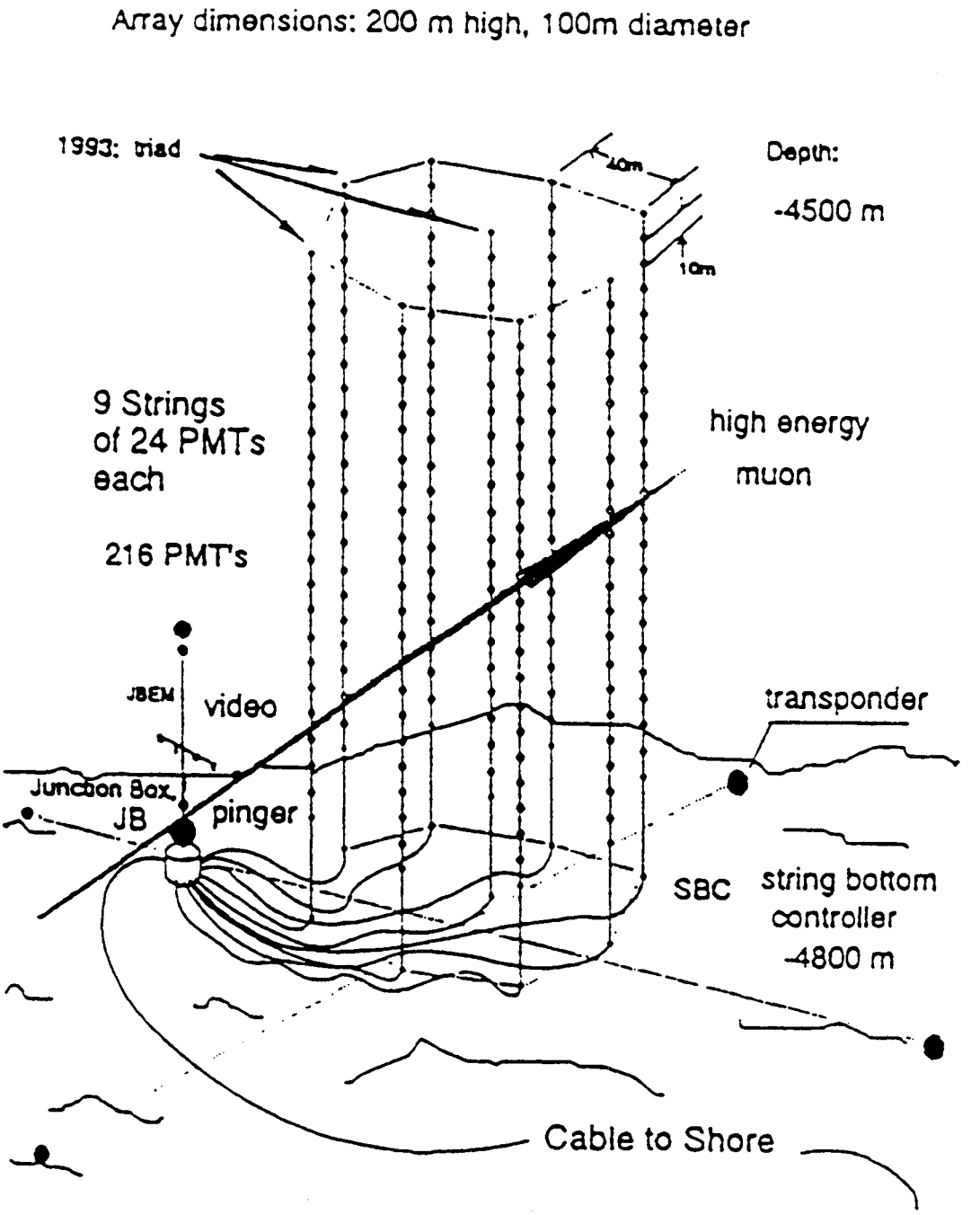

Fig. 8 The overall view of the planned DUMAND-II.

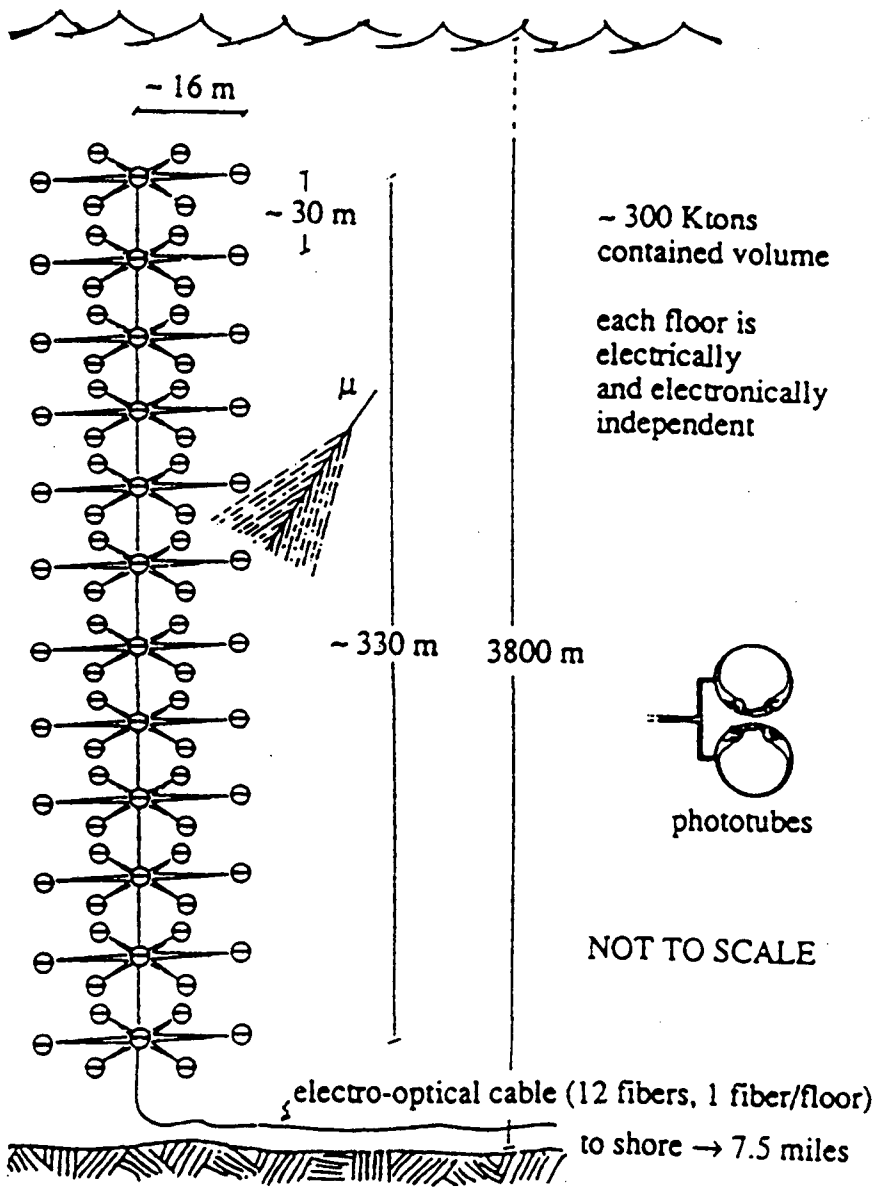

Fig. 9 Schematic view of the NESTOR neutrino telescope.

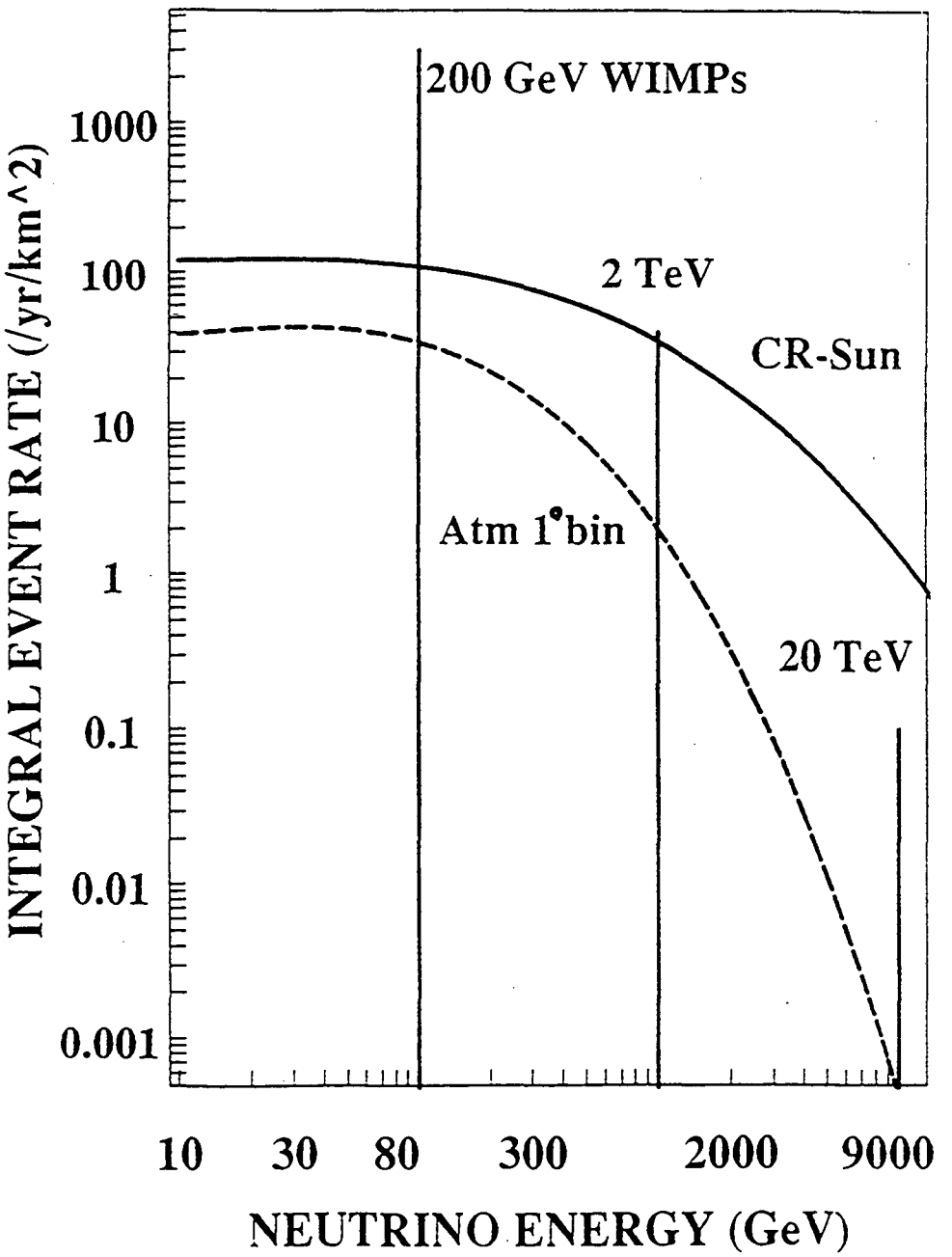

Fig. 10 The event rate as a function of neutrino energy for signal of WIMP annihilation in the Sun. For three hypothetical masses of 0.2, 2, and 20 TeV.

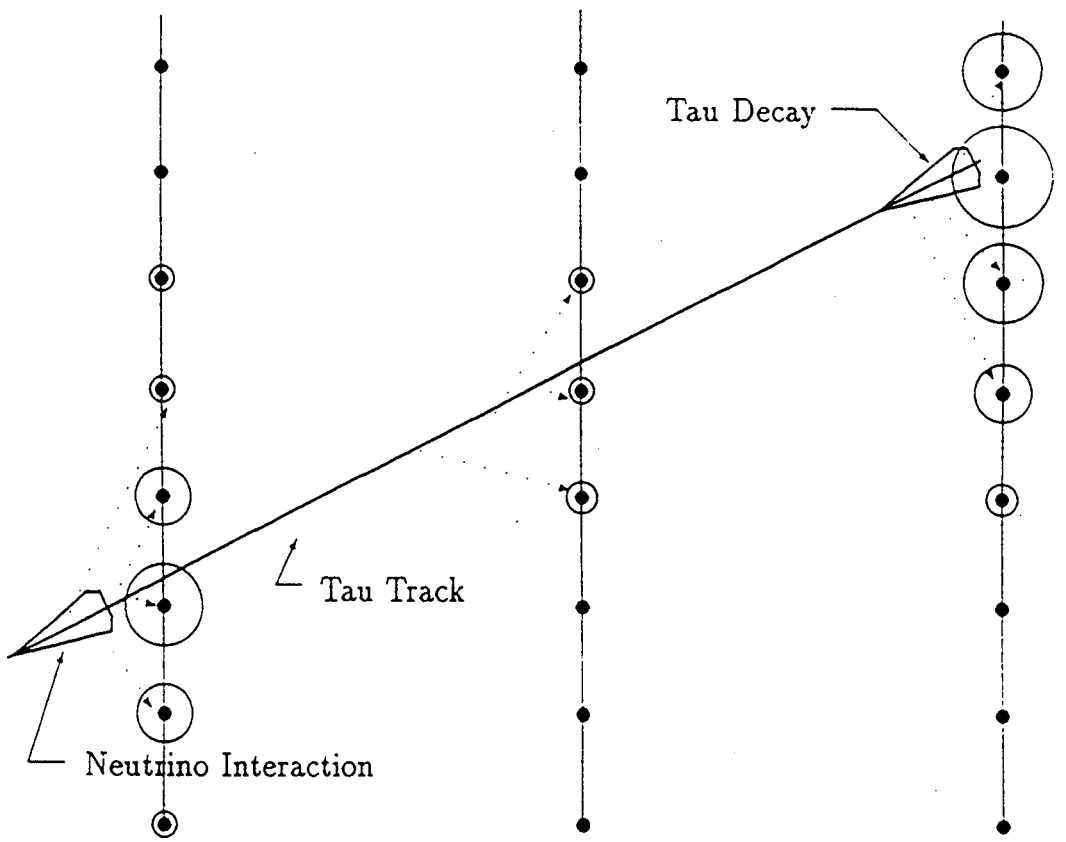

Fig. 11 A schematic view of a "double bang" event near an array of phototubes. Such cascade should be visible to detectors from hundreds of meters distance [31].

DETECTION OF DARK MATTER[1]

Yudong He[2]
Department of Physics, Space Science Laboratory
and Center for Particle Astrophysics
University of California at Berkeley, Berkeley, CA 94720, USA
and
Institute for Nuclear and Particle Astrophysics
and Nuclear Science Division
Lawrence Berkeley National Laboratory, Berkeley, CA 94720, USA

Abstract

A worldwide effort has been undertaken to search for various candidates for the missing mass that makes up more than 90% of the Universe. In this talk, I briefly review the current status and future development of dark matter detection. My talk covers key evidence for dark matter, comments on various candidates (e.g., cold dark matter vs hot dark matter, and MACHOs vs WIMPs), our understanding of its properties (e.g., density, spatial distribution, and phase space distribution), comments on observations of MACHOs, discussion on detectability of favorable candidates – WIMPs (e.g., required sensitivity, expected event rate, and possible signature), examination of current limits on WIMP cross section, and my personal perspectives.

1 The Dark Matter Problem

One of the most puzzling aspects of our Universe is that most of its mass seems to be nonluminous. There is an increasing number of observations that support the notion that the Universe contains more than 90% matter that does not emit light [1]. Its nature is unknown, except that it cannot be made of normal stars, dust, or gas, as they could be easily detected. Therefore, one of the most important problems confronting astrophysics and cosmology is to understand what constitutes most of the mass in the Universe. This could be of equal importance for particle physics, as some favorable candidates are basically particles to be discovered beyond the standard model. General reviews on dark matter problem can be found in Refs. [2, 3] and expert reviews on dark matter detection are available in Refs. [4, 5].

How do we know dark matter is there if it is nonluminous? We know it is there through the effect of its gravitational interaction. There is considerable evidence for its existence

[1]This topic is one of a series of lectures on "Current Trends in Non-Accelerator Particle Physics" given at CCAST Workshop on Tibet Cosmic Ray Experiment and Related Physics Topics and CCAST workshop on Ultrarelativistic Heavy Ion Collisions, Beijing, April 4-13, 1995. This work was supported in part by the U. S. Department of Energy under Contract No. DE-AC03-76SF00098.

[2]Mailing address: Department of Physics, University of California, Berkeley, CA 94720, USA. Email address: yudong@physics.berkeley.edu.

at various scales. Galaxies have a massive halo, extending well beyond their visible radius $R_{\rm vis}$. This evidence comes from rotation curves of spiral galaxies. A rotation curve is the velocity of the rotating emitters relative to the galactic center $v(R)$ as a function of distance R from the center. The curve is obtained from detection of Doppler shifted characteristic emission lines (e. g., 21 cm) from thin gas and stars gravitating around a given galaxy. We denote the galactic mass within a centered sphere of radius R as $M(R)$. Newtonian mechanics leads one to expect $v(R) \propto R^{-1/2}$ for $R > R_{\rm vis}$. However, observations gave completely different results: $v(R)$ stays approximately constant at 200 to 300 km sec^{-1} well beyond $R_{\rm vis}$, out to a certain $R_{\rm H}^{\rm min}$, beyond which the signal is too weak to be observed. The minimum mass of the invisible halo $M(R_{\rm H}^{\rm min})$ for some galaxies is 5 to 10 times larger than $M(R_{\rm vis})$. A typical rotation curve is shown in Fig. 1. The observed flat rotation curve implies that $M(R) \propto R$ or $\rho_{\rm dm} \propto R^{-2}$. We also find, as shown in Fig. 2, that our own galaxy has a dark halo similar to that of other observed spiral galaxies. The halo extends well beyond the position of the Sun.

Other evidence for the existence of dark matter comes from the early observation of random peculiar velocities of galaxies which exceeded the escape velocity, if all of the mass of the galactic center cluster were that observed. Observations of X-rays from clusters of galaxy also provide evidence. Recently gravitational lensing has provided an independent means of establishing the need for such enhanced mass on the scale of galactic clusters.

It is important to point out that evidence for dark matter exists on various scales as shown in Fig. 3 and that dark matter on different scales may be different. Since the density of matter ρ is usually compared to the critical density $\rho_{\rm crit}$, we define a dimensionless quantity $\Omega \equiv \rho/\rho_{\rm crit}$ ($\Omega = 1$, > 1, or < 1 corresponds to a flat, closed, and open Universe). Most determinations of Ω are made by measuring the ratio of mass to light M/L of the system and then multiplying this by the average luminosity density of the Universe $j_o = (1.7 \pm 0.6) \times 10^8\ h^{-1}\ L_\odot/M_\odot$ with $h = 0.4 - 1$. The uncertainty in h represents the uncertainty in the determination of Hubble constant $H = 100h$ km s^{-1} Mpc^{-1}. Almost all determinations of Ω use this method. For example, in the solar neighborhood $M/L = 5$ and $\Omega_{\rm lum} = 0.003h^{-1} = 0.003$ to 0.007. If the solar neighborhood is typical, the amount of matter in stars, dust, and gas is far below the critical. At largest possible scale, the recent study of large scale flows provides important information [6].

Though the dominant view today is that more than 90% of matter in the Universe is made of gravitationally-existing dark matter, I would like to point out some other possibilities. For example, one possibility would be that the simple law of Newtonian gravitational theory might be wrong when applied to something as large as galaxy, as suggested in the literature [7, 8]. In fact, modifications of Newtonian nonrelativistic dynamics at low acceleration would lead to some success. Most cosmologists consider this possibility is unlikely but nevertheless it cannot yet be totally ruled out based on present observations[3]. Another possibility would be a solution that belongs to "none of the above" category. The history of science has recorded many surprises in our past exploration and there is no reason not to expect more in future.

[3]I note that this interesting direction has not been fully explored, due at least partially to what I call the social and psychological influence of science.

2 Possible Candidates for Dark Matter

The dark matter can be classified into baryonic and non-baryonic as shown in Fig. 4. The success of nucleosynthesis theory in predicting the abundance in the Universe of ^{2}H, ^{2}H, ^{4}He, and ^{7}Li, as well as three flavors of neutrinos, gives confidence that Ω from baryons is bounded by $0.01 \leq \Omega_b h^2 \leq 0.015$. The observed baryonic matter gives only $\Omega_b \simeq 0.07$, indicating some fraction of dark matter may exist but $\Omega_b < 0.1$. The baryonic dark matter probably exists in the form of bodies with masses ranging from that of a large planet to a few solar masses. Such objects, known now collectively as massive compact halo objects (MACHOs), might be brown dwarfs or Jupiters ("stars" too small to have initiated nuclear burning), neutron stars, old white dwarfs, or black holes of mass $< 10^{-6} M_\odot$ or $> 10^6 M_\odot$ outside the range of detectability by normal means.

While it is difficult to reconcile the nucleosynthesis limit with dark matter needed on very large scales, the main argument for non-baryonic dark matter is the apparent necessity to have $\Omega = 1$ from rather solid argument of inflation theory, assuming a zero cosmological constant[4]. Non-baryonic dark matter appears to be necessary to account for galaxy formation.

Among the non-baryonic candidates there are several classes of particles which are distinguished by how they came to exist in large quantity during the early Universe, and also how they are most easily detected. The axion is motivated as a possible beautiful solution to the strong CP problem and is in a class by itself. The largest class is the weakly interacting massive particle (WIMP) class, which consists of many suggested particles. Finally, if the tau or muon neutrino had a mass in the 5 eV to 100 eV range, it could make up all or much of the dark matter.

Among the particle dark matter candidates another important distinction is whether the particles were created thermally in the early universe, or whether they were created non-thermally in phase transition. This distinction is important for dark matter detection, since the thermal and non-thermal relics have a different relationship between their relic abundance Ω and their properties such as mass and couplings. For example, the WIMP class can be defined as those particles which are created thermally, while dark matter axions come mostly from non-thermal processes. For WIMPs, the relic density can be calculated after "freeze out" from thermal equilibrium:

$$\Omega_{\rm WIMP} \simeq \frac{10^{-26}\ {\rm cm}^3\ {\rm s}^{-1}}{< \sigma v >}, \tag{1}$$

where $< \sigma v >$ is the thermally averaged cross section for two WIMPs to annihilate into ordinary particles. The remarkable fact is that for $\Omega = O(1)$, as required by the dark matter problem, the annihilation cross section for any thermally created particle turns out to be just what would be predicted for particles with electroweak scale interactions. Hence the name. It is interesting that theories such as supersymmetry, invented for entirely

[4]A zero cosmological constant is set as *ad hoc*. For example, the "best fit" universe requires a non-zero cosmological constant.

different reasons, typically predict just such a particle, making WIMP a favorable dark matter candidate.

WIMPs can be either Dirac particles with predominantly spin-independent (vector) couplings or Majorana particles with spin-dependent (axial) couplings. To be the main component of dark matter, a Majorana neutrino with Fermi coupling, for example, must be in a narrow range of mass (e.g., 5 to 8 GeV for a weak isodoublet neutrino), as determined by the annihilation rate of these particles when they were in thermal equilibrium. In contrast, Dirac particles can have a wide range of mass, since an initial particle-antiparticle asymmetry may have existed, enabling the annihilation rate to be adjusted suitably.

Regardless of the exact identity of the dark matter, its kinetic energy at the time when dark matter domination begins determines the subsequent evolution of the density perturbations that seed galactic and large structure. If at that time, the dark matter is relativistic, we call it "hot" dark matter (HDM). In this case, only largest (supercluster) structures survive and they must fragment to form galactic structures. Whereas if it is nonrelativistic we call it "cold" (CDM). In this case, structure on all scales is preserved. The distinction between CDM and HDM comes mainly from studies of galaxy formation. Since HDM cannot cluster on galaxy scales until it has cooled down to non-relativistic speeds, it gives rise to a considerably different primordial fluctuation spectrum. Of the candidates discussed above only the light neutrinos would be HDM; all the others would be CDM. Most recently, a mixed CDM + HDM model seems to be favored in light of large scale structure formation [9]. The neutrino masses required in this model are consistent with those inferred from studies of solar neutrinos and atmospheric neutrinos, as well as recent results of LSND.

The most popular candidate for WIMPs is the neutralino from supersymmetry theory (SUSY). The lightest supersymmetric particle (LSP) is stable if R-parity is conserved. The most likely LSP is a neutralino:[5]

$$\chi = a_1\tilde{B} + a_2\tilde{W}_3 + a_3\tilde{H}_1^o + a_4\tilde{H}_2^o, \tag{2}$$

where $\tilde{B}$ and $\tilde{W}_3$ are U(1) and SU(2) gauginos and $\tilde{H}_1^o$ and $\tilde{H}_2^o$ are Higgsinos. The combination is determined by a_1, a_2, a_3, and a_4 mass matrix. The precise components of the combination are determined by the parameters of the underlying supersymmetric model, and there are many of these. Typically, one considers the minimal supersymmetric model (MSSM), which is the supersymmetric extension of the Standard Model with the minimal number of new particles. While supersymmetry relates many coupling and masses, there are still dozens of free parameters in the most general MSSM. In much of the parameter space calculation of the relic abundance predicts Ω of the order of unity in neutralinos [10, 11].

[5]This is equivalent to the notation: $\chi = a_1'\tilde{\gamma} + a_2'\tilde{Z}^o + a_3\tilde{H}_1^o + a_4\tilde{H}_2^o$, with $\tilde{\gamma} = \cos\theta_W\tilde{B} + \sin\theta_W\tilde{W}_3$ and $\tilde{Z} = -\sin\theta_W\tilde{B} + \cos\theta_W\tilde{W}_3$.

3 Dark Matter Distribution in Our Galaxy

We are forced to conclude that the Universe must contain a huge amount of nonluminous matter. However, there is no way of telling what this dark matter exactly consists of. Nevertheless, we have a reasonable idea as to its properties such as how much of it there is in the galaxy (density), how it is distributed (spatial distribution), and how fast it is moving (phase space distribution). Of particular relevance to an experiment is the density and velocity distribution in the solar neighborhood, as experimental searches take place on the Earth. This knowledge, derived mainly from the rotation curve, is so crucial to all the experimental searches for dark matter that I shall give a rather detailed account below.

From the flat rotation curve of our galaxy which has been measured inside the solar circle of $R_o \sim 8.5$ kpc, we first want to estimate the total mass density in the solar neighborhood ρ_m. Gravitationally, ρ_m is related to the total potential ϕ by Poisson's equation:

$$\nabla^2 \phi = 4\pi G \rho_m. \tag{3}$$

This equation takes the following form with the assumption of axial symmetry:

$$\frac{\partial^2 \phi}{\partial z^2} + \frac{1}{\omega}\frac{\partial}{\partial \omega}\left(\omega \frac{\partial \phi}{\partial \omega}\right) = 4\pi G \rho_m. \tag{4}$$

Cowsik [12] argued that $(\partial\phi/\partial\omega)$ is negligible not only for a thin disc-like system such as our galaxy but also for the distribution of dark matter in our galaxy which could be in the form of an extended halo. The radial part of the Laplacian could be dropped from the above equation. To ascertain the conditions under which the radial term can be neglected, note that:

$$\omega \frac{\partial \phi}{\partial \omega} = v_c^2. \tag{5}$$

Since the rotation velocity near the solar circle v_c is nearly constant, its derivative becomes very small near the solar circle:

$$\left|\frac{\partial}{\partial \omega}\left(\omega \frac{\partial \phi}{\partial \omega}\right)\right|_{\omega=\omega_o} = \left|\frac{\partial v_c^2}{\partial \omega}\right|_{\omega=\omega_o} \sim 0. \tag{6}$$

We know that the number density of any particular type of stars has a distribution which is controlled by the Jeans equation:

$$\frac{1}{\nu}\frac{\partial}{\partial z}(\nu < v_z^2 >) = -\frac{\partial \phi}{\partial z}. \tag{7}$$

In this case, eqn. (4) becomes:

$$\frac{d}{dz}\left[\frac{1}{\nu}\frac{d}{dz}(\nu < v_z^2 >)\right] = 4\pi G \rho_m. \tag{8}$$

Thus by astronomical observations of $\nu(z)$ and $< v^2(z) >$, the value of $\rho_{\rm dm}$ is normalized:

$$\rho_{\rm m} = \rho_{\rm star} + \rho_{\rm gas} + \rho_{\rm dm} \tag{9}$$

with

$$\rho_{\rm dm} = 0.4 - 1 \text{ GeV cm}^{-3}. \tag{10}$$

The spatial distribution of dark matter in our galaxy seems to be spherical and isotropic. The following parameterization is usually used:

$$\rho_{\rm x}(R) = \rho_{\rm dm}\frac{a^2 + R_{\rm o}^2}{a^2 + R^2}, \tag{11}$$

where $R_{\rm o} \sim 8.5$ kpc is the distance of the Sun from the galactic center, $a \sim 5.6$ kpc is the core radius of the halo, and $\rho_{\rm dm} \sim 0.4$ to 1 GeV cm^{-3} is the local density of dark matter near the Sun (i.e., solar neighborhood). It should be noted that this distribution is not well established. For instance, it is possible that the galactic halo is flattened into an ellipsoid, and there may be a component of the halo velocity which is rotational and not isotropic.

The phase space distribution, or specifically, the velocity distribution $f(\vec{v})$, is an important characteristic of dark matter that one has to know in an experimental search. The mass distribution in and around the galaxy satisfies the stationary collisionless Boltzman equation:

$$\vec{v} \cdot \nabla f - \nabla\phi \cdot \frac{\partial f}{\partial \vec{v}} = 0. \tag{12}$$

Assuming the form of solution to the above equation is:

$$f = \left(\frac{1}{\pi}\right)^{3/2}\left(\frac{\rho_{\rm o}}{m_{\rm x}}\right)\left(\frac{1}{v_{\rm halo}^3}\right)e^{-(\frac{1}{2}v^2+\phi)/\frac{1}{2}v_{\rm halo}^2}, \tag{13}$$

where contributions to the potential ϕ arise from both density of the visible matter $\rho_{\rm vis}$ which is known in principle and from the dark matter $\rho_{\rm dm}$ which should satisfy the equation:

$$\nabla^2 \phi_{\rm dm} = 4\pi G\rho_{\rm dm}, \tag{14}$$

with

$$\rho_{\rm dm} = \int d^3v[m_{\rm x}f(v)] = \rho_{\rm o}m_{\rm x}e^{-(\phi_{\rm vis}+\phi_{\rm dm})/\frac{1}{2}v_{\rm halo}^2}. \tag{15}$$

Thus we have:

$$\nabla^2 \phi_{\rm dm} = 4\pi G\rho_{\rm o}m_{\rm x}e^{-(\phi_{\rm vis}+\phi_{\rm dm})/\frac{1}{2}v_{\rm halo}^2}. \tag{16}$$

Table 1: Summary of galactic WIMP parameters related to an experimental search.

Quantity	Value	Meaning
ρ_o	$\sim 0.4 - 1$ GeV cm^{-3}	Local density of WIMPs in our galaxy
m_x	$\sim 10 - 10^5$ GeV	WIMP mass
σ_{xt}	$\sim 10^{-38}$ cm^2	WIMP cross section with target nucleus
v_{halo}	$\sim 9.0 \times 10^{-4}$ c	Mean velocity of WIMPs in halo
v_{cut}	$\sim 2.1 \times 10^{-3}$ c	Cutoff velocity of WIMPs in halo
v_{sun}	$\sim 7.3 \times 10^{-4}$ c	Velocity of the Sun around the galactic center
v_{earth}	$\sim 5.0 \times 10^{-5}$ c	Velocity of the Earth around the Sun

We then solve for ϕ_{dm} for a given value of v_{halo} according to the above equation and use ϕ_{dm} to calculate $v(R)$ according to eqn. (5). In order to match the observed $v(R)$, one finds:

$$v_{halo} = \sqrt{< v^2 >} \sim 270 \text{ km s}^{-1}. \tag{17}$$

Thus we obtain a Maxwellian velocity distribution with a cutoff. That is, for $v < v_{cut}$, we have:

$$f(v) = \left(\frac{1}{\pi}\right)^{3/2} \left(\frac{\rho_o}{m_x}\right) \left(\frac{1}{v_{halo}^3}\right) e^{-v^2/v_{halo}^2}, \tag{18}$$

and for $v > v_{cut}$, $f(v) = 0$ because particles with $v > v_{cut}$ cannot be trapped by the system and will escape the galaxy.

We should note that the solar system is moving through this "gas" of dark matter particles with a velocity $\vec{v}_{sun}$ and the Earth is moving around the Sun with a velocity $\vec{v}_{earth}$. Therefore, in lab frame, the velocity distribution becomes:

$$f(v) = \frac{dn}{dv} = \left(\frac{1}{\pi}\right)^{3/2} \left(\frac{\rho_o}{m_x}\right) \left(\frac{1}{v_{halo}^3}\right) e^{-(\vec{v}+\vec{v}_{sun}+\vec{v}_{earth})^2/v_{halo}^2}, \tag{19}$$

and the flux is then given as:

$$\frac{dI}{dv} = v\frac{dn}{dv}. \tag{20}$$

Parameters involved in eqn. (19) are collected in Table 1. We will use this equation when we calculate the recoil energy spectrum.

It is worthwhile to note that there are uncertainties in the above model for the density and velocity distributions of the galactic dark matter. The parameters of our galaxy and especially of the dark halo are not well known: $v_c = 190 - 250$ km s^{-1}, $R_o = 7 - 9$ kpc, and $a = 2 - 10$ kpc. In addition, the halo may not be spherical, but may be flattened

into an ellipsoidal configuration, and the rotation curve may be gently rising or falling at $\sim 15\%$ level. These uncertainties have great impact on the design and interpretation of experimental search. For example, in a WIMP search the detection rate is proportional to ρ_o and $< v >$. In an axion search, the rate is proportional to ρ_o. In a MACHO search, the rate is a complicated function of all the parameters in the halo model.

4 Search for MACHOs via Microlensing

The concept of gravitational microlensing in astronomy has been known for a long time. The idea of using microlensing to observe MACHOs was proposed by Paczyński [13] in 1986. If a large nonluminous object in the halo of our galaxy passes between us and any of the stars in nearby galaxies being monitored, its gravity would act as a microlens, temporarily amplifying the apparent brightness of the star. The method is sensitive to any objects with mass between $10^{-8}\ M_\odot$ and $10^3\ M_\odot$, just the range in which such objects are allowed to exist.

Three collaborations (MACHO [14], EROS [15], and OGLE [16]) are currently conducting searches for MACHOs via gravitational microlensing. Using large optical telescopes equipped with CCD imaging system, they monitored millions of stars, either in Large Magellanic Clouds (LMC) or in the galactic bulge, for signals of microlensing. Three teams all found events with microlensing signature [14, 15, 16].

The beautiful and unique principle in MACHO detection deserves a brief description here. Let D be the distance to a star in target galaxy (for LMC, $D \sim 50$ kpc) and x be the distance to a MACHO in units of D. Let b be the distance of the MACHO from the line of sight between the observer and the star ("impact parameter") and $v_{\rm T}$ be the MACHO velocity in the transverse plane. The magnitude of amplification A as a function of time is given as:

$$A(t) = \frac{u(t)^2 + 2}{u(t)[u(t)^2 + 4]^{1/2}}, \tag{21}$$

and the time duration of the amplification τ is given as:

$$\tau = \frac{r_{\rm e}}{v_{\rm T}}, \tag{22}$$

in which

$$u(t) = \sqrt{\frac{b^2 + v_{\rm T}^2 t^2}{r_{\rm e}^2}}, \tag{23}$$

and $r_{\rm e}$ is the Einstein radius that is given as:

$$r_{\rm e} = \sqrt{\frac{4Gm}{c^2}}\sqrt{Dx(1-x)}. \tag{24}$$

The symmetric light curve of microlensing is easily distinguished from other non-symmetric ones due to variable stars. In Fig. 5, I show several beautiful microlensing events reported

by MACHO collaboration. In an experiment, one measures the symmetric profile $A(t)$, which is characterized by two quantities $A_{\max}$ and τ. However, there are 4 unknowns: x, b, m, and v_{T}. In order to determine mass (and the distribution) of MACHOs, one has to make assumptions and to obtain good satistics. Assuming an isothermal spherical distribution of MACHOs and $dN/dm = \delta(m)$, one can get: $\tau \sim 64\ \mathrm{day}\sqrt{m/m_{\odot}}$ and the most probable masses are $0.01 - 0.4\ M_{\odot}$.

At present, we can conclude that gravitational microlensing has been experimentally established. MACHOs seem to exist either in the galactic halo or in the disc. To determine their masses model-independently, there is a need to have a control. Based on the present statistics, it is still not clear whether the objects that caused the microlensing are numerous enough to make up the galactic dark matter. Recently, the MACHO collaboration [17] asserted that their measurements of nonluminous objects constitute the definite observation of halo dark matter in our galaxy. Furthermore, they calculated that for a standard halo model, MACHOs add up to $\sim 7.6 \times 10^{10}\ M_{\odot}$ and that the MACHO fraction of this dark halo $\leq 20\%$. Further detailed studies are needed to pin down these determinations as more data are accumulated.

5 Experimental Detection of WIMPs

How would we detect WIMPs? If WIMPs fill the galaxy, they must be all around us. The number density $\mathcal{N}$ is estimated to be:

$$\mathcal{N} = \frac{\rho_{\mathrm{x}}}{m_{\mathrm{x}}} \sim 0.01\ \mathrm{cm}^{-3}\left(\frac{\rho_{\mathrm{x}}}{1\ \mathrm{GeV\ cm}^{-3}}\right)\left(\frac{100\ \mathrm{GeV}}{m_{\mathrm{x}}}\right). \tag{25}$$

The average flux $\mathcal{F}$ is then roughly estimated as:

$$\mathcal{F} = \mathcal{N} < v > \sim 10^5\ \mathrm{cm}^{-2}\ \mathrm{sec}^{-1}\left(\frac{\mathcal{N}}{0.01\ \mathrm{cm}^{-3}}\right)\left(\frac{< v >}{10^{-3}\ c}\right). \tag{26}$$

This means that about 10^{14} WIMPs would pass through a human body each day. However, since the cross section is so small (weak scale $\sim 10^{-38}\ \mathrm{cm}^2$) that the majority would pass through us and the Earth unaffected and only ~ 10 per day would interact with atoms in our body. Our goal is to detect and identify WIMPs through their interactions.

5.1 Detection Techniques

The detection of WIMPs is a challenge. The present methods rely upon the fact that when a WIMP collides with a target nucleus, the elastic scattering will cause the target nucleus to recoil. The recoil energy is calculable based on kinematics:

$$E_{\mathrm{r}} = \frac{m_*^2}{m_{\mathrm{t}}} v^2 (1 - \cos\theta), \tag{27}$$

where m_* is the reduced mass of the collision system:

$$m_* = \frac{m_x m_t}{m_x + m_t}, \tag{28}$$

m_t is the target nucleus mass, m_x and v are the mass and velocity of WIMPs, and θ is the scattering angle in center-mass-system. Inputing a typical set of parameters, one immediately finds that:

Signal is weak, on the order of ~ 1 keV amu^{-1}

Nevertheless, this small signal of nuclear recoil can be detected and measured in several ways as shown in Fig. 6.

(1) An atom recoiling from a dark matter collision with nuclei in a semiconductor such as Si and Ge would release free electric charge (ionization) in the material. This can be collected and measured with a good resolution. Semiconductors have a threshold that is suitable for dark matter search. The limitations are the microphonics problem at low energies, the electronic noise, and more importantly the technical difficulties with increasing mass of the crystals.

(2) In some crystals or liquids the recoiling atom causes the emission of a weak but measurable flash of scintillation light. Such scintillation light can be detected by photomultipliers even if only a few photons of light (e. g., ~ 40 photons per keV in NaI) are released. Although scintillators have a reasonably low cost/mass ratio, their resolution is rather poor compared to semiconductors. The advantages are possible pulse shape discrimination and ability to chose non-zero spin target nuclei (such as ^{23}Na, ^{127}I, ^{19}F, ^{129}Xe) which may lead to high axial coupling (e.g., ^{19}F) and the high estimated quenching factor (e.g., liquid Xe).

(3) If a moving atom slows down in a crystal, it will lose its energy in the form of vibrations of phonons which can be detected at temperature close to the absolute zero. A semiconductor or superconductor thermometer enables us to measure phonons and ionization simultaneously, which is crucial for background suppression and/or rejection. The R & D shows promising results and the problem is to reach a stable running conditions with large mass of detectors.

(4) In some crystals like mica, the recoil energy can cause a measurable change in the chemical etching property and the collision events can be traced by measuring small etch pits due to nuclear recoils. The search using ancient mica has the advantage of long exposure time (~ 1 Gyr). The combination of track-etch technique and an atomic force microscope provides reason for optimism that this technique may be the most sensitive one.

I point out that all these techniques have been demonstrated using known particles such as photons or neutrons. The techniques discussed above have been used or under development for WIMP search.

5.2 Expected Signals in Detectors

Now I turn to the expected WIMP recoil signal. The recoil energy spectrum (per unit time and per unit detector mass) can be calculated from:

$$\frac{dN}{dE_r}(E_r) = f_t\left(\frac{N_A\rho_t}{A_t}\right)\left(\frac{\rho_x}{m_x}\right)\int_{v_{min}}^{v_{max}} dv\left\{vf(v)\left[\frac{d\sigma}{dE_r}(v,E_r)\right]\right\}, \tag{29}$$

in which f_t is the fraction of atoms that are responsible for recoils and $(N_A\rho_t/At)$ is the total number of atoms in the material. The integral limits are:

$$v_{min}(E_r) = \sqrt{\frac{m_t E_r}{2m_*}}, \tag{30}$$

and v_{max} is a function of v_{cut}, v_{sun}, and v_{earth}, depending on the time of observation. The velocity distribution of dark matter particles $f(v)$ in eqn. (29) is given in eqn. (19). The differential WIMP cross section $\frac{d\sigma}{dE_r}(v,E_r)$ is usually complicated. In the low energy range of concern here, it can be factorized:

$$\frac{d\sigma}{dE_r}(v,E_r) = \frac{d\sigma}{dE_r}(v,0)\times[F(E_r)]^2, \tag{31}$$

with

$$\frac{d\sigma}{dE_r}(v,0) = \frac{\sigma_{xt}}{E_r^{max}}, \tag{32}$$

$$E_r^{max} = E_r(\theta=\pi) = 2v^2\frac{m_*^2}{m_t}. \tag{33}$$

The nuclear form factor $F(E_r)$ represents the effect due to the finite size of the nucleus and is usually given as:

$$F(E_r) = 3\left[\frac{j_1(qr_o)}{qr_o}\right]e^{-\frac{1}{2}r_*^2q^2}, \tag{34}$$

in which $q^2 = 2m_tE_r$ is momentum transfer, j_1 is spherical Bessel function of index 1, $r_* = 1$ fm, $r_o = (r^2 - 5r_*^2)^{1/2}$, and $r = r_1A^{1/3}$ ($r_1 \sim 1.2$ fm). The nuclear form factor $F(E_r)$ leads to a suppression in the cross section, typically $\sim 1-100\%$. The recoil energy spectrum then becomes:

$$\frac{dN}{dE_r} = \left(\frac{R_o}{< E_r^{max} >}\right)[F(E_r)]^2G(E_r), \tag{35}$$

with

$$R_o = f_t\left(\frac{\rho_t N_t}{A_t}\right)\left(\frac{\rho_x}{m_x}\right)\sigma_{xt} < v >, \tag{36}$$

$$G(E_r) = \frac{< v^2 >}{< v >}\left\langle\frac{1}{v}\right\rangle, \tag{37}$$

where the average of x ($= v^2$, v, and $1/v$) is made for velocity distribution $f(v)$:

$$< x >= \int_{v_{\min}}^{v_{\max}} dv[xf(v)]. \tag{38}$$

If a detector measures a quantity K that is related to E_r by $K = K(E_r)$ and the detector's response function $\mathcal{D}(E_r, K)$ is known, the observed spectrum will be:

$$\frac{dN}{dK} = \int dE_r \left\{ \left[\frac{dN}{dE_r}(E_r) \right] \times \mathcal{D}(E_r, K) \right\}. \tag{39}$$

In some experiments, the range of recoil nuclei, instead of recoil energy, is measured. Since recoil range R_r is a monotonic function of recoil energy E_r for a given detector medium, the above formulation can be easily translated to recoil range spectrum (dN/dR_r). For example, in the mica experiment, one measures the projected range spectrum of recoil nuclei perpendicular to a cleavage plane, $(dN/dR_r^{\perp})$.

The total number of events observed above a threshold E_{th} is obtained as:

$$N(E_{th}) = \int_{E_{th}}^{E_r^{\max}} dE_r \left\{ \left[\frac{dN}{dE_r}(E_r) \right] \times \epsilon(E_r) \right\}, \tag{40}$$

where $\epsilon(E_r)$ is the efficiency of the detector as a function of E_r.

5.3 Event Rate and Background Consideration

Given the WIMP flux and its interaction cross section σ_{xt} with a known target nucleus, the event rate $\mathcal{R}$ is easy to estimate. For a typical set of parameters, we have:

$$\mathcal{R} \sim 0.01\ \mathrm{kg}^{-1}\ \mathrm{day}^{-1} \left(\frac{T_{\exp}}{1\ \mathrm{day}}\right)\left(\frac{W_t}{1\ \mathrm{kg}}\right)\left(\frac{f_t}{10\%}\right)\left(\frac{1\ \mathrm{GeV}}{m_t}\right)$$
$$\times \left(\frac{\rho_{\mathrm{halo}}}{1\ \mathrm{GeV\ cm}^{-3}}\right)\left(\frac{100\ \mathrm{GeV}}{m_x}\right)\left(\frac{\sigma_{xt}}{10^{-38}\ \mathrm{cm}^2}\right)\left(\frac{v_{\mathrm{halo}}}{300\ \mathrm{km\ s}^{-1}}\right). \tag{41}$$

For this set of typical parameters, one finds that:

Event rate is low, on the order of $\sim 0.01\ \mathrm{day}^{-1}\ \mathrm{kg}^{-1}$

Therefore, background, or more precisely signal/noise ratio, is a critical concern for WIMP search. Potential backgrounds come from (1) cosmic ray muons and neutrons and (2) radioactivity both external and internal to the detector. The first source could be avoided by performing the experiment deep underground and by appropriate shielding. The external radioactivity would be minimized by appropriate shielding and by careful choosing surrounding materials. The internal would be minimized by selection and purification of detector material. However, to eliminate/reduce residual radioactivity both external and internal or to increase signal/noise ratio, one has to increase the intrinsic background rejection power of the detector by taking advantage of their different response to the background (electrons) and to the signal (recoil nuclei). This can be done with a pulse shape discrimination (in scintillator) or by the simultaneous measurements of two physical quantities (heat and ionization in bolometer).

5.4 On-going Experiments and Current Limits

Many groups around the world have been trying to detect WIMPs. Three types of detectors (semiconductor, scintillator, and track-etch mica) have been used in the on-going search. Bolometers are in the R & D phase and will be soon used in *in-situ* measurement. Tremendous progress has been made over the past several years, as one sees in Table 2 in which I list most of the searches.

None of the completed experiments so far have found a signal of WIMPs. These negative results are usually presented in the following way. Let me recall that (dN/dE_r) [or equivalently (dN/dR_r)] depends on WIMP parameters: ρ_x, σ, and m_x. Suppose that at a level of $[(dN/dE_r)$ versus $E_r]_{null}$ or $[(dN/dR_r^{\perp})$ versus $R_r^{\perp}]_{null}$, one detects no signal or runs into background. One can then use this null observation to bound on exclusive region in the parameter space (ρ_x, σ, m_x). As a common practice, one assumes $\rho_x \sim 0.4 - 1$ GeV cm^{-3} as known in order for WIMPs to account for all dark matter and considers σ and m_x as unknown. Therefore, a negative result at a level of $[(dN/dE_r)$ versus $E_r]_{null}$ or $[(dN/dR_r^{\perp})$ versus $R_r^{\perp}]_{null}$ is converted to an exclusive plot in a space of (σ versus $m_x)_{\rho_x=\rho_{dm}}$. Caution needs to be expressed in this conversion especially when using these limits to place constraints on the SUSY particle parameters. One needs to consider details in each experiment as event rates depend on whether the interaction cross section of WIMPs with a specific target nucleus used is coherent or incoherent and is spin-dependent [axial coupling $\propto \lambda^2 J(J+1)$] or spin-independent (scalar coupling).

The experimental results obtained from three different techniques are shown in Figs. 7, 8, and 9. We note that the current cross section limit is around 10^{-32} cm^2 for most favorable mass. This limit is several orders of magnitude higher than expected – an indication of how much work remains to be done.

5.5 Signature of WIMPs in Detectors

None of the current experiments are in practice capable of obtaining the signature of WIMPs. The signature that has been discussed extensively in the literature is the annual and seasonal modulation of recoil energy spectrum (not just rate!). However, as one can estimate based on eqns. (19) and (29), the effect is quite small:

Signature is unrobust, a few percent annual or seasonal modulation

Extracting this signature is a challenge when considering low signal/noise ratio and requires large mass detectors and very stable running conditions.

The directionality of a detector is the key to WIMP's signature. In a proposed active search using annealed mica [38], one expects to observe tracks in mica due to WIMPs with forward/backward ratio as high as ~ 100. The signature in this experiment is significant and would be unambiguously identified [39].

Of course, one would identify WIMPs based on the spectrum shape of recoil energy. However, a spectrum is difficult to obtain when one does not have a control (one can not turn off the WIMP flow). Moreover, it is not a valid method for a "threshold"

Table 2: Summary of WIMP search experiments.

Collaboration	Completed	Planned	Site (m.w.e.)	Ref.
SEMICONDUCTOR				
UCSB/UCB/LBL	2×900g Ge	-	Oroville (500)	[18]
Avignone/Drukier	250-1000g Ge	-	Homestake (4400)	[19]
Caltech/Psi/Neuchatel	800g Ge	-	St. Gotthard (3000)	[20]
Zaragoza/PNL/USC	234g Ge	-	Canfranc (675)	[21]
Heidelberg/Moscow	2900g Ge	15kg	Gran Sasso (3500)	[22]
UCSB/UCB/LBL/Saclay	4×17g Si	-	Oroville (500)	[23]
SCINTILLATOR				
Beijing/Paris/Roma/Saclay	7kg NaI(Tl)	100kg	Gran Sasso (3500)	[24]
Beijing/Paris/Roma/Saclay	360g CaF_2(Eu)	-	Gran Sasso (3500)	[24]
Zaragoza/PNL/USC	3×10.7kg NaI(Tl)	-	Canfranc (675)	[25]
Osaka (Japan)	36.5kg NaI(Tl)	-	Kamioka (2400)	[26]
Imp. Coll./Oxford/Rutherford	1kg NaI	50kg	Boulby (3000)	[27]
Imp. Coll./Oxford/Rutherford	CaF_2 (Eu)	-	Boulby (3000)	[28]
Imp. Coll./Oxford/Rutherford	C_6F_6	-	Boulby (3000)	[28]
DAMA (Roma)	3.5kg Liq. Xe	-	Gran Sasso (3500)	[29]
Imp. Coll./Oxford/Rutherford	1kg Solid Xe	-	Boulby (3000)	[30]
BOLOMETER				
CfPA/Stanford/UCSB/INR	60g Ge	1kg	Stanford (17)	[31]
Munich	31g Al_2O_3	1kg	Gran Sasso (3500)	[32]
CEA/IN_2P_3/INSU	24g Al_2O_3	-	Fréjus (4800)	[33]
Tokyo	2.8g LiF	1kg	Kamioka (2400)	[34]
Imp. Coll./Oxford/Rutherford	32g LiF	-	Boulby (3000)	[35]
Milano	100g LiF	-	Gran Sasso (3500)	[36]
Milano	30g NaF	-	Gran Sasso (3500)	[36]
TRACK-ETCH				
Berkeley (Passive)	0.08mm^2 ancient mica	-	–	[37]
Berkeley (Active)	1m^2 annealed mica	-	Berkeley (90)	[38]

detector. The mica technique measures, in principle, the spectrum of projected recoil range. However, due to residual fission tracks, there is only a narrow window for WIMPs, making it like a "threshold" detector. Other identifications may include the behavior of the signal as a function of the material and the spatial distribution of the energy deposition in the detector.

6 Concluding Remarks

Nothing is more puzzling than the fact that more than 90% of matter in the Universe is dark. In the quest for understanding what makes up the majority of the Universe, the crucial point and real challenge is to detect and identify this unknown matter. Much progress has been made in the past couple of years and is highlighted by microlensing observations of MACHOs and competitive searches for WIMPs.

In MACHO search, the microlensing technique has been experimentally established. However, many questions remain unanswered including the key one: "Is the galactic halo made of MACHOs only?" The current data seem to show some confusions. To make it extreme, as new results come to exist, more questions are being raised than answered. To be certain that the objects responsible for microlensing events are unambiguously caused by MACHOs and to determine $\Omega_{\rm MACHO}$ in the galactic halo with good accuracy, further studies with much higher statistics are needed in the upcoming years.

In WIMP search, the experimental challenge, as I demonstrated before, is triply difficult:

$$\boxed{\textbf{WIMP Detection} \Longleftrightarrow \textbf{Weak Signal} \oplus \textbf{Low Rate} \oplus \textbf{Unrobust Signature}}$$

In other words, detectors need to be operated near threshold with small signal/noise ratio, and yet the signature is not robust. The short-term goal is to improve the background rejection power and increase the mass of the detectors.

Further improvement with semiconductor ionization detectors operated at liquid nitrogen temperature is expected. But the improvement will be limited, as we will reach the detector limit soon. With scintillators it has proved to be practical to increase the mass (like NaI) and to have spin-dependent nuclei (like CaF_2). There is some hope to study annual modulation effect of WIMP signal in the next BPRS run. Calorimeters represent the most ambitious R & D, particularly by measuring two physical quantities (heat + ionization or heat + scintillation). The technique has potential to reject background and to provide more stringent limits when it starts *in-situ* run. The ancient mica search will soon improve the limit by a factor of ~ 100 or so.

Other searches include those for candidates like axions, light neutrinos, and other exotics. In particular, the axion is a very attractive scenario. If it is discovered, it will solve not only dark matter problem but also the strong CP problem. There are also many indirect searches for WIMPs which I did not cover in my talk. Interested readers may find discussions in Ref. [4].

There is no doubt that the discovery of dark matter particles would be of great significance in cosmology, astrophysics, and particle physics. An improvement of several orders

of magnitude in sensitivity is necessary if one is to carry out a meaningful search for SUSY candidates. Needless to say, a positive result is a prize worth winning. However, as we all know, the game of any search has its intrinsic feature that a negative return is always a possibility. What if one does not succeed? Well, the first thing I can imagine is that we are still left wondering what the Universe is about (the dark matter problem is still there!). Second thing might be that we would place some tight constraints on the SUSY or even rule out the theory under the assumption that LSP makes $\Omega = 1$. This is wonderful, but to me in some sense, is no more interesting than saying that "SUSY is too naive for $\Omega_{\rm LSP} \sim O(1)$" or "SUSY may be still right but $\Omega_{\rm LSP} << 1$". Let me close my talk by saying that things puzzling or beyond our reach today may turn out be natural and simple tomorrow. The large portion of the dark matter story, either optimistic or pessimistic, remains to be told.

Acknowledgements

My interest in dark matter has been developed through my peripheral involvement in the Berkeley mica project with Dr. Dan Snowden-Ifft and Prof. Buford Price over the past several years, to whom I am indebted. Prof. Linkai Ding, Prof. Buford Price, Prof. Bernard Sadoulet, and Dr. Dan Snowden-Ifft have read the manuscript and made useful comments.

References

[1] V. A. Trimble, Rev. Astron. Astrophys. **25**, 425 (1987).

[2] P. J. E. Peebles, *Principles of Physical Cosmology*, (Princeton, 1993).

[3] E. W. Kolb and M. S. Turner, *The Early Universe*, (Addison-Wesley, 1990).

[4] J. R. Primack, D. Seckel, and B. Sadoulet, Ann. Rev. Nucl. Part. Sci. **38**, 751 (1988).

[5] P. F. Smith and J. D. Lewin, Phys. Rep. **187**, 203 (1990).

[6] A. Dekel, Nucl. Phys. B **S38**, 425 (1995).

[7] R. H. Sanders and K. G. Begeman, Mon. Not. Roy. Astron. Soc. **267**, 283 (1994); R. H. Sanders, Astron. Astrophys. **2**, 1 (1990).

[8] H. H. Soleng, General Relativity and Gravitation, **27**, 367 (1995).

[9] J. R. Primack, J. Holtzman, A. Klypin, and D. O. Caldwell, Phys. Rev. Lett. **74**, 2160 (1995).

[10] M. Drees and M. M. Nojiri, Phys. Rev. D **48**, 3483 (1993).

[11] G. L. Kane, Nucl. Phys. B **38**, 300 (1993).

[12] R. Cowsik, in *Proc. Intern. Cosmic Ray Conf.*, Dublin ,**5**, 82 (1991).

[13] B. Paczyński, Astrophys. J. **304**, 1 (1986).

[14] C. Alcock *et al.* (MACHO Coll.), Nature **365**, 621 (1993).

[15] E. Aubourg *et al.* (EROS Coll.), Nature **365**, 623 (1993).

[16] A. Udalski *et al.* (OGLE Coll.), Acta Astron. **43**, 289 (1993).

[17] C. Alcock *et al.* (MACHO Coll.), Phys. Rev. Lett. **74**, 2867 (1995).

[18] D. O. Caldwell *et al.*, Phys. Rev. Lett. **61**, 510 (1988).

[19] A. K. Drukier *et al.*, Nucl. Phys. B (Proc. Suppl.) **28A**, 293 (1992).

[20] D. Reusser *et al.*, Phys. Lett. B **255**, 143 (1991).

[21] E. Garcia *et al.*, Phys. Rev. D **51**, 1458 (1995).

[22] M. Beck *et al.*, Phys. Lett. B **336**, 141 (1994).

[23] D. O. Caldwell *et al.*, Phys. Rev. Lett. **65**, 1305 (1990).

[24] C. Bacci *et al.*, (BPRS Coll.), Phys. Lett. B **293**, 460 (1992).

[25] M. S. Sarsa (Zaragoza/PNL/USC Coll.), TAUP'93 (Gran Sasso).

[26] K. Fushimi *et al.*, Phys. Rev. C **47**, R425 (1993).

[27] G. J. Davies *et al.*, Phys. Lett. B **321**, 156 (1994).

[28] G. J. Davies *et al.*, Phys. Lett. B **322**, 159 (1994).

[29] P. Belli *et al.*, Nucl. Instr. Meth. A **336**, 336 (1993).

[30] G. J. Davies *et al.*, Phys. Lett. B **320**, 395 (1994).

[31] T. Shutt *et al.*, Physica B **194** 1201 (1994); Phys. Rev. Lett. **69**, 3425 (1992).

[32] W. Seidel *et al.*, J. Low Temperature Phys. **93**, 797 (1993).

[33] N. Coron *et al.*, Astron. Astrophys. **278**, L31 (1993).

[34] M. Minowa *et al.*, Nucl. Instr. Meth. A **327**, 612 (1993).

[35] P. F. Smith *et al.*, Phys. Lett. B **265**, 454 (1990).

[36] A. Alessandrello *et al.*, Nucl. Instr. Meth A **344**, 243 (1994).

[37] D. P. Snowden-Ifft, E. S. Freeman, and P. B. Price, Phys. Rev. Lett. **74**, 4133 (1995).

[38] D. P. Snowden-Ifft, Y. D. He, and P. B. Price, in *Proc. Intern. Conf. on Trends in Astroparticle Physics*, Santa Monica, California, eds. D. B. Cline and R. Peccei, (World Scientific, Singapore, 1992), 440.

[39] Y. D. He, "Direct detection of WIMPs with mica", Report (unpublished) (1991).

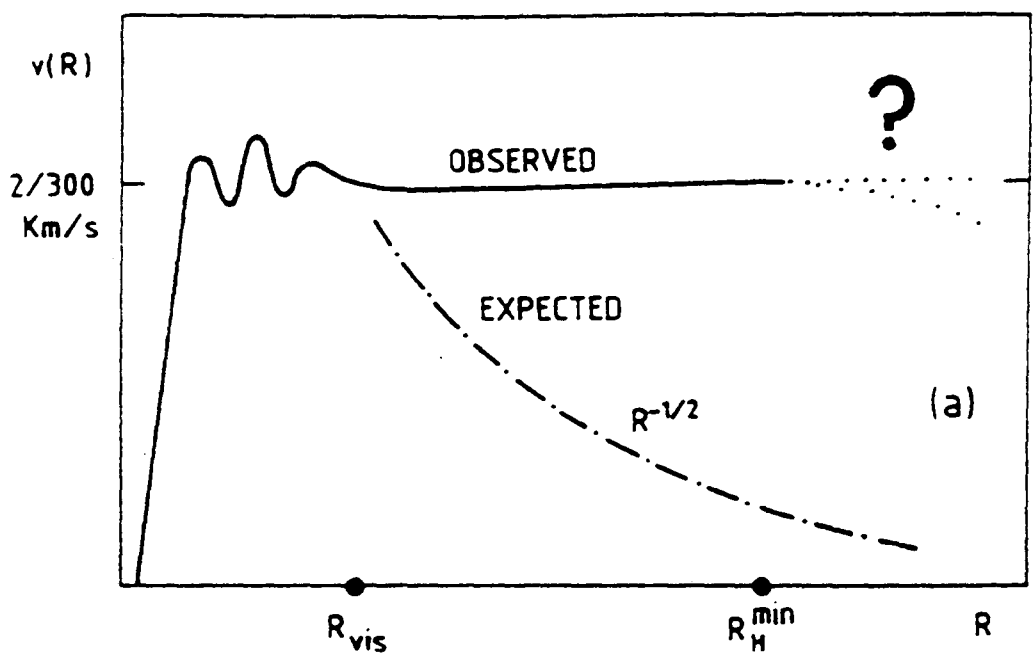

Fig. 1 A schematic example of rotation curves for spiral galaxies. The rotation velocity reaches constant at 200 km s^{-1} when $R > R_{vis}$.

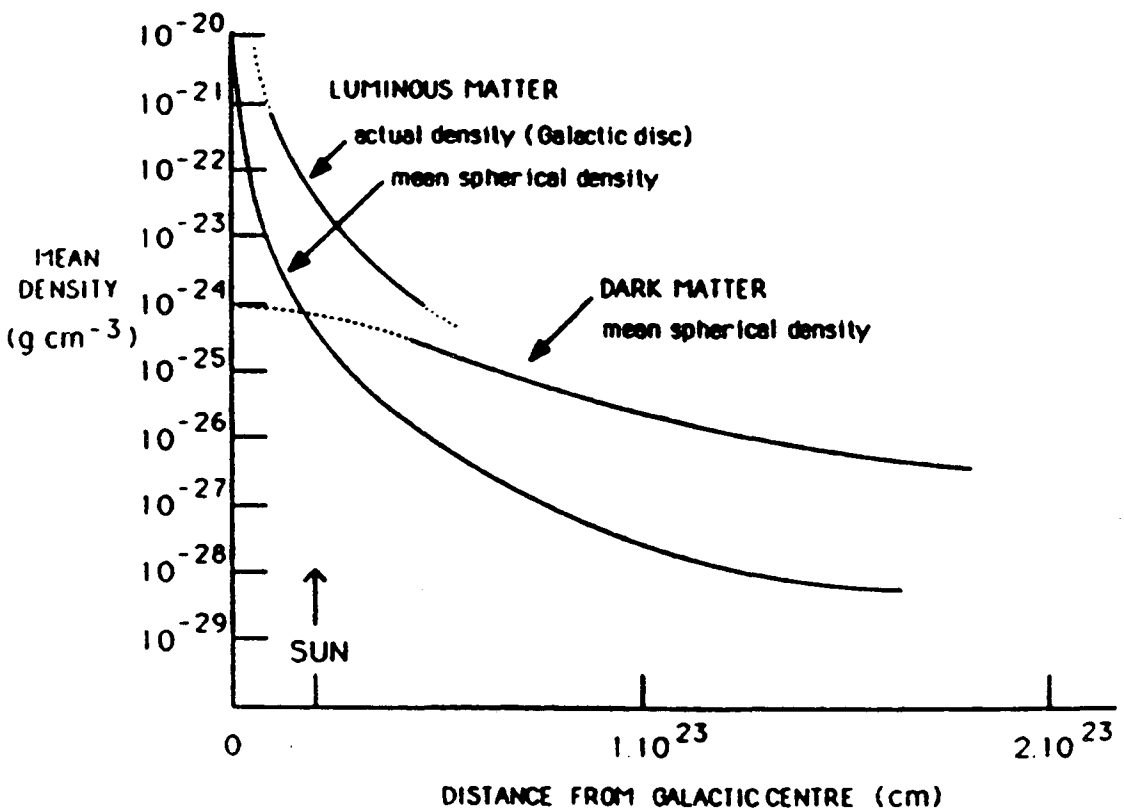

Fig. 2 Radial distribution of luminous and dark matter in the galaxy. There is a dark halo which extends well beyond the visible matter and counts for $\sim$ 90% of the total galactic mass.

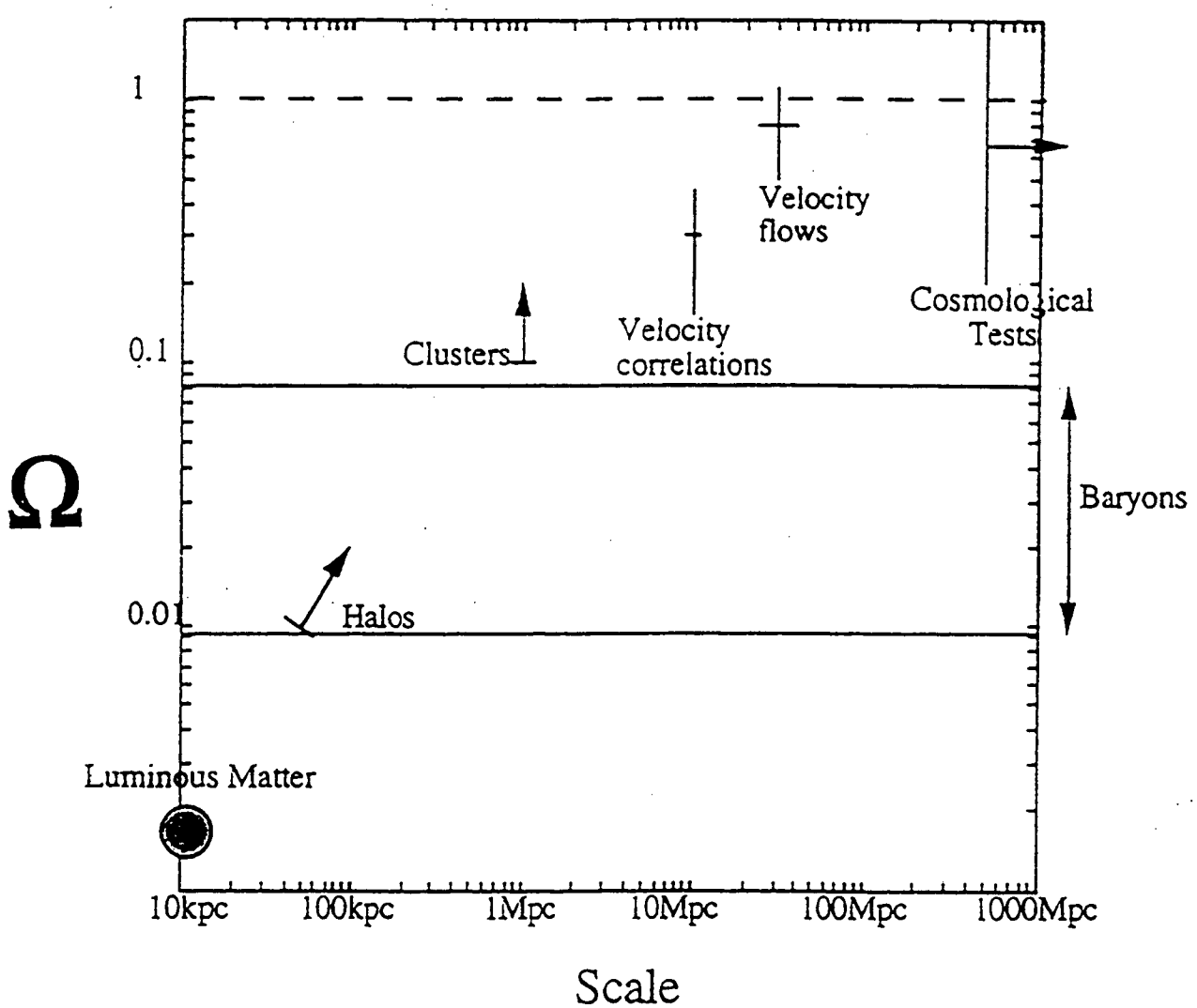

Fig. 3 Matter abundance measured at various scales in our Universe, indicating the mass deficits on all scales.

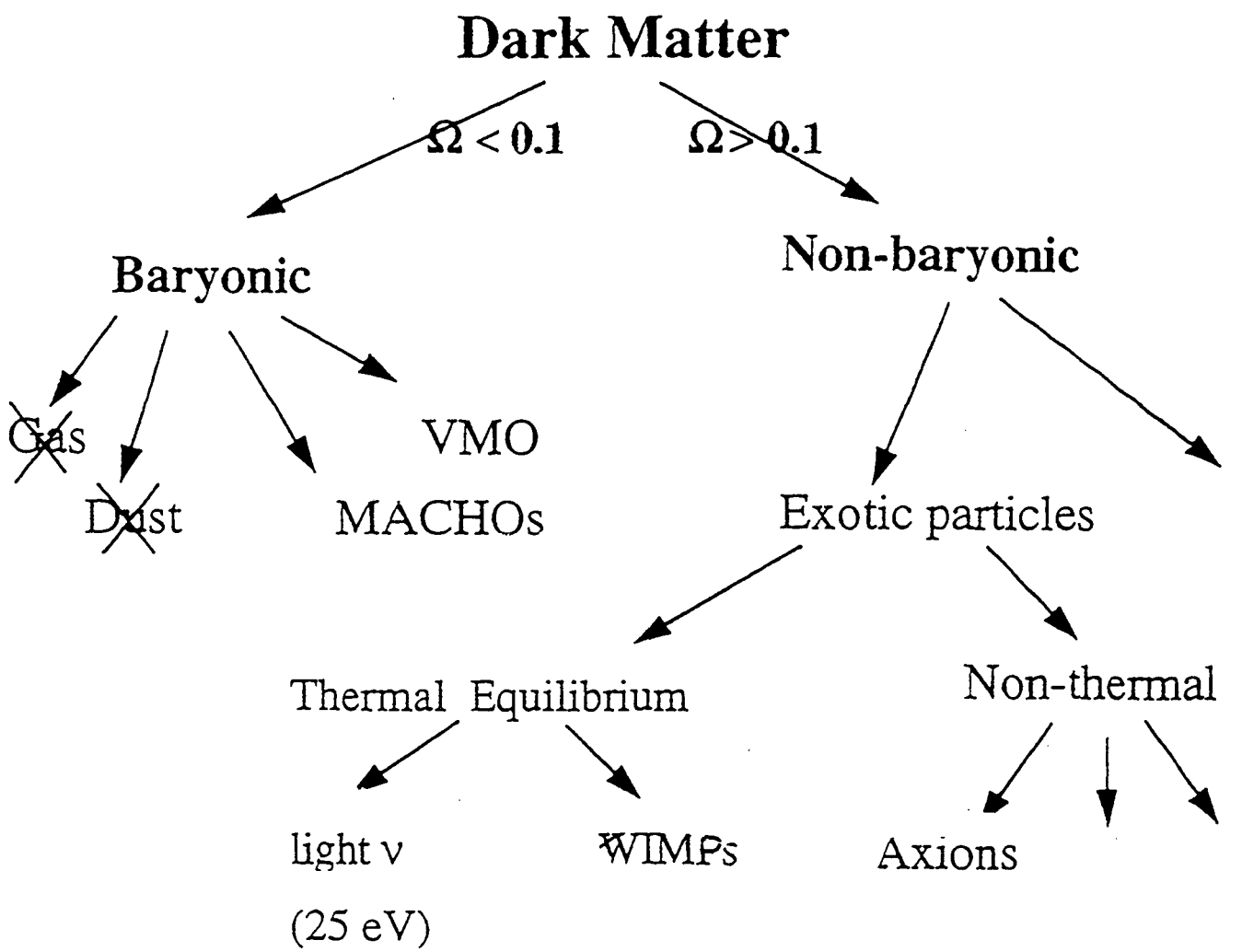

Fig. 4 Present classification of dark matter candidates. See text for detailed discussions.

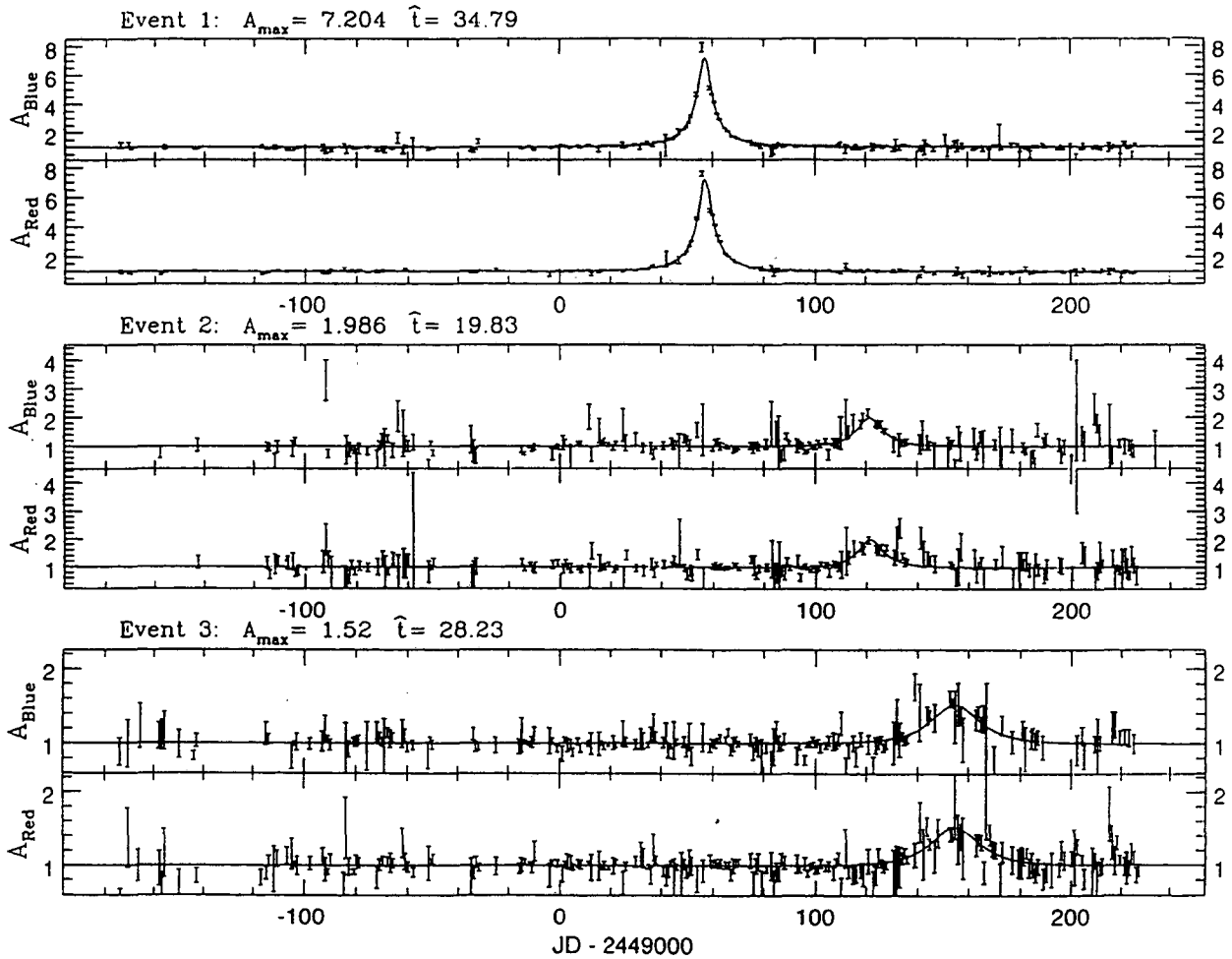

Fig. 5 Some gravitational microlensing events observed by MACHO collaboration. The light curves are taken from [17].

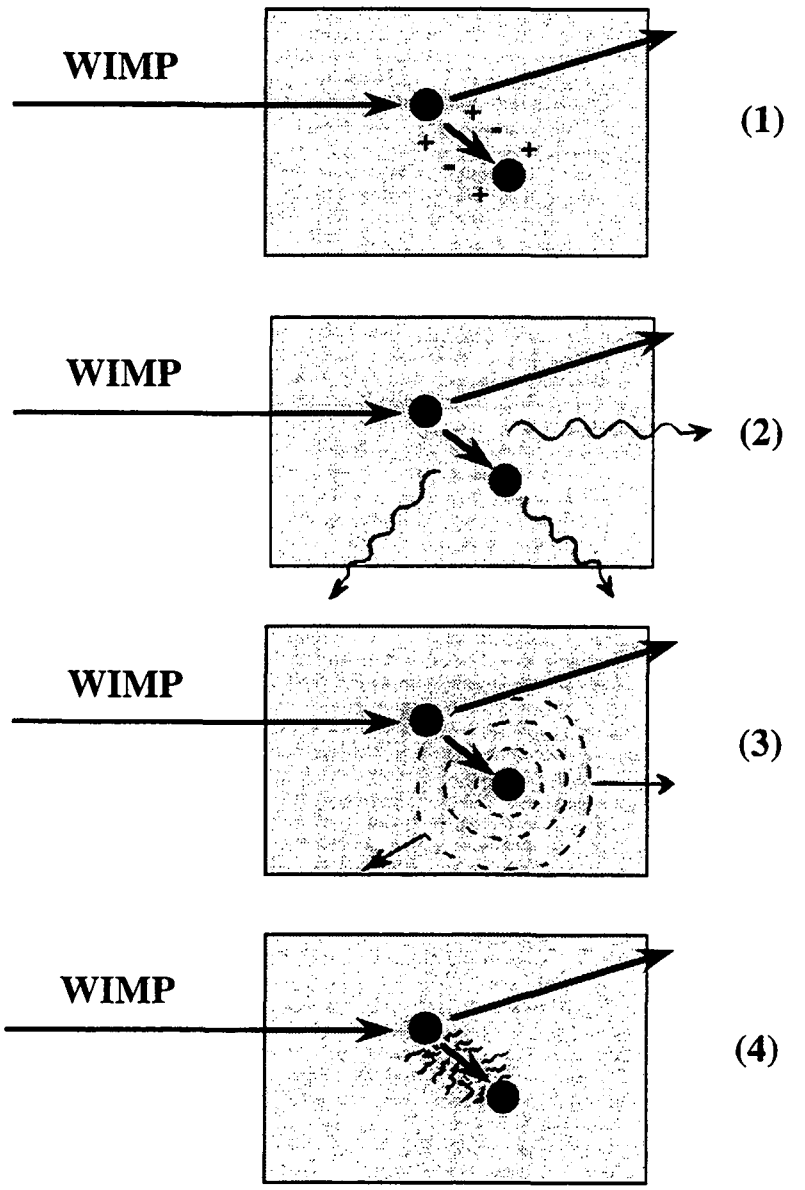

Fig. 6 A WIMP is "detected" by measuring nuclear recoil that WIMP imparts to a target nucleus in an elastic collision of WIMPs via (1) a small current arising from ionization in semiconductors; (2) a flash of scintillation lights in crystal or liquid scintillators; (4) a shower of phonons or a tiny increase in temperature in superconductor; or (4) an etching-revealable damage in solid state track detectors.

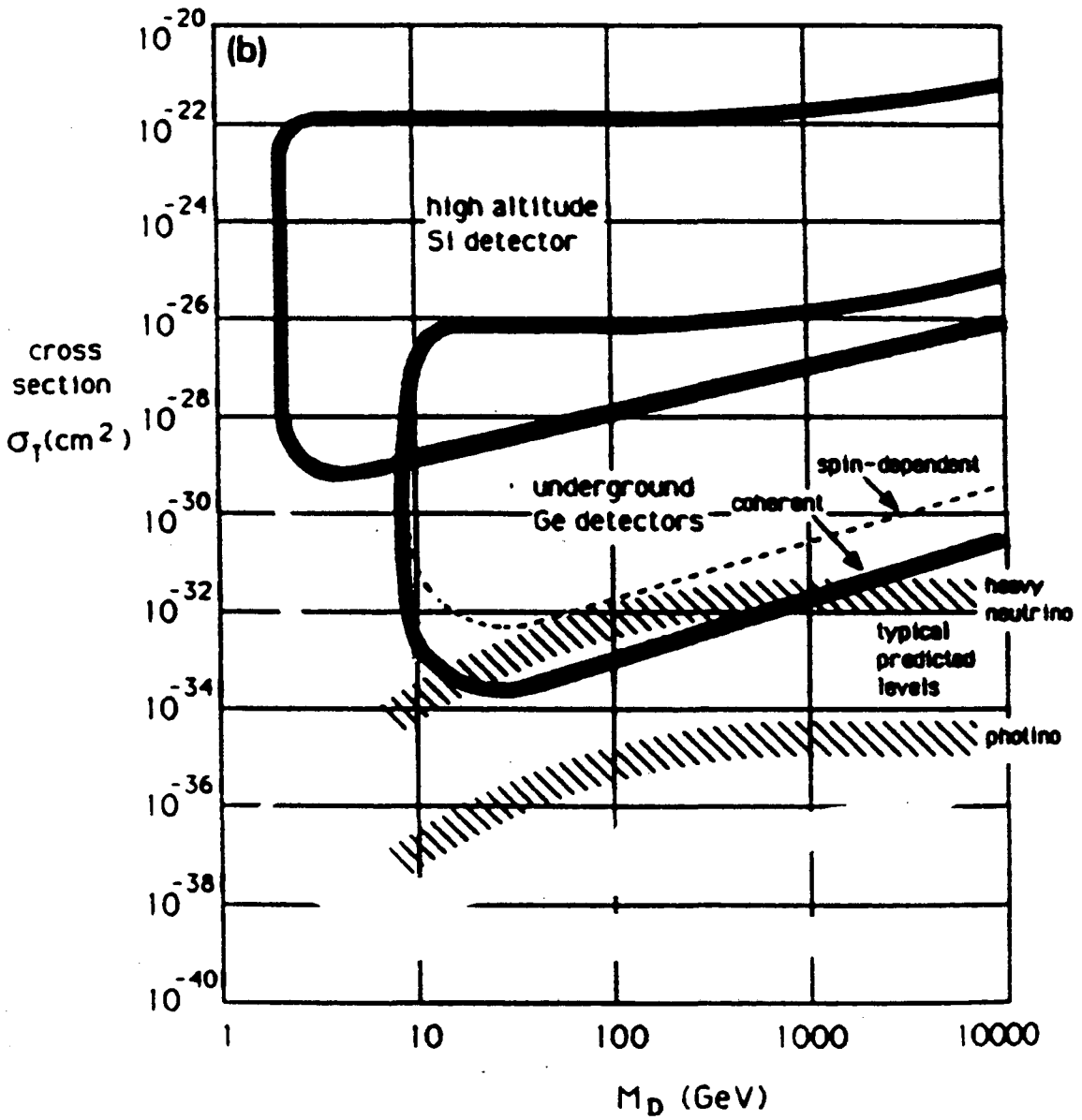

Fig. 7 Exclusive plot of WIMP cross section as a function of WIMP mass obtained by Ge experiment [18].

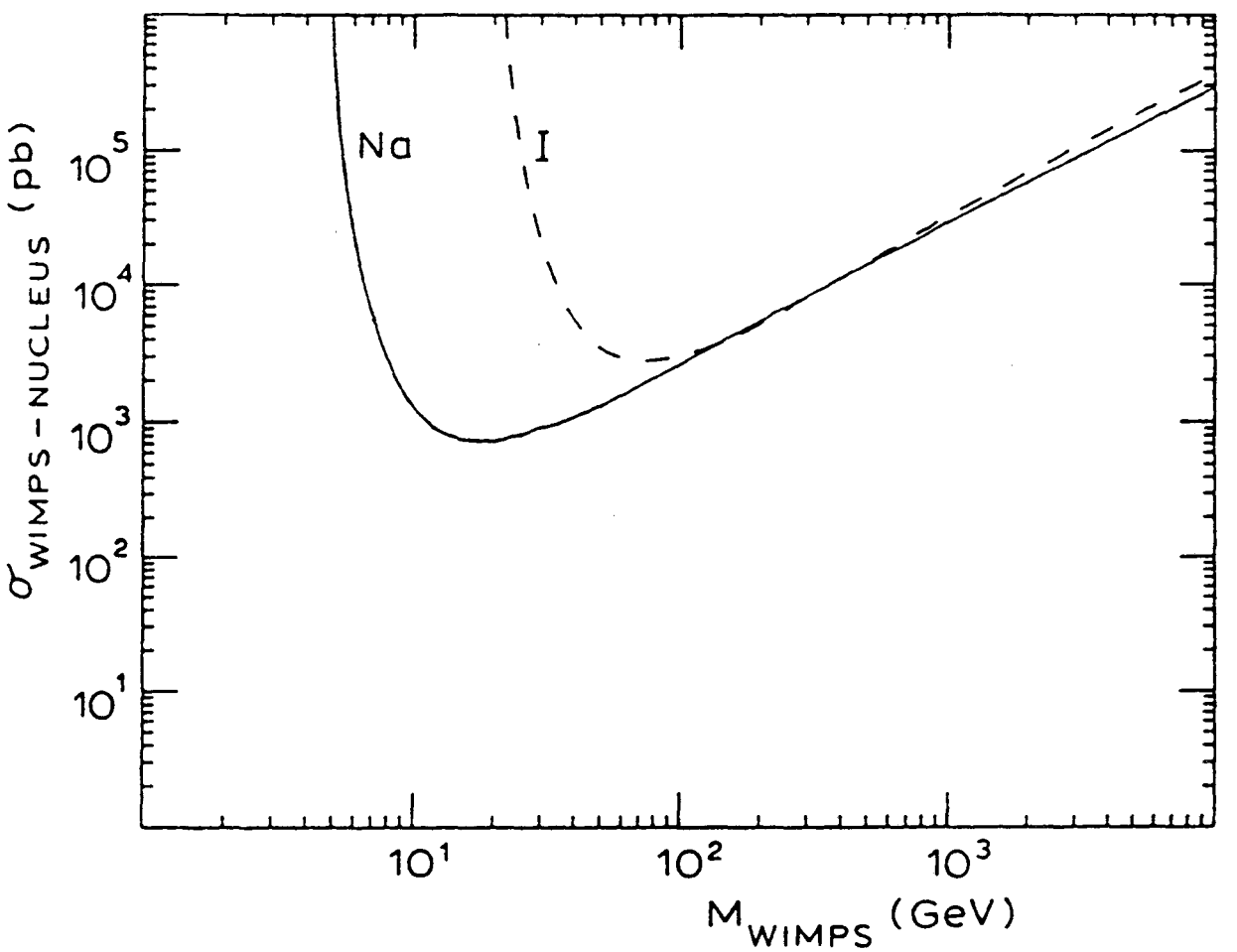

Fig. 8 Exclusive plot of WIMP cross section as a function of WIMP mass obtained with NaI by BPRS collaboration [24].

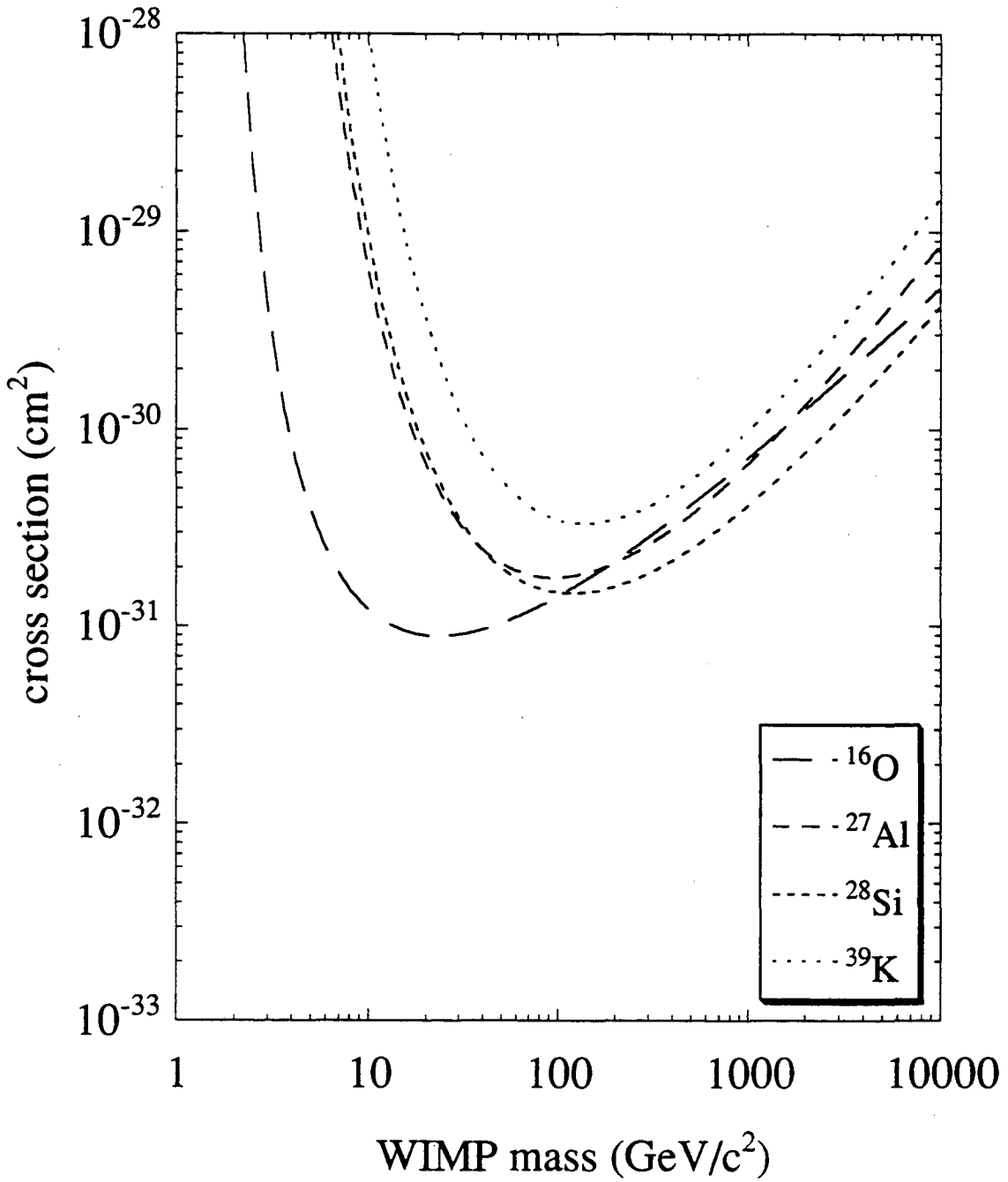

Fig. 9 Exclusive plot of WIMP cross section as a function of WIMP mass obtained using ancient mica [37].

SEARCH FOR STRANGE QUARK MATTER[1]

Yudong He[2]
Department of Physics, Space Science Laboratory
and Center for Particle Astrophysics
University of California at Berkeley, Berkeley, CA 94720, USA
and
Institute for Nuclear and Particle Astrophysics
and Nuclear Science Division
Lawrence Berkeley National Laboratory, Berkeley, CA 94720, USA

Abstract

In the last decade, considerable theoretical and experimental interests have focused on the fascinating possibility that quark matter consisting of up, down, and strange quarks may be metastable or might even be absolutely stable. I first review the theoretical background of this hypothetical matter. I then discuss some interesting consequences of strange matter in cosmology and astrophysics. I finally summarize various searches for strange quark matter in terrestrial materials, in galactic cosmic rays, and in heavy ion collisions. Future directions are also discussed from an experimentist point of view.

1 Physics of Strange Quark Matter

In 1984 Witten [1] conjectured that quark matter consisting of roughly equal numbers of up, down, and strange quarks may be more stable than ordinary nuclear matter. Calculations by Farhi and Jaffe [2] using the MIT bag model indicate that this may be indeed the case for a wide range of parameters including the strange quark mass m_s, the bag constant B, and the QCD coupling α_c[3]. Fig. 1 shows contours of energy per baryon for a bulk strange quark matter in a parameter space of m_s versus B for $\alpha_c = 0$, 0.3, 0.6, and 0.9. There have been attempts to study the properties of strange matter in bulk and in finite lumps ($100 < A < 10^7$) which are often called strangelets [3]. Recent study of Gilson and Jaffe [4] addressed the stability of very small strangelets. They found that for system parameters such that strange matter is unbound in bulk, there may still exist strangelets with $A < 100$ that are metastable. However, they cannot determine whether the lifetime

[1]This topic is one of a series of lectures on "Current Trends in Non-Accelerator Particle Physics" given at CCAST Workshop on Tibet Cosmic Ray Experiment and Related Physics Topics and CCAST Workshop on Ultrarelativistic Heavy Ion Collisions, Beijing, April 4-13, 1995. This work was supported in part by the U. S. Department of Energy under Contract No. DE-AC03-76SF00098.

[2]Mailing address: Department of Physics, University of California, Berkeley, CA 94720, USA. Email address: yudong@physics.berkeley.edu.

[3]$B^{1/4}$ is the energy difference between the vacuum energy and the energy inside the bag. Parameters obtained from bag model fits to light hadron spectra are $B^{1/4} = 100 - 200$ MeV, $m_s = 100 - 300$ MeV, and $\alpha_s = 0 - 0.9$.

of these strangelets is sufficient to detect them in current accelerator experiments. An excellent introduction to the subject can be found in Ref. [5].

1.1 Formation of Strange Quark Matter

Nuclear matter is believed to undergo a phase transition to quark matter when the temperature and density are sufficiently high. When formed from protons and neutrons, quark matter is composed mostly of up and down quarks immediately after the phase transition. If the chemical potential of the quark gas is higher than the mass of the strange quark, weak interactions such as $\mathrm{u} + \mathrm{d} \leftrightarrow \mathrm{u} + \mathrm{s}$ or $\mathrm{u} \leftrightarrow \mathrm{s} + \mathrm{e}^+ + \nu_\mathrm{e}$ will convert up and down quarks to strange quarks. The strange quarks introduce more degrees of freedom and consequently lower the energy of the system as illustrated in Fig. 2. The conversion to strange quarks will continue until the Fermi energies of all flavors are the same and the energy per baryon has dropped by a factor of r [$r = (2/3)^{1/4} \simeq 0.904$ for $m_\mathrm{s} = 0$; if $0 < m_\mathrm{s} < 300$ MeV, $0.904 < r < 1$]. I emphasize that flavor equilibrium is established via weak interaction. Note that other flavor of quarks (charm, beauty, and top) do not appear because their masses are larger than the Fermi energy of the nonstrange quark system (~ 300 MeV). It is certain, in the light of energy, that the 3-flavor strange quark matter is more bound than the 2-flavor nonstrange quark matter. The fact that symmetry and energy consideration favor the appearance of strange quarks in quark matter at and above nuclear matter densities was certainly well known in 70's [4]. For example, Bodmer [7] has discussed the idea of strange multiquark droplets. Chin and Kerman [8] speculated that such a strange multiquark matter may exist as long-lived exotic forms of nuclear matter inside stars. The possibility that strange quark matter could actually have lower energy than nuclear matter is the key point of Witten's proposal [1].

1.2 Mass Formula for Strange Quark Matter

To predict the energy per baryon (E/A) of strange quark matter ${}^S A^Z$, a mass formula was developed by Berger and Jaffe using a phenomenological approach [9]. The formula was modified later by Madsen [10] to include curvature contributions. The energy per baryon is expressed as a function of the charge Z, the baryon number A, and the hypercharge $Y = A + S$. There are three parameters in the formula: the energy per baryon in the bulk limit ϵ_o[5], the mass of strange quark matter m_s, and the uncertainty in the curvature term c. Their values are not well known, but $\epsilon_\mathrm{o} \sim 850$ to 900 MeV, $m_\mathrm{s} \sim 150$ MeV, and $c \sim 0.5$ to 1. This formula assumes that $-S/A \sim 1$ so that all of the quarks are roaming freely inside of the nuclear "bag". In other words, the quarks are not confined to separate particles such as protons, neutrons, lambdas, etc. Including the curvature term, the mass formula can be expressed as:

[4] Alcock and Olinto [6] noted that "There is nothing in Witten's seminal paper that could not have been done in 1974". It is somehow really curious that the strange quark matter was not raised earlier, given the long history of discussions on quark matter.

[5] Note ϵ_o carries the same information as the bag constant B.

$$E({}^{S}A^{Z}) = \epsilon_o A + \frac{1}{2}\Delta_Y(Y - Y_{\min})^2 + \frac{1}{2}\Delta_Z(Z - Z_{\min})^2 + c\left(4\pi\Omega_{s,s,o}\rho_o^2 A^{2/3} + \frac{g\mu^2\rho_o}{6\pi}A^{1/3}\right), \quad (1)$$

analogous to the Bethe-Weizsäcker semiempirical mass formula in nuclear physics. In eqn. (1), the coefficients depend on ϵ_o, m_s, and c and all can be found in Ref. [9, 10]. Desai *et al.* [11] developed an approximation to this formula for $m_s = 150$ MeV that is very accurate for changes in ϵ_o within the interested range:

$$E({}^{S}A^{Z}) = \epsilon_o\left\{A + \frac{0.10}{A}(Y - Y_{\min})^2 + \left[\frac{0.10}{A} + \frac{0.0010}{A^{1/3}}\right](Z - Z_{\min})^2 + c(0.097A^{2/3} + 0.32A^{1/3})\right\}, \quad (2)$$

where

$$Y_{\min} = 0.24 \times 10^{-3}(\text{MeV})^{-1}\epsilon_o A, \quad (3)$$

$$Z_{\min} = \frac{9.7A}{A^{2/3} + 96.0}. \quad (4)$$

However, coefficients in eqn. (2) must be reevaluated using eqn. (1) for changes in m_s.

1.3 Strange Hadronic Matter

As strangeness remains a largely unexplored degree of freedom in strongly interacting systems, there also have been wide discussions on strange hadronic matter, a large class of bound multistrange hadronic objects. Strange hadronic matter or metastable exotic multihypernuclear objects (MEMOs) would be formed from combinations of p, n, Λ, Ξ baryons, which are stable against strong decay. This is quite different from strange quark matter, as strange quark matter is quark matter in which the quarks (u, d, and s in approximately equal numbers) are confined to a single large bag where the binding arises from residual gluon interactions. Hadronic matter are bound states of hyperons and nucleons where the binding arises from attractive nuclear fields. In this case, the strange quarks are localized within individual hyperons, which are assumed to retain their identity in the bound system. Hyperons are distinguishable from nucleons, and so can occupy shell-model states of the same orbital angular momentum and total spin as nucleons. A similar mass formula has been developed for strange hadronic matter by Dover and Gal [12]. Discussions on this topic and related references can be found in Schaffner *et al.* [13] and Dover and Gal [12].

1.4 Problems in Theory

Is strange quark matter really stable from a theoretical point of view? The immediate answer is "we do not know". First, uncertainties in the model parameters make this difficult to determine definitely. Second and more important, the applicability of perturbative QCD theory in the strong coupling limit is questionable. Present calculations are in fact incapable of deciding if strange matter is stable or not. No QCD based calculation schemes predict the energy per baryon of strange matter to even 100 MeV accuracy

which is much worse than the accuracy needed to answer the question. Furthermore, is strangeness a good observable degree of freedom? Is the mass of strange quarks we are talking about algebra mass, current mass, or something else? Apparently, the theory that embodies our current understanding of physics does not enable us to answer these questions, but pointing toward an attractive possibility. Answers to these questions can be only obtained from astrophysical observations and laboratory experiments.

Strange quark matter would fill the void of 55 orders of magnitude between known nuclides and the ultradense neutron stars as shown in Fig. 3. In this window, no form of nuclear matter has been discovered so far and is called nuclear desert. It is amusing why physics forbid nuclear particles from assembling themselves into objects that could fill in this "desert". Could this nuclear desert be actually filled with new forms of matter, different in structure from ordinary nuclear matter, that we have failed to find?

The hypothesis of strange quark matter has many striking phenomenological consequences in cosmology, astrophysics, physics, and chemistry as shown in Fig. 4. One of potential applications is to grow drops of strange matter to provide a compact energy source [14]. Applications in chemistry are also possible but will not be discussed in this paper.

2 Cosmological Consequences of Strange Matter

2.1 Quark Nuggets: Dark Matter Candidates?

Strange quark matter was originally conceived by Witten [1] as a dark matter[6] candidate that might have been made in the early Universe when temperature was $T \sim 100$ to 200 MeV. The quark nuggets as relics of the phase transition are an attractive candidate for cold dark matter. However, subsequent work has shown that strange matter could not survive later than one second in the early Universe and therefore is not a plausible dark matter candidate. In particular, Witten's model for the formation of quark nuggets was criticized by Applegate and Hogan [15]. Possible influence of quark nuggets on primordial nucleosynthesis of light elements was considered by Schaeffer *et al.* [16]. Madsen and Riisager [17] have particularly discussed big bang helium synthesis. Boyd and Saito [18] have discussed the production of light strange quark matter nuggets from spallation. Schaeffer [19] also studied primordial fluctuations in a universe dominated by quark nuggets.

2.2 Evaporation and Boiling: Survival or Not?

Alcock and Farhi [20] showed, on the grounds of thermodynamic consideration, that even if nuggets of strange quarks were formed, they would have evaporated as the Universe cooled down to $T \sim 2$ MeV. However, this calculation was criticized by Madsen *et al.* [21]. Madsen and Olesen [22] studied the boiling of strange quark matter. Lee and Lee

[6]For an introduction to dark matter problem, see Yudong He, "Detection of Dark Matter", this proceedings.

[23] pointed out that boiling is an important mechanism by which strange quark lumps may be dissolved as the temperature goes down. They showed that it is unlikely that any strange matter lumps formed in the early Universe could have survived boiling. They concluded that quark nuggets with A as low as 10^{46} might survive evaporation.

2.3 Flux of Quark Nuggets or Nuclearites

As the issue of survival of quark nuggets is so controversial, no one has realistically calculated the flux of relic quark nuggets. Instead, one can assume that the relic quark nugget constitutes a certain fraction of dark matter, and then use experimental limits to constrain the theoretical model of evaporation and creation of quark nuggets. In a later section, I will discuss experimental searches for quark nuggets in galactic cosmic rays.

3 Astrophysical Consequences of Strange Matter

3.1 Neutron Stars or Strange Stars?

In astrophysics, strange matter is conjectured to appear in late stages of stellar evolution like neutron star and type II supernova. If the strange matter is stable it is likely that what were thought of as neutron stars are probably made of strange matter, not of neutron matter, and should be called strange stars. It is possible that the central density of an ordinary neutron star is high enough so that a conversion to 2-flavor quark matter occurs. The 2-flavor quark matter readily converts to strange matter so that the star would have strange central core. This core would be surrounded by neutrons and will absorb neutrons, so that the core would grow, consuming the entire star. Comments on strange stars have been made by Bethe *et al.* [24]. The question is: What are the observable properties that would distinguish strange stars from conventional neutron stars?

3.2 Global Properties of Strange Stars

The global properties of strange stars have been discussed by Witten [1], Haensel *et al.* [25], and Alcock, Farhi, and Olinto [26]. In particular, the structure of stellar objects composed of strange matter was studied by Alcock, Farhi, and Olinto [26]. Strange stars have very different equations of state from ordinary neutron stars. An ordinary neutron star is held together gravitationally and the equation of state has a property such that as the pressure goes to zero the density goes to zero. Strange stars have a nonvanishing density at zero pressure and small lumps, which are not gravitationally bound, are self-bound. Consequently, its relation between mass and radius ($M \propto R^3$) is different from that of neutron stars (M decreases with increasing R). In Fig. 5, the relation for strange stars is compared to those calculated using different conventional equations of state for neutron stars. However, all neutron/strange stars for which masses have been determined have masses near $1.4M_\odot$, where the two models of compact stars have very similar radii.

Should a very low mass compact star be discovered, the two pictures would be easily distinguishable.

Since a strange star is more compact than a neutron star, it would rotate more rapidly than a neutron star. Glendenning [27] has discussed this issue. The observation of 0.5 ms pulsar would be a strong evidence for a strange star since ordinary neutron stars cannot spin this rapidly. In addition, test of a strange matter pulsar by observation of the neutrino flux has been proposed [28].

3.3 Surface Properties of Strange Stars

A strange star would be made exclusively of strange matter if strange matter is absolutely stable. However, as pointed out by Alcock *et al.* [26], a bare strange star may lead to a photon luminosity of 10^{38} erg s^{-1} that well exceeds the Eddington limit. They calculated the dispersion relation for photons in strange matter and concluded that a strange matter surface would have a low emissivity for X-ray photons. There is another consequence of the electrical properties of this surface. This consequence requires a gap between ions at the base of the crust and the quark surface in which a Coulomb barrier prevents direct nuclear reactions between the crust and the strange matter. Putting these arguments together, they reached a possibility that the surface of a strange star is made of the same material as the surface of a neutron star, making no difference in the surface properties between strange stars and neutron stars.

3.4 Pulsar Glitches

Pulsar glitch is a phenomenon in which the period of a radio pulsar decreases with time steadily. This has been explained as a result of the loss of angular momentum by magnetic dipole radiation. A model has been developed for this phenomenon involving the behavior of superfluid neutrons in the inner crust of a neutron star [29]. No equivalent for this model involving strange stars has been found. However, one should not claim that the success of the superfluid neutron model provides a model-independent argument against the strange matter hypothesis.

3.5 Conversion to Strange Stars

Several conversion modes from neutron matter to strange matter have been explored. These modes include conversion via two-flavor quark matter, clustering of lambdas, kaon condensates, direct burning, and seeding from the outside. As Alcock and Olinto pointed out, the uncertainties in each of these are so large that estimates of conversion rates cannot be made with confidence. For the seeding case, Olinto [30] concluded that a droplet of strange matter in a neutron star could consume a neutron star, changing it from a neutron star to a strange star in less than a minute. If this conversion happens just after the supernova explosion one expects a neutrino signature of 10^{52} ergs over a period between minutes and hours. Next generation neutrino detectors will be able to detect neutrinos

from nearby supernovae and this signature can be tested. If the conversion happens in an active pulsar, a huge glitch will be observed because of the change in moment of inertia. An old defunct pulsar will convert even faster, and a γ-ray burst will be its signature.

4 Experimental Searches

Strange quark matter is stable against fissioning and can, in principle, be found in lumps ranging from nuclear to stellar dimensions. Small lumps of it, either as relic quark nuggets from the Big Bang or as matter from strange stars, might be accelerated in the same processes that accelerate ordinary cosmic ray particles, giving rise to a galactic flux. Since Z of strange quark matter grows only slowly with A, it behaves chemically like a very massive isotope of ordinary nuclear matter. Thus, many stable strangelet isotopes should exist for each value of Z and should easily be distinguished from ordinary cosmic ray particles.

Another form of strange quark matter that might be present in cosmic rays and would be detectable is nuclearites. These lumps of strange quark matter have not been accelerated to cosmic ray energies, but have velocities on the order of galactic virial velocities ($\sim$ 250 km sec^{-1}). With such low velocities, they would be electrically neutral due to pickup of electrons as they traverse the galaxy. Experimental methods suitable, at least in principle, for the detection of nuclearites were discussed by De Rújula and Glashow [33, 34].

Experimentally, strange matter may be signaled by its unusually small ratio of $|Z|/A$ as compared to normal nuclear matter, possible negative Z, and arbitrarily large A. Searches done so far include those in terrestrial materials, in galactic cosmic rays, and in heavy ion collisions.

4.1 Searches in Terrestrial Materials

The search for strange quark matter in terrestrial materials can be carried out by using different techniques. I discuss three below.

4.1.1 Heavy Ion Activation

Farhi and Jaffe [35] proposed to use heavy ion activation to search for small impurities of strange matter in laboratory samples of ordinary matter. Lumps of strange matter with baryon number less than $\sim 10^{16}$ are possibly light enough to be materially bound to ordinary matter at the surface of the Earth. The proposal was to expose a sample of material which may contain strange matter to a low-energy beam of heavy ions. The beam energy is adjusted to be just below the Coulomb barrier of the nuclei in the sample. If there is no strange matter impurity no nuclear reactions will occur. Since the Coulomb barrier of strange matter is typically lower than that of ordinary nuclei, the beam may interact with whatever strange matter is in the sample. Each interaction would characteristically result in a high multiplicity, isotropic burst of photons, which should present an unmistakable

signature. Such an experiment has been performed at LBL but no results has been reported [36].

4.1.2 Mass Spectroscopy

Blackman and Jaffe [37] have used existing limits on concentration of heavy isotopes obtained from mass spectroscopy to place exclusion limits on the presence of stable strange quark matter of baryon number $A < 2500$ in terrestrial materials. Fig. 6 summarizes the concentration limits on heavy isotopes of low-Z materials like H, Li, Be, B, C, O, F, and Na obtained from various experiments [38]. These limits can be translated to exclusion plots in the parameter space of ϵ_o versus m_s where strange matter is proposed to be stable. Since the maximum size of possible terrestrial strange matter, constrained by gravitational consideration, is as large as $A \sim 10^{16}$, windows are still open for $2500 < A < 10^{16}$. Further mass spectrograph experiments with wide dynamical range of Z/A would be required to extend the search to large A region for high-Z materials.

4.1.3 Rutherford Backscattering

Brügger *et al.* [39] have conducted a search for supermassive nuclei by using Rutherford backscattering [40] of ions as heavy as ^{238}U. The method is sensitive to a broad range of masses extending to those that exceed the projectile mass by several orders of magnitude. Upper limits for the abundance of strange nuggets with masses $A \sim 400$ to 10^7 were found to be in the range 10^{-10} to 10^{-14} per nucleus in a sample of Fe-meteorite. More recent search [41] improved the limits by a factor of ~ 100 as shown in Fig. 7. Their results can also be interpreted as giving upper limits for the abundance of supermassive relic particles that are bound to nuclei by hadronic interactions so that they cannot be detached in a collision process. Liu *et al.* [42] have independently carried out a search for $Z \sim 100$ and $A \sim 1000$ in meteorite samples using a He heavy ion beam. The limit they obtained is 2×10^{-6} per nucleus.

4.2 Searches in Galactic Cosmic Rays

The ingredients that are necessary for a search for nuclearites in cosmic radiations were discussed by De Rújula and Glashow [33]. However, I point out that their formulae for calculating ionization rate of nuclearites have not been experimentally established.

4.2.1 Flux Limits on Quark Nuggets

I summarize here all the searches in galactic cosmic rays in Table 1. Techniques used include solid nuclear track detectors, scintillators, and gravitational detectors. Published upper limits on magnetic monopoles have been used to obtain a flux limit for nuclearites. Most searches excluding those I will discuss later led to negative results. I compile all the upper limits in Fig. 8. These upper limits are compared to a flux calculated assuming that all dark matter particles are made of quark nuggets. The bottom line is that the strange

Table 1: Summary of experimental searches for quark nuggets in galactic cosmic rays.

Group	Detector	Depth ($g\ cm^{-2}$)	Acceptance (m^2 yr str)	Refs.
Shirk and Price	Lexan	1	0.84	[43]
Kinoshita and Price	CR-39	603	10	[44]
Barwick *et al.*	CR-39	603	16	[45]
Doke *et al.*	cellulose nitrate	1000	271	[46]
Price *et al.*	mica	2×10^6	6.2×10^5	[48]
Price and Salamon	mica	2×10^6	6×10^7	[49]
Nakamura *et al.*	scintillator	1000	0.29	[50]
Barish *et al.*	scintillator	1000	1.74	[51]
Liu and Barish	gravitational detector	1000	0.73	[52]
Nakamura *et al.*	CR-39	700	107	[54]
Orito *et al.*	CR-39	10^4	4200	[55]
Porter *et al.*	Čerenkov detector	1000	--	[56]
Ahlen *et al.*	streamer tube + scintillator	400w.e.m.	--	[57]
Astone *et al.*	gravitational detector	1000	--	[58]

matter as a dark matter candidate has been ruled out in the mass region of $M = 10^9$ to 10^{16} GeV at a level down to $\sim 10^{-10}$. However, if strange quark matter is being produced from processes like strange star collisions, the flux is hard to calculate and this hypothesis cannot be ruled out by this type of experiment.

4.2.2 Candidate Events: Evidence for Strange Matter?

Several cosmic ray events have been (and more exotic events can be) interpreted as candidates for strange quark matter.

The Centauros, mini-Centauros, and Geminion events observed in emulsion experiments [59] were interpreted as manifestations of the formation of strange quark matter in collisions of heavy primaries with nuclei in deep atmosphere by Halzen and Liu [60]. They claimed that these anomalous fireballs in emulsion show indeed features of stable strange quark matter.

The famous event discovered by Price *et al.* [61] in a balloon experiment in 1975 fits very well to a slow supermassive object with $\beta \equiv v/c \simeq 0.4$, $Z \sim 46$, and $A > 10^{3-4}$. This notion was in fact carefully discussed by Price *et al.* [61] in their paper as one of the three classes of hypothetical particles that are compatible with their data.

At sea level, Yock [62] found 4 events that are difficult to account for in terms of known nuclei and are consistent with singly charged long-lived particles with $A > 4.5$ at a flux of $2 \times 10^{-9}\ cm^{-2}\ sec^{-1}\ sr^{-1}$.

In a recent balloon counter experiment, Saito *et al.* [63] observed two events which cannot be accounted for by conventional background. These events are found to be consistent with the assumption of objects with $Z = 14$ and $A \sim 350$ at energy of 450 A MeV. The existence of strange quark matter has not been excluded at a flux of $\sim 6 \times 10^{-9}$ $\mathrm{cm}^{-2}\ \mathrm{sec}^{-1}\ \mathrm{sr}^{-1}$.

Additionally, the event found in Yunnan Station Experiment in 1976 is also consistent with the hypothesis that it was a particle with $Z = 1$ and $A \sim 10$ [64].

Several puzzling astrophysical phenomena reported in the literature have been linked to the existence of strange quark matter. Baym *et al.* [31] discussed the possibility that Cygnus X-3 may be strange in nature based on the unusual observation of exotic hadron emissions. They suggested that very small strangelets are produced at the exposed strange surface and accelerated to high energies. Spallation reactions in the atmosphere of the companion create neutral strangelets that propagate to the Earth. Collisions in the atmosphere produce the neutrinos that in turn produce the deep underground muons observed in large detectors. Alcock *et al.* [32] considered a model for the 5 March 1979 γ-ray transient based on strange matter hypothesis. Other unusual events can be linked to strange matter one way or other. This is nothing but the fact that the observational information is so limited that there is room for speculation and imagination.

4.3 Searches in Heavy Ion Collisions

The possibility of creating and detecting a new form of matter – quark-gluon-plasma (QGP) – via high energy nucleus-nucleus collisions in laboratory is one of the major activities in current nuclear physics research. In ultrarelativistic heavy ion collisions, nuclear matter will be heated to temperatures reached only within the cores of dense stars and within the first microsecond after the origin of the Universe. At such temperatures nuclear matter "melts" and is predicted to form a deconfined plasma of quarks and gluons. The quest of theoreticians and experimentalists alike in this field is to identify QGP uniquely and to study its properties. The QGP and the possible hadron-QGP phase transition are beyond the scope of this paper and a number of excellent reviews are available for interested readers [65]. In the following, I focus on the search for strangelet production in ultrarelativistic heavy ion collisions.

Shortly after the idea of strange matter was proposed, Liu and Shaw [66] suggested that strangelets or metastable droplets of quark matter might be formed in heavy ion collisions. The formation of the strangelets requires the creation of strange quarks, which occurs via the production of $s\bar{s}$ pairs. Recent study suggests that an equilibrium abundance of $s\bar{s}$ at the local temperature is produced in QGP. The s and $\bar{s}$ quarks must separate and enhance before condensation from the QGP in order to prevent their annihilation. This requirement may be satisfied due to the existence of a larger number of u and d quarks than $\bar{u}$ and $\bar{d}$ quarks. Since more K^+ and K° mesons are freely created than K^- and $\overline{K}^\circ$ mesons, entropy and more antistrangeness is carried away from the system, leaving behind an excess of strangeness $[n_s = (n_{K^+} + n_{K^\circ}) - (n_{K^-} + n_{\overline{K}^\circ})]$, with which small strangelets might be formed. The separation and enhancement of strangeness is an important topic in

Table 2: Summary of experimental searches for strangelet production in high energy heavy ion collisions.

Acceleator	Group	Detector	Signal	Sensitivity	τ (sec)	Refs.
BNL AGS	E814	Spectrometer	A and Z	10^{-4}/int	10^{-7}	[71]
	E878	Spectrometer	limited A/Z	$10^{-12}/\pi$	10^{-7}	[72]
	E864	Spectrometer	A and Z	3×10^{-11}/int	10^{-7}	[73]
	E882	CR-39	$Z > 6$	$\sim 10^{-8}$/int	10^{-9}	[74]
CERN SPS	NA52	Spectrometer	A and Z	2.3×10^{-11}/int	10^{-6}	[75]

current QGP study. Other mechanisms have been also suggested by Greiner *et al.* [67, 68]. The production probability that a given droplet might form is difficult to calculate due to uncertainties in current theory, and the results turn out to be highly model dependent[7]. Crawford *et al.* [69, 70] developed an oversimplified model to calculate the production rate for experimental design. In Fig. 9, I sketch the production model for strangelets in heavy ion collisions.

Several searches in heavy ion collisions are underway using beams of 14.5 A GeV Si and 11.4 A GeV Au at Brookhaven AGS and beams of 200 A GeV S and 160 A GeV Pb at CERN SPS. In Table 2, I summarize the experimental activities concerning strangelet search at both places. In Fig. 10, I present an upper limit, as representative, reported by an experiment at CERN.

The key issue in accelerator search that one has to realize is that if strangelets are indeed produced in heavy ion collisions, their lifetime will be very short, typically on the order of $\sim 10^{-9}$ sec. Most of searches have been carried out using quite large scale detection system, on the order of 100 m in length, corresponding to a lifetime of a detected particle of 10^{-6} sec. Experiments with lifetime sensitivity as short as 10^{-9} sec are needed to maximize the possibility of a successful detection.

5 Discussions and Conclusions

It is an interesting fact that we do not know exactly the true ground state of the strong interaction at present. The hypothetical strange quark matter is certainly a very attractive scenario. The fact that the applicability of perturbative QCD theory in the strong coupling limit is in question makes this uncertain. At the moment, no one knows how to model quark matter in QCD accurately. On the other hand, lattice calculations are as yet unable to cope with systems at nonzero chemical potential. In conclusion, present calculations are incapable of deciding if strange matter is stable or not. Answers need to be found

[7]Using a toy model, I find that the production rate of strangelets with $A = 20$ in Au + Au collisions at 11.4 A GeV drops 3-4 orders of magnitude if ϵ_0 increases from 880 MeV to 900 MeV.

experimentally.

If the strange quark matter hypothesis is correct, it must have many striking consequences in physics, in astrophysics, in cosmology, and even in chemistry. Even though several events have been interpreted in favor of this hypothesis, observational experiments done so far have not enabled us to reach a conclusion. In the past 5 years, interests have been shifted away from searches for strange quark matter in cosmic radiations as relics from the Big Bang. No dedicated experiments have been designed for detecting astrophysical signals of strange matter from neutron stars and supernovae. Laboratory searches in the hope of creating the "Little Bang" with high energy heavy ion beams are underway and high sensitivity data will become available both from BNL AGS and CERN SPS soon.

From an experimentalist point of view, in a quest for detection of strangelets, one faces a fundamentally important question that can only be answered by "yes" or "maybe" (instead of "yes" or "no"). This is so because it is very difficult to rule out the hypothesis of strange quark matter based on a negative result either from cosmic ray experiments or from heavy ion collision experiments. Of course, the discovery of strange quark matter would create a new domain of nuclear physics and would change our current understanding of strong interactions. The search is definitely a prize worth winning. However, it is to me not a pleasant case for an experimentalist. I am happy to be contradicted with regard to my pessimism on this issue. One would agree with me that the future of this field depends to large extent on what we are going to learn from on-going experiments both at AGS and at CERN in the next couple of years.

Acknowledgements

My interest in this topic has been developed through many stimulating discussions with Professor Buford Price over the past several years.

References

[1] E. Witten, Phys. Rev. D **30**, 272 (1984).

[2] E. Farhi and R. L. Jaffe, Phys. Rev. D **30**, 2379 (1984).

[3] For a review, see *Proc. Intern. Workshop on Strange Quark Matter in Physics and Astrophysics*, Aarhus, Demmark (1991), eds J. Madsen and P. Haensel [Nucl. Phys. (Proc. Suppl.) **B24**, (1991)].

[4] E. P. Gilson and R. L. Jaffe, Phys. Rev. Lett. **71**, 332 (1993).

[5] H. J. Crawford and C. H. Greiner, Scientific American **270**, 72 (1994).

[6] C. Alcock and A. Olinto, Ann. Rev. Nucl. Part. Sci. **38**, 161 (1988).

[7] A. R. Bodmer, Phys. Rev. D **4**, 1601 (1971).

[8] S. Chin and A. Kerman, Phys. Rev. Lett. **43**, 1292 (1971).

[9] M. S. Berger and R. L. Jaffe, Phys. Rev. C **35**, 213 (1987).

[10] J. Madsen, Phys. Rev. Lett. **70**, 391 (1993).

[11] M. S. Desai, H. J. Crawford, and G. L. Shaw, Phys. Rev. D **47**, 2063 (1993).

[12] C. B. Dover and A. Gal, Nucl. Phys. A **560**, 559 (1993).

[13] J. Schaffner *et al.*, Phys. Rev. Lett. **71**, 1328 (1993).

[14] G. L. Shaw, M. Shin, R. H. Dalitz, and M. Desai, Nature (London) **337**, 436 (1989).

[15] J. H. Applegate and C. J. Hogan, Phys. Rev. D **30**, 3037 (1985).

[16] R. Schaeffer, P. Delbourgo-Salvador, and J. Audouze, Nature (London) **317**, 407 (1985).

[17] J. Madsen and K. Riisager, Phys. Lett. B **158**, 208 (1985).

[18] R. N. Royd and T. Saito, Phys. Lett. B **298**, 6 (1993).

[19] R. Schaeffer, Astron. Astrophys. **157**, L13 (1985).

[20] C. Alcock and E. Farhi, Phys. Rev. D **32**, 1273 (1985).

[21] J. Madsen, H. Heiselberg, and K. Riisager, Phys. Rev. D **34**, 2847 (1987).

[22] J. Madsen and M. L. Olesen, Phys. Rev. D **43**, 1069 (1991).

[23] C. H. Lee and H. K. Lee, Phys. Rev. D **44**, 398 (1991).

[24] H. A. Bethe, G. E. Brown, and J. Cooperstein, Nucl. Phys. A **462**, 791 (1987).

[25] P. Haensel, J. L. Zdunik, and R. Schaeffer, Astron. Astrophys. **160**, 121 (1986).

[26] C. Alcock, E. Farhi, and A. Olinto, Astrophys. J. **310**, 261 (1986).

[27] N. K. Glendenning, Mod. Phys. Lett. A **5**, 2197 (1990).

[28] G. L. Shaw, G. Benford, and D. L. Silverman, Phys. Lett, B **169**, 275 (1986).

[29] D. Pines and M. A. Alpar, Nature (London) **316**, 27 (1985).

[30] A. V. Olinto, Phys. Lett. B **192**, 71 (1987).

[31] G. Baym *et al.*, Phys. Lett B. **160**, 181 (1985).

[32] C. Alcock, E. Farhi, and A. Olinto, Phys. Rev. Lett. **57**, 2088 (1986).

[33] A. De Rújula and S. L. Glashow, Nature (London) **312**, 734 (1984).

[34] A. De Rújula, Nucl. Phys. **434**, 605c (1985).

[35] E. Farhi and R. L. Jaffe, Phys. Rev. D **32**, 2452 (1985).

[36] M. D. Deleplanque *et al.*, private communication (1995).

[37] E. G. Blackman and R. L. Jaffe, Nucl. Phys. B **324**, 205 (1989).

[38] T. K. Hemmick *et al.*, Phys. Rev. D **41**, 2074 (1990) and therein references 11-19.

[39] M. Brügger *et al.*, Nature (London) **337**, 434 (1989).

[40] M. Overbeck *et al.*, Nucl. Instr. Meth. A **288**, 413 (1990).

[41] S. Polikanov *et al.*, Z. Phys. A **338**, 357 (1991).

[42] S. J. Liu, B. Z. Xie, Y. Wu, and X. W. Tang, High Energy Phys. Nucl. Phys. **13**, 103 (1989).

[43] E. K. Shirk and P. B. Price, Astrophys. J. **220**, 719 (1978).

[44] K. Kinoshita and P. B. Price, Phys. Rev. D **24**, 1707 (1981).

[45] S. W. Barwick, K. Kinoshita, and P. B. Price, Phys. Rev. D **28**, 2338 (1983).

[46] T. Doke *et al.*, Phys. Lett. B **129**, 370 (1983).

[47] P. B. Price, Phys. Lett. B **140**, 112 (1984).

[48] P. B. Price *et al.*, Phys. Rev. Lett. **52**, 1265 (1984).

[49] P. B. Price and M. H. Salamon, Phys. Rev. Lett. **56**, 1126 (1986).

[50] K. Nakamura *et al.*, Phys. Lett. B **161**, 417 (1985).

[51] B. Barish, G. Liu, and C. Lane, Phys. Rev. D **36**, 2641 (1987).

[52] G. Liu and B. Barish, Phys. Rev. Lett. **61**, 271 (1988).

[53] P. B. Price, Phys. Rev. D **38**, 3813 (1988).

[54] S. Nakamura *et al.*, Phys. Lett. B **263**, 529 (1991).

[55] S. Orito *et al.*, Phys. Rev. Lett. **66**, 1951 (1991).

[56] N. A. Porter, D. J. Fegan, G. C. MacNeill, and T. C. Weekes, Nature (London) **316**, 49 (1985).

[57] S. P. Ahlen *et al.*, Phys. Rev. Lett. **69**, 1860 (1992).

[58] P. Astone *et al.*, Phys. Rev. D **47**, 4770 (1993).

[59] C. M. G. Lattes, Y. Fujimoto, and S. Hasegawa, Phys. Rep. **65**, 151 (1978).

[60] F. Halzen and H. C. Liu, Phys. Rev. D **32**, 1716 (1985).

[61] P. B. Price, E. K. Shirk, W. Z. Osborne, and L. S. Pinsky, Phys. Rev. Lett. **35**, 487 (1975); Phys. Rev. D **18**, 1382 (1978).

[62] P. C. M. Yock, Phys. Rev. D **34**, 698 (1986).

[63] T. Saito, Y. Hatano, Y. Fukada, and H. Oda, Phys. Rev. Lett. **65**, 2094 (1990).

[64] A. X. Huo, private communication (1995).

[65] For a review on Quark Gluon Plasma, see *Proc. of Quark Matter.*

[66] H. C. Liu and G. L. Shaw, Phys. Rev. D **30**, 1137 (1984).

[67] C. Greiner, P. Koch, and H. Stöcker, Phys. Rev. Lett. **58**, 1825 (1987).

[68] C. Greiner and H. Stöcker, Phys. Rev. D **44**, 3517 (1991).

[69] H. J. Crawford, M. S. Desai, and G. L. Shaw, Phys. Rev. D **45**, 857 (1992).

[70] H. J. Crawford, M. S. Desai, and G. L. Shaw, Phys. Rev. D **48**, 4474 (1993).

[71] J. Barrette *et al.*, Phys. Lett. B **252**, 550 (1990).

[72] H. J. Crawford *et al.*, Nucl. Phys. A (Proc. Suppl.) **24**, 251 (1991).

[73] J. Sandweiss *et al.*, Nucl. Phys. A (Proc. Suppl.) **24**, 234 (1991).

[74] Y. D. He and P. B. Price, to be published (1995).

[75] K. Borer *et al.*, Phys. Rev. Lett. **72**, 1415 (1994).

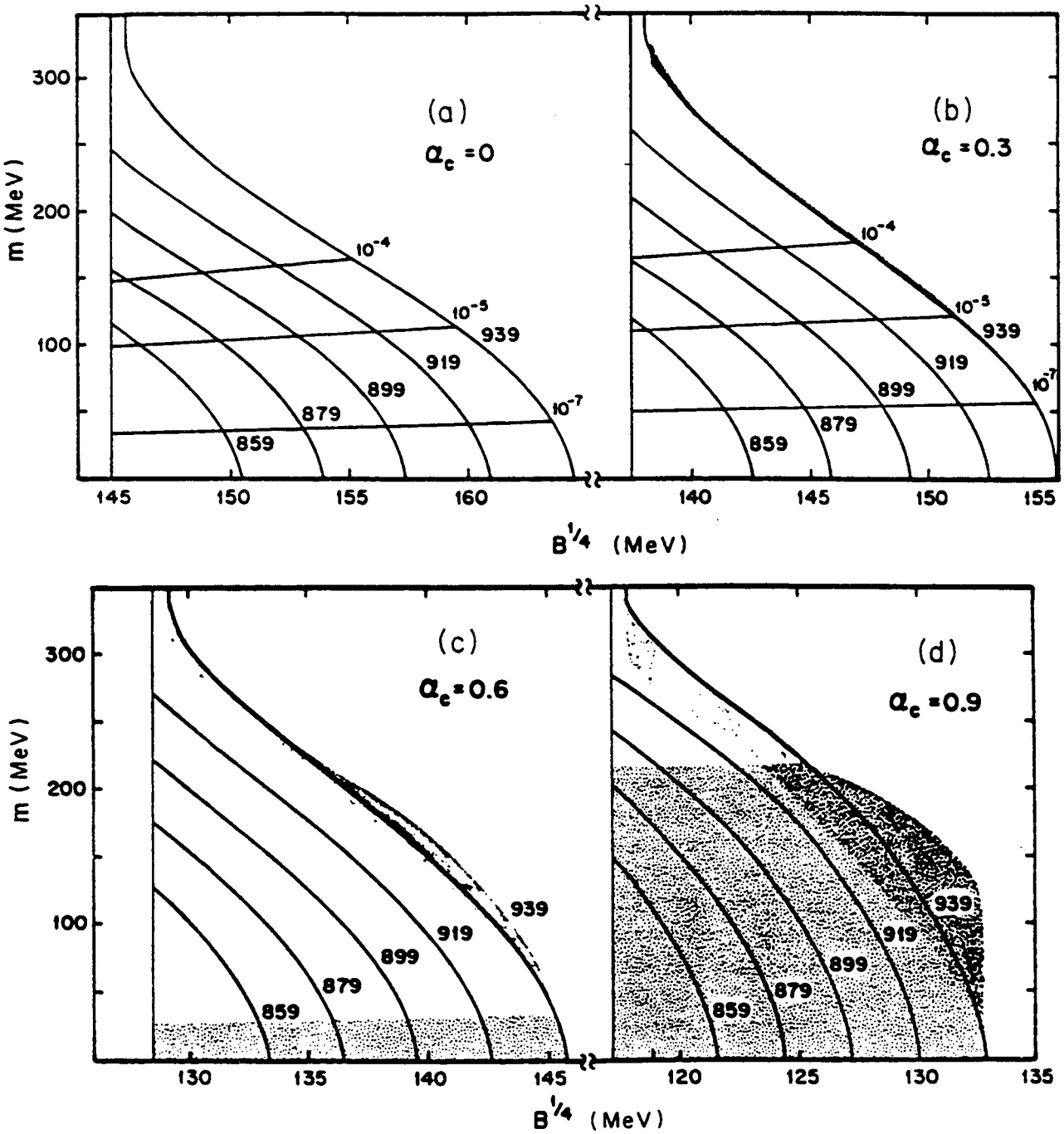

Fig. 1 Contours of energy per baryon (E/A) in the plan of $B^{1/4}$ versus m_s for $\alpha_c = 0$ (a), 0.3 (b), 0.6 (c), and 0.9 (d). This figure is taken from Farhi and Jaffe [2].

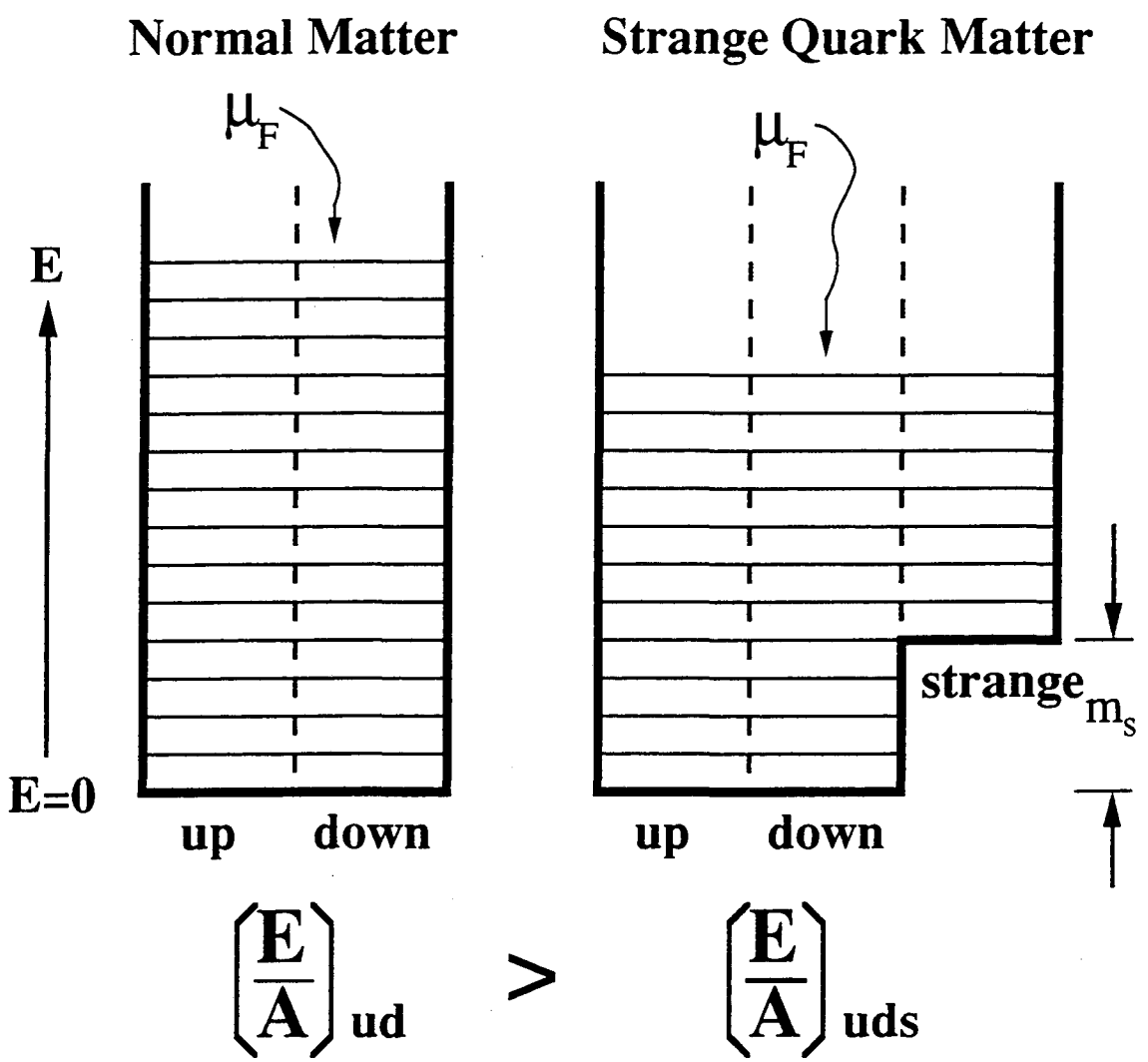

Fig. 2 2-flavor nonstrange quark matter system and 3-flavor strange quark matter system. The strange quarks introduce new degree of freedom in the system and lower the energy of the system.

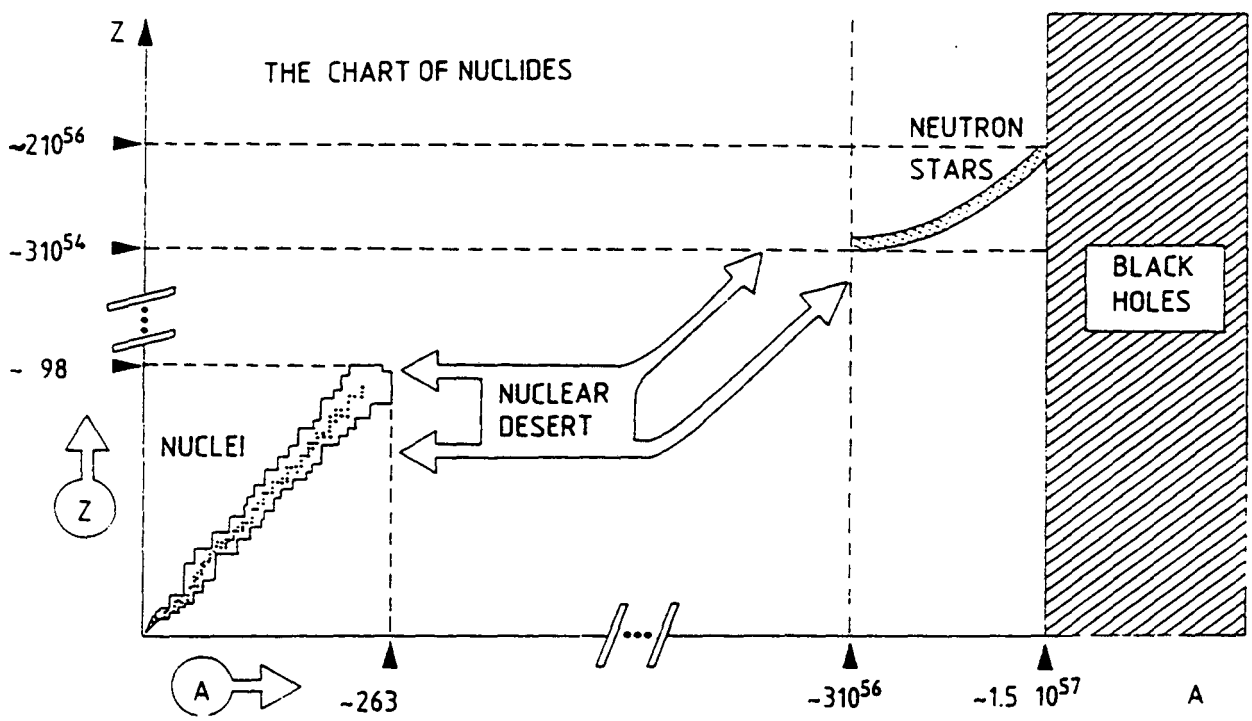

Fig. 3 The nuclear "desert" – a region between ordinary nuclides and neutron stars would be filled with strange quark matter.

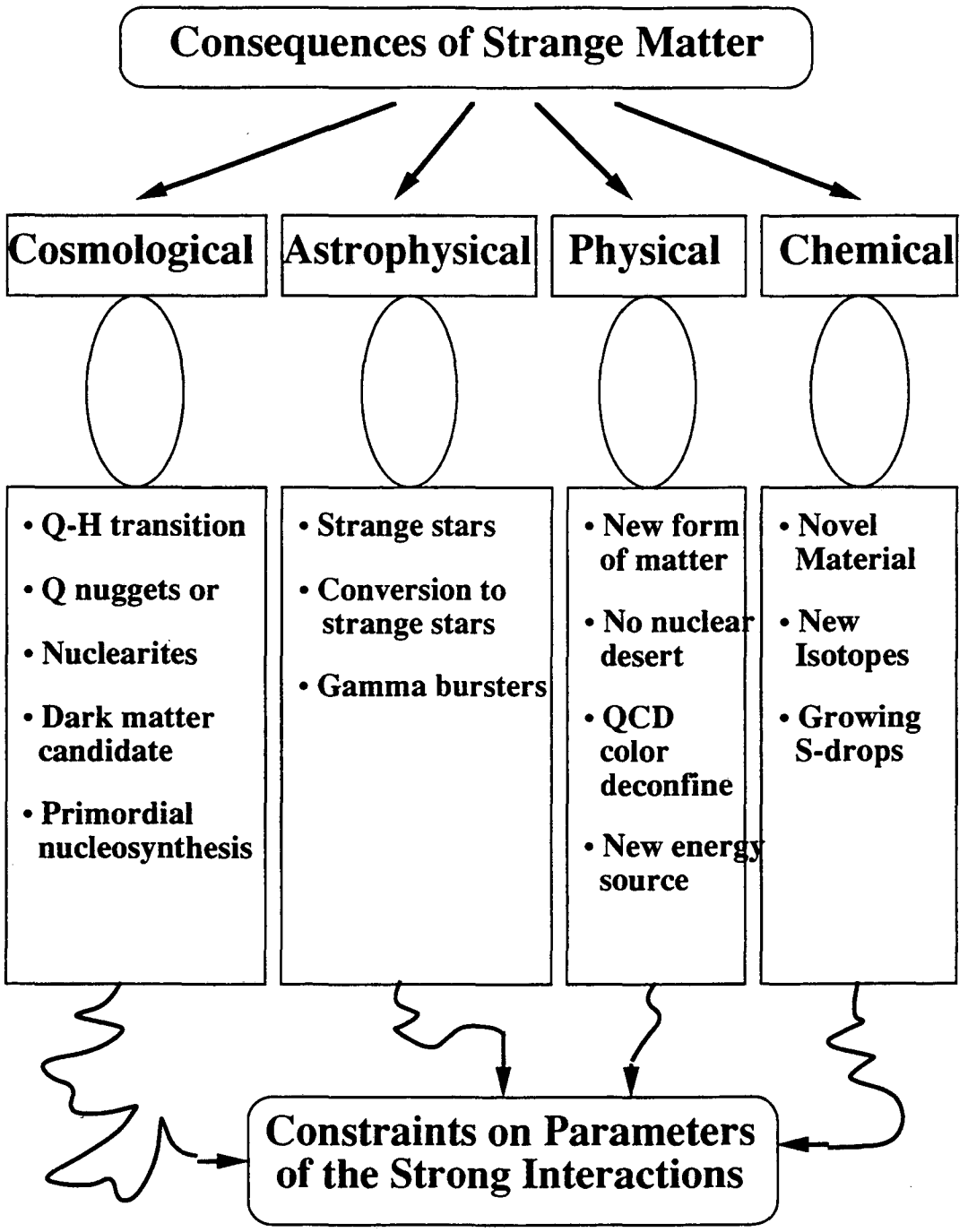

Fig. 4 Possible consequences of strange quark matter. Observations may be used to rule out or provide constraints on the strange matter hypothesis.

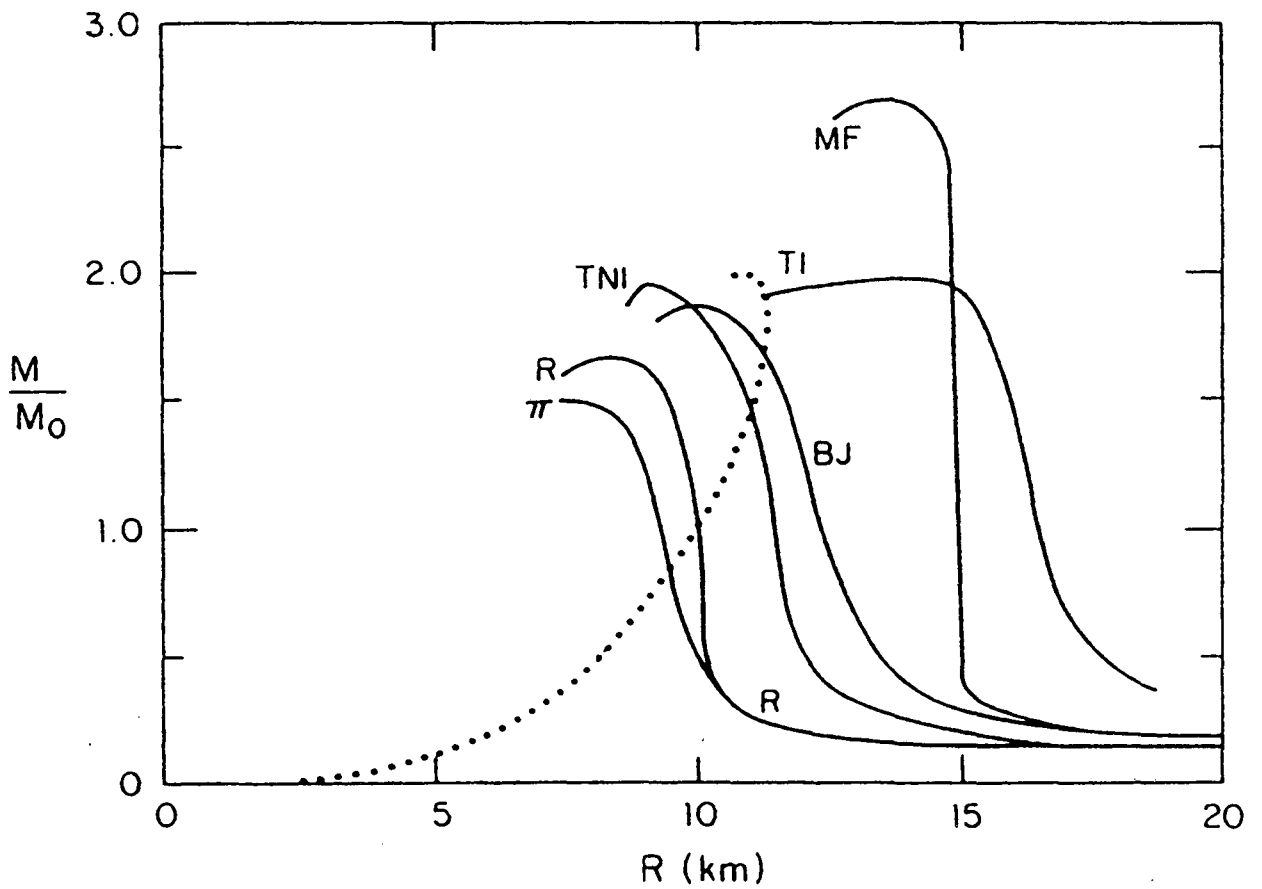

Fig. 5 The relation between mass and radius for strange stars (dotted line) and for various models of neutron stars (solid lines).

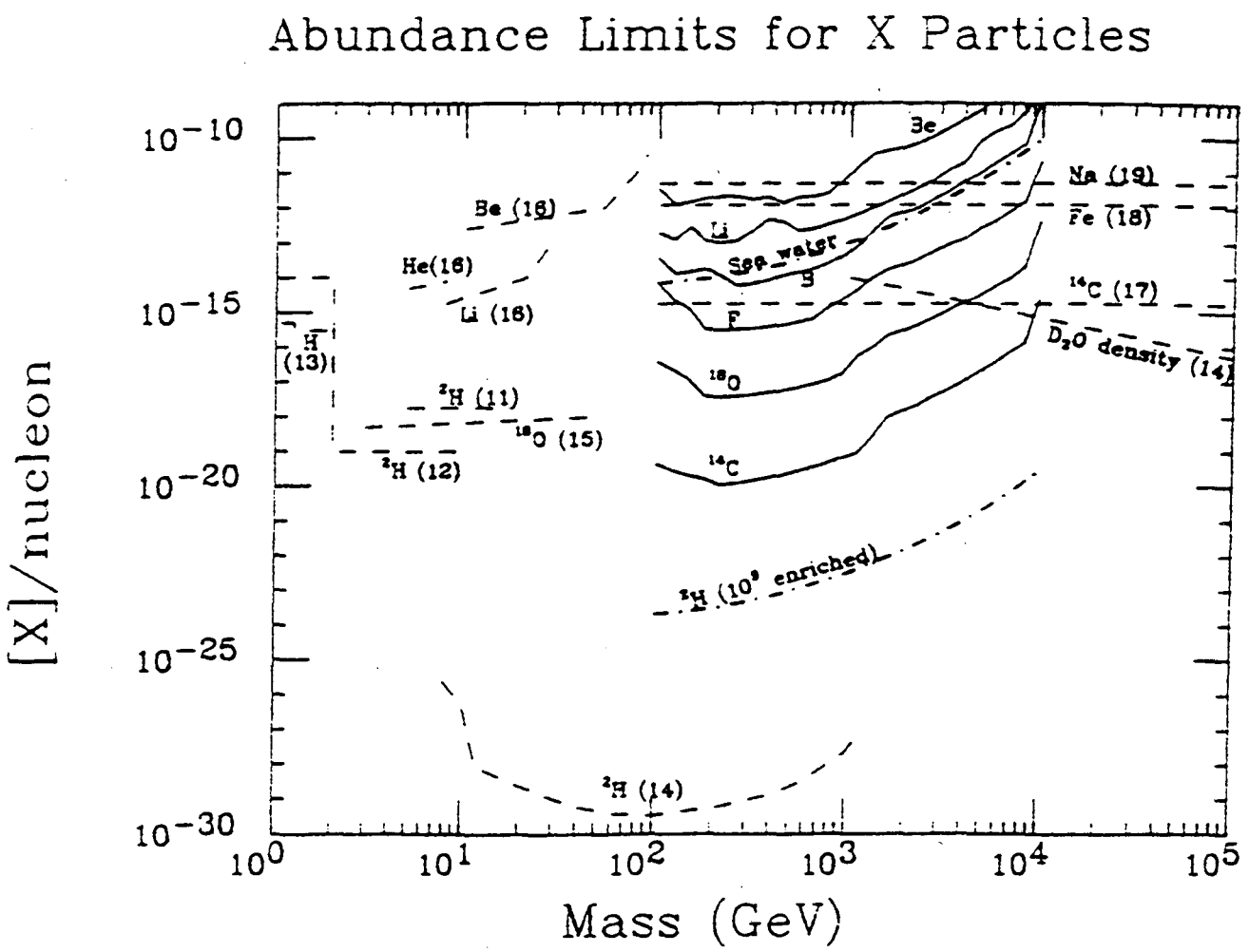

Fig. 6 Concentration limits on heavy isotopes of low-Z materials obtained from various mass spectroscopy experiments [38].

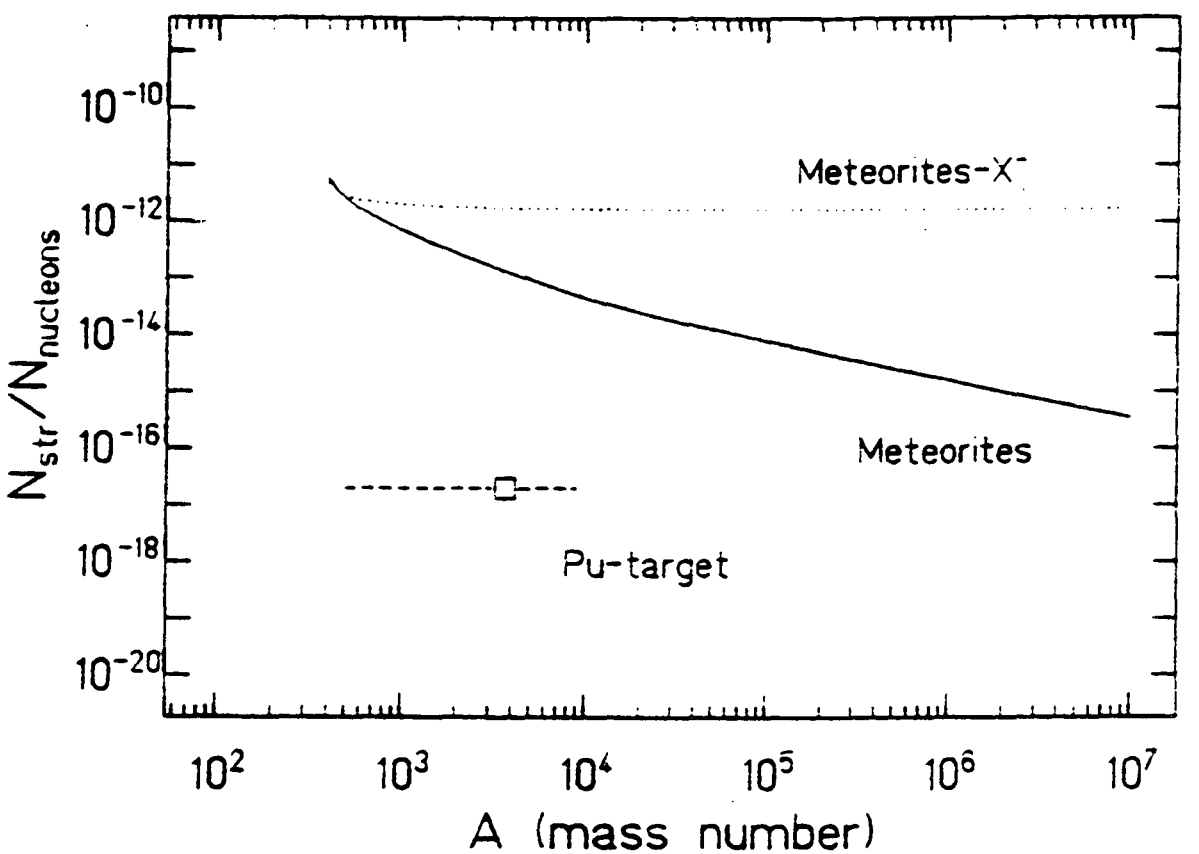

Fig. 7 Upper limits to the abundance of strange quark matter obtained in Rutherford backscattering experiment [39, 41].

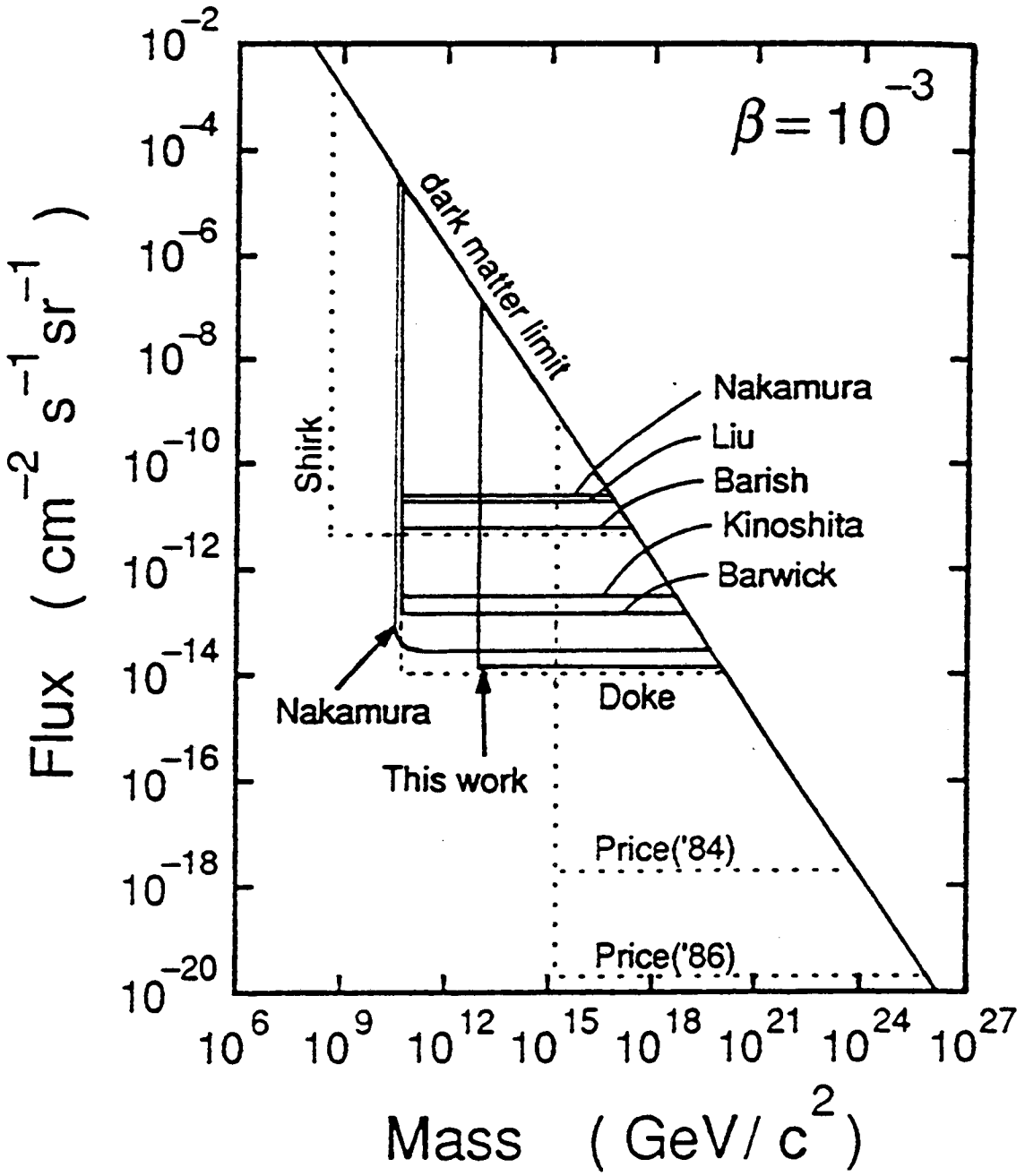

Fig. 8 Compiled flux limits to nuclearites in galactic cosmic rays as a function of the mass.

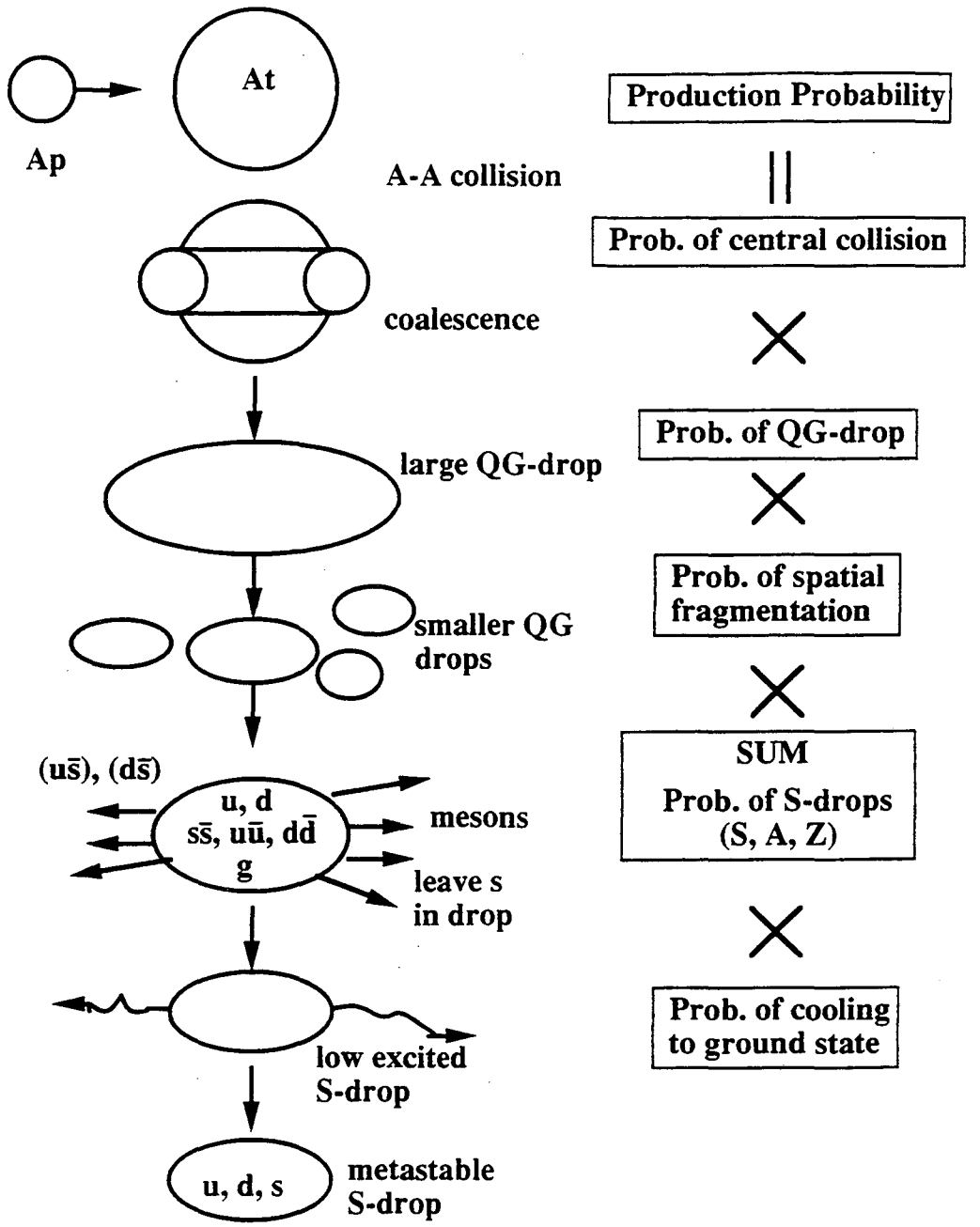

Fig. 9 A model for production of strangelets in high energy heavy ion collisions.

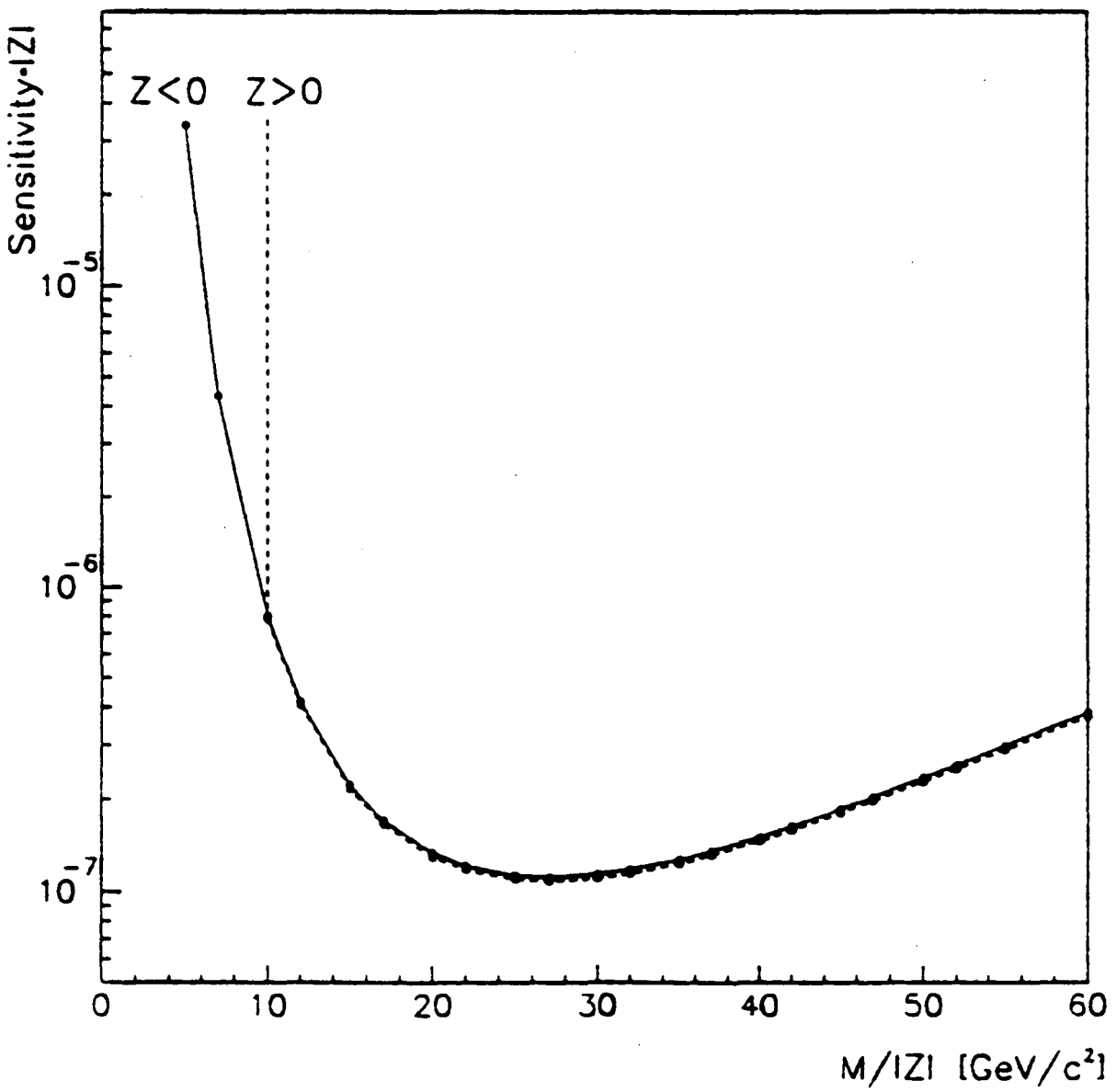

Fig. 10 Upper limits to strangelet production rate obtained by NA52 in S + W collisions at 200 A GeV [75].

MAGNETIC MONOPOLE SEARCHES[1]

Yudong He[2]
Department of Physics, Space Science Laboratory
and Center for Particle Astrophysics
University of California at Berkeley, Berkeley, CA 94720, USA
and
Institute for Nuclear and Particle Astrophysics
and Nuclear Science Division
Lawrence Berkeley National Laboratory, Berkeley, CA 94720, USA

Abstract

The magnetic monopole, either the classical point-like Dirac one or the modern structured GUT one, has been discussed by theorists and sought after by experimentalists for decades. The Dirac monopole-antimonopole pairs have been suggested to be produced in high energy collisions and various searches have been carried out at available accelerators. In the cosmic radiation, a small flux of supermassive GUT monopoles is expected as a topological defect that might have been created in the early Universe. The search for relic monopoles has formed an important aspect of recent experimental efforts. This paper reviews the recent development of experimental searches for magnetic monopoles both at accelerators and in cosmic radiation.

1 Magnetic Monopoles: from Dirac to GUTs

The magnetic monopole was introduced as early as 1931 by Dirac [1]. He found that if there exists at least one free magnetic charge, the quantization of the electric charge can be naturally explained. He then established a relationship between the elementary electric charge e and the magnetic charge g [2]:

$$g = n\frac{\hbar c}{2e} = n\frac{e}{2\alpha} = 68.5en, \tag{1}$$

in which $n = \pm 1, \pm 2, ...$ is a non-zero integer. The elementary magnetic charge is obtained by setting $n = 1$ in eqn. (1): $g_o = 68.5e = 3.29 \times 10^{-8}$ CGS units. Here we assume that the elementary electric charge is that of electrons. If the elementary electric charge were found be to that of quarks, $(1/3)e$, one would have an elementary magnetic charge 3 times larger.

[1]This topic is one of a series of lectures on "Current Trends in Non-Accelerator Particle Physics" given at CCAST Workshop on Tibet Cosmic Ray Experiment and Related Physics Topics, Beijing, April 4-13, 1995. This work was supported in part by the U. S. Department of Energy under Contract No. DE-AC03-76SF00098.

[2]Mailing address: Department of Physics, University of California, Berkeley, CA 94720, USA. Email address: yudong@physics.berkeley.edu.

It is important to point out that the existence of Dirac magnetic monopoles was not necessarily required by any theory or observation, but it would symmetrize the form of Maxwell's equations for electromagnetism and would explain the quantization of electric charge. The requirement for the existence of Dirac magnetic monopoles was nothing but a consequence of consideration of the simplicity and beauty of the theory. Except for the relation of the magnetic charge to the electric charge, there was no prediction for other properties of the Dirac monopole. For example, its mass was not related to its electromagnetic properties and was not known at all. Assuming the classical electron radius to be equal to the classical monopole radius, a naive guess of the monopole mass can be obtained as: $m_{\rm M} \simeq g_{\rm o}^2 m_{\rm e}/e^2 \simeq 4695 m_{\rm e} \sim 2.4$ GeV. Predictions of the mass vary upwards from Dirac's original guess of 0.5 GeV [3].

A revival of monopoles occurred in 1974 when it was realized that the existence of monopoles is naturally implied and the electric charge is naturally quantized in unified gauge theories of the fundamental interactions [4, 5]. In such theories electromagnetism is embedded in a spontaneously broken gauge theory. This was an important stimulation for the experimental search, since the theories not only imply its existence, but also predict its calculable properties. In the context of the Grand Unification Theories (GUTs) of strong and electroweak interactions [6], magnetic monopoles appear at the phase transition corresponding to the spontaneous breaking of the unified group into subgroups. The mass of monopoles is related to the masses of the vector and Higgs bosons ($M_{\rm V}$ and $M_{\rm S}$), which are carriers of the unified interaction. In the so-called Prasad-Sommerfield limit ($M_{\rm S}/M_{\rm V} \to 0$) [7], the monopole mass is given as: $m_{\rm M} \geq M_{\rm V}/\alpha_{\rm G}$ where $\alpha_{\rm G}$ is the dimensionless unified coupling constant. In general, the monopole mass is a monotonically increasing function of $M_{\rm S}^2/M_{\rm V}^2$. Since the energy scale of GUTs is expected to be $\sim 10^{14}$ GeV, the magnetic monopoles associated with GUTs are supermassive: $m_{\rm M} \sim 10^{16}$ GeV. Lighter magnetic monopoles have been also offered by some GUTs. In the same time, even more massive monopoles have been predicted in the Kaluza-Klein theories and in supersymmetry theories.

The existence of the 't Hooft-Polyakov monopole solution has spurred new interest, because unlike the Dirac monopole, which could or could not be put into the theory at the theorist's whim, these topological monopoles must necessarily exist. They arise not only as fundamental entities in the theory but also as classical solutions to the field equations. If magnetic monopoles are indeed present in the Universe, they have a myriad of interesting astrophysical and cosmological consequences. One of them is the resulting monopole flux in the Universe as a relic of phase transition in the very early Universe. An estimate with an uncertainty up to a few orders of magnitude can be made for the current flux of this relic monopoles. It involves lengthy arguments related to details of GUTs and cosmology. Kolb and Turner [8] pointed out that cosmology seems to make two firm predictions about the relic monopole abundance: That there should be equal numbers of north and south magnetic poles, and that either far too few to detect, or far too many to be consistent with the standard cosmology, should have been produced. Even though no one has realistically calculated the flux of relic supermassive monopoles to within an order of magnitude, we can be reasonably certain that the flux of relic monopoles is small

based on some astrophysical considerations.

The velocity of monopoles is important for monopole detection schemes, for determining the astrophysical effects, and for calculating the resulting monopole flux. The typical velocity of relic monopoles is estimated to range from $\beta \sim 10^{-5}$ to 0.1, depending on whether the GUT monopoles are bound to planets such as the Earth ($\beta \sim 4 \times 10^{-5}$), bound to the solar and other stellar systems ($\beta \sim 10^{-4}$), bound to the galaxy or local supercluster ($\beta \sim 10^{-3}$), or not gravitationally bound to the galaxy or supercluster ($\beta \geq 10^{-3}$).

For more detailed discussions on the properties of the GUT monopole and its role in the early Universe, readers are referred to Refs. [8, 9]. Experimental issues can be found in Refs. [10, 11, 12] and an excellent review up to 1986 can be found in Ref. [13].

2 Detectability of Monopoles and Techniques

The detection of magnetic monopoles would be of great significance, either for the Dirac point-like type or for the GUT structured type. For the first type, the detection of one monopole would provide a way to explain the quantization of electric charge and would make the Maxwell's equations in a symmetric form. For the second type, the detection of a single superheavy monopole would help us to test GUTs and understand the physics that occurred in the very early Universe.

Methods for the direct detection of magnetic monopoles can be classified into two categories: induction and ionization. The induction experiment relies upon the fact that when a monopole moves through N loops of wire, it induces a current $\Delta I = 4\pi N n g_o / L$ due to the change in magnetic flux in the loop where L is the inductance of the loop. This is simply an analogy to the fact that a moving electric charge can induce a magnetic field. The amplitude of induction should be determined by the magnetic charge, independent of all other properties of monopoles, such as velocity, mass, and catalysis of nucleon decay. The typical change of current is so small ($\Delta I \sim 10^{-9}$ A for $L \sim$ few μH) that a very sensitive superconducting quantum interferometer device (SQUID) is needed to detect the signal. For experiments with well shielded superconducting loops, the signal of monopoles should in principle be clean. However, such sensitive devices are difficult to build on a scale sufficiently large to make them competitive with the other detectors.

Ionization detectors rely upon the fact that as a monopole moves through matter it loses energy through its interactions with atomic electrons. One of the advantages of ionization detectors is that it is relatively easy to scale the detectors to large areas. Ionization detectors that have been used in the monopole search include scintillation counters and track-etch solid detectors. Calculations of the energy loss and scintillation light yield of a magnetic monopole are complicated and the results have been reviewed by Ahlen [14]. In short, the ionization of a monopole is found to be characteristically different from that of an electrically charged particle [14, 15, 16, 17]. Of particular interest to an experimentalist is that dE/dx for a monopole increases with its velocity for $\beta > 10^{-4}$, and is large for relativistic monopoles. This is illustrated by an example of calculated dE/dx

for a monopole in hydrogen as shown in Fig. 1. For Dirac monopoles with GeV mass scale that might be produced in high energy interactions, they would be relativistic and their ionization would be a factor of $n^2(g_o/e)^2 \sim 4700n^2$ larger than that of a minimum ionizing electrically charged particle. This huge dE/dx makes it easy to detect relativistically moving monopoles. However, the ionization rate of GUT monopoles moving at $\beta \sim 10^{-3}$ is small. For example, in CR-39, a type of track-etch detector used in monopole detection, $dE/dx < 100$ MeV cm^2 g^{-1} and the detection of a bare monopole becomes difficult based on its ionization.

Fortunately, there is one way to get around it. The interaction of the monopole magnetic charge with nuclear magnetic dipoles could lead to the formation of a monopole-nucleus bound system [15]. Such a bound system is called a monopolic atom in the literature. The binding energy is found to range from 1 to 100 keV, depending on the nucleus in the system. The typical size of the bound system would be of the order of ~ 10 fm. Monopoles may also be bound in atomic nuclei by electrons, in a way similar to the chemical binding of molecules. Such a bound system is called a monopolic molecule. Its binding energy would be on the order of ~ 1 eV and its dimension would be on the order of ~ 1 Å. A useful consequence of the formation of the monopolic atoms and molecules is the effect of the energy loss and cross section for the monopole catalysis of nucleon decay. Fig. 2 presents calculated restricted energy loss (REL) as a function of velocity for the bare monopoles and monopole-nucleus bound systems. The REL for monopole-nucleus bound states is enhanced by a large factor compared to that for bare monopoles, making it possible to detect them in track-etch detectors which are sensitive to REL. Monopole-proton bound states may be formed via radiative capture. For a slowly moving monopole with $\beta \sim 10^{-4} - 10^{-3}$, the cross section may be on the order of 1-10 mb. The monopole-nucleus bound systems should exist for nuclei which have a relatively large gyromagnetic factor. For example, the capture cross section for the radiative capture of a moving monopole with $\beta \sim 10^{-3}$ in ^{27}Al nuclei is estimated to be ~ 0.3 mb. One estimate of the binding energy in the ground state of the bound system is ~ 0.56 eV.

A GUT monopole may catalyze proton decay through $p + M \rightarrow M + e^- + \pi^\circ$ [18]. The cross section for this process would be comparable to that of strong interactions [19, 20, 21]. The catalysis cross section is usually expressed as: $\sigma_{\text{catalysis}} \simeq 0.62\sigma_{\text{R}}/\beta$ mb where σ_{R} quantifies our ignorance. The cross section for the capture of a nucleus by a monopole is $\sigma_{\text{capture}} \simeq 10^{-3}/\sqrt{\beta}$ mb. When $\beta \leq 4 \times 10^{-3}$, we have $\sigma_{\text{catalysis}} \geq \sigma_{\text{capture}}$. Therefore, it is possible for a monopole to capture a proton and then subsequently catalyze the proton decay. It is also possible for a monopole to capture a nucleus and then catalyze the proton decay. In the case of nuclei, the cross section is enhanced. The monopole catalysis of proton decay can be used as an indirect way to detect monopoles. The signature of the monopole-catalyzed nucleon decay should be different from that of a spontaneous nucleon decay.

Table 1: Concentration limits obtained from searches in bulk materials.

Material Studied	Magnetic Charge (g_o)	Concentration Limit (gram^{-1})	Detection Technique	Refs.
Iron Ore	> 0.6	$< 2 \times 10^{-7}$	Induction	[22]
Iron Aerosols	$> 1/3$	$< 1 \times 10^{-14}$	Spectrometer	[23]
Air, Sea Water	–	$< 6 \times 10^{-4}$	Scintillator	[24]
Natural Materials	> 0.04	$< 5 \times 10^{-1}$	Induction	[25]
Lunar Rock	> 0.05	$< 2 \times 10^{-4}$	Induction	[26]
Sea Water	< 140	$< 6 \times 10^{-7}$	Scintillator	[27]
Manganese Nodules	< 120	$< 1 \times 10^{-2}$	Plastic	[28]
Manganese	> 0	$< 1 \times 10^{-4}$	Plastic	[29]
Magnetite, Meteor	$< 1 - 3$	$< 2 \times 10^{-3}$	Emulsion	[30]
Meteorite	–	$< 2 \times 10^{-2}$	Scintillator	[31]

3 Search for Classical Monopoles

3.1 Searches in Natural Materials

Searches have been carried out in natural materials in which magnetic monopoles might have been trapped in bulk paramagnetic and ferromagnetic materials. No candidate event has been found so far. The negative results are usually expressed as limits on the concentration density. There has been no activities in recent years. Table 1 summarizes the previous results.

3.2 Searches in e^+e^-, pp, $p\overline{p}$ and pA Interactions

Dirac magnetic monopole-antimonopole pairs have been suggested to be produced in high energy particle collisions [32, 33]. Since the highly structured monopoles of 't Hooft and Polyakov may have a large mass ($m_{\rm M} \sim 10^{15}$ GeV), it is unlikely to produce them in current accelerators. Because of form factor suppression, the cross section for producing objects with extended structure may be impossibly low [32]. Therefore, experiments carried out at accelerators have focused only on the Dirac point-like monopoles. In contrast to the case of GUT monopoles, the mass of a point-like Dirac monopole is unspecified. Consequently, Dirac monopoles have been sought both in cosmic rays and at each accelerator that opens up a new mass regime.

A number of searches have been carried out in e^+e^-, pp, $p\overline{p}$, and pA collisions at various high energy accelerators. There are also searches using beams of ν, neutron, and γ in fixed target experiments. In each of these, an upper limit on its production cross section has been placed. Table 2 summarizes the recent results obtained by various groups using

different detectors. Note that each limit is valid for only its sensitive magnetic charge and the accessible mass. In all these collisions, the monopole pairs are expected to be produced via Drell-Yan mechanism. Fig. 3 presents some upper limits as a function of the monopole mass. Note that some of limits were obtained from indirect searches in which a series of targets made of compacted ferromagnetic tungsten powder was used. Monopoles that might be produced in collisions should have lost their energy and be brought to rest inside the target. Then the targets were placed in front of a pulsed solenoid, capable of giving a magnetic field of more than 200 kG, large enough to extract and accelerate the monopoles. The extracted monopoles, if any, are detected in nuclear emulsion or in track-etch detectors.

3.3 New Searches in Heavy Ion Collisions

Recently, we have proposed that a similar search be carried out in high energy nucleus-nucleus collisions using heavy ion beams available at BNL AGS and CERN SPS. In nucleus-nucleus collisions, in addition to the Drell-Yan mechanism, the thermal production of monopole pairs has been predicted [65]. However, no specific predictions of the production cross section have been made. Nevertheless, the monopole-antimonopole pair production in nucleus-nucleus collisions seems to be more favorable than in e^+e^-, pp, $p\overline{p}$, and pA collisions.

Beased on an upper limit that we have placed on the production cross section for ultradense nuclear matter in collisions of 11.4 A GeV Au with Pb in 1992 [64], we are able to set an upper limit on the production of monopoles with $n \geq 2$ in nuclear collisions. The experiment was carried out at BNL AGS using BP-1 glass detectors with 10^9 Au ions. This upper limit is also listed in Table 2. With a new search that we began last year at BNL AGS, we expect to have two orders of magnitude improvement in the sensitivity [66]. We have also proposed to use the intense beams of 160 A GeV Pb at CERN SPS by the end of this year to conduct another high-statistics search [67].

Since the search for the monopole production in heavy ion collisions is relatively new, let me discuss it in some detail. We exploit one of the useful features of the track-etch detector BP-1: its sensitivity can be tuned by a suitable choice of chemical etchants [68]. Fig. 4 shows the dependence of the etch rate ratio on Z/β – a curve often called the response curve. One sees from Fig. 4 that the detection threshold and dynamic range can be chosen by using different etchants. In the experiment designed to search for monopoles, we use 1N NaOH at 50 °C, which yields a threshold in dE/dx corresponding to $Z/\beta > 83$. In Fig. 5, I present the ratio of the equivalent charge to velocity as a function of velocity for monopoles with $n = 1$ and $n = 2$. We estimate that our detector is sensitive to a $n = 2$ magnetic monopole with $\beta > 0.2$ and with various possible masses. The detector module consists of 20 sheets BP-1 glass detectors and a Pb target as shown in Fig. 6. On each surface of the glass, we are able to obtain an instantaneous value of dE/dx averaged over a distance of 50 μm for a highly-ionizing particle created in the target. With the two plates of BP-1 glass placed upstream from the target we can veto beam particles and fragments which have energies much lower than the beam energy so that they register as $Z/\beta > 83$

Table 2: Summary of experimental searches for Dirac monopole production in high energy e^+e^-, pp, $p\overline{p}$, pA, and AA collisions using different techniques.

Collision System	Energy (GeV)	Magnetic Charge (g_o)	Mass (GeV)	Cross Section (cm^2)	Detector Technique	Refs.
e^+e^-	88-94	1	< 45	$< 3 \times 10^{-37}$	Plastic	[34]
	88-94	2	< 41.6	$< 3 \times 10^{-37}$	Plastic	[34]
	89-93	0.2-1	< 44.9	$< 7 \times 10^{-35}$	Plastic	[35]
	50-61	1	< 29	$< 1 \times 10^{-37}$	Plastic	[36]
	50-61	2	< 18	$< 1 \times 10^{-37}$	Plastic	[36]
	35	< 1	< 17	$< 1 \times 10^{-38}$	Scintillator	[37]
	50-52	1	< 24	$< 8 \times 10^{-37}$	Plastic	[38]
	50-52	2	< 22	$< 1.3 \times 10^{-35}$	Plastic	[38]
	10.6	< 0.15	< 4	$< 9 \times 10^{-37}$	CLEO	[39]
	29	< 3	–	$< 3 \times 10^{-38}$	Plastic	[40]
	34	< 6	< 10	$< 4 \times 10^{-38}$	Plastic	[41]
	29	< 3	< 30	$< 9 \times 10^{-37}$	Plastic	[42]
$p\overline{p}$	1800	≥ 0.5	< 850	$< 2 \times 10^{-34}$	Plastic	[43]
	1800	≥ 1	< 800	$< 1.2 \times 10^{-33}$	Plastic	[44]
	1800	≥ 1	< 800	$< 3 \times 10^{-32}$	Plastic	[45]
	540	1,3	–	$< 1 \times 10^{-31}$	Plastic	[46]
pp	52	–	< 20	$< 8 \times 10^{-36}$	Scintillator	[47]
	63	< 24	< 20	$< 1 \times 10^{-37}$	Scintillator	[48]
	56	< 3	< 30	$< 1 \times 10^{-37}$	Plastic	[49]
	60	< 3	< 30	$< 2 \times 10^{-36}$	Plastic	[50]
pA	300	–	–	$< 4 \times 10^{-33}$	Spark Chamber	[51]
	70	< 2	< 5	$< 1 \times 10^{-40}$	Scintillator	[52]
	400	< 10	< 12	$< 5 \times 10^{-43}$	Induction	[53]
	400	< 24	< 13	$< 5 \times 10^{-42}$	Scintillator	[54]
	300	< 24	< 12	$< 6 \times 10^{-42}$	Scintillator	[55]
	70	–	< 5	$< 1 \times 10^{-41}$	Emulsion	[56]
	28	< 2	< 3	$< 1 \times 10^{-40}$	Emulsion	[57]
	30	< 2	< 3	$< 2 \times 10^{-40}$	Scintillator	[58]
	28	< 4	< 3	$< 1 \times 10^{-35}$	Scintillator	[59]
	6	1	< 1	$< 2 \times 10^{-35}$	Emulsion	[60]
nA	300	–	–	$< 2 \times 10^{-30}$	OSPK	[61]
νA	8	–	–	$< 1 \times 10^{-38}$	HLBC	[62]
γA	0.001	1	tachyonic	$< 2 \times 10^{-36}$	Scintillator	[63]
AA	11.4	≥ 2	< 3	$< 2 \times 10^{-32}$	Glass	[64]

before reaching the target. With the 18 downstream plates we look for central collisions leading to products with $Z/\beta > 83$ emitted from the target. For these products, we have many measurements of dE/dx along their trajectories. These measurements of dE/dx, as a function of penetrating depth, enable us to determine Z and β simultaneously for each registered particle. As demonstrated in our previous studies, Z can be measured to ± 2 and β can be measured to within $3-5\%$.

Three classes of events can register in our experiment: (1) a Dirac magnetic monopole is signaled by a decrease of dE/dx with penetrating depth; (2) candidates for an ultradense nuclear matter are recognizable by $Z > 83$ and $\beta > \beta_{cm}$; (3) background would be projectile fragments that slowed through a large thickness of beam pipe or in interactions leading to fragments with intermediate rapidity emitted in nearly the forward direction. We show these three classes of events in Fig. 7. As the flight distance is only 20 mm, our detector is sensitive to particles with a lifetime as short as $\sim 10^{-10}$ sec.

We use a fully automated scanning measurement system developed at Berkeley to scan all glass plates and measure the geometry of each identified track. The system consists of a CCD camera, a microscope, an image processor, and a computer. The on-line image analysis algorithm identifies tracks and extracts parameters of elliptical fit to tracks. We look for penetrating tracks and obtain a series of values of Z/β at every 0.3 g cm^{-2} interval along its trajectory. In off-line analysis, we use a dE/dx code and our calibration response curve to determine Z and β for each event by minimizing χ^2 of the fits to our measured Z/β values as a function of penetrating depth.

No one has realistically calculated the cross section for monopole production. A meaningful search for monopole pair production requires a sensitivity below the Drell-Yan cross section for pair production. In Fig. 8, I present the calculated Drell-Yan cross section based on an empirical formulae [69]. The Drell-Yan cross section serves as a rough point of reference for production of monopole pairs via an intermediate massive virtual photon, multiple virtual photons, or gluon-gluon fusion. Our limit on the cross section is lower than the estimated cross section for monopole production for values of monopole mass up to at least 3 GeV for 11.4 A GeV Au.

4 Search for GUT Monopoles

A small flux of GUT monopoles has been predicted to reach the Earth as a cosmological relic from the phase transition in the very early Universe. The possible velocity ranges from $\beta \sim 10^{-5}$ to 0.1, depending on the choice of the monopole mass. Three types of searches have been carried out: (1) direct searches for a flux of monopoles reaching the Earth now; (2) searches for signals of monopole interactions preserved in certain materials over a long period of time; and (3) searches for monopoles based on monopole catalysis of proton decay.

Table 3: Summary of flux limits for GUT monopoles obtained with superconducting induction devices.

Experimental Group	Magnetic Chage (g_o)	Velocity Range	Galactic Flux Limit ($cm^{-2}\,s^{-1}\,sr^{-1}$)	Refs.
Stanford	1	all β	$< 4.4 \times 10^{-12}$	[70]
Stanford	1	all β	$< 7.2 \times 10^{-13}$	[71]
IBM/BNL	1	all β	$< 3.8 \times 10^{-13}$	[72]
Stanford	1	all β	$< 7.2 \times 10^{-13}$	[73]
Kobe	1	all β	$< 1.0 \times 10^{-10}$	[74]
Imperial College	1	all β	$< 5.0 \times 10^{-14}$	[75]
NBS	1	all β	$< 5.0 \times 10^{-12}$	[76]
CFM	1	all β	$< 7.0 \times 10^{-11}$	[77]
IBM/BNL	1	all β	$< 5.0 \times 10^{-12}$	[78]
Imperial College	1	all β	$< 6.0 \times 10^{-12}$	[79]
Kobe	1	all β	$< 6.0 \times 10^{-10}$	[80]
IBM/BNL	1	all β	$< 7.0 \times 10^{-12}$	[81]
Stanford	1	all β	$< 4.0 \times 10^{-11}$	[82]
Stanford	1	all β	$< 6.0 \times 10^{-10}$	[83]

4.1 Direct Searches in Galactic Cosmic Rays

Superconducting induction devices, scintillation detectors, and track-etch detectors have been used in active searches for GUT monopoles. In 1982, Cabrera recoreded a single current jump that is consistent with a monopole of $g = g_o$ in a four-turn coil of 5 cm diameter [83]. In 1985, Caplin also found one event [75]. But no other jump was observed in subsequent runs with much larger areas by the same group and other groups, leaving these two events unconfirmed. No other candidate has been found. I summarize all the results obtained by various groups using induction devices in Table 3. I recall that these limits are valid for monopoles with all possible masses and velocities because the induction signal depends solely on the magnetic charge. The results obtained using track-etch detectors including CR-39 plastic and ancient mica are summarized in Table 4. In Table 5, I summarize all the flux limits obtained from searches using scintillator counters, proportional wire chamber, and water Čerenkov detectors.

4.2 Searches for Preserved Signals of Monopoles

A unique search was carried out using ancient mica as a track-etch detector by Price *et al.* [92]. Mica crystals are usually found in deep mines and have lifetimes on the order of Gyr. As seen from Fig. 2, the ionization of a bare monopole moving at a speed as slow as $\beta \leq 10^{-3}$ is too low to produce a damage in mica to form a track that is

Table 4: Summary of flux limits for GUT monopoles with track-etch detector CR-39 plastic and ancient mica.

Experimental Technique	Velocity Range (in units of c)	Flux Limit ($cm^{-2}\,s^{-1}\,sr^{-1}$)	Comments	Refs.
Plastic	$0.0004 - 1$	$< 3.7 \times 10^{-15}$	limits vary with β	[84]
	$0.00004 - 0.0002$	$< 2 \times 10^{-14}$		[85]
	$0.001 - 1$	$< 2 \times 10^{-14}$		[85]
	$0.0001 - 1$	$< 1 \times 10^{-13}$		[86]
	$0.007 - 1$	$< 1 \times 10^{-12}$		[87]
	$0.01 - 1$	$< 5 \times 10^{-15}$		[88]
	$0.001 - 1$	$< 1 \times 10^{-13}$		[89]
Ancient Mica	$0.0003 - 0.0015$	$< 1 \times 10^{-18}$	limits vary with β	[90]
	$0.0004 - 0.001$	$< 1 \times 10^{-18}$	limits vary with β	[91]
	$0.0006 - 0.002$	$< 1 \times 10^{-16}$	limits vary with β	[92]

chemically revealable. However, if a monopole captures a nucleus of charge $Z \geq 10$ (e.g., Al) on its journey through the Earth, the enhanced ionization of the bound state will cause measurable damage in the mica (see Fig. 2). Thus, in the entire lifetime of the mica, it served as a monopole detector. The signal should have been preserved as long as the temperature of the mica has remained low enough not to erase any tracks due to monopole-nucleus system. The mica that Price *et al.* used in their search was found at a depth of $\sim$ 5 km and its age was determined to be as old as 0.45×10^9 years. The authors used ancient tracks due to spontaneous fission of ^{238}U impurities in the mica to measure its fission-track age. To ensure that the temperature of the mica has remained low so that no tracks were erased in the entire history of the mica, they also measured the ratio of number of α-interaction tracks to number of fission tracks to establish the thermal history of the mica.

The advantage of this search is the long exposure time. Even for a small area, the collecting power is impressively large. For the area of 13.5 cm^2 they scanned, the collecting power corresponds to 6×10^9 cm^2 yr. No candidate of monopole tracks was found. Based on reasonable assumptions about the capture cross section, one can translate this negative result into flux limit. One finds this limit is the most stringent one among all the published limits to date. Similar searches were carried out later [91, 90] and all limits are listed in Table 4. Some of flux limits are presented in Fig. 9.

4.3 Searches Using Catalysis of Proton Decay

The idea of monopole catalysis of proton decay has been used to place upper limits on the relic flux of GUT monopoles. Several underground experiment groups working on proton

Table 5: Summary of flux limits for GUT monopoles with scintillator counters, proportional wire chambers, and Čerenkov detectors.

Experimental Group	Velocity Range (in units of c)	Flux Limit ($cm^{-2}\,s^{-1}\,sr^{-1}$)	Comments	Refs.
IMB	$0.00001 - 0.1$	$< 1.0 \times 10^{-15}$	Catalysis of p decay	[93]
MICRO	$0.00018 - 0.003$	$< 5.6 \times 10^{-15}$	Catalysis of p decay	[94]
Soudan II	$0.002 - 0.91$	$< 8.7 \times 10^{-15}$	Catalysis of p decay	[95]
INRM	< 0.001	$< 5 \times 10^{-16}$	Catalysis of p decay	[96]
Soudan I	$0.00001 - 1$	$< 1 \times 10^{-13}$	Catalysis of p decay	[97]
CalTech	$0.0003 - 0.005$	$< 5 \times 10^{-12}$		[98]
Texas A&M	$0.0009 - 0.01$	$< 5 \times 10^{-14}$		[99]
ICRR	$0.0004 - 1$	$< 1.7 \times 10^{-13}$		[100]
La Jolla	$0.0001 - 1$	$< 2 \times 10^{-14}$		[101]
Akeno	$0.0007 - 1$	$< 1 \times 10^{-13}$		[102]
KGF	$0.0012 - 1$	$< 3 \times 10^{-15}$	Catalysis of p decay	[103]
Frejus	$0.0008 - 0.1$	$< 5 \times 10^{-14}$		[104]
Kamioka	$0.00005 - 0.001$	$< 3 \times 10^{-15}$	Catalysis of p decay	[105]
IMB	$0.001 - 0.1$	$< 3 \times 10^{-15}$	Catalysis of p decay	[106]
ICRR	$0.0003 - 0.001$	$< 7 \times 10^{-13}$		[107]
ICRR	$0.0003 - 0.1$	$< 2 \times 10^{-12}$		[108]
Tokyo	$0.00005 - 1$	$< 6 \times 10^{-13}$		[109]
KGF	$0.001 - 1$	$< 2 \times 10^{-14}$		[110]
Berkeley	$0.0006 - 0.002$	$< 4 \times 10^{-13}$		[111]
Berkeley	$0.0006 - 0.002$	$< 4 \times 10^{-13}$		[112]
Soudan I	$0.001 - 0.01$	$< 4 \times 10^{-13}$		[113]
Bologna	$0.001 - 0.4$	$< 3 \times 10^{-13}$		[114]
AHT	$0.0005 - 0.05$	$< 3 \times 10^{-12}$	Catalysis of p decay	[115]
IMB	$0.0001 - 0.1$	$< 8 \times 10^{-15}$	Catalysis of p decay	[116]
Mayflower	$0.0001 - 0.03$	$< 5 \times 10^{-12}$		[117]
Tokyo	$0.0006 - 1$	$< 2 \times 10^{-12}$		[118]
M Blanc 1	$0.02 - 1$	$< 5 \times 10^{-13}$		[119]
Baksan	0.003	$< 1 \times 10^{-13}$		[120]
Bologna	$0.007 - 0.6$	$< 2 \times 10^{-12}$		[121]
Tokyo	$0.01 - 0.1$	$< 2 \times 10^{-11}$		[122]
BNL	$0.0003 - 0.001$	$< 5 \times 10^{-11}$		[123]

decay have published flux limits. The results obtained by several experiments are listed in Table 5.

Similar searches can be carried out with underwater or underice neutrino detector arrays such as BAIKAL and AMANDA. With an array of photomultiplier modules, the catalysis of proton decay in some certain range of monopole velocity will produce a detectable signal in the detector. In fact, an upper limit has been already placed by BAIKAL group using 6 photomultipliers [124].

It should be pointed out that the flux limits obtained from the catalysis of proton decay depend on the catalysis cross section. When one compares these limits, one should check with conditions of each limit and especially the catalysis cross section each experiment assumes.

5 Astrophysical and Cosmological Limits

Many authors have shown that the existence of GUT monopoles may have a myriad of astrophysical and cosmological consequences. In turn, these astrophysical and cosmological arguments have been used to provide severe constraints on the present relic flux of GUT monopoles. In this section, I will briefly discuss several examples.

5.1 Limit from Mass Density of the Universe

If the Universe is flat as favored by the theoretical prejudice such as inflation theory, the mass density of the Universe is equal to the critical density ($\Omega = 1$). An increasing number of observations support that the Universe consists largely of dark matter. Monopoles are certainly a candidate for the dark matter in galaxies and for providing closure density. By requiring that the present monopole mass density be smaller than the critical density, a bound on the monopole flux can be obtained for three cases.

If monopoles are uniformly distributed and have a typical velocity $\beta \sim 10^{-3}$, the average flux limit is:

$$\mathcal{F}_{\mathrm{M}} \leq 10^{-14}\,\mathrm{cm}^{-2}\,\mathrm{s}^{-1}\,\mathrm{sr}^{-1}\left(\frac{10^{16}\,\mathrm{GeV}}{m_{\mathrm{M}}}\right). \tag{2}$$

If monopoles cluster in galaxies, ours in particular, the local galactic flux can be significantly higher. The flux limit is:

$$\mathcal{F}_{\mathrm{M}} \leq 5 \times 10^{-10}\,\mathrm{cm}^{-2}\,\mathrm{s}^{-1}\,\mathrm{sr}^{-1}\left(\frac{10^{16}\,\mathrm{GeV}}{m_{\mathrm{M}}}\right). \tag{3}$$

Taking the local monopole mass density to be less than the local halo density, a more realistic flux limit is obtained:

$$\mathcal{F}_{\mathrm{M}} \leq 10^{-10}\,\mathrm{cm}^{-2}\,\mathrm{s}^{-1}\,\mathrm{sr}^{-1}\left(\frac{10^{16}\,\mathrm{GeV}}{m_{\mathrm{M}}}\right). \tag{4}$$

Comparing the last limit to those listed in Tables 3-5, one can conclude that the experimental search limits are more stringent than this limit by few orders of magnitude, indicating that GUT relic monopoles, if any, do not constitute the majority of the dark matter in our galaxy. In other words, $\Omega_{\rm monopole} << 1$.

5.2 Limit from the Galactic Magnetic Field

A monopole by virtue of its magnetic charge will be accelerated by any magnetic field it encounters, and in the process it can gain kinetic energy. The magnetic field in our galaxy is stretched in the azimuthal direction along the spiral arms, and it is probably due to the non-uniform rotation of the galaxy. The field is complicated, but is characterized by strength $B \simeq 3 \times 10^{-6}$ G, the coherent length $l \simeq 300$ pc, the size of the field region $r \sim 30$ kpc, and the rotation period $\tau \simeq 3 \times 10^7$ yr. A flux limit can be obtained by requiring that the kinetic energy gained per unit time by magnetic monopoles be equal to or less than the magnetic energy generated by the dynamo effect. The flux limit obtained this way is called Parker limit [127]. The Parker limit was reexamined by taking into account the complicated chaotic nature of the galactic magnetic field. The current limit is [125]:

$$\mathcal{F}_{\rm M} \leq 10^{-15}\,{\rm cm}^{-2}\,{\rm s}^{-1}\,{\rm sr}^{-1}\left(\frac{B}{3\times 10^{-6}\,{\rm G}}\right)\left(\frac{3\times 10^7\,{\rm yr}}{\tau}\right)\left(\frac{r}{30\,{\rm kpc}}\right)\left(\frac{300\,{\rm pc}}{l}\right)^{1/2}, \quad (5)$$

for $m_{\rm M} \leq 10^{17}$ GeV and

$$\mathcal{F}_{\rm M} \leq 10^{-16}\,{\rm cm}^{-2}\,{\rm s}^{-1}\,{\rm sr}^{-1}\left(\frac{m_{\rm M}}{10^{16}\,{\rm GeV}}\right)\left(\frac{3\times 10^7\,{\rm yr}}{\tau}\right)\left(\frac{300\,{\rm pc}}{l}\right), \quad (6)$$

for $m_{\rm M} \geq 10^{17}$ GeV. The Parker limit has served as a benchmark for the sensitivity of monopole search experiments.

5.3 Limit from Intercluster Magnetic Fields

Parker's argument can be applied to the survival of other astrophysical magnetic fields. Raphaeli and Turner [135] assumed the existence of intercluster field $B_{\rm IC} \sim 3 \times 10^{-8}$ G with a regeneration time $\tau_{\rm IC} \sim 10^9$ year. They obtained a flux limit that is about three orders of magnitude more stringent than the original Parker limit. But the limit is less reliable than that obtained from our own galaxy, because our knowledge of the existence of the persistence time of intercluster fields is less secure.

5.4 Limit from Monopole Catalysis of Nucleon Decay

The most stringent flux limit follows from considering neutron stars with some model dependence [133]. A variety of approaches have been used to obtain limits to the luminosities of neutron stars. A review can be found in Ref. [130]. Limits obtained from other astrophysical and cosmological considerations are all listed in Table 6. It should be

Table 6: Flux limits of GUT monopoles derived from astrophysical and cosmological considerations.

Argument	Flux Limit ($cm^{-2}\,s^{-1}\,sr^{-1}$)	Comments	Refs.
Galactic field	$< 1 \times 10^{-16}$	Improved Parker Limit	[125]
	$< 1 \times 10^{-12}$	Reexamined Parker Limit	[126]
	$< 1 \times 10^{-16}$	Parker Limit	[127]
Jovian planets	$< 1 \times 10^{-23}$	Catalysis of p decay	[128]
Solar trapping	$< 1 \times 10^{-16}$	–	[129]
Neutron stars	$< 3 \times 10^{-23}$	–	[130]
	$< 1 \times 10^{-18}$	Catalysis of p decay	[131]
	$< 1 \times 10^{-23}$	Catalssis of p decay	[132]
	$< 5 \times 10^{-22}$	Catalysis of p decay	[133]
Pulsars	$< 7 \times 10^{-22}$	Catalysis of p decay	[134]
Intergalactic field	$< 1 \times 10^{-18}$	Catalysis of p decay	[135]
Galactic halo	$< 5 \times 10^{-15}$	–	[136]

emphasized that these limits listed in Table 6 would not be taken seriously to within a few orders of magnitude accuracy due to various astrophysical uncertainties.

6 Discussions and Conclusions

The discovery of a monopole should be of fundamental importance and have great impact on physical theories. A number of searches carried out for Dirac monopoles in high energy collisions of e^+e^-, pp, $p\overline{p}$, and pA at various accelerators have all led to negative results. Upper limits have been placed on the cross section for the monopole production for various masses accessible. In heavy ion collisions the production of monopoles is more likely than in e^+e^- and pp (or $p\overline{p}$) collisions due to the possible thermal production mechanism. A search for monopole production in high energy nucleus-nucleus collisions has been carried out at BNL AGS using 11.4 A GeV Au ions. A new search has been planned at CERN SPS using the newly available beam of 160 A GeV Pb.

The supermassive monopoles are predicted by GUTs with calculable properties. They might have played an important role in the earliest moment of the Universe. Along with neutrino mass and proton decay, monopoles are one of the few predictions of GUTs that can be studied in our present low energy environment. The relic supermassive monopoles are expected to be present in galactic cosmic rays, but their flux cannot be calculated realistically to within an order of magnitude. The massive GUT monopoles created in the early Universe have many interesting astrophysical and cosmological consequences. Some

of them are so conspicuous (and thus far not seen) that they can be used to place severe constraints on the possible flux of relic monopoles. However, this type of argument serves only as a consistency check for the theory, but not a test, because it can only be used to rule out the theory, but not confirm the theory. The flux limits obtained in this way indicates how far one needs to go in order to perform a meaningful search. The unique way to test the theory is to detect the relic flux for which there is no substitute.

The question then is at what level a non-detection should be of significance for GUT and/or cosmology of the early Universe. While there is no solid calculation of the relic flux, most researchers believe that searches below the Parker limit should be of significance for GUTs. But I am not aware of any concrete argument or any detailed calculation to demonstrate how it goes.

When one compares the published flux limits of GUT monopoles, one should be aware of the condition under which each limit was derived. I have following comments.

The limits from track-etch detector CR-39 were obtained assuming that the response of CR-39 to a given value of dE/dx is the same at low energies as at high energies and that nuclear stopping has the same effectiveness as electronic stopping [86]. In the Japanese experiment, the CR-39 is the only detector used to record monopole candidates. In MACRO, the CR-39 is used to confirm the existence of a monopole when the scintillation counters and streamer tubes that are used in conjunction with the CR-39 array indicate a candidate. Detection of monopoles in a low velocity regime requires that the detector is sensitive not only to electronic stopping, but also to nuclear stopping, with total $dE/dx > (dE/dx)_{th} \sim 100\,\mathrm{MeV\,g^{-1}\,cm^2}$. Therefore, the determination of the detector threshold in dE/dx and effectiveness of nuclear stopping in comparison with electronic stopping in CR-39 is essential for these searches. A recent study by Snowden-Ifft and Price using a scanning electron microcope (SEM) reported that nuclear stopping is only $20 \pm 10\%$ as effective as electronic stopping at affecting the response of the CR-39 made by American Acrylics [137]. The threshold of this type of CR-39 in the effective dE/dx is extrapolated to be $\sim 1\ \mathrm{GeV\,g^{-1}cm^2}$. Consequently, this type of CR-39 is believed to be insensitive to a low velocity monopole. Cecchini *et al.* [138] have recently calibrated the CR-39 used in MACRO experiment using the SEM technique. They claimed that for MACRO CR-39 the response to low energy ions is the same as to high energy ions for the equivalent value of dE/dx with the same efficiency for nuclear stopping and electronic stopping. Their work raises the need for further study of the response of CR-39 to low energy ions, and especially to determine the effectiveness of nuclear stopping in track formation. We have recently demonstrated that an atomic force microscope (AFM) can be used to measure low energy ion tracks in CR-39 [139]. This technique might be used to determine the effectiveness of nuclear stopping and to determine the threshold of CR-39.

Some limits were obtained assuming the catalysis of nucleon decay by monopoles. These limits are valid for the assumed catalysis cross section and some different values have been used by different groups.

The mica limit is valid when monopoles do not catalyze nucleon decay and is valid for those monopoles that did not capture a proton in the early Universe and that did capture a nucleus with $Z > 10$ before reaching the mica sample at a depth of ~ 3 km. The fraction

of monopoles that would reach the Earth without having captured a proton is a function of only the binding energy of the monopole-proton bound state and baryon/photon ratio. The uncertainty in this fraction ranges from 0.02 to 0.9 [140].

Limits obtained using induction device do not depend on other properties of monopoles such as the monopole velocity and mass.

To summarize, the accelerator searches are sensitive only to monopoles with limited masses ($m_M \leq 850$ GeV). Searches for GUT monopoles with large masses ($m_M \sim 10^{16}$ GeV) have been carried out in galactic cosmic rays. I want to point out that even though the mass regimes of these two types of experiments are very different, they in fact attack the same physics from different approaches. In the accelerator experiments, one measures the cross section for monopole creation either thermally or via pair production. In the cosmic ray experiments, one measures the flux of monopoles produced in the very early Universe. It is interesting to compare the limit on production cross section for monopoles obtained from accelerator experiments to the limit on the flux of monopoles obtained from cosmic ray experiments in the same mass range. Starting with an assumed monopole-antimonopole annihilation cross section, an expanding universe, and detailed balance, the present flux of thermally produced monopoles of mass m_M is estimated to be [126]:

$$f_M \simeq 10^{12}\ \mathrm{cm}^{-2}\,\mathrm{s}^{-1}\,\mathrm{sr}^{-1}\left(\frac{m_M}{T_i}\right)^3 \exp\left(-\frac{2m_M}{T_i}\right), \tag{7}$$

in which $T_i \sim 10^{14}$ GeV is the temperature of the Universe when production of monopoles took place. Let us assume that the null detection of monopoles at the highest energy pp collider rules out the monopole with $m_M \leq 100$ GeV. So for a monopole mass of 100 GeV, we have $f_M \sim 10^{-23}\ \mathrm{cm}^{-2}\,\mathrm{s}^{-1}\,\mathrm{sr}^{-1}$, which is about a factor of 10^8 below the best limits obtained from cosmic ray experiments so far. Of course, searches for GUT monopoles with larger masses will have to be carried out in galactic cosmic rays.

Acknowledgements

I thank Professor Buford Price for reading the manuscript.

References

[1] P. A. M. Dirac, in *Proc. Roy. Soc.* London, Ser. A **133**, 60 (1931).

[2] P. A. M. Dirac, Phys. Rev. **74**, 817 (1948).

[3] T. Goldman and D. Ross, Phys. Lett. B **84**, 20 (1979).

[4] G. 't Hooft, Nucl. Phys. B **79**, 276 (1974).

[5] A. M. Polyakov, JETP Lett. **20**, 194 (1974).

[6] H. Georgi and S. L. Glashow, Phys. Rev. Lett. **32**, 438 (1974); H. Georgi, H. R. Quinn, and S. Weiberg, Phys. Rev. Lett. **33**, 451 (1974).

[7] M. K. Prasad and C. M. Sommerfield, Phys. Rev. Lett. **35**, 760 (1975).

[8] E. W. Kolb and M. S. Turner, *The Early Universe* (Addison-Wesley, 1990).

[9] J. Preskill, Ann. Rev. Nucl. Part. Sci. **34**, 461 (1984).

[10] R. A. Carrigan and W. P. Trower, Sci. Am. **246**, No 4, 106 (1983).

[11] R. A. Carrigan and W. P. Trower, Nature **305**, 673 (1983).

[12] G. Giacomelli, Riv. Nuovo Cimento **7**, 1 (1984).

[13] D. E. Groom, Phys. Rep. **140**, 323 (1986).

[14] S. P. Ahlen, Rev. Mod. Phys. **52**, 121 (1980).

[15] G. F. Drell *et al.*, Nucl. Phys. B **209**, 45 (1980).

[16] S. P. Ahlen and K. Kinoshita, Phys. Rev. D **26**, 2347 (1982).

[17] S. P. Ahlen and G. Tarlé, Phys. Rev. D **27**, 688 (1983).

[18] C. R. Dokos and T. N. Tomaras, Phys. Rev. D **21**, 2940 (1980).

[19] V. A. Rubakov and M. S. Serebryakov, Nucl. Phys. B **218**, 240 (1983).

[20] V. A. Rubakov, JETP Lett. **33**, 644 (1981); Nucl. Phys. B **203**, 311 (1982).

[21] G. G. Callan, Phys. Rev. D **26**, 2058 (1982).

[22] T. Ebisu and T. Watanabe, Phys. Rev. D **36**, 3359 (1987).

[23] V. F. Mikhailov, Phys. Lett. B **130**, 331 (1983).

[24] R. A. Carrigan, F. A. Nezrick, and B. P. Strauss, Phys. Rev. D **13**, 1823 (1976).

[25] B. Cabrera, Ph. D. Thesis, Stanford (1975).

[26] R. R. Ross, P. H. Eberhard, L. W. Alvarez, and R. D. Watt, Phys Rev. D **8**, 698 (1973).

[27] H. H. Kolm, F. Villa, and A. Odian, Phys. Rev. D **4**, 1285 (1971).

[28] R. L. Fleischer *et al.*, Phys. Rev. **177**, 2029 (1969).

[29] R. L. Fleischer *et al.*, Phys. Rev. **184**, 1392 (1969).

[30] E. Goto, H. H. Kolm, and K. W. Ford, Phys. Rev. **132**, 387 (1963).

[31] V. A. Petukhov and M. N. Yakimenko, Nucl. Phys. **49**, 87 (1963).

[32] A. K. Drukier and S. Nussinov, Phys. Rev. Lett. **49**, 102 (1982).

[33] L. E. Roberts, Nuovo Cimento A **92**, 247 (1986).

[34] J. L. Pinfold *et al.*, Phys. Lett. B **316**, 407 (1993).

[35] K. Kinoshita *et al.*, Phys. Rev. D **46**, R881 (1992).

[36] K. Kinoshita *et al.*, Phys. Lett. B **228**, 543 (1989).

[37] W. Braunsch *et al.* (TASSO Coll.), Z. Phys. C **38**, 543 (1988).

[38] K. Kinoshita *et al.*, Phys. Rev. Lett. **60**, 1610 (1988).

[39] T. Gentile *et al.*, Phys. Rev. D **35**, 1081 (1987).

[40] D. Fryberger *et al.*, Phys. Rev. D **29**, 1524 (1984).

[41] P. Musset, M. Price, and E. Lohrmann, Phys. Lett. B **128**, 333 (1983).

[42] K. Kinoshita, P. B. Price, and D. Fryberger, Phys. Rev. Lett. **48**, 77 (1982).

[43] M. Bertani *et al.*, Europhys. Lett. **12**, 613 (1990).

[44] P. B. Price, G. R. Jing, and K. Kinoshita, Phys. Rev. Lett. **65**, 143 (1990).

[45] P. B. Price, G. X. Ren, and K. Kinoshita, Phys. Rev. Lett. **59**, 2523 (1987).

[46] B. Aubert *et al.*, Phys. Lett. B **120**, 465 (1983).

[47] G. F. Dell *et al.*, Nucl. Phys. B **209**, 45 (1982).

[48] R. A. Carrigan, B. P. Strauss, and G. Giacomelli, Phys. Rev. D **17**, 1754 (1978).

[49] H. Hoffmann *et al.*, Lett. Nuovo Cimento **23**, 357 (1978).

[50] G. Giacomelli *et al.*, Nuovo Cimento A **28**, 21 (1975).

[51] D. M. Stevens *et al.*, Phys. Rev. D **14**, 2207 (1976).

[52] V. P. Zrelov *et al.*, Cze. J. Phys. B **26**, 1306 (1976).

[53] P. Eberhard, LBL Report 4289 (1975).

[54] R. A. Carrigan, F. A. Nezrick, and B. P. Strauss, Phys. Rev. D **10**, 3876 (1974).

[55] R. A. Carrigan, F. A. Nezrick, and B. P. Strauss, Phys. Rev. D **8**, 3717 (1973).

[56] I. I. Gurevich *et al.*, Phys. Lett. B **38**, 549 (1972).

[57] E. Amaldi *et al.*, Nuovo Cimento **28**, 773 (1963).

[58] E. Purcell *et al.*, Phys. Rev. **129**, 2326 (1963).

[59] M. Fidecaro, G. Finocchiaro, G. Giacomelli, Nuovo Cimento **22**, 657 (1961).

[60] H. B. Bradner and W. M. Isbell, Phys. Rev. **114**, 603 (1959).

[61] D. L. Berke *et al.*, Phys. Lett. B **60**, 113 (1975).

[62] R. A. Carrigan and F. A. Nezrick, Nucl. Phys. B **91**, 279 (1975).

[63] D. F. Bartlett and M. D. Lahana, Phys. Rev. D **6**, 1817 (1972).

[64] Y. D. He and P. B. Price, Phys. Rev. C **48**, 647 (1993).

[65] T. Dobbins and L. E. Roberts, Nuovo Cimento A **106**, 1295 (1993).

[66] Y. D. He and P. B. Price, in preparation (1995).

[67] Y. D. He and P. B. Price, A Proposal to CERN SPS (1995).

[68] Y. D. He, A. J. Westphal and P. B. Price, Nucl. Instr. Meth. B **84**, 67 (1994).

[69] R. Vogt, Atomic Data Nucl. Tables **50**, 343 (1992).

[70] R. D. Gardner *et al.*, Phys. Rev. D **44**, 622 (1991).

[71] M. E. Huber *et al.*, Phys. Rev. D **44**, 636 (1992).

[72] S. Bermon *et al.*, Phys. Rev. Lett. **64**, 839 (1990).

[73] M. E. Huber *et al.*, Phys. Rev. Lett. **64**, 835 (1990).

[74] T. Ebisu and T. Watanabe, Phys. Rev. D **36**, 3359 (1987).

[75] A. D. Caplin *et al.*, Nature **321**, 402 (1986).

[76] M. W. Cromar *et al.*, Phys. Rev. Lett. **56**, 2561 (1986).

[77] J. Incandela *et al.*, Phys. Rev. D **34**, 2637 (1986).

[78] S. Bermon *et al.*, Phys. Rev. Lett. **55**, 1850 (1985).

[79] A. D. Caplin *et al.*, Nature **317**, 234 (1985).

[80] T. Ebisu and T. Watanabe, J. Phys. G **11**, 883 (1985).

[81] J. Incandela *et al.*, Phys. Rev. Lett. **53**, 2067 (1984).

[82] B. Cabrera, M. Taber, R. Gardner, and J. Bours, Phys. Rev. Lett. **51**, 1933 (1983).

[83] B. Cabrera, Phys. Rev. Lett. **48**, 1378 (1982).

[84] S. Orito *et al.*, Phys. Rev. Lett. **66**, 1951 (1991).

[85] K. Nakamura *et al.*, Phys. Lett. B **183**, 395 (1987).

[86] P. B. Price, Phys. Lett. B **140**, 112 (1984).

[87] S. W. Barwick, K. Kinoshita, and P. B. Price, Phys. Rev. D **28**, 2338 (1983).

[88] T. Doke *et al.*, Phys. Lett. B **129**, 370 (1983).

[89] K. Kinoshita and P. B. Price, Phys. Rev. D **24**, 1707 (1981).

[90] D. Ghosh and S. Chatterjea, Europhys. Lett. **12**, 25 (1990).

[91] P. B. Price and M. H. Salamon, Phys. Rev. Lett. **56**, 1126 (1986).

[92] P. B. Price, S. L. Guo, S. P. Ahlen, and R. L. Fleischer, Phys. Rev. Lett. **52**, 1265 (1984).

[93] R. Becker-Szendy *et al.* (IMB Coll.), Phys. Rev. D **49**, 2169 (1994).

[94] S. P. Ahlen *et al.* (MACRO Coll.), Phys. Rev. Lett. **72**, 608 (1994).

[95] J. L. Thron *et al.* (Soudan-II Coll.), Phys. Rev. D **46**, 4846 (1992).

[96] L. B. Bezrukov *et al.*, Sov. J. Nucl. Phys. **52**, 54 (1990).

[97] J. Bartelt *et al.* (Soudan Coll.), Phys. Rev. D **36**, 1990 (1987).

[98] B. Barish, G. Liu, and C. Lane, Phys. Rev. D **36**, 2641 (1987).

[99] M. J. Shepko *et al.*, Phys. Rev. D **35**, R2917 (1987).

[100] T. Tsukamoto *et al.*, Europhys. Lett. **3**, 39 (1987).

[101] G. E. Masek *et al.*, Phys. Rev. D **35**, 2758 (1987).

[102] T. Hara *et al.*, Phys. Rev. Lett. **56**, 553 (1986).

[103] M. R. Krishnaswamy *et al.* (KGF Coll.), Nuovo Cimento C **9**, 167 (1986).

[104] Ch. Berger *et al.*, Nucl. Phys. B **313**, 509 (1986).

[105] T. Kajita *et al.*, J. Phys. Soc. Japan **54**, 4065 (1985).

[106] H. S. Park *et al.* (IMB Coll.), Nucl. Phys. B **252**, 261 (1985).

[107] F. Kajino *et al.*, Phys. Rev. Lett. **52**, 1373 (1984).

[108] F. Kajino *et al.*, J. Phys. G **10**, 447 (1984).

[109] K. Kawagoe *et al.*, Lett. Nuovo Cimento **41**, 315 (1984).

[110] M. R. Krishnaswamy *et al.* (KGF Coll.), Phys. Lett. B **142**, 99 (1984).

[111] T. M. Liss, S. P. Ahlen, and G. Tarlé, Phys. Rev. D **30**, 884 (1984).

[112] G. Tarlé, S. P. Ahlen, and T. M. Liss, Phys. Rev. Lett. **52**, 90 (1984).

[113] J. Bartelt *et al.* (Soudan 1 Coll.), Phys. Rev. Lett. **50**, 655 (1983).

[114] R. Bonarelli *et al.*, Phys. Lett. B **126**, 137 (1983).

[115] P. C. Bosetti *et al.*, Phys. Lett. B **133**, 265 (1983).

[116] S. Errede *et al.* (IMB Coll.), Phys. Rev. Lett. **51**, 245 (1983).

[117] D. E. Groom, E. C. Loh, H. N. Nelson, and D. M. Ritson, Phys. Rev. Lett. **50**, 573 (1983).

[118] T. Mashimo *et al.*, Phys. Lett. B **128**, 327 (1983).

[119] G. Battistoni *et al.*, Phys. Lett. B **133**, 454 (1983).

[120] E. N. Alexeyev *et al.*, Lett. Nuovo Cimento **35**, 413 (1982).

[121] R. Bonarelli *et al.*, Phys. Lett. B **112**, 100 (1982).

[122] T. Mashimo *et al.*, J. Phys. Soc. Japan **51**, 3067 (1982).

[123] J. D. Ullman, Phys. Rev. Lett. **47**, 289 (1981).

[124] L. B. Bezrukov *et al.* (BAIKAL Coll.),in *Proc. Intern. Conf. on High Energy Phys.* Leipzig (1984).

[125] F. C. Adams *et al.*, Phys. Rev. Lett. **70**, 2511 (1993).

[126] M. S. Turner, E. N. Parker, and T. Bogdan, Phys. Rev. D **26**, 1296 (1982).

[127] E. N. Parker, Astrophys. J. **160**, 383 (1970).

[128] J. Arafune, M. Fukugita, and T. Yanagita, Phys. Rev. D **32**, 2586 (1985).

[129] L. Bracci *et al.*, Nucl. Phys. B **258**, 726 (1985).

[130] E. W. Kolb and M. S. Turner, Astrophys. J. **286**, 702 (1984).

[131] J. A. Harvey, Nucl. Phys. B **236**, 255 (1984).

[132] S. Dimopoulos, J. Preskill, and F. Wilczek, Phys. Rev. Lett. **119**, 320 (1982).

[133] E. W. Kolb, S. Colgate, and J. A. Harvey, Phys. Rev. Lett. **49**, 1373 (1982).

[134] K. Freese, M. S. Turner, and D. Schramm, Phys. Rev. Lett. **51**, 1625 (1983).

[135] Y. Raphaeli and M. S. Turner, Phys. Lett. B **121**, 115 (1983).

[136] E. E. Salpeter, S. L. Shapiro, and I. Wasserman, Phys. Rev. Lett. **49**, 1114 (1982).

[137] D. P. Snowden-Ifft and P. B. Price, Phys. Lett. B **288**, 250 (1982).

[138] S. Cecchini *et al.*, MACRO Internal Memo. 20/93 (1993).

[139] Y. D. He and C. I. Hancox, Rev. Sci. Instr. (1995) in press.

[140] P. B. Price, Phys. Rev. Lett. **73**, 1305 (1994).

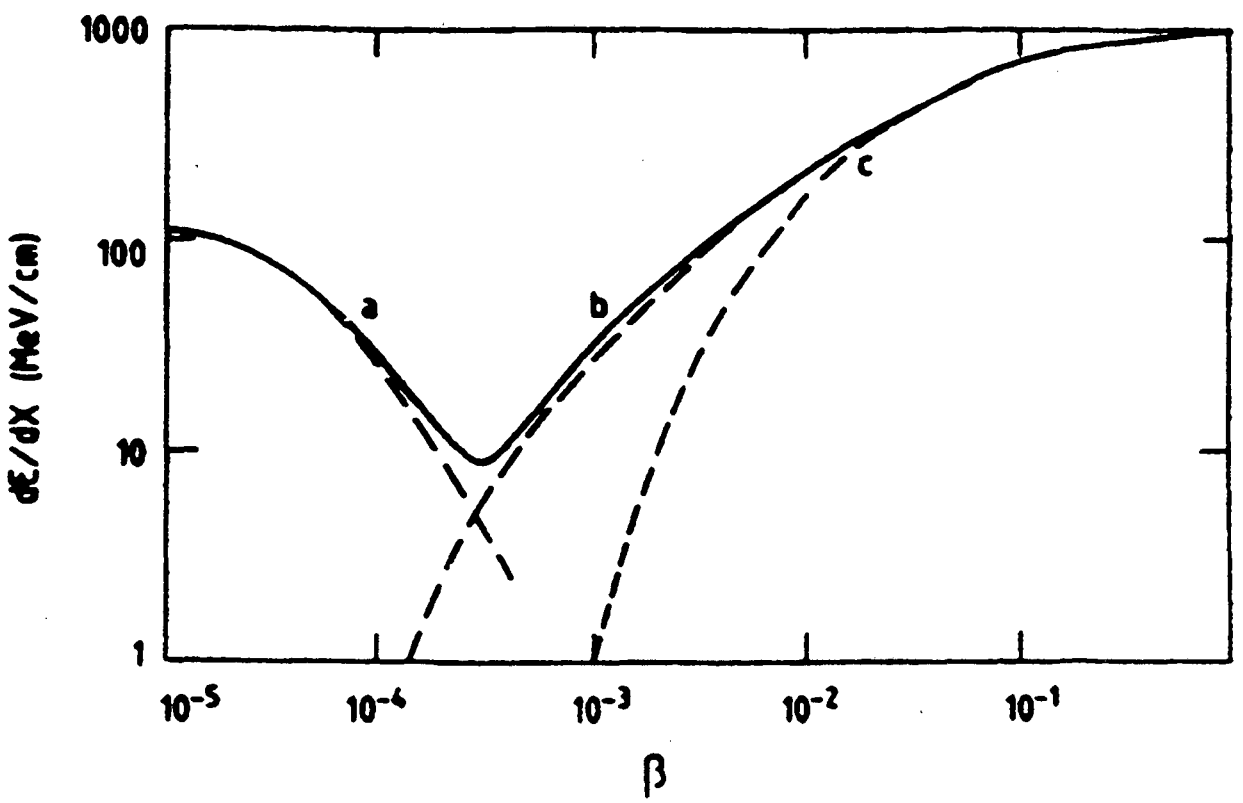

Fig. 1 dE/dx for a monopole in hydrogen due to (a) elastic scattering, (b) interactions with level crossing, and (c) ionization loss. The total is shown as the solid line.

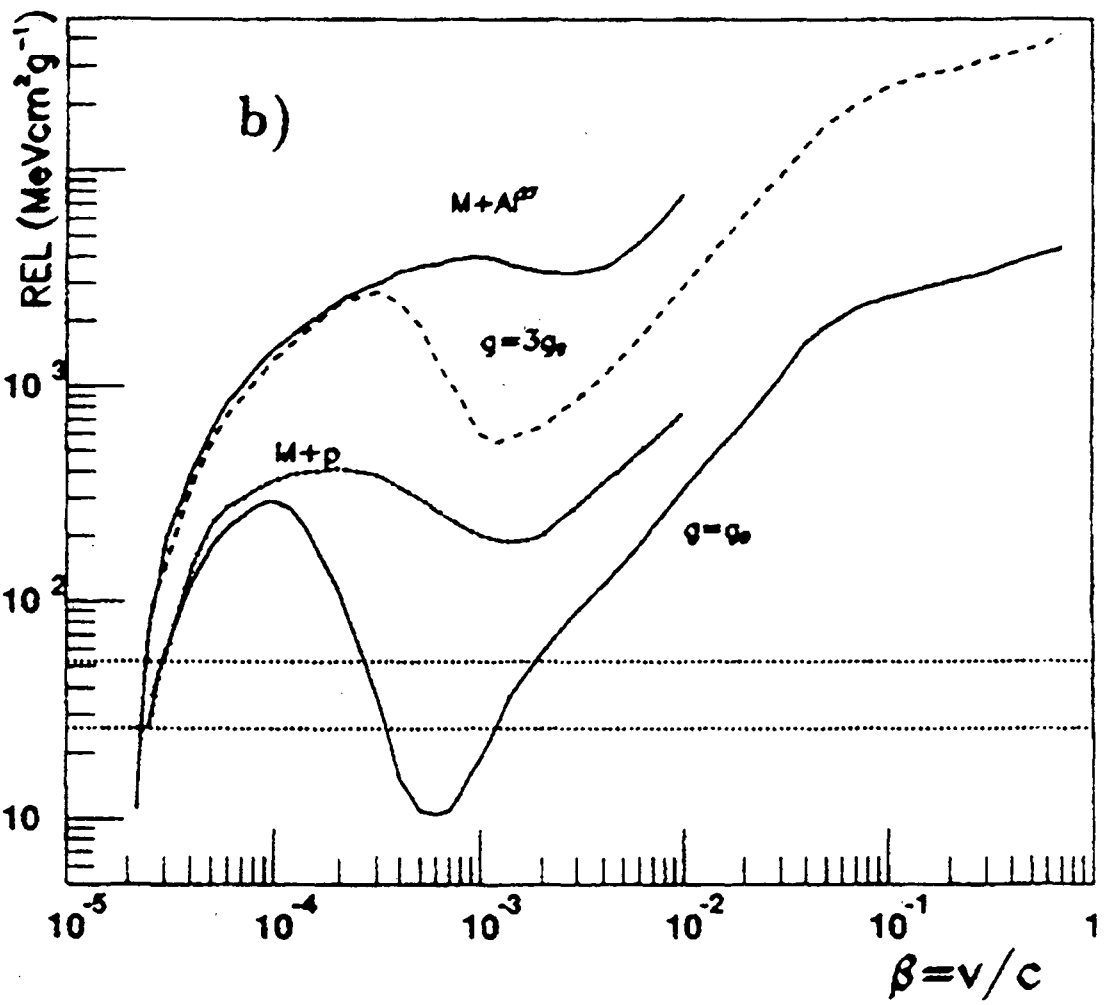

Fig. 2 The calculated REL for the bare and bound monopole as a function of the velocity. The detector threshold is around 100 MeV $cm^2\,g^{-1}$.

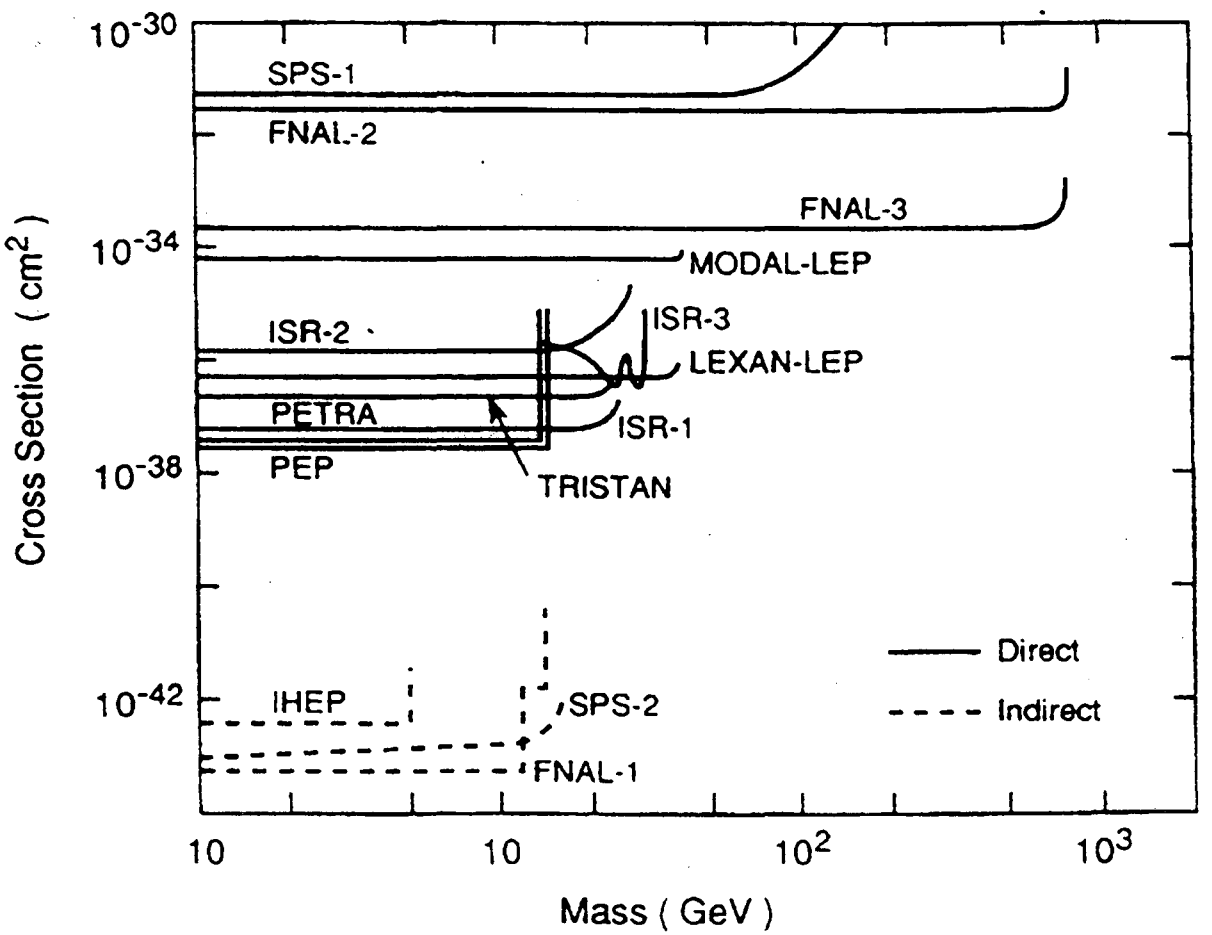

Fig. 3 Summary of upper limits on the production cross section of Dirac monopoles in high energy particle accelerators.

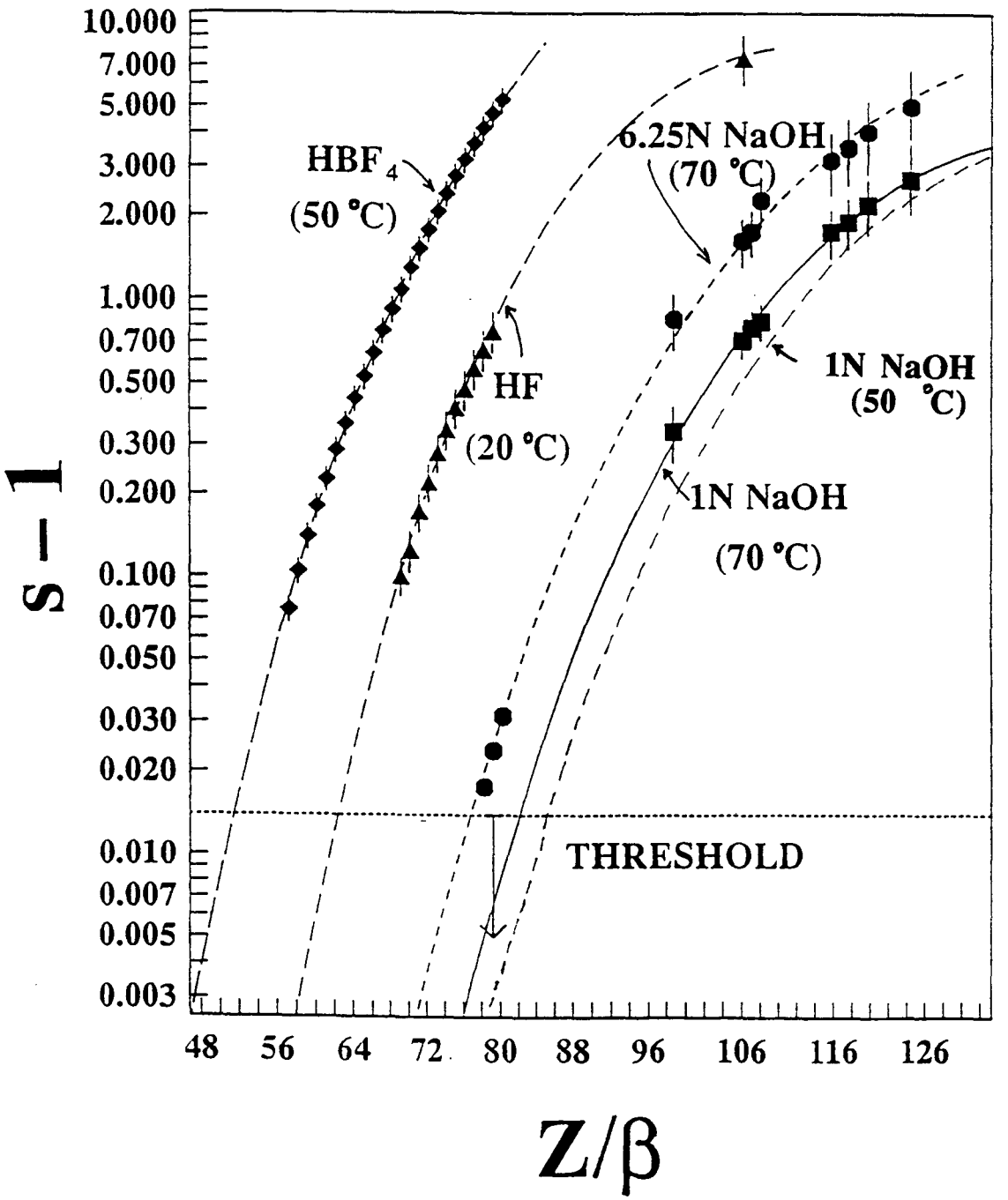

Fig. 4 The calibrated response curves for BP-1 glass etched in various etchants: 49% HBF_4 at 50 °C, 49% HF at 18 °C, 6.25N NaOH at 50 °C, 1N NaOH at 70 °C, and 1N NaOH at 50 °C. The detector signal $(s-1)$ is shown as a function of Z/β.

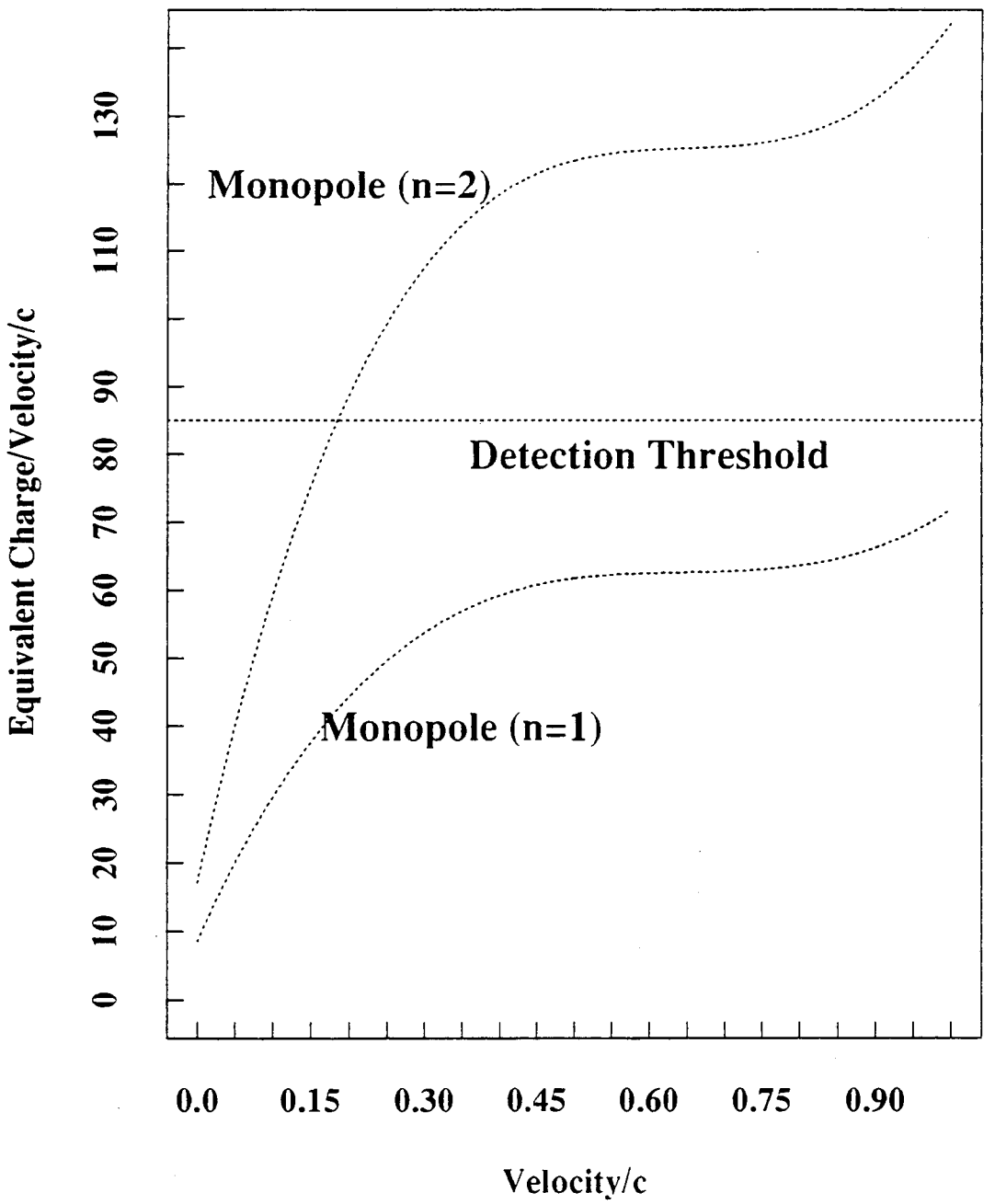

Fig. 5 The ratio of the equivalent charge Q to the velocity of a Dirac monopole as a function of velocity. Monopole with $n = 2$ and $\beta > 0.2$ are detectable.

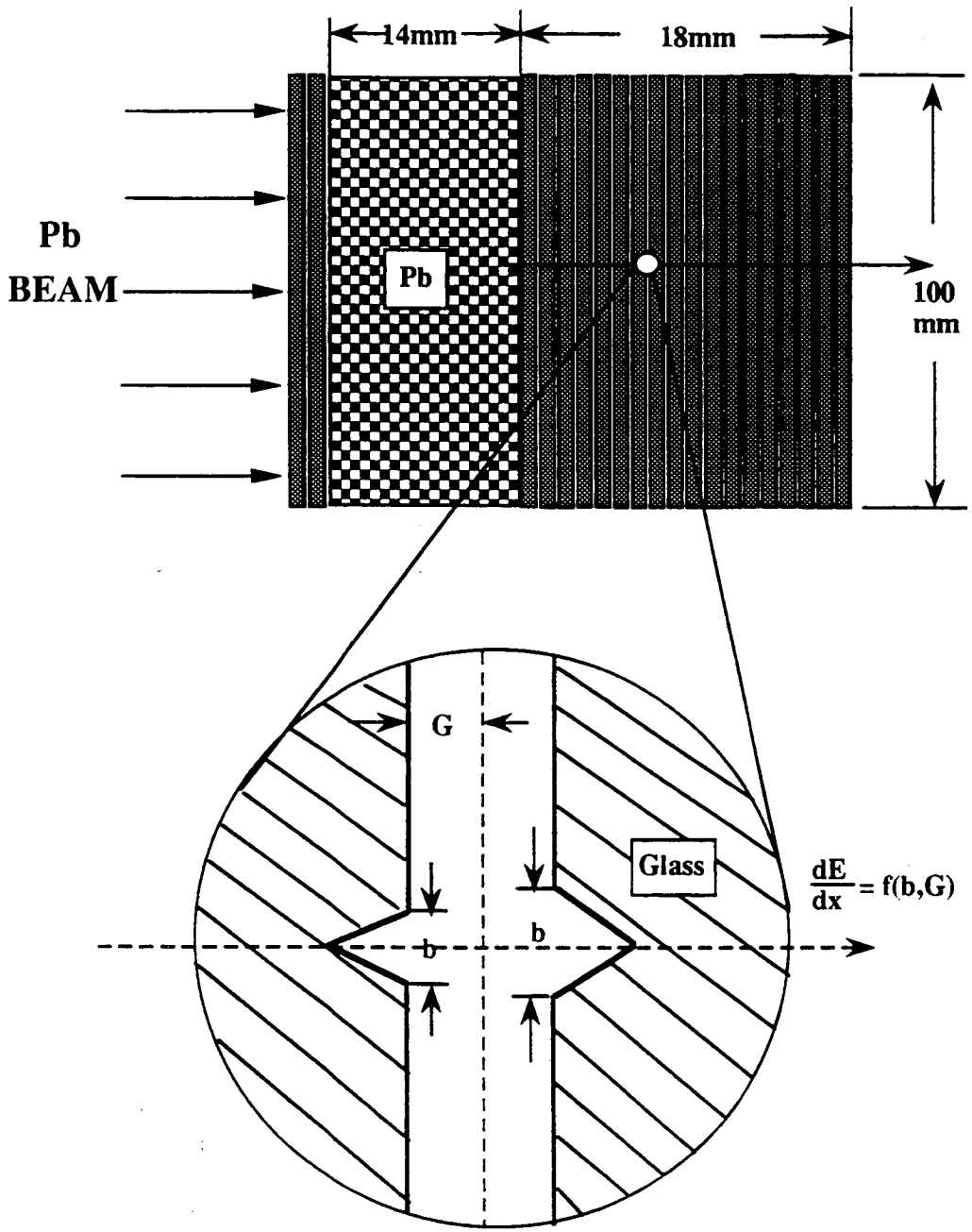

Fig. 6 The experimental setup used in a recent high statistics search for Dirac monopole production. The dE/dx is measured at various depths as a particle passes through the detector system.

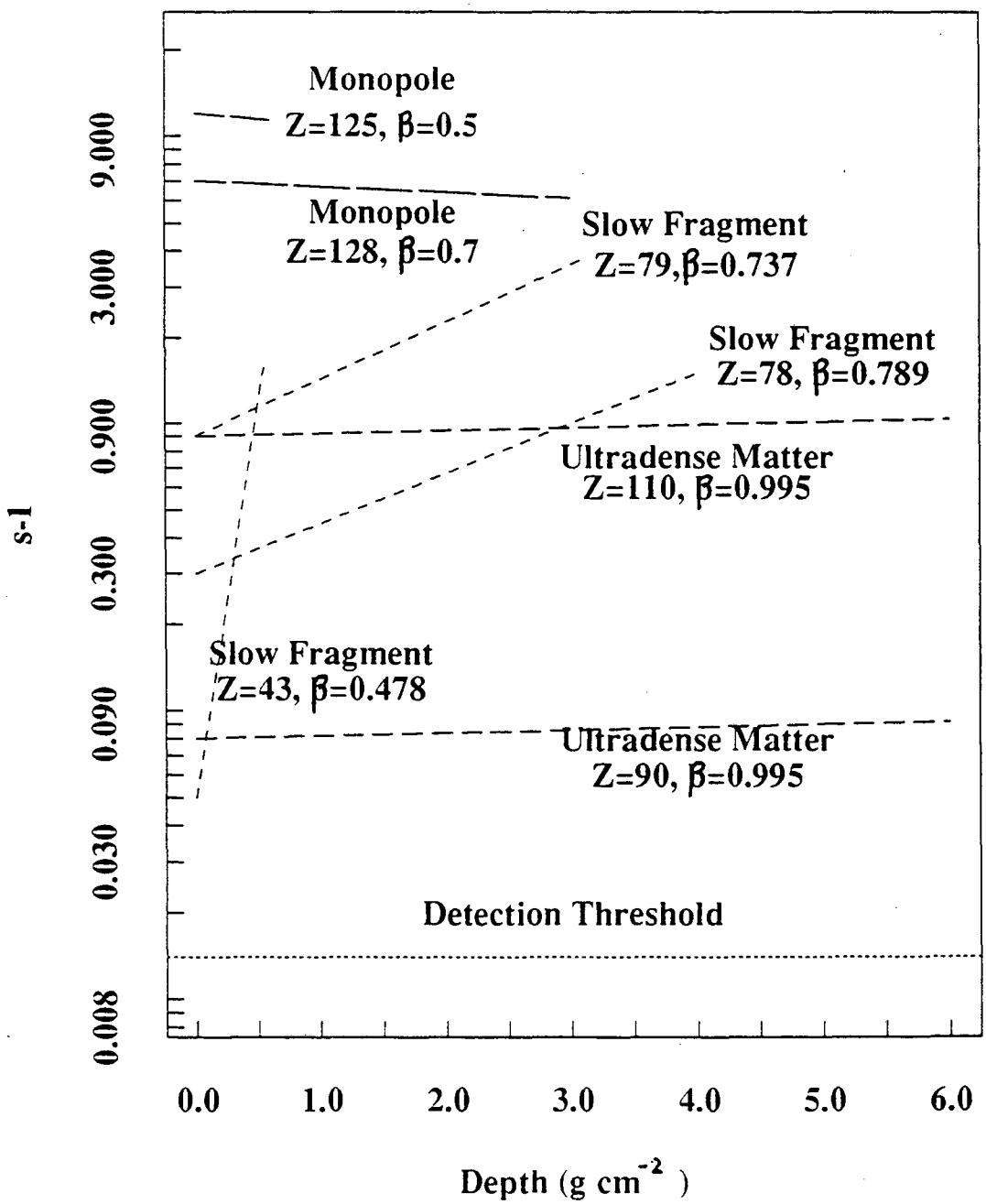

Fig. 7 Measurements of the signal dE/dx at various penetrating depths allow the equivalent charge and velocity of a particle to be determined simultaneously. Shown in the figures are three classes of events. See text for details.

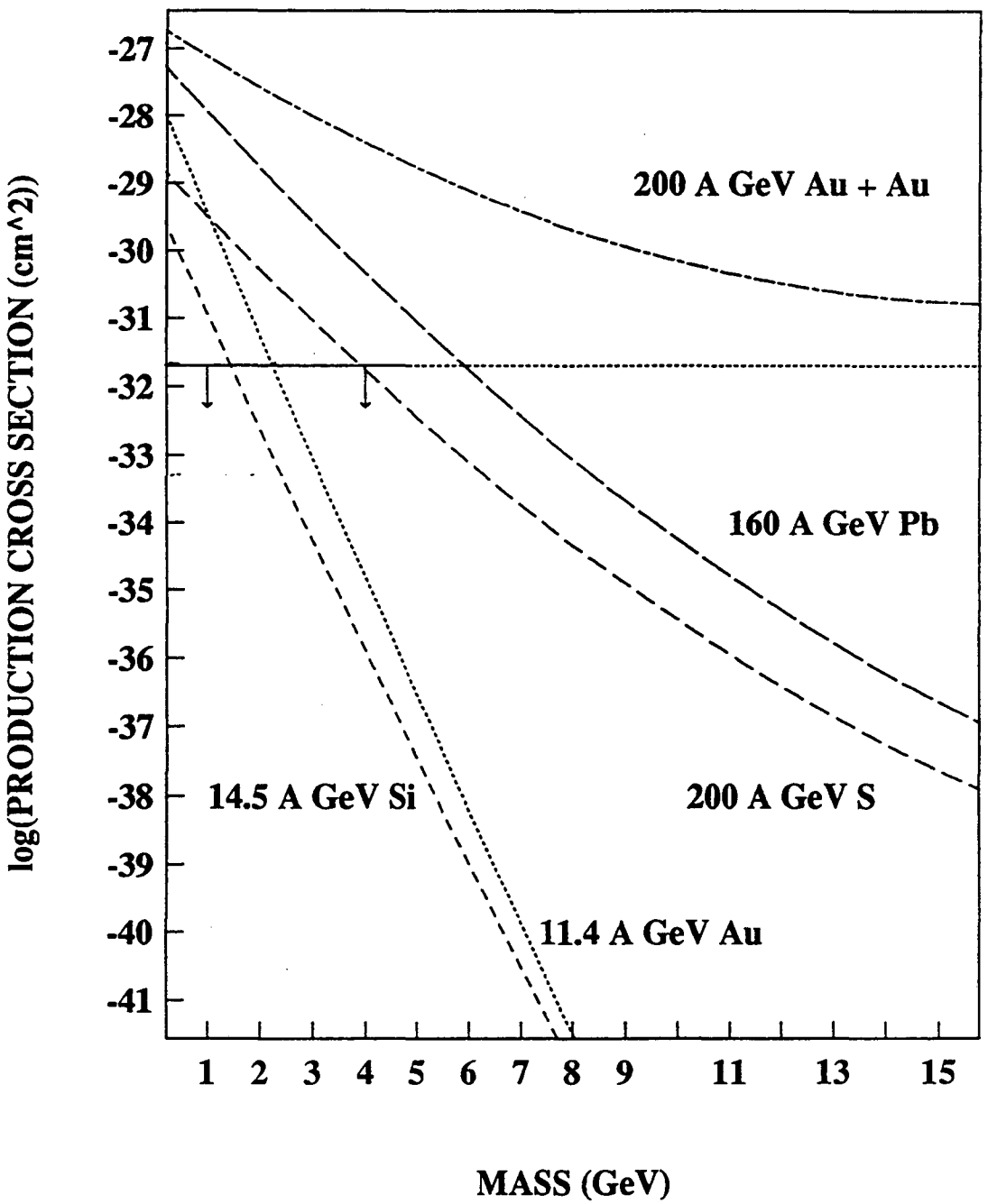

Fig. 8 The upper limit on the production cross section for Dirac monopoles. The Drell-Yan cross section is shown for comparison.

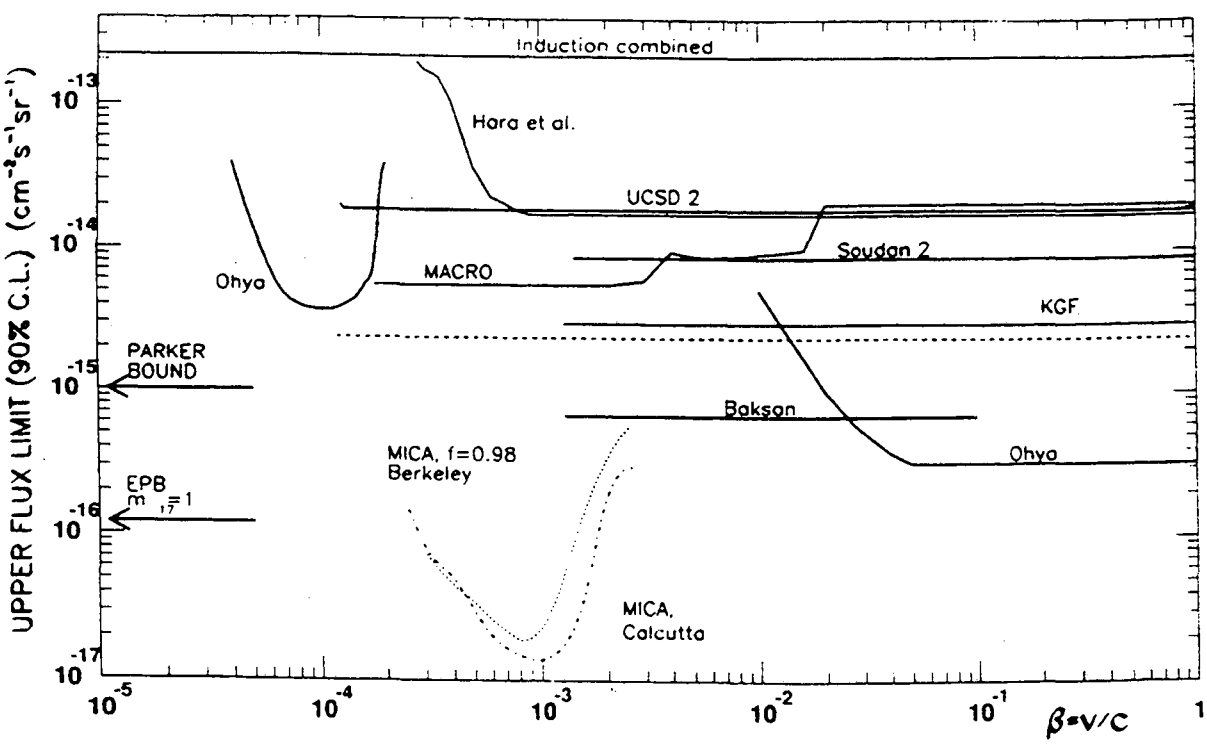

Fig. 9 Summary of flux limits on monopoles in galactic cosmic radiation.

LAWRENCE BERKELEY LABORATORY
UNIVERSITY OF CALIFORNIA
TECHNICAL INFORMATION DEPARTMENT
BERKELEY, CALIFORNIA 94720